

School of Doctoral Studies in Biological Sciences

University of South Bohemia in České Budějovice

Faculty of Science

**The bioenergetics of the bloodstream form of  
*Trypanosoma brucei*:  
Is the mitochondrion capable of ATP production?**

Ph.D. Thesis

**Gergana Taleva, MSc.**

Supervisor: RNDr. Alena Panicucci Zíková, Ph.D.

Institute of Parasitology

Biology Centre of the Czech Academy of Sciences

&

Faculty of Science

University of South Bohemia

České Budějovice, 2023

This thesis should be cited as:

Gergana Taleva, 2023: **The bioenergetics of bloodstream form of Trypanosoma brucei: Is the mitochondrion capable of ATP production?** Ph.D. thesis. University of South Bohemia, Faculty of Science, School of Doctoral Studies in Biological Sciences, České Budějovice, Czech Republic, pp.

## Declaration

I hereby declare that I am the author of this dissertation and that I have used only those sources and literature detailed in the list of references.

České Budějovice, December 2023

Gergana Taleva

This thesis originated from a partnership of **Faculty of Science, University of South Bohemia**, and **Institute of Parasitology AS CR**, supporting doctoral studies in the Molecular and Cell Biology and Genetics study programme.



Přírodovědecká  
fakulta  
Faculty  
of Science



Parazitologický ústav,  
Biologické centrum AV ČR  
Institute of Parasitology  
Biology Centre, AS CR

## Financial support:

This work was supported by the Czech Science Foundation grant number 18-17529S and 20-14409S, by the ERC CZ LL1205 grant and by the MSMT grant number CZ.02.1.01/0.0/0.0/16\_019/0000759.

## ACKNOWLEDGEMENTS

I would like to thank Alena for the immense support not only professionally, but also personally. You have always believed in me even when I did not believe in myself. Thank you for your guidance and at the same time the freedom you gave me, the fruitful straight-to-the point discussions and your passion in science!

I would like to thank Brian for his trust and support, and for teaching me all the techniques with the greatest precision of detail.

I would like to thank all lab members of the Laboratory of Functional Biology of Protists for the help during the years – especially Ondra and Eva for their calmness, patience, and readiness to always help, and Míša K. for her incredible sense of humor that helped me a lot!

I would like to thank everyone from the whole Department of Molecular Parasitology for the wonderful and supportive environment making it an incredible place to work at, for the memorable drinking nights and fun we had and for the amazing friendships I made.

Finally, I thank my family for not giving up on the idea that I will ever graduate! I thank my better half for not asking all the time: ‘Will you graduate already?’. I especially thank my mother and my mother-in-law not only for the support, but also for taking care of my daughters all summer, so that the thesis can be written.

## LIST OF PAPERS:

- I.** **Taleva G**, Husová M, Panicucci B, Hierro-Yap C, Pineda E, Biran M, Moos M, Šimek P, Butter F, Bringaud F, Zíková A. Mitochondrion of the *Trypanosoma brucei* long slender bloodstream form is capable of ATP production by substrate-level phosphorylation. PLoS Pathog. 2023 Oct 11;19(10):e1011699. doi: 10.1371/journal.ppat.1011699. PMID: 37819951; PMCID: PMC10593219, (IF 7.4).

GT generated the double knock-outs cell lines and performed the majority of the experiments and data analysis. She also contributed significantly to the writing process. She is sharing the first authorship with Michaela Husová.

- II.** Zoltner M, Campagnaro GD, **Taleva G**, Burrell A, Cerone M, Leung KF, Achcar F, Horn D, Vaughan S, Gadelha C, Zíková A, Barrett MP, de Koning HP, Field MC. Suramin exposure alters cellular metabolism and mitochondrial energy production in African trypanosomes. J Biol Chem. 2020 Jun 12;295(24):8331-8347. doi: 10.1074/jbc.RA120.012355. Epub 2020 Apr 30. PMID: 32354742; PMCID: PMC7294092, (impact factor 4.8).

AZ performed part of the experiments and analysed the corresponding data. Her contribution was: 30%.

## SUMMARY OF THE PUBLISHED PAPERS:

### **I. Mitochondrion of the *Trypanosoma brucei* long slender bloodstream form is capable of ATP production by substrate-level phosphorylation**

Taleva G, Husová M, Panicucci B, Hierro-Yap C, Pineda E, Biran M, Moos M, Šimek P, Butter F, Bringaud F, Zíková A.

The (Taleva et al., 2023) research paper summarizes the main findings of my Ph.D. studies, together with a few additional optimized experiments that further support the conclusions of my Ph.D. thesis.

The study examines the way in which the mitochondrion of the long slender bloodstream form (BF) *T. brucei* is supplied with ATP, which is then hydrolyzed by F<sub>0</sub>F<sub>1</sub>-ATP synthase to sustain the vital mitochondrial (mt) membrane potential ( $\Delta\Psi_m$ ). For a long time, it was assumed that ATP was only produced glycolytically and imported from the cytosol into the mitochondrion via an ADP/ATP carrier (AAC). Understanding the molecular mechanisms behind the maintenance of the  $\Delta\Psi_m$  of the infectious form of the parasite is crucial since the delivery of the most commonly used drugs to treat Animal African Trypanosomiasis depends on the  $\Delta\Psi_m$  and its reduction is associated with resistance to these drugs (Wilkes et al., 1997), (Eze et al., 2016), (Carruthers et al., 2021).

In this study we show that AAC is indeed the only carrier that can import ATP into the mt matrix to power the hydrolytic activity of the F<sub>0</sub>F<sub>1</sub>-ATP synthase and that its deletion has no effect on the parasite growth, virulence, levels of  $\Delta\Psi_m$  and overall parasite metabolism. This strongly suggests that mt ATP production by substrate-level of phosphorylation (SUBPHOS) occurs in the long slender BF *T. brucei*. The viability of AAC double knock-out (DKO) cells together with the lack of increase of mt ATP levels upon glucose stimulation indicate that the standard culture conditions must provide enough nutrients to support mt ATP production by mt SUBPHOS pathways.

This is further supported by the fact that deletion of succinyl-CoA synthetase (SCoAS or SCS in the paper), the key mt enzyme that produces ATP through SUBPHOS, results in lower parasite virulence, altered metabolic landscape and reduced mt ATP content.

The study also finds that in SCoAS DKO cells, AAC appears to be completely reversed (i.e. supplying ATP to the mitochondrion) to compensate for SCoAS loss. This is evidenced by the lower mt ATP steady-state

levels observed in the SCoAS DKO mutant with unchanged  $\Delta\Psi_m$ , and the greatly increased (25-fold) sensitivity of the DKO mutant to the AAC inhibitor CATR.

The study not only proves that the mitochondrion of the long slender BF is capable of ATP production by SUBPHOS, but also shows that it is important especially when the cells are grown in nutrient-limiting conditions, such as in Creek's Minimal Media (CMM) or in CMM supplemented with glycerol instead of glucose (CMM\_gly). It seems that under CMM\_gly conditions, where cytosolic ATP is limited, the reverse AAC activity is no longer sufficient to compensate for the absence of mt SUBPHOS. Such conditions are more similar to the natural environment of the parasite. Therefore, it can be speculated that the ATP production by the mt SUBPHOS allows parasites to exploit different host environments in which the glucose concentration can be limited.

Furthermore, the study reveals amazing flexibility of the BF *T. brucei* in its cellular bioenergetics, allowing the parasite to quickly adapt and survive various challenging environments of its mammalian host by responding to sudden changes in intracellular ATP levels while still maintaining viable levels of the  $\Delta\Psi_m$  across the mt inner membrane.

## **II. Suramin exposure alters cellular metabolism and mitochondrial energy production in African trypanosomes**

Zoltner M, Campagnaro GD, Taleva G, Burrell A, Cerone M, Leung KF, Achcar F, Horn D, Vaughan S, Gadelha C, Zíková A, Barrett MP, de Koning HP, Field MC

The first-line treatment for first stage sleeping sickness caused by *T. b. rhodesiense* is still suramin. Although suramin was introduced a century ago, the exact mechanism of its trypanocidal activity remains unclear. The study aims to shed light on the mechanisms of action of the drug on the BF *T. brucei*.

The research (Zoltner et al., 2020) shows that suramin has a significant impact on the bioenergetics of the parasites. While suramin treatment of the *T. brucei* form caused a significant decrease in cellular ATP levels in the blood, mt ATP content was slightly increased, which is consistent with the observed increase in mt metabolism. Suramin treatment also resulted in a time- and dose-dependent depolarization of the mt membrane, but with no effect on  $F_0F_1$  ATP synthase proton pumping activity.

The study also showed that suramin had no apparent effects on glycosomes and on the glycolytic pathway, which produces the majority of cellular ATP. However, it appears that the drug activates the pentose phosphate metabolic pathway (supported by proteomics and metabolomics data) as well as parts of the mt-Kreb cycle (supported by proteomics data and increased mt-ATP production), likely in the cells' attempt to cope with cellular stress and decreased cellular ATP levels, respectively.

In summary, the study suggests that the reason for trypanosome cell death upon suramin treatment is the breakdown of cellular ATP. (Zoltner et al., 2020)

I was responsible for the *in vivo* measurement of the steady-state ATP levels in both cytosolic and mt cell compartments upon suramin treatment using the previously generated luciferase-based reporter assay. I also tested the effect of 8 hours suramin treatment on the ability of F<sub>0</sub>F<sub>1</sub>-ATPase to energize the mt membranes. I used the ability of safranin O to quench in the energized mitochondrion in digitonin-permeabilized cells and presence of ATP, allowing for monitoring of  $\Delta\Psi_m$  change over time.

## **Co-author agreement**

RNDr. Alena Panicucci Zíková, Ph.D., the supervisor of this Ph.D. thesis and co-author of papers I-II, fully acknowledges the stated contribution of Gergana Taleva to these manuscripts.

RNDr. Alena Panicucci Zíková, Ph.D.

RNDr. Alena Panicucci Zíková, Ph.D., lead author of paper I, acknowledges the stated contribution of Gergana Taleva to this manuscript.

RNDr. Alena Panicucci Zíková, Ph.D.



## ABBREVIATIONS (ALPHABETICAL ORDER):

$\Delta\Psi_m$	mitochondrial membrane potential
1,3BPGA	1,3-bisphosphoglycerate
AAC	ADP/ATP carrier
AAT	animal African trypanosomiases
Ab	antibody
AceCS	acetyl-CoA synthetase
ACH	acetyl-CoA thioesterase (also called acetyl-CoA hydrolase)
ADP	adenosine diphosphate
AKCT	2-amino-3-ketobutyrate coenzyme A ligase
ALT	alanine aminotransferase (formerly called transaminase)
AOB	amino oxobutyrate
ApoL1	apolipoprotein L1
APRT	adenine phosphoribosyltransferase
A-SCoAS	ATP-specific SCoAS
ASCT	acetate:succinate CoA transferase
AST	aspartate aminotransferase
ATF	adipose tissue forms
ATP	adenosine triphosphate
BCDHC	branched-chain dehydrogenase complexes
BF	bloodstream form
CATR	carboxyatractyloside
cDNA	copy DNA
CDS	coding sequence
CI	complex I
CII	complex II
CIII	complex III
CIV	complex IV
CMM	Creek's Minimal Media
CMM+glc	Creek's Minimal Media supplemented with glycerol instead of glucose
CMM+gly	Creek's Minimal Media (the same as CMM)
CoASH	coenzyme A
COX	cytochrome c oxidase
CV	complex V
cyto	cytosolic
DHAP	dihydroxyacetone-phosphate
Dk	dyskinetoplasmic
DKO	double knock-out
DNDi	Drugs for Neglected Diseases Initiative
DTNB	5,5'-Dithiobis 2-nitrobenzoic acid
<i>E.coli</i>	<i>Escherichia coli</i>
EC <sub>50</sub>	half maximal effective concentration
ETC	electron transport chain
FACS	fluorescence-activated cell sorting
FCCP	carbonyl cyanide 4-(trifluoromethoxy) phenylhydrazone
FHc	cytosolic fumarase
FHg	glycosomal fumarase

FHm	mt fumarase
FRDg	glycosomal fumarate reductase
FRDg	glycosomal fumarate reductase
FRDm	mt fumarate reductase
FRDm	mt fumarate reductase
G-3-P	glyceraldehyde-3-phosphate
G418	geneticin
GCC	glycine cleavage complex
GDH	glutamate dehydrogenase
GK	glycerol kinase
Gly-3-P	glycerol-3-phosphate
Gly3PDH	glycerol-3-phosphate dehydrogenase
GMP	guanosine monophosphate
GPI	glycosylphosphatidylinositol
G-SCoAS	GTP-specific SCoAS
HAT	human African trypanosomiasis
HK	hexokinase
HSP70	heat-shock protein 70
IC <sub>50</sub>	inhibitory concentration 50
IF1	inhibitory factor 1
IND	induced
LipDH	lipoamide dehydrogenase
LY266500	2-(3-chloro-4-fluorophenyl)-2,3-dihydro-1,2-thiazol-3-one
MCF	mitochondrial carrier family
MCP	mt carrier protein
MDH(c)	(cytosolic) malate dehydrogenase
MEc	cytosolic malic enzyme
MEm	mitochondrial malic enzyme
MPC1/2	mt pyruvate carrier 1 and 2
mt	mitochondrial
MTS	mitochondrial targeting sequence
NAD <sup>+</sup>	Nicotinamide adenine dinucleotide (oxidised)
NADH	Nicotinamide adenine dinucleotide (reduced)
NDH <sub>2</sub>	type 2 alternative NADH dehydrogenase
NECT	nifurtimox–eflornithine combination therapy
NMR	nuclear magnetic resonance
NON	non-induced
OLM	oligomycin
ORF	open reading frame
org	organellar
OXPPOS	oxidative phosphorylation
P5C	Δ-pyrroline-5-carboxylate
P5CDH	P5C dehydrogenase
PARP	procyclic acidic repetitive protein
PCR	polymerase chain reaction
PDH	pyruvate dehydrogenase complex
PEP	phosphoenolpyruvate
PEPCK	phosphoenolpyruvate carboxykinase
PF	procyclic form
PPDK	pyruvate phosphate dikinase

PRODH	proline dehydrogenase
PTS	peroxisomal targeting sequence
PYK	pyruvate kinase
QC1	quinazolinecarboxamide compound
qPCR	quantitative polymerase chain reaction
RBP6	RNA-binding protein 6
RNAi	RNA interference
ROS	reactive oxygen species
RT	reverse transcriptase
SCoAS	succinyl-CoA synthetase
SHAM	salicylhydroxamic acid
SKO	single knock-out
SM	single marker
SRA	serum resistance-associated
SUBPHOS	substrate level phosphorylation
<i>T. b. equiperdum</i>	<i>Trypanosoma brucei equiperdum</i>
<i>T. b. evansi</i>	<i>Trypanosoma brucei evansi</i>
<i>T. b. gambiense</i>	<i>Trypanosoma brucei gambiense</i>
<i>T. b. rhodesiense</i>	<i>Trypanosoma brucei rhodesiense</i>
<i>T. brucei</i>	<i>Trypanosoma brucei</i>
<i>T. congolense</i>	<i>Trypanosoma congolense</i>
<i>T. simiae</i>	<i>Trypanosoma simiae</i>
<i>T. suis</i>	<i>Trypanosoma suis</i>
<i>T. vivax</i>	<i>Trypanosoma vivax</i>
TAO	Trypanosoma alternative oxidase
TbHpHbR	T. b. haptoglobin-haemoglobin receptor
TbIscU	T. b. iron-sulfur cluster assembly enzyme
TET	tetracyclin
TETD	Tetraethyl thiuram disulfide
TgsGP	VSG-like glycoprotein
TLF	trypanosome lytic factor
TMRE	tetramethylrhodamine, ethyl ester
TPMP	methyltriphenylphosphonium chloride
UK5099	2-Cyano-3-(1-phenyl-1H-indol-3-yl)-2-propenoic acid
VSG(s)	variant surface glycoprotein(s)
WB	western blot
WCL	whole cell lysate
WCL	whole cell lysates
WHO	World Health Organization
WT	wild type
$\alpha$ -KG	$\alpha$ -ketoglutarate
$\alpha$ -KgDH	$\alpha$ -KG dehydrogenase

# TABLE OF CONTENTS

1. Introduction.....	1
1.1. Human and animal African trypanosomiasis .....	2
1.1.1. Animal African Trypanosomiasis (AAT) .....	2
1.1.1. Human African Trypanosomiasis (HAT) .....	2
1.1.1.1. HAT: Stages.....	3
1.1.1.2. HAT: Host-pathogen interactions.....	4
1.2. <i>T. brucei</i> life cycle .....	6
1.3. Bioenergetics of <i>T. brucei</i> .....	8
1.3.1. Bioenergetics of procyclic form (PF) of <i>T. brucei</i> .....	8
1.3.1.1. Energy sources .....	12
1.3.1.2. Proline metabolism in glucose-depleted conditions .....	13
1.3.1.2.1. From proline to glutamate.....	13
1.3.1.2.2. From glutamate to $\alpha$ -ketoglutarate.....	13
1.3.1.2.3. From $\alpha$ -ketoglutarate to pyruvate .....	14
1.3.1.2.4. From pyruvate to acetate .....	15
1.3.1.3. Proline metabolism in PF in glucose – rich conditions.....	16
1.3.1.4. Glucose metabolism in PF .....	16
1.3.1.4.1. NAD <sup>+</sup> /NADH balance in glycosomes.....	17
1.3.1.4.2. ADP/ATP balance in glycosomes.....	18
1.3.1.4.3. Cellular ATP production pathways.....	18
1.3.1.5. Threonine metabolism .....	19
1.3.1.5.1.1. The fate of acetate .....	19
1.3.1.6. Glycerol as a carbon source .....	20

1.3.1.7. Lipids as energy and carbon source.....	21
1.3.1.8. Alternative energy sources.....	21
1.3.1.9. Electron transport chain (ETC) and complex V (CV) .....	22
1.3.1.9.1. Complex I (CI) .....	23
1.3.1.9.2. Type 2 alternative NADH dehydrogenase (NDH2).....	23
1.3.1.9.3. Glycerol-3-phosphate dehydrogenase.....	23
1.3.1.9.4. Complex II (CII).....	24
1.3.1.9.5. From ubiquinol to oxygen.....	24
1.3.1.9.6. Complex III (CIII) and Complex IV (CIV).....	24
1.3.1.9.7. Trypanosoma alternative oxidase (TAO).....	24
1.3.1.9.8. Complex V (CV) .....	25
1.3.2. Bioenergetics in bloodstream form of <i>T. brucei</i> .....	25
1.3.2.1. Energy sources .....	27
1.3.2.2. Glucose metabolism .....	27
1.3.2.2.1. From glucose to pyruvate.....	27
1.3.2.2.2. The fate of pyruvate.....	29
1.3.2.3. Threonine metabolism .....	31
1.3.2.4. Glutamine/ $\alpha$ -ketoglutarate metabolism.....	32
1.3.2.4.1. From glutamine to $\alpha$ -ketoglutarate .....	32
1.3.2.4.2. Form $\alpha$ -ketoglutarate to succinate .....	33
1.3.2.5. Proline and other AAs as energy source .....	34
1.3.2.5.1. Fatty acids as energy source.....	34
1.3.2.5.2. Glycerol as energy and carbon source .....	35
1.3.2.6. Electron transport chain (ETC) and complex V (CV) .....	37
1.3.2.6.1. Complex I (CI) .....	37
1.3.2.6.2. Type 2 alternative NADH dehydrogenase (NDH2).....	37

1.3.2.6.3. Glycerol-3-phosphate dehydrogenase.....	37
1.3.2.6.4. Complex II (CII).....	38
1.3.2.6.5. Complex III (CIII) and Complex IV (CIV).....	38
1.3.2.6.6. Trypanosoma alternative oxidase (TAO).....	38
1.3.2.6.7. Complex V (CV) .....	38
1.4. Succinyl-CoA synthetase (SCoAS) .....	39
1.5. ADP/ATP carrier (AAC).....	40
2. Hypotheses.....	43
3. Results .....	44
3.1. AAC is not essential in BF trypanosomes <i>in vitro</i> .....	44
3.1.1. AAC expression is developmentally regulated.....	44
3.1.2. AAC RNAi cell line shows no growth phenotype .....	44
3.1.3. Lack of AAC has no effect on BF growth.....	45
3.2. Functional analysis of BF trypanosomes upon AAC loss .....	48
3.2.1. Membrane potential is not affected in BF cells upon AAC loss.....	48
3.2.2. Expression levels of SUBPHOS enzymes and F <sub>0</sub> F <sub>1</sub> -ATPase subunits are not affected upon AAC loss.....	49
3.2.3. AAC DKO cells show increased sensitivity towards TPMP, a SUBPHOS II inhibitor.....	50
3.3. AAC appears to be the only mt ADP/ATP carrier in BF trypanosomes .....	54
3.4. Succinyl-CoA synthetase (SCoAS) is expressed and active in BF trypanosomes - SCoAS activity assay .....	56
3.5. SCoAS is not essential in BF trypanosomes <i>in vitro</i> in standard medium, but becomes potentially important in minimal medium.....	58
3.5.1. SCoAS RNAi cells show growth phenotype in minimal medium .....	58
3.5.2. SCoAS DKO cell line has no growth defects .....	61
3.6. $\Delta\Psi_m$ is not changed upon SCoAS loss.....	64
3.6.1. SCoAS DKO has no detectable SCoAS activity.....	64

3.6.2. $\Delta\Psi_m$ was not changed upon SCoAS loss.....	65
3.7. SCoAS DKO parasites are less virulent in mice than AAC DKO parasites, which are fully virulent .....	66
3.8. One clone, but not the other of SCoAS DKO cells become more dependent on the activity of AAC .....	67
3.8.1. AAC expression levels in SCoAS DKO cells.....	67
3.8.2. CATR sensitivity in SCoAS DKO cells.....	68
3.9. Conditional SCoAS DKO cell line generation.....	69
3.10. SCoAS DKO/AAC RNAi cell line.....	72
3.11. Importance of $F_0F_1$ -ATPase activity in AAC and SCoAS DKO cell lines.....	73
3.11.1. Oligomycin sensitivity in AAC DKO and SCoAS DKO cells.....	74
3.11.2. $\Delta\Psi_m$ is OLM sensitive in AAC DKO cells.....	75
3.12. ATP measurements indicate a contribution of SCoAS to the mt ATP pool.....	76
3.12.1. <i>In vitro</i> ATP measurements.....	77
3.12.2. <i>In vivo</i> ATP measurements.....	78
3.13. AAC DKO/ASCT RNAi cell line - Increased sensitivity towards TPMP suggests SUBPHOS I and II activity.....	83
3.14. Exometabolic analysis supports the SUBPHOS activity.....	84
3.15. <i>In vitro</i> studies using glycerol as an energy source support the mt SUBPHOS activities.....	87
3.15.1. Glycerol studies: AAC DKO and SCoAS DKO cells.....	87
3.15.2. Glycerol studies: SCoAS RNAi.....	88
4. Discussion.....	90
4.1. AAC is active yet not essential in BF <i>T. brucei</i> .....	90
4.2. SUBPHOS pathways are present and active in BF mitochondrion.....	91
4.3. Interplay between the two pathways: AAC and SUBPHOS I/II work together and can compensate for each other.....	92
4.4. Both SUBPHOS I and II are active and compensate for the AAC loss.....	94
4.5. SCoAS is essential in glycerol medium as well as in the mouse model.....	96

5. Materials and methods .....	99
5.1. Cultivation media.....	99
5.2. Cell lines .....	100
5.2.1. Bloodstream form (BF) WT cell line .....	100
5.2.2. BF Single-marker (SM) cell line.....	101
5.2.3. AAC RNAi (GT).....	101
5.2.4. SCoAS RNAi.....	101
5.2.5. AAC DKO .....	102
5.2.6. SCoAS DKO.....	103
5.2.7. AAC DKO/ASCT RNAi .....	103
5.2.8. Conditional SCoAS DKO.....	103
5.2.9. SCoAS DKO/AAC RNAi .....	104
5.3. Mitochondrial or cytosolic luciferase expression in AAC DKO, SCoAS DKO and BF WT cells	104
5.4. Transfections of <i>T. brucei</i> .....	105
5.5. Western blots .....	106
5.6. Quantitative reverse transcriptase-PCR (qRT-PCR).....	106
5.6.1. Total RNA isolation (Phenol-Chloroform extraction).....	106
5.6.2. DNase treatment.....	107
5.6.3. Copy DNA (cDNA) synthesis .....	107
5.6.4. Quantitative PCR (qPCR) and data analysis.....	108
5.7. Membrane potential measurements by TMRE .....	109
5.7.1. Cell staining.....	110
5.7.2. FACS measurements.....	110
5.8. Membrane potential measurement by quenching mode of Safranin-O.....	110
5.9. Oligomycin treatment .....	111
5.10. <i>In vitro</i> ATP measurements.....	111
5.10.1. Sample preparation – subcellular fractionation.....	111



5.10.2. ATP measurements .....	112
5.11. <i>In vivo</i> ATP measurements – luciferase assay .....	112
5.12. Animal experiments .....	113
5.13. Alamar blue assay .....	113
5.14. Succinyl-CoA synthetase (SCoAS) activity assay .....	114
5.14.1. Sample preparation – digitonin subcellular fractionation: .....	114
5.14.2. Sample preparation of the mitochondrial matrix-rich fraction .....	115
5.14.3. Activity assay - measurements .....	115
5.15. Exometabolomics .....	116
6. Reference list (alphabetical order): .....	117
7. CURRICULUM VITAE .....	140

# 1. INTRODUCTION

*Trypanosoma brucei* (*T. brucei*) is a unicellular eukaryotic parasite belonging to the family Trypanosomatidae, order Kinetoplastida, phylum Euglenozoa (Cayla et al., 2019). Trypanosomatids include organisms of huge medical relevance, including *T. brucei*, *Trypanosoma cruzi* (causative agent of Chagas disease) and *Leishmania spp.* (causative agent of leishmaniasis). *T. brucei* is the causative agent of African sleeping sickness in humans and nagana in cattle. *T. brucei* has a digenetic life cycle, alternating between the forms residing in the tse-tse fly (*Diptera*, genus *Glossina*) and the forms that reside in a mammalian host (www.cdc.gov). There are 31 species and subspecies of tsetse flies inhabiting forests, river areas or savannah (Büscher et al., 2017). Both male and female flies are haematophagous (blood-feeding) and are responsible for trypanosome transmission, making elimination of *T. brucei* extremely challenging to impossible.

The parasite's cell consists of a single copy elongated mitochondrion, where the kinetoplast is positioned. The kinetoplast, hence the name of the order Kinetoplastida, is the catenated mitochondrial (mt) DNA. The kinetoplast consists of maxicircles (~ 50 copies) and minicircles (~ 10000). The maxicircles encode mt proteins, whereas the minicircles encode short guide RNAs. The kinetoplast is linked to the parasite single flagellum through a basal body. The kinetoplast and basal body are in turn connected by a tripartite attachment complex. The place where the flagellum exits (the most posterior part) is formed the flagellar pocket, being the only site of endo- and exocytosis. The cell has many glycosomes, specialized peroxisome-like organelles, where the glycolytic reactions are compartmentalized. The cell nucleus contains 11 pairs (the organism is diploid) of megabase conventional chromosomes. The genome contains in addition more than 100 approximately 50 kb minichromosomes, harboring the variant surface glycoprotein (VSG) genes, each of them flanked by a 177 bp repeat (Matthews, 2005).

*T. brucei* includes 3 subspecies which are morphologically indistinguishable. While *T. brucei brucei* (hereafter referred to as *T. brucei* for simplicity) causes animal African trypanosomiasis (AAT) and is not infective to human beings, *T. brucei rhodesiense* and *T. brucei gambiense* can infect humans and cause human African trypanosomiasis (HAT).

## 1.1. Human and animal African trypanosomiases

The diseases caused by *T. brucei* as well as other trypanosome species are collectively referred to as African trypanosomiases. They cause human and animal diseases with huge medical and economic impact across sub-Saharan Africa, and animal only disease across Asia and South America (Morrison et al., 2023).

### 1.1.1. Animal African Trypanosomiases (AAT)

Animal African trypanosomiases (AAT, also known as nagana) are caused by multiple species. In sub-Saharan Africa the main pathogenic species are *T. congolense*, *T. vivax* and *T. brucei* infecting cattle, sheep, goats, equids, and wild animals, *T. simiae* and *T. suis* infecting pigs. *T. b. equiperdum* causes venereally-transmitted AAT in horses and donkeys in the region. In North Africa, South America and Asia (*T. b. evansi* only), *T. b. evansi* and *T. vivax* infect cattle, equids, camels, and Asian buffalo (Morrison et al., 2023). The body wasting, and eventual death of domesticated animals has huge economic implications such as restrictions in agricultural development and poverty in the affected areas.

Although drugs against AAT are available, the development of trypanocide resistance in herds is a major problem. This is mainly due to lack of knowledge of the farmers and poor practices in West and Eastern Africa, such as inappropriate dosage and timing of drug administration, lack of veterinary supervision, overuse, or unavailability of the drugs (Kasozi et al., 2022).

### 1.1.1. Human African Trypanosomiases (HAT)

Human African Trypanosomiasis (HAT, also known as sleeping sickness) is a neglected tropical disease which is transmitted by a tsetse fly bite. It occurs in sub-Saharan African belt where the vector is present. HAT is caused by two variants (or subspecies) of *T. brucei* - *T. b. rhodesiense* and *T. b. gambiense*. *T. b. gambiense* is divided into two subtypes - Group 1 which represents about 80 % of *T. b. gambiense* and it has a homogenous genetic composition, whereas Group 2 represents about 20% of the parasites and it is quite heterogenous (Gibson, 1986).

*T. b. rhodesiense* is spread out in eastern and southern Africa causing the fast developing acute disease progressing within weeks or months. The main reservoir for *T. b. rhodesiense* is domestic and wild animals. The main vectors for *T. b. rhodesiense* are *Glossina fuscipes*, *Glossina morsitans* and *Glossina pallidipes* (Büscher et al., 2017).

*T. b. gambiense* is spread out in western and central Africa causing the chronic slow-progressing disease within years (Büscher et al., 2017). The main reservoir of *T. b. gambiense* are humans although wild and even domestic animals (sheep, pigs, goats, dogs) can most probably also contribute as reservoirs (Boundenga et al., 2022), (Njiokou et al., 2010), (Vourchakbé et al., 2020). The main vectors for *T. b. gambiense* are *Glossina fuscipes* and *Glossina palpalis* (Büscher et al., 2017).

*T. b. brucei* does not infect humans because of the presence of the trypanosome lytic factor in the human blood, as will be explained in more detail later .

#### **1.1.1.1. HAT: Stages**

HAT proceeds in two well-known stages (Morrison et al., 2023). In the first stage (haemolymphatic stage) the tsetse fly bites the human host and deposits the parasites to the skin from where they are distributed to the lymphatic and vascular system. At this stage the patient has typically fever, headache, lymphadenopathy, weakness, hepatosplenomegaly, and endocrine dysfunction. The second stage (meningoencephalitic stage) begins when the parasites penetrate the blood-brain barrier and enter the brain. The symptoms include motor and sensory impairment and speech and sleep disorder hence the name sleeping sickness. If the HAT is not treated it leads in almost all cases to coma and ultimately death. Very often the progression rate from first to second stage determines the virulence of the trypanosomes. There is a treatment for both stages.

The first-line treatment for the first stage HAT caused by *T. b. gambiense* is pentamidine isethionate with efficacy against the disease 95-98%. It is usually well tolerated with adverse effect such as hypoglycemia, hypotension, stomach and intestine problems and pain (Büscher et al., 2017). The first-line treatment for first stage HAT caused by *T. b. rhodesiense* is suramin. The side effects are usually mild and reversible such as pyrexia, nephrotoxicity, peripheral neuropathy, agranulocytosis, and thrombocytopenia (Büscher et al., 2017).

For the second stage of HAT caused by *T. b. gambiense* the first-line treatment is nifurtimox–eflornithine combination therapy (NECT). NECT has 95-98% cure rates, less than 1% mortality rates and less severe adverse effects (abdominal pain, headache, vomiting) (Büscher et al., 2017). It is effective and well tolerated also in children, pregnant or breastfeeding women (Kuemmerle et al., 2021). For the second stage of HAT caused by *T. b. rhodesiense* the first-line treatment is melarsoprol due to lack of a better alternative. The melarsoprol is very toxic causing an encephalopathic syndrome which causes death in in 5% of the patients. It also causes trypanosomal resistance in about 30% of the cases (Babokhov et al., 2013).

Although the available drugs are free of charge, they are toxic, difficult to administer (mostly by intravenous injection), not always effective and cause severe side effects. In addition, the parasite is rapidly developing resistance to these old drugs.

The path to HAT elimination should be facilitated by the new drug fexinidazole, which has been on the market since 2018 (Dickie et al., 2020). It was developed by Sanofi-Aventis in collaboration with DNDi. It is the first oral drug effective in both stages of HAT caused by *T. b. gambiense*. One of the few drawbacks is that absorption of the drug is dependent on food intake, so its effect may not be maximal in an area of malnutrition. However, another oral drug, acoziborol, will hopefully be on the market soon and is considered a dream drug because it appears to require only one dose to be fully effective (Dickie et al., 2020). Combined with a greater number of health care providers, active surveillance, and the new treatments, HAT is on its way to elimination.

Only 992 and 663 cases of HAT were reported in 2019 and 2020, respectively. WHO has set an ambitious goal of interrupting of *T. b. gambiense* transmission and eliminating HAT caused by *T. b. rhodesiense* by 2030 (Franco et al., 2022). If successful, HAT would be the first disease eliminated solely through the use of drugs rather than a vaccine.

#### **1.1.1.2. HAT: Host-pathogen interactions**

The HAT progression outcome depends on the genetic diversity in both trypanosome parasite and human host.

*T. b. gambiense* Group 1 has primarily an anthroponotic nature and typically causes chronic infection which can take months or even years to progress. In contrast, *T. b. rhodesiense* and *T. b. gambiense* Group 2 are zoonotic with large animal reservoir and often cause more acute infections with critical complications within days (Morrison et al., 2023). An important factor is also the human individual genetic factors which is an ongoing research area. For example, high interleukin 10 and low TNF $\alpha$  is linked with increased risk of HAT development whereas high interleukin 8 is associated with low risk (Morrison et al., 2023).

There has been a significant progress in the combat against HAT – from more than 30 000 cases per year at the turn of the century greatly reduced to 663 cases in 2020 (Franco et al., 2022). It was all due to the sustain of good surveillance and the expansion of health facilities for diagnosis and HAT treatment. It seems promising the goal of the World Health Organization (WHO) to eliminate the disease of public health importance by 2030 (Franco et al., 2022). The *T. b. gambiense* HAT seems easier to be controlled since the

main reservoirs are humans while the rhodesiense HAT could be more difficult for elimination due to the zoonotic nature of the parasite.

The development of vaccines is still a challenge due to several reasons (Morrison et al., 2023). The well-studied *T. brucei* large gene family of VSGs effectively evade the host immune response. At a particular moment only one type of densely packed VSG protein is expressed on the surface of each cell through a monoallelic expression system, and the immune system develops VSG-specific antibodies. Before the antibodies manage to clear the parasites with the respective VSG, the cell changes the identity of the VSG thus rechallenging the immune system. The VSG genes and pseudogenes are positioned at the telomeric regions of the chromosomes, and the repertoire is enormous - it constitutes approximately 20% of the coding genome of *T. brucei*. The mechanism responsible for the VSG switch is either the transcriptional switching between telomeric expression sites or recombination of the VSG genes (Cestari & Stuart, 2017). VSGs can move freely across the cell surface and in combination with the cell motility induced by the flagellum causes the hydrodynamic pressure on the cell to direct the bound antibodies towards the flagellar pocket where they are cleared by endocytosis. Another important aspect of immune system impairment is the ability of the trypanosomes to kill B memory cells. This was observed in mice and some breeds of cattle and leads to loss of the immunological memory towards previous infection (Frenkel et al., 2016), (O’Gorman et al., 2009).

Many African primates have developed a mechanism for protection against trypanosomes including humans. A well-studied mechanism constitutes the main component of the human trypanosome lytic factor (TLF) 1 and 2, with the lytic component apolipoprotein L1 (ApoL1) present on both. TLFs are present in the human, gorilla, and baboon serum (Wheeler, 2010). The mammalian bloodstream form of *T. b. brucei* expresses in the flagellar pocket the haptoglobin-haemoglobin receptor (TbHpHbR), which primary function is the uptake of haem. TbHpHbR is partially responsible for the uptake of TLF due to its recognition and binding of the ApoL1 component. ApoL1 reaches the cytosol and forms a pH-dependent ionic pore in the lysosomes of the parasite causing swelling of the organelle and ultimately death of the trypanosome by cell lysis (Morrison et al., 2023), (Wheeler, 2010). *T. b. gambiense* and *T. b. rhodesiense*, the human-infective trypanosome species, however, have developed a way to overcome the ApoL1-induced cell lysis. *T. b. rhodesiense* is able to neutralize directly ApoL1 by secreting the serum resistance-associated (SRA) protein (Morrison et al., 2023), (Wheeler, 2010). *T. b. gambiense* Group 2 shows resistance to human trypanosome lytic factor in a similar manner as *T. b. rhodesiense*, although the exact mechanism is still unknown (Cooper et al., 2016). *T. b. gambiense* Group 1 has evolved a different mechanism to escape ApoL1 toxicity – mutation (Horáková et al., 2022) or decreased expression of the TbHpHbR gene, resulting in ApoL1 decreased uptake, inactivation and increased degradation (Kieft et al., 2010). Another mechanism

leading to reduced sensitivity of *T. b. gambiense* Group 1 towards ApoL1 is the expression of specific cysteine protease which acts most probably by increasing TLF and/or APOL1 proteolysis (Alsford et al., 2014). In addition, expression of VSG-like glycoprotein TgsGP also was found to confer TLF resistance in *T. b. gambiense* probably by stiffening the endosomal membranes (Uzureau et al., 2013).

## 1.2. *T. brucei* life cycle

The life cycle of *T. brucei* is nicely summarized in (Matthews, 2005). *T. brucei* life cycle alternates between the parasite forms found in the tse-tse fly insect vector and the forms that reside in a mammalian host (see Fig.1). During its life cycle, the parasite remains extracellular.

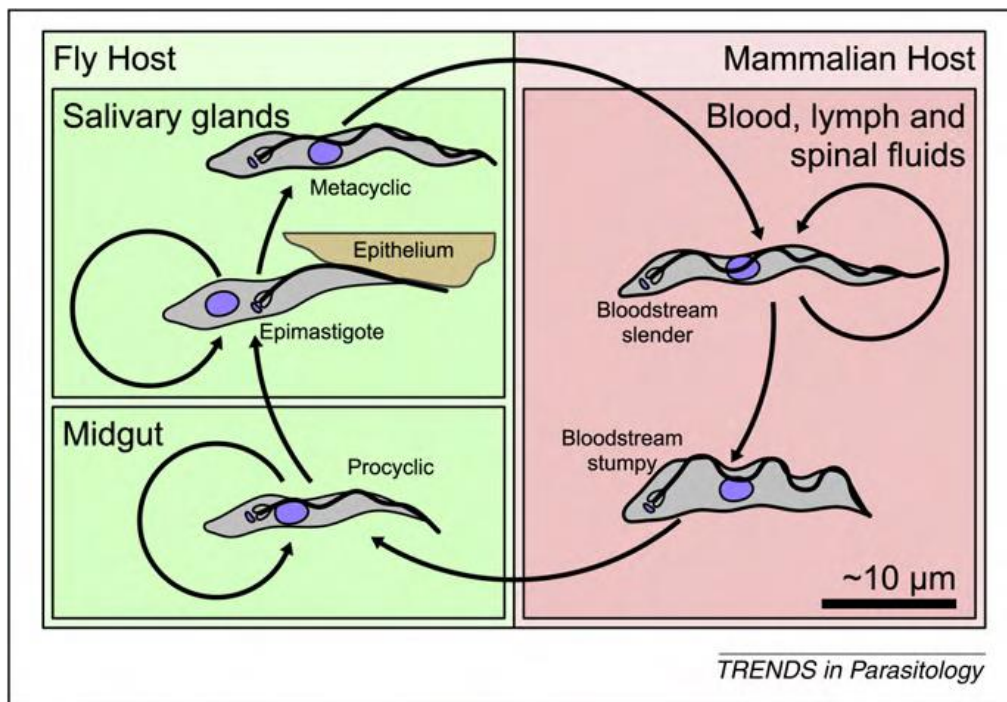


**Fig.1** Life cycle of *T. brucei* (adapted from (Wheeler, 2010)). In the mammalian host the parasite proliferates in the body fluids in the form of a long slender bloodstream form. There they proliferate and differentiate into non-proliferative stumpy form. Upon tsetse bloodmeal, the stumpy forms are ingested and transform into procyclic form cells in the midgut of the fly. The cells migrate to the salivary gland where they differentiate into epimastigotes via an asymmetric division producing short and long forms. Most probably only the short epimastigotes attach to the epithelium of the salivary gland by the flagellum. Next, the cells detach and transform into non-proliferative metacyclic forms, ready to be injected into a new host during bloodmeal of the fly.

Upon tsetse bite, the metacyclic trypomastigotes enter the bloodstream of the mammal where they proliferate as a long slender bloodstream form (BF). After a few days, the parasites spread through the blood and lymph to various organs and tissues, still being extracellular. Next, the BF trypanosomes penetrate the brain parenchyma leading to a local inflammation and tissue damage (Kristensson et al., 2013). As a BF the parasite evades the immune system of the host through the expression of the VSGs.

When the parasites reach high numbers, they are replaced by the non-proliferative stumpy form which is taken up by the fly during blood meal. It should be noted that in this thesis, the long slender bloodstream form only and not the stumpy form is referred to as BF although both are present in the bloodstream of the host. The stumpy forms are considered important for the regulation of the parasite number in the host ensuring its longer survival. Another important reason is the uniform cell arrest ensures the uniform re-entry into the cell cycle once the parasite is transmitted into the insect vector (Matthews, 2005).

When the stumpy form reaches the midgut of the tsetse fly, it transforms into procyclic form (PF) which is no longer infectious to mammals. During the transition the most important changes include the replacement of the VSG surface coat with other proteins (mainly procyclins hence the name), repositioning of the kinetoplast between the posterior end and the nucleus and elaboration of the mt cristae which is linked to changes in the parasite metabolism (Sharma et al., 2009).

In the tsetse midgut the PF parasites proliferate and then they migrate to the proventriculus (the end part of the foregut), where they elongate, and become epimastigotes. In the proventriculus the PF parasites penetrate the newly formed and still immature peritrophic matrix (protective chitinous structure) and evade the ectoperitrophic space (the space between the peritrophic matrix and the epithelial cells) (Rose et al., 2020). The epimastigotes have repositioned their kinetoplast next to the nucleus in the anterior end. The parasite continues to proliferate however asymmetrically, producing long and short epimastigote. Long epimastigote most probably degenerates and the short epimastigote moves to and attaches to the epithelial wall of the salivary gland and attaches there through extensions of the flagellum (Sharma et al., 2009).

Finally, the parasites undergo division arrest and transform into metacyclic trypomastigotes. The metacyclic trypanosomes regain the VSG surface coat and are released in the lumen of the tsetse gland ready for transmission into the mammalian host.

Most research has been focused mainly on PF midgut form and the long slender BF trypanosomes since those forms are readily cultured. However, studies have appeared investigating other forms of the parasite in the tsetse vector, after publishing a protocol for in vitro differentiation of PF cells to epimastigote and metacyclic forms by overexpression of RNA-binding protein 6 (RBP6) (Kolev et al., 2012).



### **1.3. Bioenergetics of *T. brucei***

The life cycle of *T. brucei* is quite complex and involves infection of various tissues of mammalian and insect hosts and consequently, the parasite must adapt to different environments. Being a tsetse fly resident, PF of the parasite depends on the fly haemolymph, in which the main carbon sources are amino acids. When residing in the mammalian host bloodstream, BF of the parasite depends mainly on glucose. The adaptations include both morphological and metabolic changes (Bringaud et al., 2006). The morphological adaptations comprise the change in the shape of the whole cell as well as the repositioning of the kinetoplast. Other obvious transformations occur in the morphology of the *T. brucei* single mitochondrion, as it transitions from a highly branched network that occupies a vast proportion of the PF cell to a long and slender tubule that lacks obvious cristae structures in the BF parasite. These physical changes correlate with the substantive metabolic reorganization that occurs as the fully developed PF mitochondrion becomes a less active organelle in the BF cell, although this notion is gradually changing with the accumulation of new data. Regardless the mt changes, the organelle always retains vital processes such as ion homeostasis, calcium signaling, RNA editing, fatty acid synthesis and Fe-S cluster assembly (Verner et al., 2015). In the following sections the bioenergetics of PF and BF trypanosomes will be discussed and compared as most research has been done on these stages of the *T. brucei* life cycle.

#### **1.3.1. Bioenergetics of procyclic form (PF) of *T. brucei***

PF parasites have a fully developed mitochondrion that efficiently produces chemical energy in the form of ATP for the entire cell. ATP in PF cells like in other eukaryotes can be produced in 2 different ways – by oxidative phosphorylation (OXPHOS) or by substrate level phosphorylation (SUBPHOS). During OXPHOS, the electrons released from the oxidation of nutrients flow through the electron transport chain (ETC) to the final electron acceptor, oxygen. The energy released in these redox reactions is used to pump protons across the inner mt (mt) membrane. The proton motive force generated is used by F<sub>0</sub>F<sub>1</sub>-ATP synthase, which allows protons to return to the mt matrix according to their concentration gradient and produces ATP. This ATP is then transported out into the cytosol by ADP/ATP carrier (AAC) while the ADP is transported from the cytosol into the mitochondrion. ATP is utilized for cellular needs. On the other hand, SUBPHOS produces ATP in various cell compartments which involves a chemical reaction with a direct transfer of a phosphoryl group to ADP from a phosphorylated compound.

The electrons feeding the ETC come from reduced molecules of NADH and FADH<sub>2</sub> which are produced by the TCA cycle. However, despite the presence of the TCA enzymes, the TCA cycle in PF cells is

classically believed not to function in a canonical way since not all the reactions were shown to happen (Van Hellemond, Opperdoes, et al., 2005). The idea of an incomplete TCA cycle was first suggested when the ablation of aconitase, and then other TCA cycle enzymes, did not affect cell growth and viability (Van Weelden et al., 2003), (Bochud-Allemann & Schneider, 2002). Furthermore, majority of acetyl-CoA does not enter the TCA cycle but is rather converted to acetate while ATP is being produced by substrate phosphorylation (Van Hellemond, Opperdoes, et al., 2005). It should be noted that those experiments were performed in glucose and nutrient-rich medium and it has to be considered the limiting sensitivity of the methods used. This notion of incomplete TCA cycle in trypanosomes is starting to change since new data is emerging. A recent study demonstrated that in PF cells malate can be converted to succinate using both reducing and oxidative TCA cycle steps in the presence of 2mM proline and absence of glucose (Villafranz et al., 2021). The same study using radiolabeled substrates in combination with various enzyme mutant cell lines clearly demonstrates that TCA cycle in PF *T. brucei* parasites is fully and canonically functional under certain growth conditions resembling physiological environment.

The pathways by which the PF produce energy are shown on **Fig. 2** and **3** and will be discussed in detail in the following sections.

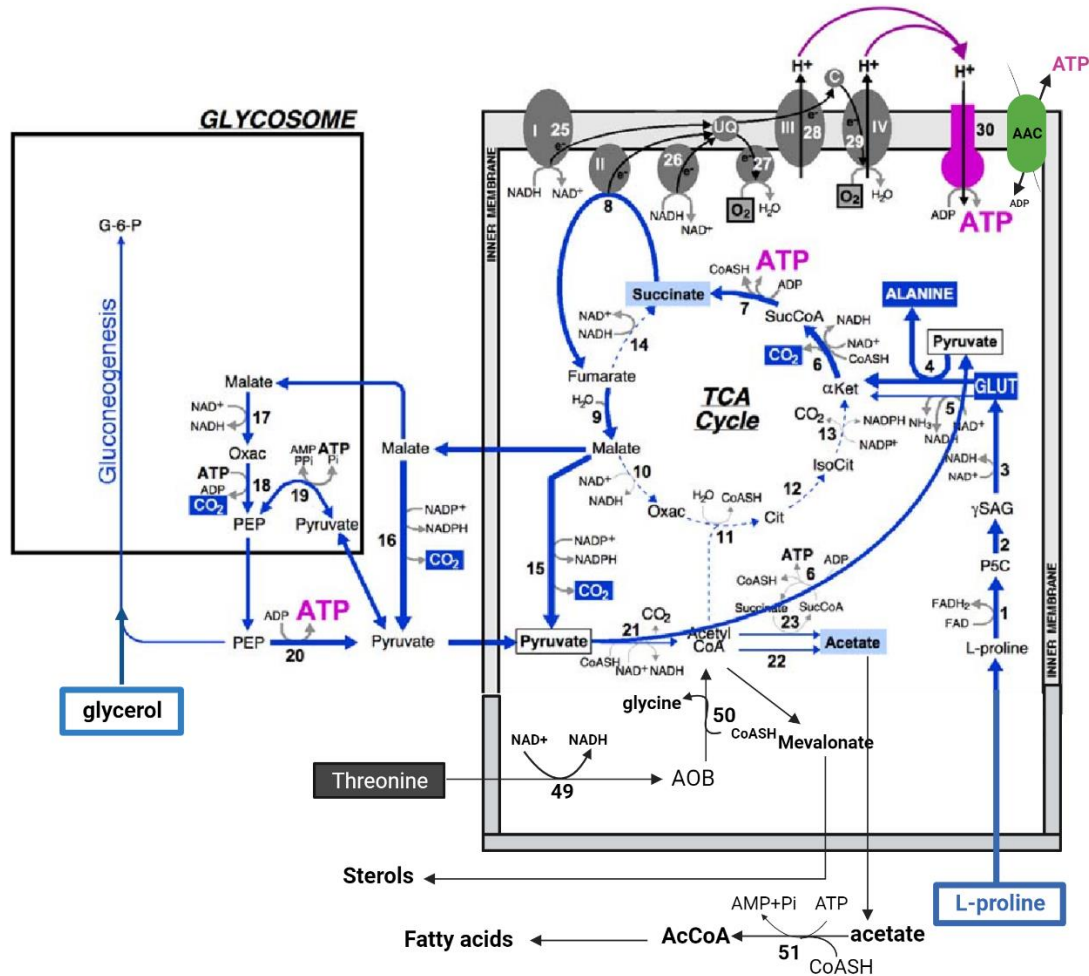


**Fig.2** Scheme of the bioenergetics of procyclic *T. brucei* growing in glucose-depleted medium (adapted from (Bringaud et al., 2012), (Millerioux et al., 2013)). Blue arrows represent enzymatic steps of proline metabolism. Excreted end products are in white characters on a blue background (major end products: L-alanine, L-glutamate and CO<sub>2</sub>) or in black characters on a light blue background (minor end products: acetate and succinate). At reversible steps, only the presumed or demonstrated direction of the reaction is represented. Dashed arrows indicate steps considered to occur at background level or not at all under glucose-depleted growth conditions. The glycosomal and mt compartments, the tricarboxylic acid cycle (TCA cycle) and gluconeogenesis are indicated. Glycerol as a substrate for gluconeogenesis is indicated, threonine metabolism is indicated with black arrows. Abbreviations: AAC, ADP/ATP carrier, AcCoA, Acetyl-CoA, C, cytochrome c; Cit, citrate; CoASH, coenzyme A; DHAP, dihydroxyacetone phosphate; G-6-P, glucose-6- phosphate; GLUT, glutamate; Gly-3-P, glycerol-3-phosphate; IsoCit, isocitrate; 2Ket, 2-ketoglutarate; Oxac, oxaloacetate; P5C, pyrroline-5-carboxylate; PEP, phosphoenolpyruvate; Pi, inorganic phosphate; PPI, inorganic pyrophosphate;  $\gamma$ SAG, glutamate  $\gamma$ - semialdehyde; SucCoA, succinyl-CoA; UQ, ubiquinone pool. Enzymes: 1, proline dehydrogenase (PRODH); 2, spontaneous reaction; 3, pyrroline-5 carboxylate dehydrogenase (P5CDH); 4, L- alanine aminotransferase (ALT); 5, glutamate dehydrogenase (GDH); 6,  $\alpha$ -ketoglutarate dehydrogenase complex; 7, succinyl-CoA synthetase (SCoAS); 8, succinate dehydrogenase (SDH; complex II of the respiratory chain); 9, mt fumarase; 10, mt malate dehydrogenase; 11, citrate synthase; 12, aconitase; 13, NADP-dependent isocitrate dehydrogenase; 14, mt NADH-dependent fumarate reductase (FRDm); 15, mt malic enzyme (ME<sub>m</sub>); 16, cytosolic malic enzyme ME<sub>c</sub>); 17, glycosomal malate

dehydrogenase; 18, phosphoenolpyruvate carboxykinase (PEPCK); 19, pyruvate phosphate dikinase (PPDK); 20, pyruvate kinase (PYK); 21, pyruvate dehydrogenase complex; 22, unknown enzyme; 23, acetate:succinate CoA-transferase (ASCT); 25, complex I of the respiratory chain; 26, rotenone-insensitive NADH dehydrogenase; 27, trypanosome alternative oxidase (TAO); 28, complex III of the respiratory chain; 29, complex IV of the respiratory chain; 30, F<sub>0</sub>F<sub>1</sub>-ATP synthase (ATP<sub>s</sub>), 49, threonine 3-dehydrogenase (TDH); 50, 2-amino-3-ketobutyrate coenzyme A ligase; 51, AMP-dependent acetyl-CoA synthetase (AceCS).  
Created with BioRender.com.

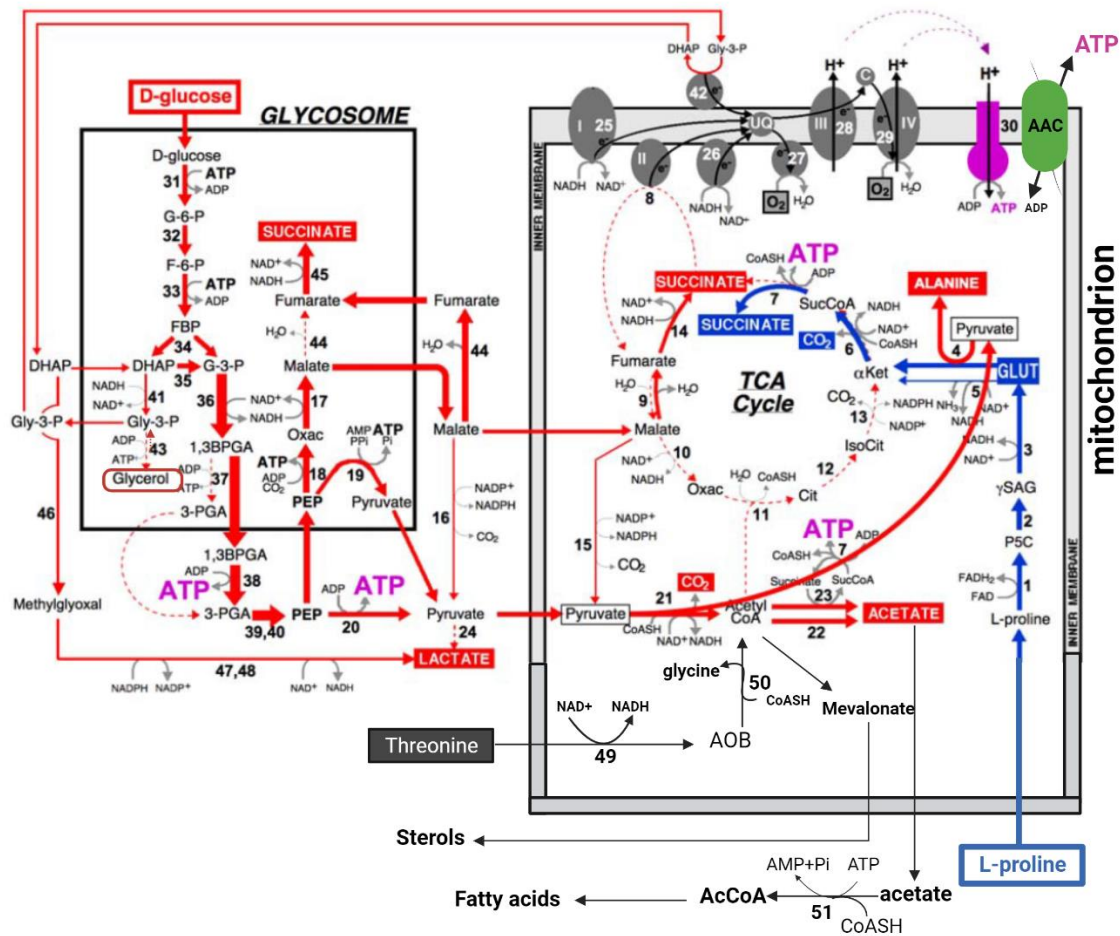


**Fig.3** Scheme of the bioenergetics of procyclic *T. brucei* growing in glucose-rich medium (adapted from (Bringaud et al., 2012), (Millerioux et al., 2013)). See Figure 2 for the legend. Red arrows represent enzymatic steps of glucose and glycerol metabolism. Excreted end products are in white characters on a red background. Threonine metabolism is indicated with black arrows. Abbreviations not used in Figure 2: 1,3BPGA, 1,3-bisphosphoglycerate; F-6-P, fructose-6- phosphate; FBP, fructose-1,6- bisphosphate; G-3-P, glyceraldehyde-3-phosphate; Gly-3-P, glycerol-3-phosphate; 3-PGA, 3- phosphoglycerate. Enzymes not shown in Figure 2: 24, lactate dehydrogenase; 31, hexokinase; 32, glucose-6-phosphate isomerase; 33, phosphofructokinase; 34, aldolase; 35, triose-phosphate isomerase; 36, glyceraldehyde-3-phosphate dehydrogenase; 37, glycosomal phosphoglycerate

kinase; 38, cytosolic phosphoglycerate kinase; 39, phosphoglycerate mutase; 40, enolase; 41, NADH-dependent glycerol-3-phosphate dehydrogenase; 42, FAD-dependent glycerol-3-phosphate dehydrogenase; 43, glycerol kinase; 44, cytosolic fumarase; 45, glycosomal NADH-dependent fumarate reductase (FRDg); 46, nonenzymatic reaction; 47, NADPH-dependent methylglyoxal reductase; 48, NAD<sup>+</sup>-dependent-lactaldehyde dehydrogenase. Created with BioRender.com.

### 1.3.1.1. Energy sources

The PF of *T. brucei* resides in the midgut of the tsetse fly, therefore it is adapted to rely on the nutrients presented in the haemolymph of the vector. The haemolymph is rich in amino acids, whereas glucose is only available during short periods of time immediately after blood-meal.

One of the most abundant amino acids in the tsetse fly is proline, the concentration of which in the fly midgut is about 1-2mM (Balogun, 1974). Proline cannot be synthesized by the parasite, and it must be provided from the environment (Mantilla et al., 2017). Proline has been shown to be important source of energy for the fly itself especially during its flight (Bursell, 1963). In contrast to the conditions found in the tsetse fly, the PF parasites have been grown in the laboratory in a glucose and nutrient-rich medium, namely the commonly used SDM-79 medium containing 6mM glucose. Under these conditions the parasite preferentially utilizes glucose (Lamour et al., 2005), (Bringaud et al., 2006). Consequently, in the past the glucose catabolism had been investigated intensively and proline as carbon and energy source was neglected. However, when the glucose-depleted media was developed, the essential role of the proline metabolism was addressed (Bringaud et al., 2012). PF parasites were shown to grow well in glucose-depleted medium when proline was present (Furuya et al., n.d.), (Lamour et al., 2005), (James C. Morris, 2002). In addition, when glucose is absent, proline is the only amino acid that can sustain the culture and its rate of consumption increases up to 6 folds in those conditions (Lamour et al., 2005), (C. Ebikeme et al., 2010). Proline was shown to be essential for the PF cells to colonize the midgut of the fly (Mantilla et al., 2017). Therefore, on **Fig.2** the current scheme of PF metabolism is shown in glucose-depleted conditions when the cells rely mainly on proline for energy production.

Another amino acid found to be consumed in high quantities and used as a carbon and energy source in PF trypanosomes is threonine (Millerioux et al., 2013), (G. A. Cross et al., 1975), (Lamour et al., 2005), (Linstead & Cross, 1977). Interestingly, glycerol, but not fatty acids, was shown to be utilized by PF for energy needs. Surprisingly, glycerol was even the preferred carbon source when glucose was available (Allmann et al., 2021). Recently, it was found that some glycolytic and TCA cycle intermediates can be

used as energy sources given the right conditions (Villafray et al., 2021). All mentioned sources of energy for PF trypanosomes will be discussed in detail in the following section.

### **1.3.1.2. Proline metabolism in glucose-depleted conditions**

In the next few sections, more attention will be given to proline metabolism in PF trypanosomes when glucose is not available to the parasite due to different reasons - cell mutants used, inhibition of relevant pathways or growing cells in glucose-depleted media (SDM-80).

#### **1.3.1.2.1. From proline to glutamate**

When proline enters the cell through plasma membrane probably via transporters of the AAT7-B family (Haindrich et al., 2021) then it reaches the mt matrix, where it is oxidized to glutamate like in other organisms (Coustou et al., 2008), (Van Weelden et al., 2005), see **Fig.2**. The reaction is achieved by oxidation of proline to  $\Delta$ -pyrroline-5-carboxylate (P5C) by the membrane associated flavoenzyme proline dehydrogenase (PRODH) (**Fig.2, step 1**), (Mantilla et al., 2017), (Lamour et al., 2005) followed by P5C non-enzymatic hydrolyzation to glutamic semialdehyde ( $\gamma$ SAG), **Fig.2, step 2**.  $\gamma$ SAG is in turn oxidized to glutamate by mt NAD-dependent P5C dehydrogenase (P5CDH) with the concomitant reduction of  $\text{NAD}^+$  to NADH (Mantilla et al., 2017), **Fig.2, step 3**. Electrons feed ETC either directly by the proline dehydrogenase which transfers them to ubiquinone (Moxley et al., 2011) or indirectly via NADH produced by P5C dehydrogenase. The produced NADH is further oxidized to  $\text{NAD}^+$  by complex I or type 2 alternative NADH dehydrogenase (NDH2) (Bringaud et al., 2012).

#### **1.3.1.2.2. From glutamate to $\alpha$ -ketoglutarate**

Next, glutamate is converted to  $\alpha$ -ketoglutarate ( $\alpha$ -KG) (**Fig.2**) in two ways – by alanine aminotransferase (formerly called transaminase), ALT, **Fig.2, step 4**, or mt glutamate dehydrogenase (GDH, **Fig.2, step 5**). The first, and probably the most contributing reaction is the conversion by ALT which catalyzes the transamination of glutamate to pyruvate with concomitant production of  $\alpha$ -KG and alanine, and excreting alanine (Evanst & Brown, 1972). ALT has been shown to be essential in PF when they are grown in glucose-depleted conditions with proline being the main carbon source (Spitznagel et al., 2009). Although it seems that ALT in both PF and BF cells is cytosolically localized, recent analysis of TrypTag data focusing on mtly localized proteins has also placed this enzyme into the mitochondrial matrix (Pyrih et al., 2023). The second possible reaction is oxidative deamination of glutamate to  $\alpha$ -KG by GDH and it is considered to be

negligible although it may be involved in the reverse reaction to the synthesis of glutamate, which is likely the case when  $\alpha$ -KG is utilized as an energy source (Bringaud et al., 2012), (Villafranz et al., 2021).

### 1.3.1.2.3. From $\alpha$ -ketoglutarate to pyruvate

$\alpha$ -KG is further metabolized to succinyl Co-A as part of the TCA cycle by the multi-enzyme complex, the  $\alpha$ -KG dehydrogenase ( $\alpha$ -KgdH) (**Fig 2, step 6**). In prokaryotes and eukaryotes,  $\alpha$ -KgdH is a well characterized and important enzyme that has a similar structure and even shares common subunits with the pyruvate dehydrogenase complex (PDH), which is responsible for converting pyruvate into the acetyl-CoA (Perham, 2000). PDH and  $\alpha$ -KgdH are composed of three subunits: E1 (p for PDH or k for  $\alpha$ -KgdH), E2 (p or k) and E3. The E3, also known as lipoamide dehydrogenase (LipDH) subunit and it is a common subunit for both PDH and  $\alpha$ -KgdH and also for branched-chain dehydrogenase complexes (BCDHC) and the glycine cleavage complex (GCC) (Rex Sheu & Blass, 1999).

In *T. brucei*, all 3 subunits of  $\alpha$ -KgdH are transcribed in both life stages.  $\alpha$ -KgdH in PF cells shown to be highly active (Durieux I et al., 1991), but the essentiality of the enzyme is doubtful. Downregulation of E3 subunit in PF indicates that  $\alpha$ -KgdH is essential, because the observed growth phenotype could not be rescued by the addition of thymidine suggesting that the growth arrest is not caused by dysfunctional GCC (Roldán et al., 2011). In addition, knock-out of KgdH E2 in glucose-depleted media also shows severe growth defect (Villafranz et al., 2021).while downregulation of KgdH E1 subunit in the presence of glucose didn't produce any growth phenotype (Bochud-Allemann & Schneider, 2002).

In the next step, the production of succinate from succinyl-CoA is coupled to SUBPHOS ATP production, and the succinate is mostly excreted (Bringaud et al., 2012) , **Fig 2, step 7**. This particular step and the SCoAS enzyme performing the reaction will be discussed later in more detail. Part of the succinate can be converted to malate through TCA cycle reactions (**Fig 2, steps 8 and 9**). These reactions are essential for PF trypanosomes grown in glucose-depleted conditions (Coustou et al., 2008).

Finally, malate is converted to pyruvate, which is a substrate necessary for the ALT previously discussed (**Fig.2, step 4**). In glucose-depleted conditions pyruvate can be produced from malate in three possible ways: (i) in the mitochondrion by mt malic enzyme (MEM, **Fig.2, step 15**), (ii) in the cytosol by the cytosolic malic enzyme (MEc, **Fig.2, step 16**), (iii) in a three-step pathway which includes the glycosomal malate dehydrogenase (**Fig.2, step 17**), the glycosomal phosphoenolpyruvate carboxykinase (PEPCK, **Fig.2, step 18**), and the cytosolic pyruvate kinase (PYK, **Fig.2, step 20**). The final **step 20** can be performed also by the glycosomal pyruvate phosphate dikinase (PPDK, **Fig.2, step 19**) in a forward way. It can be also performed in a reversible manner for gluconeogenesis (Allmann et al., 2013). Interestingly, the

conversion of malate to pyruvate by the MEm and MEc (**Fig.3, step 15 and 16**) is essential and represents the bridge between succinate and acetate branches (Coustou et al., 2008).

#### 1.3.1.2.4. From pyruvate to acetate

Minor amounts of proline – derived pyruvate enters mitochondrion via mt pyruvate carrier 1 and 2 (MPC1/2) (Štáfková et al., 2016) where it is converted to acetyl-CoA by the mt pyruvate dehydrogenase complex (PDH, **Fig.2, step 21**) and then to acetate (Coustou et al., 2008), (Bringaud et al., 2012). PF cells with RNAi-depleted E1 subunit of PDH are viable however with reduced growth rate (Bochud-Allemann & Schneider, 2002). Acetyl-CoA is considered not to be further metabolized in the TCA cycle, but rather converted into acetate by two redundant reactions catalyzed by acetate:succinate CoA transferase (ASCT) and acetyl-CoA thioesterase (also called acetyl-CoA hydrolase, ACH) (Mochizuki et al., 2020).

The first reaction is achieved by ASCT, **Fig.2, step 23**, which transfers the CoA group of acetyl-CoA to succinate to produce acetate and succinyl-CoA (Rivière et al., 2004). The produced succinyl-CoA is immediately converted to succinate with the concomitant production of SUBPHOS ATP by succinyl-CoA synthetase (SCoAS, **Fig.2, step 7**) (Millerioux et al., 2012). ASCT was shown to be highly specific for acetyl-CoA (Mochizuki et al., 2020). Note that this reaction is the same as the SUBPHOS described in the previous section. The conversion of acetyl-CoA to acetate is coupled with ATP formation using this so called ASCT/SCoAS cycle (Van Hellemond et al., 1998). Interestingly, this rare biological event is only seen in the mitochondria of trypanosomatids, as well as in helminths and hydrogenosomes of some anaerobic organisms, such as trichomonads and some fungi (Tielens et al., 2010), (Van Hellemond et al., 1998). The fact that mitochondrion of *T. brucei* and hydrogenosomes share the ASCT/SCoAS cycle supports the common origin of both organelles.

When it was determined that the acetate levels were not significantly changed in ASCT null PF cells, it was proposed that there could be a redundant enzyme that also produce acetate (Rivière et al., 2004). Indeed, this enzyme was later identified as ACH, **Fig.2, step 22** (Millerioux et al., 2012). ACH solely removes CoA-SH group from acetyl-CoA and the concomitant production of acetate is not coupled with ATP synthesis. NMR analyses of PF parasites shows that acetate constitutes only 3.2% of the excreted end products from proline metabolism (Coustou et al., 2008), whereas the acetate excreted from glucose metabolism is up to 82% (Mazet et al., 2013), pointing that the flux through the acetate branch of proline is low. The low flux could be explained by the fact that in glucose-poor conditions threonine serves as a main amino acid carbon source for acetate production leading to fatty acid biosynthesis (Lamour et al., 2005). Threonine metabolism will be discussed later.



### 1.3.1.3. Proline metabolism in PF in glucose – rich conditions

When PF *T. brucei* are grown in SDM-79 medium containing 6mM glucose, it represents the conditions the parasites meet only during short period of time after tsetse fly blood meal. Interestingly, when glucose is abundant it seems to regulate proline metabolism in procyclic trypanosomes affecting the rate of proline consumption and determining which metabolic pathway is active (**Fig.3**).

When both glucose and proline are present in the medium, PF cells preferentially consume glucose (Lamour et al., 2005), (Bringaud et al., 2006) and the rate of proline consumption increases substantially when glucose concentration is below 200  $\mu$ M (C. E. Ebikeme et al., 2008).

In glucose – rich medium it seems that the conversion of proline-derived succinate to alanine (**Fig.3, step 4**) is impaired since NMR analysis of the excreted end products show accumulation of proline -derived glutamate and succinate (**Fig.3, steps 3 and 7, white characters on a blue background**), however barely detectable amounts of proline-derived alanine (**produced at step 4**) (Coustou et al., 2008). It seems that the proline – derived succinate does not need to be metabolized further since RNAi-mediated complex II knockdown cell line shows no growth defects when glucose is available (Coustou et al., 2008). More significant amount of glucose-derived alanine is detected (**Fig.3, step 4, white characters on a red background**) since the pyruvate required by ALT in **step 4** was shown to be a product of glucose catabolism. In addition, the metabolomic analysis identified fumarate and malate derived from glucose metabolism (Coustou et al., 2006), but not from proline (Coustou et al., 2008). It all shows that the presence of glucose regulates not only the rate of proline consumption but also which pathways are active, pointing once more to the plasticity of the *T. brucei*.

### 1.3.1.4. Glucose metabolism in PF

When available, glucose is the preferred energy source for PF parasites. Classically, it is accepted that PF trypanosomes are catabolizing glucose into partially oxidized end products – succinate and acetate, and small amounts of lactate, pyruvate and alanine (Bringaud et al., 2006) (**Fig.3**). NMR analysis shows that the amounts of the glucose-derived excreted products when glucose is the only carbon source is as follows: succinate up to 63% of the all the detected end products (Coustou et al., 2008), acetate up to 82% (Mazet et al., 2013), lactate up to 7% (Coustou et al., 2008), pyruvate up to 4% (Štáfková et al., 2016) and alanine up to 1% (Coustou et al., 2008). Since glycolysis in trypanosomes occurs in the presence of oxygen and at the same time the TCA cycle is not completely utilized, the process is known as aerobic oxidation/fermentation of glucose. Aerobic fermentation is a result of lack of Pasteur effect (glucose

consumption is inhibited when oxygen is present) (Bringaud et al., 2006). Most of the glycolytic steps occur in the peroxisome-derived organelle, glycosomes (hence the name) (Opperdoes & Borst, 1977).

Glucose metabolism in PF cells is well described in (Bringaud et al., 2012). When glucose enters the glycosomes it is mainly converted to 1,3-bisphosphoglycerate (1,3BPGA) by conventional glycolytic enzymes (**Fig.3, steps 31-36**). Next, 1,3BPGA is excreted into the cytosol where it is converted to phosphoenolpyruvate (PEP), (**Fig.3, steps 38-40**). PEP is a branching point, and it can be transported back to the glycosomes to feed the glycosomal succinate branch or it can be converted to pyruvate (**Fig.3, step 20**) to feed the succinate and acetate branches in the mitochondrion. The conversion of PEP to glycosomal succinate involves conversion to oxaloacetate (**Fig.3, step 18**) and then to malate (**Fig.3, step 17**). Malate is then converted to fumarate (**Fig.3, step 44**) by cytosolic fumarase in the cytosol and fumarate re-enters glycosomes to be converted to excreted succinate (**Fig.3, step 45**). The cytosolic malate can enter additionally the mitochondrion and be converted to fumarate and then to excreted mt succinate (**Fig.3, step 9 and 14**).

PEP is converted to pyruvate either by PYK (**Fig.3, step 20**) in the cytosol or by PPK in the glycosomes (**Fig.3, step 19**). The produced pyruvate was found not to be excreted at all (or as a minor product depending on the strain) from PF cells, but rather utilized further (Rivière et al., 2004), (Mazet et al., 2013), (Coustou et al., 2008), (Štáfková et al., 2016). When the pyruvate enters the mitochondrion, it is converted to acetyl-CoA and then primarily to acetate (**Fig.3, steps 21-23**, which were already discussed).

#### 1.3.1.4.1. NAD<sup>+</sup>/NADH balance in glycosomes

Since the glycosomal membrane is not permeable for large molecules, the balance between NAD<sup>+</sup> and NADH is strictly kept (Bringaud et al., 2012). In PF cells under glucose-rich conditions, NADH is produced in the reaction catalyzed by glyceraldehyde-3-phosphate dehydrogenase (**Fig.3, step 36**) and it is re-oxidized by glycosomal malate dehydrogenase (MDH, **Fig.3, step 17**) and fumarate reductase, thereby balanced (FRDg, **Fig.3, step 45**) (Besteiro et al., 2002), (C. Ebikeme et al., 2010). This is the so-called succinate branch. Note that in PF cells, all three isoforms of the MDH are expressed and active in the relevant compartment – glycosomes, cytosol and mitochondrion (Aranda et al., 2006), although cytosolic isoform is not presented on the **Fig. 2 and 3**. In *T. brucei* redox balance can be maintained in a different way through the glycerol-3-phosphate (Gly-3-P)/dihydroxyacetone-phosphate (DHAP) shuttle (**Fig.3, steps 41 and 42**) (Guerra et al., 2006). However, in PF in contrast to BF parasites, this pathway is negligible (C. Ebikeme et al., 2010). This Gly-3-P/DHAP shuttle consists of three parts: (i) glycosomal NADH-dependent glycerol-3-phosphate dehydrogenase (**Fig.3, step 41**), which converts DHAP to Gly-3-P, (ii)

putative glycosomal exchanger/transporter, which exchanges Gly-3-P for DHAP between the glycosomes and cytosol, (iii) mt FAD-dependent glycerol-3-phosphate dehydrogenase (Gly3PDH) (**Fig.3, step 42**), which regenerates DHAP from Gly-3-P by transferring electrons ultimately to oxygen via the mt respiratory chain (**Fig.3, steps 27-29**).

PF trypanosomes excrete glucose-derived lactate as a minor end product. Most probably the lactate is a result of diverting cytosolic DHAP as glycolytic product leading to production of the toxic methylglyoxal and further detoxification to lactate (**Fig.3, steps 46-48**). It involves NADPH-dependent methylglyoxal reductase and NAD<sup>+</sup>-dependent L-lactaldehyde dehydrogenase (**Fig.3, steps 47 and 48**). Interestingly, this system in *T. brucei* includes most probably only glyoxalase II instead of glyoxalase I and II and produces L-lactate instead of D-lactate (Greig et al., 2009).

#### **1.3.1.4.2. ADP/ATP balance in glycosomes**

Similarly to NADH, ADP/ATP balance is also maintained in the glycosomes. The glycosome compartmentalization of glycolysis ensures the balance and it is seen as a way to protect the cell from otherwise unregulated ATP consuming enzymes – hexokinase (HK) (**Fig.3, step 31**) and phosphofructokinase (**Fig.3, step 33**) (Michels et al., 2021). The main, however not the only kinase regenerating glycosomal ATP in the PF parasites is the PEPCK (**Fig.3, step 18**). It seems very plausible that ATP is regenerated also by glycosomal PPDK (**Fig.3, step 19**) especially when PEPCK is absent (C. Ebikeme et al., 2010). In addition, *T. brucei* expresses several isoforms of adenylate kinases, an enzymes responsible for interconversion of adenosine phosphates (ATP, ADP and AMP), localized in the cytosol, mitochondrion and glycosomes of both life stages of the parasite (Opperdoes FR, 1981), (Ginger et al., 2005). They are believed to contribute to ADP/ATP homeostasis in those compartments.

#### **1.3.1.4.3. Cellular ATP production pathways**

ATP in PF cells was at first considered to be produced mainly by OXPHOS and the F<sub>0</sub>F<sub>1</sub>-ATP synthase (also known as complex V, CV) in glucose-rich conditions (Williams, 1994). However, later it was shown that when glucose is available, CV function is dispensable and ATP production by SUBPHOS is essential (Coustou et al., 2008), (Coustou et al., 2003), (Bochud-Allemann & Schneider, 2002). SUBPHOS ATP is produced in **Fig.3, steps 7, 18, 19, 20 and 38**. Since PEPCK (**step 18**) and PPDK (**step 19**) maintain the glycosomal ADP/ATP balance their ATP net contribution is 0. Therefore, in PF parasites in glucose-rich

conditions the ATP is produced mainly by phosphoglycerate kinase (**step 38**), PYK (**step 20**) and SCoAS (**step 7**). Note that SCoAS is involved in both TCA and ASCT/SCoAS cycles.

However, when grown in glucose-depleted medium the ATP produced by OXPHOS becomes essential (**Fig.2**) (Coustou et al., 2008), (Dewar et al., 2022). When PF cells are grown *in vitro* without glucose and lose partially or completely OXPHOS ATP production, they either stop proliferating or die in a few days, respectively (Hierro-Yap et al., 2021). Intriguing however, the partial loss of OXPHOS ATP production does not prevent the PF cells from colonizing and establishing infection in the tsetse midgut pointing out at the possibility of higher capacity of SUBPHOS ATP production *in vivo* probably due to better availability of various substrates. However, fully functioning OXPHOS is necessary for further migration and colonization of subsequent fly organs (Dewar et al., 2022).

### **1.3.1.5. Threonine metabolism**

Another amino acid that was found to be utilized in high quantities by PF trypanosomes is threonine. In standard glucose-rich SDM-79 medium it was shown that threonine is the most rapidly consumed amino acid, however alone it could not sustain cell growth. In glucose-depleted conditions threonine was even the most highly consumed carbon source (Lamour et al., 2005). It was suggested already in the 70's that threonine catabolism leads to the production of equal amounts of glycine and acetate (G. A. Cross et al., 1975), (Linstead & Cross, 1977). When threonine enters the mitochondrion, it is converted to amino oxobutyrate (AOB) with NADH production (**Fig. 2 and 3, step 49**). Next, AOB is converted to acetyl-CoA with glycine release (**Fig. 2 and 3, step 50**). Then acetyl Co-A is converted to acetate (**Fig. 2 and 3, step 22 and 23**). Step 23 is accompanied by the concomitant SUBPHOS ATP production during ASCT/SCoAS cycle already discussed. Acetate serves as a precursor for lipid biosynthesis, which will be discussed in detail later. Threonine seems to be the main source of acetate for lipid biosynthesis in PF trypanosomes, contributing approximately 2.5-fold more than glucose-derived acetate when equimolar amounts of glucose and threonine are present in the medium (Millerioux et al., 2013). The potential source of threonine for PF cells could be the tsetse fly midgut or haemolymph, however no data is available. Another possibility is that the tsetse resident symbionts, *Wigglesworthia glossinidia* and/or *Sodalis glossinidius*, could possibly supply precursors for *de novo* threonine biosynthesis (Ong et al., 2015).

#### **1.3.1.5.1.1. The fate of acetate**

The fate of acetate in *T. brucei* except being mostly excreted from the cells through aquaglyceroporins (Uzcátegui et al., 2018) is to be utilized for *de novo* lipid biosynthesis (Loïc et al., n.d.), (Millerioux et al.,

2013). Eukaryotes typically use citrate/malate shuttle to export acetyl-CoA from mitochondria to the cytosol and it serves as a lipid precursor. Surprisingly, in trypanosomes this shuttle is not used, but instead the acetate produced from acetyl-CoA in the mitochondrion is excreted to the cytosol probably by passive diffusion where it is converted back to acetyl-CoA by cytosolic acetyl-CoA synthetase (AceCS), an ATP-consuming reaction (**Fig.2 and 3, step 51**) (Loïc et al., n.d.). AceCS plays an essential role for *de novo* lipid biosynthesis in PF cells since RNAi silencing of the enzyme is lethal for the parasites (Loïc et al., n.d.).

### 1.3.1.6. Glycerol as a carbon source

Glycerol was found to be utilized by PF parasites for gluconeogenesis to produce hexose phosphates, including glucose 6-phosphate, a precursor for essential metabolic pathways (Wagnies et al., 2018) (only indicated in **Fig.2** and more details shown on **Fig.3**). In glucose-free medium, where the proline contribution to gluconeogenesis was blocked by PEPCK/PPDK null double mutant, metabolism of glycerol was shown to be essential to generate hexose phosphates (Wagnies et al., 2018).

When glycerol enters the cell through aquaglyceroporins (Uzcategui et al., 2004), (Jeacock et al., 2017) and further reaches glycosomes, it gets phosphorylated to glycerol 3-phosphate (Gly-3-P) by glycerol kinase (GK) (**Fig.3 step 43**) and thus it cannot escape the glycosomes by active transport. Surprisingly, when both glucose and glycerol are available for PF trypanosomes, the preferred carbon source is glycerol (Allmann et al., 2021). The activity of GK is almost 80-fold higher than HK, the enzyme activating the glucose, and almost completely represses the activity of the latter enzyme (**Fig.3, steps 31 and 43**) (Allmann et al., 2021). Gly-3-P can be further converted to DHAP (**Fig.3, step 41**) and then used for gluconeogenesis. Alternatively, DHAP can also be converted to glyceraldehyde-3-phosphate (G-3-P) (**Fig.3, step 35**) and thus substitute the last steps of glycolysis (Allmann et al., 2021) (see **Fig.3**, downstream from **step 36**).

Glycerol uptake may be important for the parasite between blood meals of the fly when glucose is limited and/or immediately after flight when the proline levels are low (Bursell, 1963). Since mainly amino acids are studied in tsetse fly midgut and other organs, more comprehensive analysis is needed to determine the presence of glycerol and other relevant metabolites. Free glycerol was found in other insects such as in the plasma of pupae of the silk moth, *Hyalophora cecropia* (Wyatt & Meyer, n.d.) as well as the flesh fly *Sarcophaga crassipalpis* where they are proposed to serve as anti-desiccants and cryoprotectants (Clark & Worland, 2008).

### 1.3.1.7. Lipids as energy and carbon source

Fatty acids are important for the parasite not only as a membrane component, but also as building blocks for more complex lipids. Importantly, fatty acids comprise the membrane-attached fraction for the GPI-anchors of essential for the parasite survival surface proteins. For PF parasite those proteins are the procyclins and for the BF parasite are the VSGs. It is already well known that *T. brucei* on one hand can synthesize fatty acids *de novo*, but on the other hand it also can readily acquire them from its environment (for a comprehensive review see (Poudyal & Paul, 2022), (de Aquino et al., 2021), (Smith & Bütikofer, 2010) probably because the process of synthesis is energetically-demanding. For *de novo* lipid biosynthesis in *T. brucei* the important precursor is the cytosolic acetyl-CoA which is produced from the mt acetate (**Fig. 2 and 3, step 51**). It was shown that for PF cells glucose-derived, threonine-derived and external acetate molecules serve as substrates for *de novo* lipid biosynthesis - for fatty acids as well as for sterols (Millerioux et al., 2018), (Loi'c et al., n.d.), (Millerioux et al., 2013). Interestingly, leucine was shown to be utilized by PF cells for *de novo* sterol, but not fatty acid synthesis and proline did not participate in the lipid formation at all even in glucose/acetate/threonine-free medium (Millerioux et al., 2018).

*T. brucei* can take up free fatty acids, lysophospholipids, protein-bound lipids and lipids from lipoprotein particles. For PF trypanosomes it was shown that they can utilize external oleate and store it in the form of triacylglycerol in lipid droplets (Allmann et al., 2014) . The source of fatty acids could be the gut and/or the haemolymph. In general, the gut and haemolymph of the insects contain both free and protein/lipoprotein particles- bound fatty acids, however not sufficient data is available for the tsetse fly in particular.

The question arises whether fatty acids in *T. brucei* can be used as a carbon and energy source for oxidative metabolism? For PF parasites, it seems more plausible that they utilize fatty acids for biosynthetic purposes and do not use them as energy sources (Allmann et al., 2014).

Sterols are important for *T. brucei* as a membrane component defining its fluidity. PF cells were shown to acquire sterols from the environment via lipoprotein-cholesterol endocytosis and also, they can synthesize them *de novo* (de Aquino et al., 2021). Interestingly, leucine was found to be the main source for sterol biosynthesis using the mevalonate pathway (**Fig. 2 and 3**) (Millerioux et al., 2018).

### 1.3.1.8. Alternative energy sources

A recent study shows that besides the classical energy sources described so far such as glucose, proline, threonine, glycerol, *T. brucei* can utilize also glycolytic or TCA cycle metabolic intermediates (Villafranz et

al., 2021). The study reports that in the presence of proline, excreted end-products from glucose metabolism, such as succinate, pyruvate and to some extent alanine are re-utilized and converted to acetate by the PF cells once the glucose is consumed.

Interestingly, TCA cycle intermediates succinate, malate and  $\alpha$ -KG are shown to be as well consumed and metabolized in PF parasites when the cells are grown in physiological relevant conditions – in the presence of 2mM proline and absence of glucose. In those conditions, the TCA intermediates can even stimulate the cell growth when added individually in a 1-10mM range.  $\alpha$ -KG is of a particular interest since in contrasts to succinate or malate, when added in 10 mM concentration it managed even to support the growth of RBP6-induced epimastigotes but not procyclics when grown on 2mM proline in the absence of glucose. It is speculated that there is a higher demand for carbon sources during differentiation for procyclics to epimastigotes and therefore alternative sources are necessary, such as  $\alpha$ -KG. The question arises now, except being produced from proline, if such concentration of  $\alpha$ -KG can be found externally and then taken up by the parasite. The best scenario is to be present in the tsetse midgut/ haemolymph. However, no data is available since most studies have been focused on the tsetse fly amino acid content only. In addition, the tsetse resident symbiont, *Sodalis glossinidius*, could possibly uptake and oxidize various metabolites (N-acetylglucosamine and glutamine) and eventually produce end products that could be released into tsetse (Hall et al., 2019). Interestingly, Villafranz and colleagues also showed high excretion of  $\alpha$ -KG-derived 2-hydroxyglutarate. This is probably a one-step NADH-consuming reaction, and it is speculated to be involved in the maintenance of the mt redox balance necessary for  $\alpha$ -KG metabolism.

### 1.3.1.9. Electron transport chain (ETC) and complex V (CV)

The genome of *T. brucei* encodes the canonical ETC complexes – I, II, III and IV as well as the canonical F<sub>o</sub>F<sub>1</sub>-ATP synthase (CV) (Zíková, 2022). However, in addition to complex I, the parasite encodes the type II alternative dehydrogenase (NDH2) (Fang & Beattie, 2003) and in addition to complex IV it encodes Trypanosoma alternative oxidase (TAO) (Chaudhuri et al., 1998). In PF cells, mt membrane potential ( $\Delta\Psi_m$ ) is generated by the proton pumping complexes III and IV which is then harnessed by CV to generate chemical energy in the form of ATP by OXPHOS (Horváth et al., 2005). For schematic diagram of OXPHOS in PF trypanosomes see **Fig.2** and **3**. *T. brucei* expresses 5 enzymes which transfer electrons to the ubiquinone pool – complex I, NDH2, mt FAD-dependent glycerol-3-phosphate dehydrogenase (Gly3PDH), complex II (Acestor et al., 2011) and proline dehydrogenase.

### 1.3.1.9.1. Complex I (CI)

The role of complex I (CI, NADH:ubiquinone oxidoreductase) classically is to transfer electrons from NADH to ubiquinone while pumping protons into the intermembrane space of the mitochondria, thus contributing to the  $\Delta\Psi_m$ . It also participates in ROS production. In *T. brucei*, CI was shown to be quite large with at least 46 subunits (Acestor et al., 2011), (**Fig. 2 and 3, step 25**). Interestingly, in PF, CI does not seem to contribute significantly to re-oxidation of NADH or to  $\Delta\Psi_m$ . This was concluded from knock-out and knock-down studies of different CI subunits (Verner et al., 2011). The questionable presence of CI in the cell can be explained by the necessity of CI in other life-stages and/or ROS production as signaling molecules during differentiation from procyclics to metacyclics (Doleželová et al., 2020).

### 1.3.1.9.2. Type 2 alternative NADH dehydrogenase (NDH2)

*T. brucei* expresses an unique alternative to CI enzyme – type II alternative NADH dehydrogenase (NDH2), **Fig.2 and 3, step 26**. It plays the same role as CI - transfers electrons from NADH to ubiquinone pool, but without the ability to pump protons (Fang & Beattie, 2002). Another peculiarity is that NDH2 is a single polypeptide, and it is insensitive to rotenone. In PF trypanosomes NDH2 is essential since it contributes to the mt  $\Delta\Psi_m$  indirectly by transferring electrons to ubiquinone and further to complexes III and IV (Verner et al., 2013). It was proposed to be important for NAD<sup>+</sup>/NADH balance however since the topology of the enzyme is still a mystery (if it is facing the mt intermembrane space or the mt matrix) it is unclear if it is the cellular or mt NAD<sup>+</sup>/NADH balance that is involved in (Verner et al., 2013).

### 1.3.1.9.3. Glycerol-3-phosphate dehydrogenase

Mt glycerol-3-phosphate dehydrogenase (Gly3PDH) is a FAD-dependent and unique *T. brucei* enzyme which connects the mitochondrion with the glycosomes through Gly-3-P/DHAP shuttle (**Fig.3, step 42**) (Opperdoes & Borst, 1977). It is important that the active site of the enzyme faces the mt intermembrane space and thus its substrates are cytosolically derived. Gly3PDH oxidizes glycerol-3-phosphate to DHAP followed by electron transfer to the ubiquinone pool. The enzyme plays an essential role in maintaining the glycosomal balance of NAD<sup>+</sup>/NADH especially in BF cells. For PF parasites however, its role appears to be negligible (C. Ebikeme et al., 2010) and even in the presence of glucose the enzyme is not essential (Škodová et al., 2013).



#### **1.3.1.9.4. Complex II (CII)**

Complex II (CII, succinate dehydrogenase) is directly involved in the TCA cycle by oxidizing succinate to fumarate with the subsequent electron transfer to ubiquinone (**Fig. 2 and 3, step 8**). For PF cells CII was shown to be active regardless of the presence of glucose in the medium, however it was essential only when proline but not glucose was the available nutrient (Coustou et al., 2008), (Doleželová et al., 2020).

#### **1.3.1.9.5. From ubiquinol to oxygen**

When electrons are transferred to ubiquinone it becomes ubiquinol (the reduced form). Next, ubiquinol can be oxidized by 2 ways: the classical cytochrome-mediated pathway which consists of CIII and CIV with the cytochrome c as mediator, and the unique terminal oxidase pathway which consists of TAO (Van Hellemond, Bakker, et al., 2005).

#### **1.3.1.9.6. Complex III (CIII) and Complex IV (CIV)**

In PF trypanosomes as in other eukaryotes, Complex III (CIII, Ubiquinol:cytochrome c oxidoreductase, **Fig.2 and 3, step 28**) mediates the electron transfer from ubiquinol to cytochrome c at the same time pumps protons into the intermembrane space. Next, complex IV (CIV, cytochrome c oxidase, COX, **Fig.2 and 3, step 29**) accepts the electrons from the reduced cytochrome c and delivers them to the molecular oxygen with the production of water with the concomitant proton pump. Both CIII and CIV in PF cells are the main producers of the mt  $\Delta\Psi_m$  (Horváth et al., 2005).

#### **1.3.1.9.7. Trypanosoma alternative oxidase (TAO)**

Trypanosoma alternative oxidase (TAO) is a unique plant-like 33 kDa enzyme positioned in the inner mt membrane and catalyzing the electron transfer from ubiquinol to molecular oxygen and thus producing water however without proton pumping (Chaudhuri et al., 1998), (Chaudhuri et al., 2006), **Fig.2 and 3, step 27**. In PF parasites TAO is expressed yet at low levels (Chaudhuri et al., 1998) and it contributes only 20% of the total respiration (Gnipová et al., 2012). However, when OXPHOS is partially inhibited, TAO expression gets compensatory upregulated (Hierro-Yap et al., 2021).

### 1.3.1.9.8. Complex V (CV)

Complex V (CV, F<sub>0</sub>F<sub>1</sub>-ATP synthase/ase) in aerobic eukaryotes is the enzyme complex that harnesses mt  $\Delta\Psi_m$  generated by electron-transport chain to produce ATP by OXPHOS, (**Fig.2** and **3, step 30**). The mt  $\Delta\Psi_m$  in the form of proton gradient across the mt inner membrane is released down its concentration gradient back to the mt matrix and the free energy is utilized by CV as a rotor to phosphorylate ADP to ATP in the mt matrix. CV can also work in reverse, hydrolyzing ATP to generate mt  $\Delta\Psi_m$  usually under physiologically challenging conditions, known as F<sub>0</sub>F<sub>1</sub>-ATPase. CV in general consists of 2 domains – the membrane integrated F<sub>0</sub> part (comprising the proton-driven rotor and peripheral stalk) and the hydrophilic F<sub>1</sub> part (comprising catalytic subunits and the central stalk) (Kühlbrandt, 2019). The complex works in dimers which form long rows in lamellar cristae helping cristae biogenesis as well as energy effectiveness (Davies et al., n.d.), (Kühlbrandt, 2019).

In PF CV also functions as a dimer and plays the role to produce ATP harnessing the  $\Delta\Psi_m$  (Van Hellemond, Opperdoes, et al., 2005), (Zíková et al., 2009). CV seems to be essential for PF cells when proline is the energy source (Zíková et al., 2009) and rerouting electrons to TAO cannot compensate for the CV silencing because of the reduced cellular ATP levels (Hierro-Yap et al., 2021). Complete loss of CV prevents PF cells from fully colonizing the midgut of the tsetse vector (Dewar et al., 2022).

### 1.3.2. Bioenergetics in bloodstream form of *T. brucei*

While there are peculiar attributes of PF metabolism, the infective BF of *T. brucei* also contains some very unusual bioenergetic pathways (Michels et al., 2021), (**Fig.4**). It has been believed for a long time that BF trypanosomes depend entirely on glucose for their energy production, as this sugar is highly abundant in the mammalian blood. It is considered that the parasite can produce sufficient ATP for all cellular needs by the glycolytic pathway. Glucose is catabolized to pyruvate which instead of feeding TCA cycle it is mainly excreted from the cell. Another peculiarity of BF bioenergetics is that the BF mitochondrion lacks a cytochrome-mediated respiratory chain and thus it lacks the proton pumping activities of complexes III and IV. Therefore, the  $\Delta\Psi_m$  is maintained by the reverse activity of CV, which translocates H<sup>+</sup> into the intermembrane space at the expense of ATP (Nolan & Voorheis, 1992), (Schnauffer et al., 2005). Mt ATP supply is essential for BF parasites to maintain the  $\Delta\Psi_m$  and thus the mitochondrion itself.  $\Delta\Psi_m$  is necessary for many vital processes such as mt protein import and the operation of some mt membrane transporters. The classical view is that the ATP is produced during glycolysis in the cytosol and transported into the mt matrix via the AAC, while ADP is transported out. However, more recent data suggest that

mitochondrion of the BF parasite is more complex than originally thought and ATP could be possibly produced *in organello* in this infective stage using SUBPHOS pathway(s). The first possible SUBPHOS I pathway includes the degradation of threonine and glucose/glycerol-derived pyruvate and the second possible SUBPHOS II pathway includes the degradation of  $\alpha$ -KG alone or  $\alpha$ -KG derived from glutamine (see Fig.4, light blue circles).

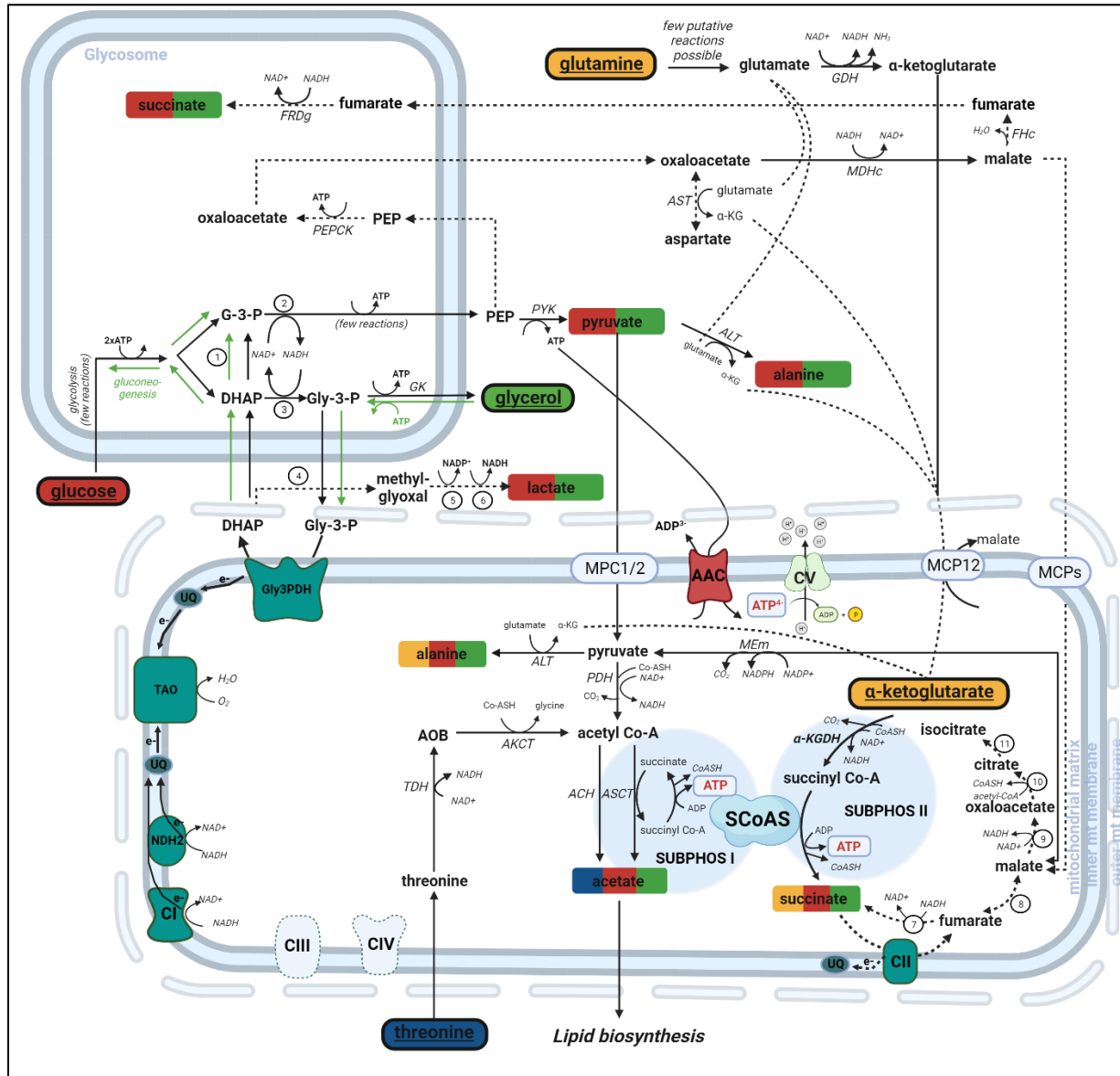


**Fig.4.** Schematic representation of carbon source metabolism in the bloodstream form of *T. brucei*. Solid lines represent the reactions which are more plausible to occur supported with experimental data. Dashed lines represent the less plausible reactions mostly based on proteomic data. Carbon sources are glucose, glycerol, threonine and glutamine/ $\alpha$ -ketoglutarate, and they are underlined and marked in red, green, blue and yellow, respectively. Glucose-derived metabolites are in red background, glycerol-

derived metabolites are in green background, threonine-derived metabolites are in blue background, glutamine/  $\alpha$ -ketoglutarate metabolites are in yellow background. The glycosomal and mt compartments are indicated. SUBPHOS I and SUBPHOS II are marked in light blue circles. Abbreviations:  $\alpha$ -KG, alpha-ketoglutarate;  $\alpha$ -KGDH, alpha-ketoglutarate dehydrogenase; AAC, ADP/ATP carrier; ACH, acetyl-CoA thioesterase; AKCT, 2-amino-3-ketobutyrate coenzyme A ligase; ALT, alanine aminotransferase; ASCT, acetate:succinate CoA-transferase; AST, aspartate aminotransferase; CI, complex I (NADH:ubiquinone oxidoreductase); CII, complex II (succinate dehydrogenase); CIII, complex III (ubiquinone:cytochrome c oxidoreductase); CIV, complex IV (cytochrome c oxidase); CV, complex V (FoF1 ATPase); DHAP, dihydroxyacetone phosphate; FHc, cytosolic fumarate hydratase (i.e., fumarase); FRDg, glycosomal NADH-dependent fumarate reductase; G-3-P, glyceraldehyde 3-phosphate; GDH, glutamate dehydrogenase; GK, glycerol kinase; Gly-3-P, glycerol 3-phosphate; Gly3PDH, mt FAD-dependent glycerol-3-phosphate dehydrogenase; MCPs, mt carrier proteins; MCP12, mt carrier protein 12; MDHc, cytosolic isoform of malate dehydrogenase; MDHm, mt isoform of malate dehydrogenase; MEm, mt malic enzyme; MPC1/2, mt pyruvate carrier 1 and 2; NDH2, type II alternative dehydrogenase; PDH, pyruvate dehydrogenase; PEP, phosphoenolpyruvate; PEPCK, phosphoenolpyruvate carboxykinase; PYK, pyruvate kinase; SCoAS, succinyl-CoA synthetase; TAO, trypanosome alternative oxidase; TDH, threonine dehydrogenase; UQ, ubiquinone; Enzymes indicated by numbers: 1, triose-phosphate isomerase; 2, glyceraldehyde-3-phosphate dehydrogenase, 3, glycosomal NADH-dependent glycerol-3-phosphate dehydrogenase; 4, nonenzymatic reaction; 5, NADPH-dependent methylglyoxal reductase; 6, NAD<sup>+</sup>-dependent lactaldehyde dehydrogenase; 7, mt NADH-dependent fumarate reductase (FRDm); 8, mt fumarase (fumarate hydratase, FHm); 9, mt malate dehydrogenase (MDHm); 10, citrate synthase; 11, aconitase. Created with BioRender.com.

### 1.3.2.1. Energy sources

The *T. brucei* parasites reside in the mammalian bloodstream, but they have also been reported to infect tissues of the skin, adipose tissue, gonads, and others (Pereira et al., 2019). However, in the following text I will mainly describe the long slender bloodstream form parasite (BF) that can be easily cultured *in vitro*. For this parasite, glucose is the main source of energy, although other energy sources such as glycerol, threonine, glutamine and  $\alpha$ -ketoglutarate are also discussed.

### 1.3.2.2. Glucose metabolism

#### 1.3.2.2.1. From glucose to pyruvate

BF of *T. brucei* is the infective form of the parasite and resides predominantly in the mammalian blood. Mammalian blood is rich in glucose (~5mM (J H Smith & Taylor, 1908)) and oxygen (95-99% oxygen saturation levels, (Smith et al., 2017)), which determines glucose as the main source of energy for BF trypanosomes during aerobic glycolysis (J. F. Ryley, 1955), (Michels et al., 2021). Aerobic glycolysis is a well-known phenomenon characteristic for cancer cells (so called Warburg effect) (Vaupel & Multhoff,

2021) as well as it is activated in mammalian effector T cells during infection (Frauwirth et al., 2002). Glucose in these T cells is catabolized to pyruvate (and then to ethanol or lactate to restore  $\text{NAD}^+$  levels) without further degradation in the TCA cycle and OXPHOS, with the net production of 2 ATP molecules from 1 glucose molecule. Despite being energetically inefficient compared to OXPHOS, the glycolytic rate is very high, and it allows the cells to meet their higher metabolic demand to divide fast. BF cells, like cancer and effector T cells, metabolize glucose mainly to pyruvate during glycolysis (**Fig.4, marked in red**). Similarly, due to high glycolytic rates the ATP produced in the cytosol seems to be sufficient for the cell to fill the needs for rapid division (~7 hours doubling time) compared to PF cells (~12 hours doubling time). Glycolysis in BF cells (excellently reviewed in (Michels et al., 2021)) takes place in the glycosomes, where glucose is oxidized to 3-phosphoglycerate, which is then exported to the cytosol where it is further catabolized to PEP and then to pyruvate in the same reactions described for PF cells. Instead of feeding the TCA cycle, pyruvate is mainly excreted from the cell (~85% of all excreted end products, (Mazet et al., 2013)). The high rate of glucose consumption together with high levels of pyruvate excretion led to the presumption that in BF parasites the glycolytic pathway alone is sufficient to produce ATP for all cellular needs.

All 7 classical glycolytic enzymes, catabolizing glucose to 3-phosphoglycerate, were found to be localized in the glycosomes (Opperdoes & Borst, 1977) – HK, glucose-6-phosphate isomerase, phosphofructokinase, aldolase, triose-phosphate isomerase, glyceraldehyde-3-phosphate dehydrogenase, glycosomal phosphoglycerate kinase (see also **Fig.3** for details, in **Fig.4** glycolysis is not shown in detail). Note that in contrast to PF cells where phosphoglycerate kinase is cytosolic, in BF cells it is localized in the glycosomes. The last 3 enzymes of glycolysis, namely phosphoglycerate mutase, enolase and PYK, are localized in the cytosol.

$\text{NADH}$ , formed during glycolysis by glyceraldehyde-3-phosphate dehydrogenase (**Fig.4, step 2**) is re-oxidized to  $\text{NAD}^+$  under aerobic conditions in the mitochondrion by the previously described Gly-3-P/DHAP shuttle. Part of DHAP is converted to Gly-3-P via glycosomal Gly3PDH (**Fig.4, step 3**) and thus regenerates  $\text{NAD}^+$ . Gly-3-P then is converted back to DHAP via mt Gly3PDH with an electron transfer to ubiquinone. In BF cells, in contrast to PF, the electron transfer from ubiquinol is not coupled to OXPHOS, but it is rather rerouted to TAO. TAO is the only mt terminal oxidase utilized by BF parasites and determines the need for oxygen during glycolysis. When oxygen is limited and the activity of TAO is inhibited, Gly-3-P is converted to glycerol in the glycosomes (J. F. Ryley, 1955). This leads to formation of equimolar amounts of pyruvate and glycerol from glucose. This conversion of Gly-3-P to glycerol is achieved by GK with the concomitant production of ATP and the reaction is reversible by nature. When glycerol is produced under these oxygen-limiting conditions it is then excreted from the cell. Although direction of the reaction

(glycerol production instead of consumption) is thermodynamically unfavorable, it happens at low ATP/ADP ratio which is provided by the glycosomal compartmentalization separating glycosomal adenine nucleotides from those in the cytosol (Hammond et al., 1985). As in PF cells, in BF maintaining the glycosomal ATP/ADP and NAD<sup>+</sup>/NADH balance is essential. The conversion of Gly-3-P to glycerol under anaerobic conditions assures this balance.

When oxygen is available to the cell, 1 glucose molecule consumed leads to the production of 2 ATP molecules in the cytosol. For 1 glucose molecule degraded, HK and phosphofructokinase consume 1 ATP molecule/reaction each (2 in total) and 2 ATP molecules are produced by glycosomal phosphoglycerate kinase to keep the glycosomal balance. The total net production of 2 ATP molecules per glucose under aerobic conditions occurs in the cytosol via PYK. However, when oxygen is not available for the cell (anaerobiosis), per 1 glucose molecule degraded, HK and phosphofructokinase also consume 1 ATP molecule/reaction each (2 in total), but 1 ATP molecule is formed by phosphoglycerate kinase and another ATP molecule by GK to balance glycosomal ATP production. Therefore, the net ATP production formed by pyruvate kinase under anaerobiosis is only 1 ATP per glucose. The decreased ATP levels under anaerobiosis lead ultimately to cell death (Helfert et al., 2001).

#### **1.3.2.2.2. The fate of pyruvate**

Next, the produced pyruvate in BF in contrast to PF cells is mostly excreted from the cell through pyruvate transporter in the plasma membrane (Sanchez, 2013). Pyruvate comprises ~85% of all end products detected (Mazet et al., 2013). The high rate of excreted pyruvate is in line with the high glycolytic rates in BF parasites. In addition to pyruvate, however, BF cells were found to produce small amounts of succinate, alanine and acetate all deriving from glucose (Mazet et al., 2013). It seems that small but significant amount of glucose-derived pyruvate enters mitochondrion via MPC1/2 (Štáfková et al., 2016) and it is further metabolized to those products. Despite the minor amounts of the products (NMR analysis shows ~5% acetate of all excreted products detected, ~1% succinate, ~9% alanine) compared to highly excreted pyruvate, this unexpected finding points out that the infective parasites have more complicated metabolism than previously thought. The percentage, with the exception of alanine, may not seem high enough compared to PF cells (see section **1.3.1.4. Glucose metabolism in PF**), however if one considers that the total glycolytic flux of the BF cells is up to 10-times higher than that in PF cells, these reactions contribute significantly to cell metabolism.

Alanine is produced from pyruvate by alanine aminotransferase (ALT) with concomitant production of  $\alpha$ -KG from glutamate, a reaction that is also active in PF parasites (Spitznagel et al., 2009), (**Fig.4, cytosolic**

**and mt forms**). Once entering the mt via MPC1/2, pyruvate could be possibly converted directly to malate, similarly to PF cells, in the organelle since proteomic data revealed mt malic enzyme (ME<sub>m</sub>) expression in the BF cells (**Fig.4**), (Zíková et al., 2017). In addition, presence of mt fumarase (FH<sub>m</sub>, aka fumarate hydratase), (**Fig.4, step 8**) and mt NADH-dependent fumarate reductase (FRD<sub>m</sub>), (**Fig.4, step 7**) explains the production of mt glucose-derived succinate utilizing the reverse TCA cycle (Zíková et al., 2017), (Gunasekera et al., 2012).

Another glucose-derived succinate can most probably be produced in the glycosomes as well. It is not possible with the current methods to discriminate whether succinate is of glycosomal or mt origin. The most probable scenario is that glycolytically formed PEP in the cytosol is transported back to the glycosomes where it is converted to oxaloacetate via PEPCK. It is supported by the fact that PEPCK is expressed in BF glycosomes (Gunasekera et al., 2012). Next, oxaloacetate is probably transported to the cytosol where it is converted to malate via cytosolic isoform of malate dehydrogenase (MDH<sub>c</sub>) (Aranda et al., 2006). Although mt and glycosomal isoforms are also present in the BF cells, their expression levels seem to be greatly reduced compared to MDH<sub>c</sub> which expression is at similar levels as to PF cells (Gunasekera et al., 2012). The following conversion of malate to fumarate probably takes place in the cytosol rather than in glycosomes via cytosolic fumarase (FH<sub>c</sub>) revealed by the slightly higher expression levels of FH<sub>c</sub> than FH<sub>g</sub> relative to PF expression (Gunasekera et al., 2012). Fumarate is probably converted to succinate in the glycosomes since glycosomal NADH-dependent fumarate reductase (FRD<sub>g</sub>) is expressed in BF trypanosomes (Gunasekera et al., 2012).

Oxaloacetate can also be converted to aspartate via aspartate aminotransferase (AST), in the cytosol not only in PF cells, but most probably also in BF cells (**Fig.4**). Importantly, in this reaction glutamate is converted to  $\alpha$ -KG which will be discussed later. In contrast to PF cells where both cytosolic and mt isoforms are expressed and active, in BF cells only the cytosolic isoform is probably active since the mt AST is strongly downregulated (Marciano et al., 2008). In addition, mt AST is highly specific towards aspartate/ $\alpha$ -KG whereas cytosolic AST shows specificity towards other dicarboxylic and aromatic amino acids as well, but not pyruvate (Marciano et al., 2008).

Interestingly, in BF parasites similarly to PF, the produced glucose-derived lactate does not come directly from pyruvate since BF cells lack lactate dehydrogenase, but rather DHAP is converted non-enzymatically to methylglyoxal, which was shown to be toxic for the cell, and consequently detoxified to the harmless lactate (Uzcátegui et al., 2018). Lactate seems to be excreted from the cell through aquaglyceroporins (Uzcátegui et al., 2018).

The detection of glucose-derived acetate shows that glycolytically-produced pyruvate enters mitochondrion where it is converted to acetyl-CoA by PDH like in PF cells. Three of the four PDH subunits are shown to be expressed in BF - PDH-E1 $\alpha$  and PDH-E2 (Mazet et al., 2013), PDH-E3, (Roldán et al., 2011). In addition, PDH is active in BF at only 4-fold lower levels than PF cells (Mazet et al., 2013). The conversion of acetyl-CoA to acetate will be discussed in the following section since threonine degradation also leads to acetate production.

### 1.3.2.3. Threonine metabolism

Although it was suggested as early as in the 1970's that threonine can be consumed by BF parasites (Cross et al., 1975), (Linstead & Cross, 1977) not much attention was given until Mazet and colleagues showed that in the infective form of the parasite not only can convert pyruvate to acetate, but also threonine to acetate (Mazet et al., 2013). Threonine in BF cells, similarly to PF cells, upon entering the mt matrix must be oxidized to AOB by TDH with the concomitant reduction of NAD<sup>+</sup> to NADH. AOB is further converted to acetyl-CoA by 2-amino-3-ketobutyrate coenzyme A ligase (AKCT), a process coupled with CoA consumption and the release of glycine. TDH is localized in the mitochondrion of *T. brucei* and it is active in both PF and BF life stages though its activity was measured to be approximately 7-fold higher in PF cells (Mazet et al., 2013).

When acetyl-CoA is produced from either pyruvate or threonine, then it is converted to acetate in the mitochondrion in the same way as in PF parasites. The production of acetate from acetyl-CoA is catalyzed by the 2 redundant enzymes already discussed – ACH and ASCT (Mochizuki et al., 2020). While ACH solely removes CoASH from acetyl-CoA, ASCT on the other hand contributes to mt ATP production through the ASCT/SCoAS cycle, catalyzing the conversion of acetyl-CoA to acetate by transferring CoASH to succinate, producing succinyl-CoA and the latter is converted back to succinate by SCoAS. A recent paper showed that ASCT/SCoAS cycle in BF cells is indeed active with a physiological CoA donor acetyl-CoA and it uses high concentration of succinate (Mochizuki et al., 2020). Both ACH and ASCT were detected in BF cells by WB (Mochizuki et al., 2020), (Mazet et al., 2013). When both enzymes simultaneously but not individually are ablated it leads to pronounced growth defects pointing at the importance of acetate production in BF parasites (Mochizuki et al., 2020). Acetate derives from both glucose (and therefore pyruvate) and threonine shown by the radiolabeled NMR (Mazet et al., 2013). In fact, BF trypanosomes excrete only approximately 1.4-times more acetate from glucose than from threonine when both carbon sources are in equal amounts (Mazet et al., 2013), whereas in PF trypanosomes, threonine rather than glucose is the main source of acetate (Millerioux et al., 2013). The observation that in BF cells both pyruvate and threonine account for acetate production is also supported by the severe growth defect



observed when PDH and TDH are depleted simultaneously, but not individually (Mazet et al., 2013). Acetate, like in PF cells, is utilized in BF cells for *de novo* fatty acid synthesis and the process is essential for the parasite (Mazet et al., 2013).

It is interesting to speculate if threonine utilization is feasible *in vivo*. The concentration of threonine in human blood is approximately 150  $\mu\text{M}$  (Lewis et al., 1980). Blocking of the acetate production from pyruvate by PDH downregulation showed no growth defects in the BF parasites when at least 150  $\mu\text{M}$  threonine (the same concentration in blood) was present in the medium (Mazet et al., 2013). It strongly suggests that threonine concentration in mammalian blood is sufficient to be utilized by the parasite for acetate production followed by for *de novo* fatty acid synthesis.

Altogether, this data clearly supports the view that in BF trypanosomes, not only pyruvate, but also threonine is utilized for the production of acetate which can be coupled via ASCT/SCoAS cycle to mt ATP production by SUBPHOS I.

#### **1.3.2.4. Glutamine/ $\alpha$ -ketoglutarate metabolism**

##### **1.3.2.4.1. From glutamine to $\alpha$ -ketoglutarate**

BF *T. brucei* were known for a long time to consume glutamine determining its addition to the medium (Hirumi et al., 1992) and later it was shown that glutamine is consumed when the pathogen is grown in both HMI-11 and Creek's Minimal Media (CMM) (Creek et al., 2013). In addition, the presence of glutamine in blood ( $\sim 0.6\text{mM}$ , (Creek et al., 2013), (Bagga et al., 2014) ) makes it a good potential source for the parasite. However only recently the glutamine degradation pathway was examined in more details (Johnston et al., 2019).

Johnston and colleagues found that almost all the glutamate and  $\alpha$ -KG have glutamine origin (37.5% and 39%, respectively keeping in mind that the labeled glutamate is 45% itself). Classically, glutamate is produced from glutamine via glutaminase, however *T. brucei* does not encode it in its genome. Other possible reactions (**Fig. 4**) though using glutamine as an amino group donor and thus converted to glutamate are suggested to happen in BF cells, such as (i) conversion of xanthosine 5'-monophosphate to guanosine monophosphate via GMP synthase, (ii) production of carbamoyl-phosphate from hydrogen carbonate via glutamine-dependent carbamoyl-phosphate synthase or (iii) production of asparagine from aspartate via asparagine synthase (Johnston et al., 2019) and references therein. In addition, those enzymes were found by proteomics that are expressed in both life stages of the parasite but without any experimental proof for their importance of the parasite (Gunasekera et al., 2012).

Next, glutamate is converted to  $\alpha$ -KG possibly by GDH in the cytosol similarly to PF cells with an NADH production. This is confirmed by the detected expression (Zíková et al., 2017) and activity (Markos A, 1989) of the enzyme in BF parasites. Other possibilities of glutamate converting to  $\alpha$ -KG is via cytosolic AST and ALT which was already discussed.

$\alpha$ -KG is also present in the human blood with concentration between 5-10  $\mu$ M (Aragonès et al., 2016), (Wagner et al., 2010) and could be potentially directly utilized by the cell.

#### 1.3.2.4.2. Form $\alpha$ -ketoglutarate to succinate

Next, in the BF parasites,  $\alpha$ -KG in the cytosol seems to enter mitochondrion probably through mt carrier protein 12 (MCP12) and probably while malate is transported out (Colasante et al., 2009).  $\alpha$ -KG is then converted to succinate via the TCA cycle enzymes similarly to PF cells. This is shown directly by the NMR analysis where around 15% of the detected succinate has glutamine origin (Johnston et al., 2019). When in the mitochondrion,  $\alpha$ -KG is oxidatively decarboxylated to succinyl-CoA by the multi-enzyme complex, the  $\alpha$ -KgdH. In BF cells all three subunits of  $\alpha$ -KgdH, the E1k, E2k and E3, are expressed (Zíková et al., 2017) and are essential, however it is suggested that those subunits play a different role in the infective stage of the BF parasites (S. Sykes et al., 2015), (S. E. Sykes & Hajduk, 2013), (Roldán et al., 2011). Nonetheless,  $\alpha$ -KgdH activity was found in BF although not consistently (Else et al., 1994), (Durieux I et al., 1991). Glutamine-derived 2-hydroxyglutarate was also detected in the BF cells (Johnston et al., 2019), detected also in PF cells (Villafray et al., 2021), which can be due to the promiscuous action of MDH on  $\alpha$ -KG (Intlekofer et al., 2017).

The detection of glutamine-derived succinate (Johnston et al., 2019) points out again at the activity of SCoAS, which produces succinate from succinyl-CoA, the connecting point of ATP production by SUBPHOS I and II.

Interestingly, the detection of small amounts of glutamine-derived malate and citrate/isocitrate (indistinguishable isomers by the assay), shows that surprisingly BF cells can actually utilize almost (why not complete) TCA cycle (Johnston et al., 2019). It is supported also by the proteomics data showing the expression of CII, mt fumarase, mt malate dehydrogenase (**Fig.4, step 9**), citrate synthase (**Fig.4, step 10**) and aconitase (**Fig.4, step 11**), (Zíková et al., 2017). Low activities of aconitase and relatively high activity of mt malate dehydrogenase were even found in BF cells (Durieux I et al., 1991). SCoAS activity was detected as well (Durieux I et al., 1991). Interestingly, NADP– dependent isocitrate dehydrogenase was found by proteomics in BF parasite (Zíková et al., 2017) together with some activity data available (Nolan

& Voorheis, 1992), it may suggest that contrary to common assumption, complete TCA cycle in BF cell might be functional.

Small amounts of glutamine-derived pyruvate and alanine (Johnston et al., 2019) further points at the functional MEm and ALT converting the glutamine-derived malate to pyruvate and then to alanine, respectively.

### **1.3.2.5. Proline and other AAs as energy source**

In PF cells proline catabolism was shown to be very important, however by contrast in BF cell it seems that although internalized by the cell it is not converted to glutamate or further catabolized in the TCA cycle (Johnston et al., 2019). Other AAs, such as tryptophan, tyrosine and phenylalanine are also required for the BF cell growth, however no evidence is available that they are utilized for energy needs (Creek et al., 2013).

#### **1.3.2.5.1. Fatty acids as energy source**

PF cells don't seem to utilize fatty acids as an energy source (Allmann et al., 2014). Interestingly however, BF parasites found recently to reside in the adipose tissues (also known as adipose tissue forms (ATFs)) are capable of oxidizing fatty acids released from adipocytes by  $\beta$ -oxidation (Trindade et al., 2016)). In the host adipose tissue, the fatty acids can comprise up to 50% of the adipocytes (Poudyal & Paul, 2022). Adipocyte release fatty acids together with glycerol (discussed in the next section) during lipolysis in the interstitial space. What most probably happens is that fatty acids acquired from interstitial spaces by BF are further shortened by  $\beta$ -oxidation and remodeled to serve as building blocks for more complicated lipids. During the process, the released acetyl-CoA can serve as a substrate for ASCT/SCoAS cycle leading to ATP production by SUBPHOS I. In this sense fatty acids seems to be able to serve as energy source when available in the environment however their contribution seems not to be significant in BF cells (Smith et al., 2017), (Poudyal & Paul, 2022).

For BF trypanosomes, other potential sources of fatty acid except adipose tissue could be the mammalian blood, lymph, interstitial spaces of CNS and skin. The blood and lymph are rich in free and protein (mostly albumin)-bound fatty acids (De Simone et al., 2021). CNS, however, does not seem to be a fatty acid source.

### 1.3.2.5.2. Glycerol as energy and carbon source

Glycerol seems to be utilized not only by PF, but also by BF parasites as an energy source (Kovářová et al., 2018). Although in contrast to PF, BF cells prefer glucose over glycerol, BF can metabolize glycerol for ATP production *in vitro* and can adapt to grow on glycerol as a sole carbon source to sustain long-term proliferation (Pineda et al., 2018) (**Fig.4, marked in green**). Glycerol, similarly to PF, enters the cell through aquaglyceroporins (Jeacock et al., 2017) and once it reaches glycosomes, it gets phosphorylated to glycerol 3-phosphate (Gly-3-P) by glycerol kinase (GK), a process consuming 1 ATP molecule. However, in contrast to PF, where Gly-3-P is converted to DHAP by glycosomal Gly3PDH, Gly-3-P in BF cells tends to be diverted to mt Gly-3-P/DHAP shuttle and subsequent electron transfer via ubiquinol to oxygen by TAO. Therefore, cells grown under glycerol conditions must rely more heavily on TAO. This is confirmed by the higher oxygen consumption (twice as much oxygen per unit carbon consumed) and 11.5-fold higher sensitivity to salicylhydroxamic acid (SHAM), the TAO inhibitor, in the presence of glycerol compared to glucose (Pineda et al., 2018).

Next, DHAP can be further used for gluconeogenesis, a process that until recently was thought not to occur in BF cells (Kovářová et al., 2018), (Pineda et al., 2018). In the absence of glucose, glycerol can be utilized for gluconeogenesis, however when both glucose and glycerol are present in the medium only glucose seems to serve as gluconeogenic precursor (Pineda et al., 2018). The detection of glycerol-derived pyruvate, acetate, alanine and succinate (**Fig.4, marked in green**) also shows that glycerol is catabolized through the same pathways as glucose.

Another interesting point is the use of glycerol instead of glucose apparently results in a lower ATP yield in the cytosol. Consumption of one glucose molecule (6 carbon atoms) leads to the production during glycolysis of 2 pyruvate molecules and 2 ATP molecules in the cytosol during glycolysis (unless diverted to other products) whereas consumption of one glycerol molecule (3 carbon atoms) leads to the production of 1 pyruvate molecule and 1 ATP molecule in the cytosol (again unless diverted to other products). Thus, twice as many glycerol molecules as glucose molecules are consumed to produce the same amount of cytosolic ATP. Pineda and colleagues indirectly show that cells grown on medium with only glucose as a carbon source, produce more ATP molecules than cells grown on glycerol medium alone (Pineda et al., 2018). In fact, the rate of glycerol consumption was slightly lower than the glucose consumption rate as the sole carbon source, meaning that when one glucose molecule is consumed for a given time, less than two glycerol molecules are consumed. Although the total end products derived from glucose are not more than twice the products derived from glycerol, including pyruvate, not all the glycerol consumed resulted in the production of pyruvate (and other metabolites).

Additionally, the cells grown in glycerol only medium seems to excrete more acetate and succinate than when grown in glucose only medium (Pineda et al., 2018). Increased acetate excretion could mean they are fueling more pyruvate through the ASCT/SCoAS cycle possibly because they need mt ATP. Increased succinate excretion could mean that significant amount of the pyruvate is diverted to PEP and finally to succinate as excreted product and thus diminishing the cytosolic ATP levels even more when glycerol is the carbon source. Another study (Kovářová et al., 2018) also supports the idea that succinate is produced from glycerol-derived PEP since they detected glycerol-derived fumarate, malate, and aspartate, which are intermediate substrates produced in the pathway. Their level was markedly increased when cells utilized glycerol since they were deprived of glucose upon hexose transporter downregulation. The study cannot discriminate between excreted and intermediate substrates since metabolomic analysis was done on whole cells and not on the spent medium, therefore it is also possible that the metabolites are produced in the TCA cycle from glycerol-derived acetyl-CoA, once again suggesting an operative TCA cycle in BF cells.

The increased activity of the glycosomal succinate shunt can be nicely justified with the need of the cell to balance glycosomal  $\text{NAD}^+/\text{NADH}$ . Since glycerol conversion to DHAP is achieved through Gly-3-P/DHAP shuttle and then the DHAP is converted to G-3-P rather than Gly-3-P, therefore when glycerol and not glucose is used as an energy source, glycosomal G3PDH is not utilized and the  $\text{NAD}^+$  produced by the enzyme does not occur (**Fig.4, step 3**). The lack of  $\text{NAD}^+$  in the glycosomes however has to be compensated for, given that NADH is produced only by glyceraldehyde-3-phosphate dehydrogenase (**Fig.4, step 2**). Therefore, increasing the succinate shunt seems to be a means of achieving it as fumarate is converted to succinate via fumarase and produces  $\text{NAD}^+$  in the glycosomes, restoring the  $\text{NAD}^+/\text{NADH}$  balance.

The physiological relevance of the glycerol consumption probably does not include the bloodstream as a natural environment for the BF cells since the concentration of the glycerol there is too low  $\sim 50\mu\text{M}$  (Samra et al., 1996), (Sjöstrand et al., 2002) compared to 10 mM in the medium used for the experiments and the glucose concentration (5mM). It rather points out that BF cells can adapt to the adipose tissue and skin, where glycerol together with fatty acids is well provided. This is speculated to be reservoirs for the parasites and the cause for patient relapses especially in asymptomatic carriers with low or even undetected blood parasites.

Glycerol is released by the adipocytes in the adipose interstitial space within relatively high concentration (ranging between 0.2 – 2.8 mM) (Sjöstrand et al., 2002), (Maggs et al., n.d.) during lipolysis together with fatty acids. Regarding the skin, glycerol concentration was found to be  $\sim 50\mu\text{M}$  (Boschmann et al., 2001). Parasites found to reside in mice and human skin have the ability to be transmitted via tsetse fly (Capewell et al., 2016).

The ability of BF cells to use glycerol may be crucial for adaptation to invade other environments, such as adipose tissue and skin, again revealing the high adaptation potential of the parasites.

### **1.3.2.6. Electron transport chain (ETC) and complex V (CV)**

An interesting peculiarity of BF bioenergetics, in contrast to PF, is that the BF mitochondrion lacks the proton pumping activities of complexes III and IV. Therefore, the  $\Delta\Psi_m$  is maintained alternatively by the reverse activity of CV, which translocates  $H^+$  into the intermembrane space at the expense of ATP (Nolan & Voorheis, 1992), explaining the lack of OXPHOS in BF cells under physiological conditions. Mt ATP supply is essential for BF parasites to maintain the vital  $\Delta\Psi_m$  and thus the mitochondrion itself. The classical view is that ATP is produced during glycolysis and transported into the matrix via the ATP/ADADPADP/ATPP carrier (AAC), while ADP is transported out. In this life stage of the parasites, the enzymes that transfer electrons to the ubiquinone pool are complex I, type II alternative NADH dehydrogenase (NDH2), mt FAD-dependent glycerol-3-phosphate dehydrogenase (Gly3PDH) and complex II (Zíková, 2022). The electrons are passed to the only terminal oxidase – trypanosome alternative oxidase (TAO).

#### **1.3.2.6.1. Complex I (CI)**

Complex I (CI, NADH:ubiquinone oxidoreductase) although assembled in BF, it is not essential *in vivo* or *in vitro* and does not seem to contribute significantly to scavenging electrons from NADH or to the proton pump (Surve et al., 2012).

#### **1.3.2.6.2. Type 2 alternative NADH dehydrogenase (NDH2)**

*T. brucei* expresses an unique alternative to CI enzyme – type II alternative NADH dehydrogenase (NDH2), which transfers electrons from NADH to ubiquinone pool without the ability to pump protons (Fang & Beattie, 2002). In BF cells it is essential like in PF cells especially when CI is ablated (Surve et al., 2017). It is still debatable if it is important for mt  $NAD^+/NADH$  balance.

#### **1.3.2.6.3. Glycerol-3-phosphate dehydrogenase**

Mt glycerol-3-phosphate dehydrogenase (Gly3PDH) oxidizes Gly-3-P to DHAP in the mitochondrion with subsequent electron transfer to the ubiquinone pool. It is essential in BF trypanosomes because it maintains

the glycosomal redox balance, that is critical for the high glycolytic flux on which the cells are completely dependent (Škodová et al., 2013). Gly3PDH is also important for the glycerol oxidation mentioned earlier.

#### **1.3.2.6.4. Complex II (CII)**

Complex II (CII, succinate dehydrogenase) is directly involved in the TCA cycle by oxidizing succinate to fumarate with the subsequent electron transfer to ubiquinone. In BF cells the complex is assembled, however is not essential shown by RNAi knockdown studies (Alkhalidi et al., 2016).

#### **1.3.2.6.5. Complex III (CIII) and Complex IV (CIV)**

In PF trypanosomes CIII and CIV are the main producers of the mt  $\Delta\Psi_m$  (Horváth et al., 2005). By contrast, in BF trypanosomes, there is no functional cytochrome - mediated respiratory chain since the cytochrome pigments are absent (Vickerman, 1965).

#### **1.3.2.6.6. Trypanosoma alternative oxidase (TAO)**

Trypanosoma alternative oxidase (TAO) is the only mt terminal oxidase in BF cells (Luévano-Martínez et al., 2020), sinking electrons from ubiquinol to oxygen without having proton pumping activity (Chaudhuri et al., 1998), (Chaudhuri et al., 2006). In BF cells TAO is indispensable (Helfert et al., 2001) and the cells rely entirely on its activity. It is apparent since those cells lack CIV activity and at the same time the electrons from ubiquinol must be oxidized (Chaudhuri et al., 2006). TAO is particularly needed to reduce electrons from the Gly-3-P/DHAP shuttle and thus assuring the high glycolytic flux.

#### **1.3.2.6.7. Complex V (CV)**

CV in BF cells, also known as  $F_0F_1$ -ATPase, has a very peculiar mode of action compared to other aerobic eukaryotes including PF parasites. CV is essential for BF parasites, and it works in its reverse mode hydrolyzing mt ATP and utilizing the energy to generate  $\Delta\Psi_m$  in the form of proton gradient in the mt intermembrane space (Nolan & Voorheis, 1992), (Schnauffer et al., 2005), (Brown et al., 2006). The reverse mode of CV generating the mt  $\Delta\Psi_m$  was first proved by inhibiting CV using oligomycin which led to mt  $\Delta\Psi_m$  collapse at similar extent as when FCCP, mt  $\Delta\Psi_m$  uncoupler, was used (Nolan & Voorheis, 1992). Generally, on aerobic cells, the ATP hydrolyzing activity is observed only in physiologically challenging

conditions usually related to hypoxia or anoxia where it is regulated by inhibitory factor 1 (IF1) (Pullman & Monroy, 1963). IF1 specifically prevents the detrimental cellular ATP hydrolysis, but not synthesis, upon mt  $\Delta\Psi_m$  collapse providing a short-term survival (Gatto et al., 2022). While it is present in PF cells where it serves as emergency break to prevent ATP depletion upon respiration inhibition, it is lacking in the BF parasites and thus assures that hydrolytic activity of CV is always possible (Panicucci et al., 2017). Although CV is essential, BF parasites can tolerate up to 90% loss of the membrane-bound part of the complex without any growth defects (Hierro-Yap et al., 2021) showing again the potential for adaptability of the parasite.

#### 1.4. Succinyl-CoA synthetase (SCoAS)

The aim of the thesis is to elucidate the mt ATP source, therefore special attention is dedicated to succinyl-CoA synthetase (SCoAS), the only known mt enzyme in BF cells that directly produces ATP, connecting SUBPHOS I and II. SCoAS catalyzes the reversible reaction of succinyl-CoA to succinate in the TCA cycle, which is coupled to the release of CoASH and ATP (or GTP) in higher eukaryotes. In *T. brucei*, SCoAS participates classically in the TCA cycle (**Fig. 2 and 3, step 7 and Fig.4, SUBPHOS II**) where the substrate succinyl-CoA derives most probably from the amino acid proline and glutamine in PF and BF cells, respectively. The glutamine (or also possibly  $\alpha$ -KG) – driven ATP production in BF cells by SCoAS is indicated as SUBPHOS II. In addition, in both life stages, SCoAS participates in the unique ASCT/SCoAS cycle as well, where the succinyl-CoA is produced from acetyl-CoA conversion to acetate via ASCT and it is fueled by glucose and threonine – derived acetyl-CoA (**Fig. 2 and 3, step 7 and Fig.4, SUBPHOS I**). This ATP producing pathway is indicated as SUBPHOS I in BF cells.

SCoAS in general is a highly conserved enzyme within the TCA cycle and it is composed of  $\alpha$  and  $\beta$  subunits, forming an  $\alpha\beta$ -dimer. SCoAS in *E. coli*, as in many other prokaryotes, is specific for ATP (Birney et al., 1996). It consists of two  $\alpha\beta$ -dimers (catalytically independent) that form a heterotetramer (Bailey et al., 1999). Additional studies in *E. coli* also revealed that the  $\alpha$  subunit has a loop containing a histidine residue (His246 $\alpha$ ) that accepts the phosphate from the enzyme-bound succinyl phosphate, thus acting as an intermediary to create ATP. This  $\alpha$  subunit also binds one of the substrates, CoASH. The  $\beta$  subunit binds the purine nucleotides at a site called the ATP-grasp of the N-terminal domain. The ATP-grasp in *E. coli* was shown to bind ADP complexed with  $Mg^{2+}$  (Joyce et al., 2000a). Although many studies have investigated the SCoAS catalysis, the precise mechanism is still debatable (Li et al., 2013).

Interestingly, SCoAS in higher eukaryotes has two isoforms, the ATP-specific SCoAS (A-SCoAS) and GTP-specific SCoAS (G-SCoAS). Both isoforms have  $\alpha$  and  $\beta$  subunits. They share the same  $\alpha$  subunit,



but the  $\beta$  subunit is less than 53% identical between the two isoforms (Johnson et al., 1998b). Thus, the  $\beta$  subunit determines the substrate specificity of the enzyme.  $\beta$  subunits of SCoAS isoforms were shown to be differentially expressed in tissues. For example, in humans, the  $\beta$  subunit of G-SCoAS in rats and mice is much more highly expressed in anabolic tissues such as liver and kidney. By contrast, the  $\beta$  subunit of A-SCoAS has increased expression in highly energetic tissues, such as testes and brain (Lambeth et al., 2004a).

In *T. brucei*, SCoAS is composed of  $\alpha$  and  $\beta$  subunits, each encoded by a single gene (Tb927.3.2230 and Tb927.10.7410, respectively). In some aspects, the PF SCoAS mechanism is similar to that described for *E. coli*, as catalysis is dependent on  $Mg^{2+}$  and a conserved histidine from  $\alpha$ -subunit becomes phosphorylated during catalysis. *T. brucei* SCoAS produces ATP instead of GTP (Bochud-Allemann & Schneider, 2002), as it was shown to phosphorylate the substrate ADP much more efficiently than GDP (Hunger-Glaser, Linder, et al., 1999). In contrast, both ATP and GTP are equally efficient phosphate donors in the reverse reaction (Hunger-Glaser, Linder, et al., 1999). The significance of *T. brucei* adaptation to produce mt ATP via SUBPHOS is revealed by RNAi functional studies in PF cells. The ablation of either the SCoAS  $\beta$  subunit or PDH/ $\alpha$ -KgdH in glucose-rich conditions results in cell growth arrest (Zhang et al., 2010), (Bochud-Allemann & Schneider, 2002). This indicates that when glucose is available ATP production *in organello* is essential for PF trypanosomes.

The function of SCoAS in BF cells is a little more complicated. Both  $\alpha$  and  $\beta$  SCoAS subunits are detected at the mRNA level, in fact  $\beta$  is a very highly expressed transcript (Zhang et al., 2010). However, the earliest reports indicated that phosphorylation of the SCoAS  $\alpha$ -subunit was only detected in PF cells (Hunger-Glaser, Linder, et al., 1999). Since this transient phosphorylation is crucial for enzymatic activity, it was presumed that SCoAS function is not required in BF cells. However, a more recent study applied a more direct genetic method to analyze the function of SCoAS. Depletion of the  $\beta$  subunit by RNAi for just 20 hours resulted in cell death (Zhang et al., 2010). This incredibly severe growth effect suggests that either the SCoAS  $\beta$  subunit has another yet unknown function in BF *T. brucei* or these cells are dependent on ATP production *in organello*. If the latter is assumed to be correct, then it implies that BF cells produce mt ATP by mt SUBPHOS I and II. Recently it has been speculated about the possibility of mt ATP production, however no direct evidence has been presented yet (Zíková et al., 2017), (Mochizuki et al., 2020), (Zíková, 2022).

### **1.5. ADP/ATP carrier (AAC)**

One of the pathways for the mt ATP supply in the infective BF parasites is via the ADP/ATP carrier (AAC) (**Fig.2, 3 and 4**). AAC is a nuclearly encoded, integral protein of the inner mt membrane that translocates

adenine ribonucleotides with two or three phosphate groups. AAC belongs to the Mt Carrier Family (MCF), and it is present in virtually all eukaryotes. AAC is a highly studied protein since it plays a central metabolic role as a supplier of ATP from mt to the cytosol. In PF *T. brucei*, the AAC functions in its classical way, by exporting ATP synthesized in the mt matrix by OXPHOS to the cytosol while importing ADP. This specific exchange of cytosolic ADP for matrix ATP occurs in an equimolar ratio (Klingenberg, 2008). However, in BF trypanosomes, because the F<sub>0</sub>F<sub>1</sub>-ATPase must hydrolyze ATP to maintain the  $\Delta\Psi_m$ , the accumulating reaction product ADP would be exported by AAC in exchange for the cytosolic substrate ATP (Schnauffer et al., 2005). Since AAC is the most obvious way to transport ATP into the BF mitochondrion, we will focus on the details about this important transporter.

All ADP/ATP carriers are proposed to share a high degree of sequence similarity and functional properties. The number of isoforms varies among the organisms. For example, humans have 4 isoforms - hANC1, 2, 3 and 4 and have differential tissue expressions (Dahout-Gonzalez et al., 2006). Yeasts have only 3 gene copies of AAC – AAC1, 2 and 3. While these isoforms have similar enzymatic properties, AAC1 and 2 are believed to be important under aerobic conditions whereas AAC3 is important for anaerobic environments (Drgoň et al., 1992), (Klingenberg, 2008).

Studies in yeast show that AAC functions as a monomer (Bamber et al., 2007), although the precise functional mechanism of AAC was debatable for some time. It was first proposed that the AAC monomer is not a single-site carrier, but rather has dual binding sites for ADP and ATP, transporting both substrates either sequentially or simultaneously (DUYCKAERTS et al., 1980). However, it is more likely that AAC functions as a single-site carrier that binds the substrates sequentially in 1:1 ratio at the same binding site in a ‘ping-pong’ mode (Klingenberg, 2008). It is now widely accepted that AAC has two ground states: the cytosolic state (c-state), where the translocation channel is open towards the cytosolic side of the inner membrane and the matrix state (m-state), where the translocation channel is open towards the matrix side (Klingenberg, 2008). Several AAC inhibitors have been very useful in resolving this mechanism as (carboxy)atractyloside locks the translocator in the c-state, while bongkreikic acid stabilizes the m-state. When the mitochondrion is respiring, the c-state allows the binding of cytosolic ADP, which induces conformational changes that define the m-state. It is proposed that the m-state involves the formation of salt bridges between the amino acids facing the cytosol, which is important for the transport cycle of AAC (King et al., 2016). ADP is then released, and the carrier is free to bind matrix ATP, followed by a conformational change to the c-state. This process can also occur in reverse as AAC can translocate ATP into the mitochondrion. Under normal physiological conditions, the nucleotide flux depends on the concentration gradient of the nucleotides and their charge due to the  $\Delta\Psi_m$  (Klingenberg, 2008). This results in the mt export of ATP produced via the OXPHOS pathway. However, when the OXPHOS pathway is

interrupted (e.g. under hypoxic conditions) and the  $\Delta\Psi_m$  dissipates, the  $F_0F_1$ -ATPase hydrolyzes mt ATP in a futile attempt to maintain the  $\Delta\Psi_m$ . Under these conditions, cytosolic ATP is imported into the mitochondrion where the ADP/ATP ratio has been drastically increased. This ratio between the nucleotides is the driving force that determines the direction of the nucleotide flow. The resolved crystal structure of the bovine AAC (Pebay-Peyroula et al., 2003) reveals that it exploits a pseudo-3-fold symmetry forming three symmetrical repeats. Furthermore, AAC contains a nucleotide binding motif represented by the consensus sequence RRRMMM and mutating any of these arginines abolishes the transport activity. Importantly, this conserved motif was also found in *T. brucei* AAC (Peña-Díaz et al., 2012).

The *T. brucei* genome encodes 2 proteins, MCP5 and MCP15, that have a high homology to the AAC present in other eukaryotes (Peña-Díaz et al., 2012). However, only MCP5 was shown to be a functionally active ADP/ATP carrier since MCP5, but not MCP15, complemented AAC function in AAC-deficient yeast (Peña-Díaz et al., 2012). In *T. brucei*, MCP5 (also referred to as TbAAC or AAC) consists of 3 identical and consecutively arranged copies: TbAACa (Tb927.10.14840), TbAACb (Tb927.10.14830) and TbAACc (Tb927.10.14820). The presence of 3 AAC gene copies can imply a high cellular demand for AAC. To date, only a few functional assays have been performed with AAC in *T. brucei*. Both the mRNA and protein data indicate that the gene product is developmentally regulated as expression levels are significantly diminished in BF stages compared to PF cells (Peña-Díaz et al., 2012). This could reflect either the overall decreased protein levels in the generally reduced mt in BF or the minor role of AAC in the BF mitochondrion. While RNAi studies determined that AAC is essential for the growth of PF trypanosomes (Peña-Díaz et al., 2012), (Gnipová et al., 2015), the data is scarce for BF life stage.

## 2. HYPOTHESES

The main aim of my thesis is to challenge the current view of how BF *T. brucei* supplies its mitochondrion with ATP that is needed for F<sub>0</sub>F<sub>1</sub>-ATP synthase (complex V, CV) to generate the essential mitochondrial membrane potential ( $\Delta\Psi_m$ ). It is widely accepted that majority of the cellular ATP is produced by highly efficient glycolysis in the cytosol and a proportion of this ATP is imported into the mt matrix via ADP/ATP carrier (AAC). We challenge this notion and hypothesize that:

- (1) ATP produced by glycolysis is not utilized for maintaining  $\Delta\Psi_m$ .**
- (2) BF mitochondrion is capable of *in organello* ATP production by SUBPHOS.**
- (3) ATP produced in the BF mitochondrion is utilized by CV for  $\Delta\Psi_m$  generation.**

In order to test the hypotheses, we:

- (1) defined potential ways of supplying mitochondrion with ATP such as:
  - ATP import to mitochondria via the activity of AAC.
  - SUBPHOS I pathway – a pathway that is fed by pyruvate, glycerol and threonine metabolism. This pathway has been shown to be active in the BF cells as it leads to the production of acetate. Acetate production is part of the acetate:succinate CoA transferase/succinyl-CoA synthetase (ASCT/SCoAS) cycle, in which ATP is generated *in organello* via SCoAS.
  - SUBPHOS II pathway – a pathway fed by glutamine and/or  $\alpha$ -ketoglutarate oxidative metabolism and leading to the production of mt succinate. This pathway involves parts of TCA cycle including SCoAS enzyme possibly generating ATP.
- (2) investigated their importance and interplay by generation of AAC and SCoAS double knock-out cell lines.
- (3) established an enzymatic assay to measure the activity of SCoAS in BF mitochondria to confirm its presence and activity.
- (4) developed luciferase-based reporter assay to measure cytosolic and mitochondrial ATP levels under *in vivo* conditions.
- (5) applied exometabolomics to measure metabolic end-products in SCoAS and AAC DKO cells.
- (6) determined the significance of mt ATP production by testing the AAC and SCoAS DKO cells under different growth conditions.

## 3. RESULTS

### 3.1. AAC is not essential in BF trypanosomes *in vitro*

Previously, AAC was shown to be essential in PF trypanosomes and to cause severe growth defects as early as day three upon RNAi induction under standard SDM-79 media conditions (Gnipová et al., 2015). This is not surprising since AAC in the insect stage operates in forward mode and its ablation prevents ATP from leaving the mt matrix, which affects cellular ADP/ATP balance. In BF trypanosomes, the AAC is thought to work in the reverse mode supplying ATP to F<sub>0</sub>F<sub>1</sub>-ATP synthase, but this has not been demonstrated experimentally. Therefore, we aimed to investigate the role of AAC in BF mitochondrion.

#### 3.1.1. AAC expression is developmentally regulated

To determine the expression levels of AAC in BF trypanosomes, we compared them with the expression levels of PF *T. b. brucei* cell lines. Western blot analysis with the equal number of cells loaded (**Fig.5A**) showed that AAC is significantly less expressed in BF compared with PF. The reduced AAC expression could be due to overall reduced mt protein content in the BF mitochondrion because of its reduction in size, activity and function.

#### 3.1.2. AAC RNAi cell line shows no growth phenotype

To determine if AAC is essential for BF *T. brucei* growth, we generated an RNAi cell line in which expression of AAC is suppressed. The *T. brucei* genome encodes for three identical and consecutive AAC gene copies: AACa (Tb927.10.14840), AACb (Tb927.10.14830) and AACc (Tb927.10.14820), resulting in the production of identical mRNAs and a single AAC protein. A construct containing a region for dsRNA production targeting AAC mRNA, was introduced to single marker (SM) BF *T. brucei* cells, encoding T7 RNA polymerase and tetracycline repressor allowing inducible expression of dsRNA upon tetracycline induction. For detailed information see section Materials and Methods. Five *T. brucei* clones were obtained after the transfection, namely B2, B3, C1, C2 and C3. The efficiency of RNAi induction was determined with clones C1, C2 and C3 clones by Western blot (WB) analysis. Cells were collected after tetracycline induction for 2, 4 and 6 days. Already at day 2 postinduction, the protein levels of AAC were significantly decreased compared to non-induced cells. At day 4, the expression of AAC was reduced to 8 % (**Fig.5B, clone 1**). A similar decrease in AAC expression was observed in clones C2 and C3.

Next, the growth rate of all five clones of AAC RNAi was measured daily under standard HMI-11 media conditions. RNAi was induced (IND) with tetracycline and the growth rate was monitored and compared with non-induced (NON) cells. No difference in growth rate between IND and NON cells was determined in all five clones. A representative growth curve of clone C1 is shown in **Fig.5C**.

We demonstrated that efficient RNAi silencing of AAC expression had no effect on growth, suggesting that AAC may not be required for BF *T. brucei*. However, there is a possibility that RNAi is not efficient enough and a residual amount of AAC remains active and stable in the RNAi-induced cells. Therefore, we generated a BF AAC double knock-out (DKO) cell line that completely lacks AAC.

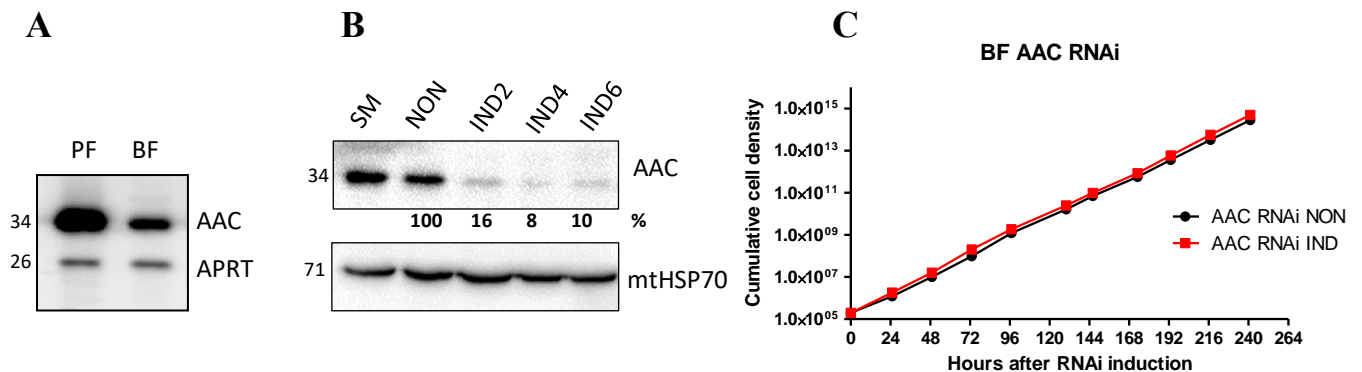
### **3.1.3. Lack of AAC has no effect on BF growth**

BF AAC DKO cell line was generated in an attempt to show conclusively that AAC is not essential in BF parasites. The strategy for generating AAC DKO is shown on **Fig.5D**. First, an AAC single knock out (SKO) cell line was engineered by replacing all three consecutively arranged AAC genes from the first allele of WT 427 BF cells with gene cassette containing T7 RNA polymerase and geneticin (G418) resistance cassette. Next, an AAC DKO cell line was generated by replacing the other three AAC genes from the second allele of the previously generated AAC SKO cells with gene cassette containing T7 promoter, tetracycline repressor and hygromycin resistance cassette. Detailed information can be found in the Materials and Methods section. The generation of the SKO was successful in the first experiment. We succeeded in generating 6 clones, of which 4 clones were tested to determine whether the first allele was replaced by the gene cassette. Using PCR with specific primers we identified one positive clone (namely clone A6). The AAC SKO A6 clone was subjected to second transfection to generate AAC DKO cells. Finally, after five unsuccessful transfection attempts to replace the second AAC allele, two clones (clones A2 and A7) were found to lack AAC CDS by PCR. We decided to work with A2 clone for all further experiments. The AAC DKO A2 cell line was verified by both PCR for gene replacement (**Fig.5E**) and by WB analysis for the lack of protein expression (**Fig.5F**). **Fig.5E** shows the PCR verification. Using specific primers that are designed so that the 5'-primer anneals upstream of the recombination site and the 3' primer anneals to the replacement cassette region that has been integrated into the genome, we verified the correct position of the gene knock-out cassettes as shown in **Fig.5D**. The 5'SKO integration site, verified by PCR amplifying 820 bp region spans a region starting upstream from the integration site and ending at T7 RNA polymerase gene. The 3'SKO integration site (1140 bp) was amplified using primer pair spans a region starting downstream from the integration site and terminating at G418 resistance cassette. Similarly, the

5'DKO primer pair spans a region starting upstream from the integration site and ending at tetracycline repressor gene and amplifies 1056 bp region. The 3'DKO primer pair spans a region starting downstream from the integration site and ending at hygromycin resistance cassette and amplifies 834 bp region. The AAC CDS primer pair amplifies 418 bp region from each of the three AAC genes, so PCR is positive when one of the AAC genes is present in the genome. PCR results show that the integration cassettes have replaced all six AAC alleles and that no AAC CDS is detectable in the AAC DKO cells.

AAC DKO cell line was also verified by WB analysis to ensure that no AAC was expressed (**Fig.5F**). Cells were cultured between one and three weeks to assure well-growing and cells were collected. They were then subjected to WB analysis probed with anti-AAC Ab and anti-mtHSP70 Ab. The latter Ab is used to determine the equal loading of the cell lysate. In contrast to BF WT where AAC was prominently expressed, no traces of AAC protein were detected in AAC DKO cells. Both PCR and WB results confirm the success of the AAC DKO cell line.

Next, we wanted to know if there is any growth defect in AAC DKO cell line. Growth of AAC DKO was monitored daily for at least seven days in either HMI-11 medium (**Fig.5.G**) or Creek's minimal medium (CMM) (**Fig.5H**). HMI-11 medium contains high concentration of glucose (25mM) together with some amino acids, whereas CMM is a simplified medium that has lowered glucose concentration (10mM), (Creek et al., 2013) which better represents although still well above the natural BF trypanosome environment – the bloodstream of the mammalian host. In both media no selectable drugs were added during the analysis since the presence of drugs themselves could influence the cell growth. Interestingly, the AAC DKO did not show any growth phenotype compared to WT in either medium. Note that both BF WT and AAC DKO cells grow more slowly in CMM medium than in HMI-11 media, which is to be expected given the lower nutrient levels in CMM. The lack of growth defect when AAC is not present clearly indicates that AAC is not required for the BF growth in culture.



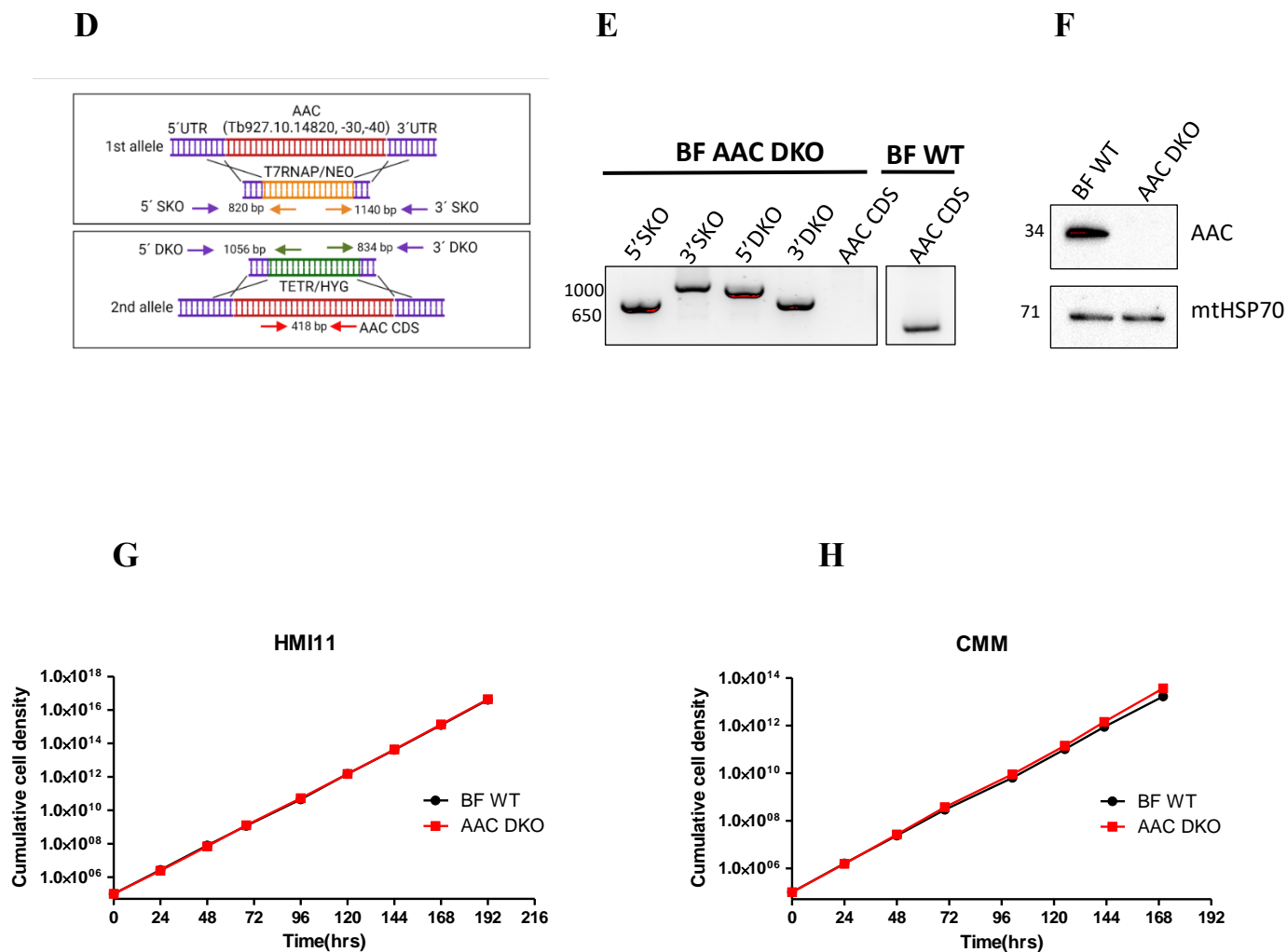


**Fig.5** AAC in BF trypanosomes. **(A)** WB analysis of AAC in PF and BF cells. Anti-APRT (adenine-phosphoribosyl transferase) antibody was used as a loading control. **(B)** WB analysis of AAC RNAi cell line, clone C1. AAC expression levels were determined after RNAi induction with tetracycline. SM – parental cell line, NON – non-induced RNAi expression, IND 2-6 – days after RNAi induction. The levels of AAC are shown in % compared to non-induced cells (100%). mtHSP70 (mt Heat Shock Protein 70) – housekeeping protein used for loading control. **(C)** A representative growth curve for AAC RNAi cell line clone C1 shown as cumulative cell density (cells/ml) measurement for 10 days. AAC RNAi non-induced (NON) cells are shown in black and the tetracycline-induced (IND) cells are in red color. **(D)** A scheme showing the strategy for AAC DKO generation. Upper panel – SKO generation (first allele replacement) and the schematic representation of the primer pairs for SKO verification. Lower panel – DKO generation (second allele replacement) and the schematic representation of the primer pairs for DKO verification. **(E)** PCR verification of AAC allele replacement by the integration cassettes of the SKO and DKO as well as the absence of AAC CDS in AAC DKO cells (clone A2). BF WT 427 used as a positive control for AAC presence. **(F)** WB analysis of lack of AAC in AAC DKO cells in contrast to BF WT. mtHSP70 antibody was used as a loading control. **(G and H)** Growth curves for AAC DKO cell line (clone A2) shown as cumulative cell density (cells/ml) in HMI-11 **(G)** and CMM **(H)** medium. BF WT is shown in black, AAC DKO in red. In panels A, B and E molecular markers are in kDa, while in D are shown in bp and on the left side.



## 3.2. Functional analysis of BF trypanosomes upon AAC loss

Neither AAC RNAi cell line nor AAC DKO cells showed any growth defect *in vitro*. Nevertheless, we continued to explore the effect of the AAC loss on mitochondria physiology and bioenergetics.

### 3.2.1. Membrane potential is not affected in BF cells upon AAC loss

AAC appears to be the sole mt ADP/ATP carrier in *T. brucei* and is proposed to import ATP into mt matrix in BF parasites. This ATP is then hydrolyzed by F<sub>0</sub>F<sub>1</sub>-ATPase to generate the essential mt membrane potential ( $\Delta\Psi_m$ ). To determine whether this was indeed true, we set to determine if the AAC loss or decrease would lead to a decrease in  $\Delta\Psi_m$ . The TMRE (tetramethylrhodamine, ethyl ester) dye was used to determine the level of  $\Delta\Psi_m$  in AAC RNAi induced cells as well as in AAC DKO cells. TMRE is a positively charged red-orange dye, which accumulates in charged mitochondria according to the levels of  $\Delta\Psi_m$ . Its fluorescence can be detected by fluorescence-activated cell sorting (FACS).  $\Delta\Psi_m$  was measured in BF AAC RNAi cells, clone C1, which were grown in regular HMI-11 medium and analyzed after tetracycline induction for 2, 5 and 7 days (**Fig.6A**). There was no significant change in  $\Delta\Psi_m$  at 2, 5 or 7 days postinduction compared to non-induced or the parental BF SM cells. BF AAC RNAi clone C2 was additionally analyzed with the same outcome (data not shown).

Next,  $\Delta\Psi_m$  was measured in BF AAC DKO cells, clone A2. The cells were grown in medium without selectable drugs at least 24 hours prior to the experiment to avoid any interference with the results. The experiment was conducted in both, glucose-rich HMI-11 (**Fig.6B**) and simplified CMM media (**Fig.6C**). The results show no significant difference in the  $\Delta\Psi_m$  between AAC DKO and the parental BF 427 WT strain neither in HMI-11 nor in CMM media.

We show that the  $\Delta\Psi_m$  was not affected in the AAC RNAi cell line, in which AAC expression is downregulated to 8% (see **Fig.5B**), nor AAC DKO cells in glucose-rich and glucose-low medium. These data suggest that the activity of AAC is not needed for proper maintenance of  $\Delta\Psi_m$  in BF parasites. This would imply that either substrate level phosphorylation (SUBPHOS) pathways in the mt matrix play an important role in alternatively supply of ATP to mitochondria or, that another, as yet unidentified mt ADP/ATP carrier is present and active.

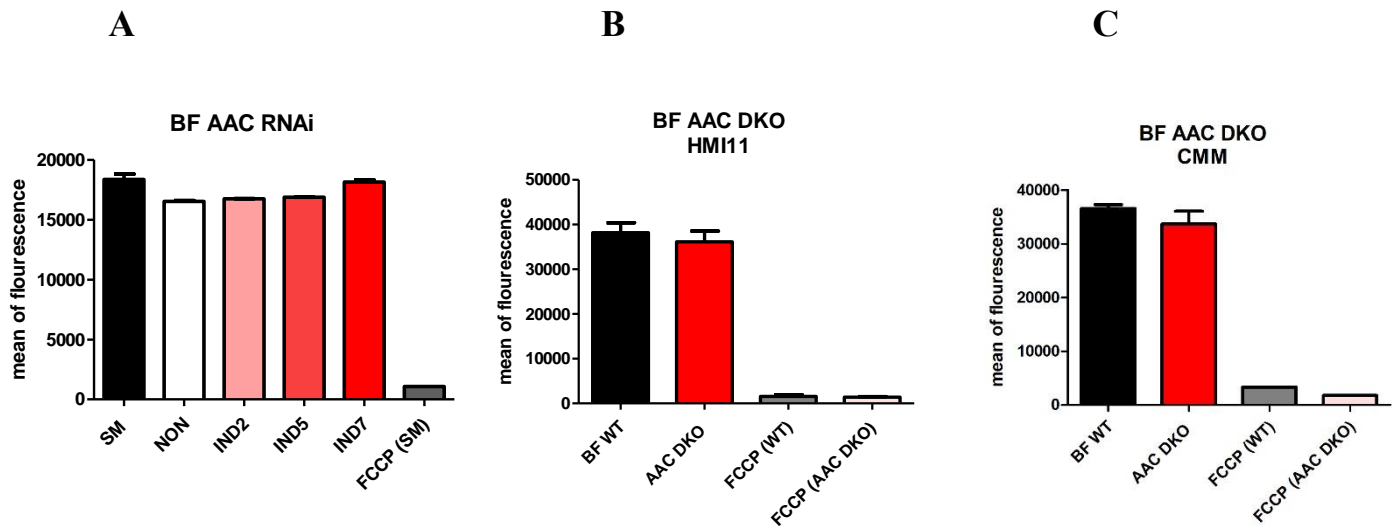


**Fig.6** Measurement of the  $\Delta\Psi_m$  ( $\Delta\Psi_m$ ) by TMRE fluorescence upon AAC loss. (A) AAC RNAi cell line, clone C1 in HMI-11 medium. SM – single marker parental cell line, NON – non-induced RNAi expression, IND 2-7 – days after RNAi induction (s.d., n=3) (B) AAC DKO cell line, clone A2 in HMI-11 medium (s.d., n=3). (C) AAC DKO cell line, clone A2 in CMM medium (s.d., n=3). FCCP (carbonyl cyanide 4-(trifluoromethoxy) phenylhydrazine).

### 3.2.2. Expression levels of SUBPHOS enzymes and F<sub>0</sub>F<sub>1</sub>-ATPase subunits are not affected upon AAC loss.

Considering the potentially important role of SUBPHOS pathways in BF parasites when AAC is lost, we first wanted to examine whether the expression levels of SUBPHOS-related enzymes might change in AAC DKO cells. WT and AAC DKO cells were grown in HMI-11 or CMM medium, and whole cell lysates were collected and analyzed by WB. Membranes were probed with available Abs against SUBPHOS enzymes: threonine dehydrogenase (TDH), acetate:succinate CoA-transferase (ASCT) and succinyl-CoA synthetase (SCoAS) (see Fig.7A-C). WB showed no visible change in protein levels of the SUBPHOS enzymes tested after the loss of AAC in AAC DKO cells compared with parental BF WT, either in HMI-11 or in CMM medium. It should be noted that there is also no change in SCoAS expression levels in WT cells when grown in HMI-11 or CMM medium (see Fig.16A). Since there is no upregulation of the SUBPHOS enzymes expression levels upon AAC loss, this could mean that BF cells already have the required levels of the SUBPHOS enzymes and produce mt ATP independently of AAC, indicating SUBPHOS activity. Nonetheless, it is also possible that the activity, but not the levels of these enzymes, need to be upregulated after the loss of AAC as a compensatory mechanism, but we have no direct means to test this.

Next, we investigated whether the levels of F<sub>1</sub> and F<sub>0</sub> ATPase subunits were altered in AAC DKO cells underscoring the functional interplay and possibly structural interactions between these two entities by possible intermolecular interactions. WB analysis of AAC DKO cells grown in either HMI-11 or CMM medium was performed, and the analysis shows no difference in the expression levels of beta (F<sub>1</sub> subunit), p18 (F<sub>1</sub> subunit), ATPaseTb2 (peripheral stalk subunit) or OSCP (peripheral stalk subunit) (**Fig.7D-G**).

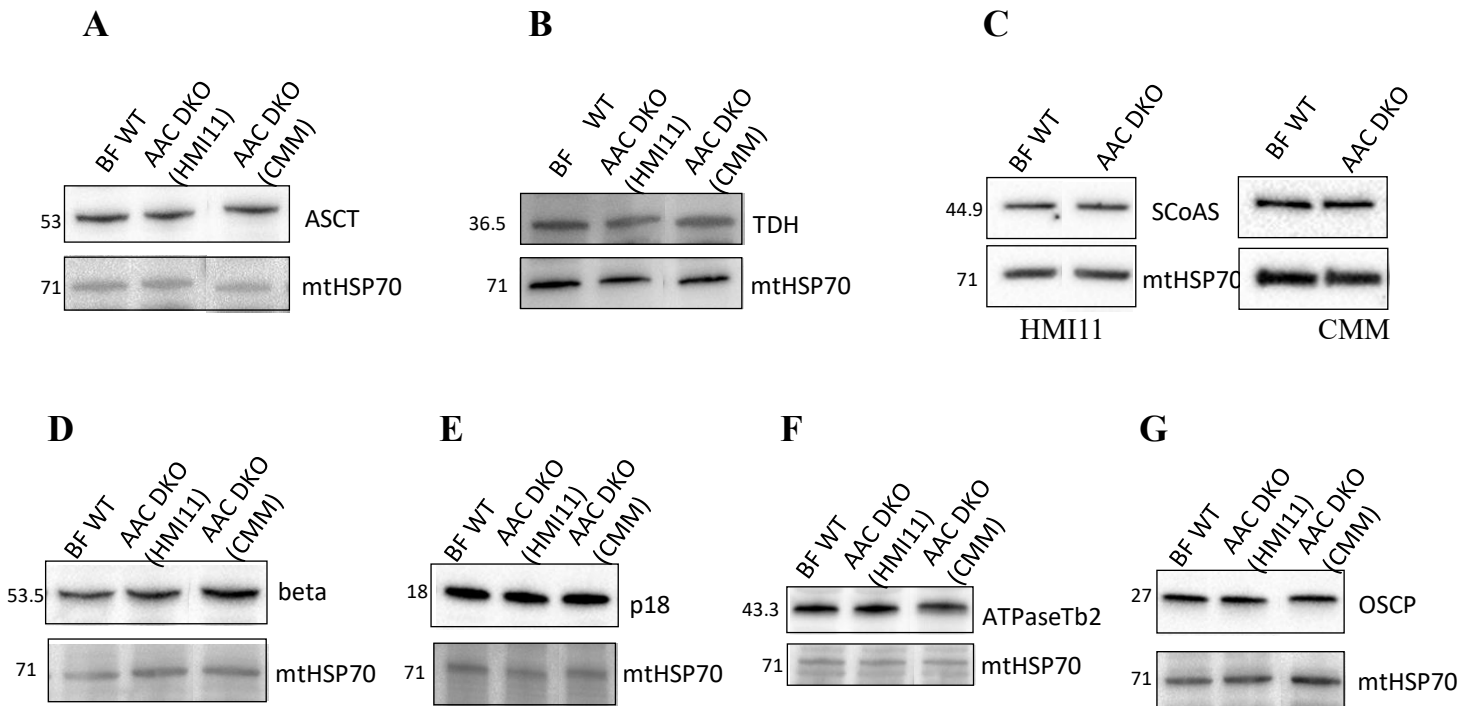


**Fig.7** WB analysis of SUBPHOS enzymes expression (**A, B** and **C**) and F<sub>1</sub> subunits of F<sub>0</sub>F<sub>1</sub>-ATPase (**D, E, F** and **G**). (**A**) ASCT expression in WT in HMI-11, AAC DKO in HMI-11 and CMM. (**B**) TDH expression in WT in HMI-11, AAC DKO in HMI-11 and CMM, (**C**) SCoAS expression in WT and AAC DKO in HMI-11 or in CMM. Lower panel shows protein expression in WT in HMI-11 and AAC DKO in HMI-11 or CMM of beta (**D**), p18 (**E**), ATPaseTb2 (**F**) and OSCP (**G**). mtHSP70 antibody was used as a loading control. Molecular marker shown on the left side in kDa.

### 3.2.3. AAC DKO cells show increased sensitivity towards TPMP, a SUBPHOS II inhibitor

While the expression levels of SUBPHOS enzymes were not altered in AAC DKO cell line (**Fig7A-C**), it does not measure the importance of these enzymes for the parasite. To determine if DKO AAC relies more

on SUBPHOS pathways when compared to BF WT, we performed alamar blue assays to calculate the sensitivity (EC<sub>50</sub> values) of AAC DKO cells towards various SUBPHOS enzyme inhibitors. We used the following inhibitors (**Fig.8A-F**):

- **SUBPHOS I** inhibitors: **UK5099** (2-Cyano-3-(1-phenyl-1H-indol-3-yl)-2-propenoic acid), (Halestrap, 1976), **arsenite** (Sodium (meta)arsenite), (Bergquist et al., 2009), **QC1** (quinazolinecarboxamide compound, (Alexander et al., 2011), **TETD** (Tetraethyl thiuram disulfide), (Linstead & Cross, 1977).
- **SUBPHOS II** inhibitors: **TPMP** (Methyltriphenylphosphonium chloride), (Elkalaf et al., 2016).
- **SUBPHOS I and II** inhibitors: **LY266500** (2-(3-chloro-4-fluorophenyl)-2,3-dihydro-1,2-thiazol-3-one), (Hunger-Glaser, Brun, et al., 1999).

See **table 1** and Materials and Methods section for more detailed information.

AAC DKO cells were grown in HMI-11 media with selectable drugs and at least 24 hours prior to the experiment the drugs were removed. EC<sub>50</sub> was determined and compared between AAC DKO and BF WT cells.

The EC<sub>50</sub> values determined for the WT cells were in the range corresponding to literature values. EC<sub>50</sub> determined for WT cells for the arsenite was 0.33 μM and according to literature for BF trypanosomes IC<sub>50</sub>=0.31μM ((Uzcátegui et al., 2013). The. The values for QC1 WT were 11.37 μM and literature showed IC<sub>50</sub>=7.8μM for BF trypanosomes (Eyram Adjogatse, 2014). EC<sub>50</sub> value for TETD was 9.98 μM, literature showed IC<sub>50</sub>=5.2 μM for BF trypanosomes (Linstead & Cross, 1977). For LY266500 we determined EC<sub>50</sub>=0.27 μM and in the literature - PF trypanosomes IC<sub>50</sub> of 0.6 μM; BF trypanosomes - 28.5 μM; *L. donovani* insect stage 2.86 μM, mammalian stage > 390 mM (Hunger-Glaser et al., 1999). Importantly, we did not observe any difference in the sensitivity of AAC DKO cells compared to WT cells towards arsenite, QC1, TETD or LY266500. (**Fig.8C-F**).

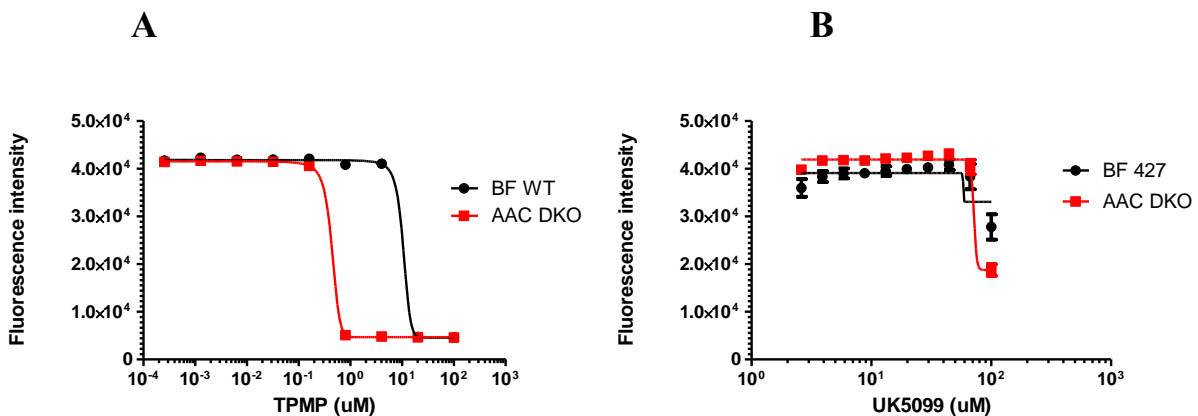
The lack of sensitivity of AAC DKO cells compared with WT cells to arsenite, a pyruvate dehydrogenase complex (PDH) inhibitor, suggests that when pyruvate cannot be converted to acetyl Co-A to feed SUBPHOS I for ATP production, the threonine is most likely compensated by the production of acetyl-Co-A and/or an active SUBPHOS II. Conversely, the lack of sensitivity of AAC DKO cells compared with WT cells to QC1 and TETD, inhibitors of threonine dehydrogenase (TDH), suggests that threonine input is compensated by pyruvate and/or active SUBPPHOS II.

The lack of shift in sensitivity in AAC DKO cells compared with WT to LY266500, a known SCoAS inhibitor, was of concern because inhibition of SCoAS in the background of AAC DKO cells would

potentially involve blockage of ATP production from both SUBPHOS pathways as well as inability to import ATP from the cytosol. It is possible that this inhibitor is not strictly specific to the identified target, but also acts on other molecules. This is supported by the observation that SCoAS DKO cells (see below) have the same sensitivity to LY266500 as WT cells although they completely lack the target of this drug, the SCoAS enzyme.

We were not able to determine the  $EC_{50}$  value for UK5099, inhibitor of mt pyruvate transporter (**Fig.8B**), neither in AAC DKO nor in WT cells. Even at the highest possible concentration of 100  $\mu$ M, the inhibitor was not cytotoxic. The maximum concentration in this case is limited by the solubility of the drug in DMSO and also by the maximum amount of DMSO that can be added to the well. This is probably a controversial result, since the literature presents the sensitivity of *T. brucei* to this drug is described in nM values (BF - 134.6 nM (J Iremonger, BSP 2018, poster 83) and the sensitivity of mouse myoblasts is determined between 10 – 15 nM (Divakaruni et al., 2013).

Interestingly, the sensitivity of AAC DKO cells ( $EC_{50}=0.17 \mu$ M) was increased approximately 30-fold compared to WT cells ( $EC_{50}=5.12 \mu$ M) to TPMP, an  $\alpha$ -ketoglutarate dehydrogenase inhibitor (Elkalaf et al., 2016) (**Fig.8A, table 1**). TPMP inhibits the production of succinyl-CoA from  $\alpha$ -ketoglutarate in the SUBPHOS-II pathway. Because this drug has not been specifically tested on *T. brucei*, its specificity may be questioned. However, AAC DKO parasites expressing an ectopic v5-tagged AAC (a cell line generated by Michaela Husová) had TPMP  $EC_{50}$  levels returned to the sensitivity observed in the BSF 427 cell line (Taleva et al., 2023). This confirms that the increased significance of KgdDH is due to the loss of AAC. The result suggests that AAC DKO is more dependent on at least the SUBPHOS II pathway.



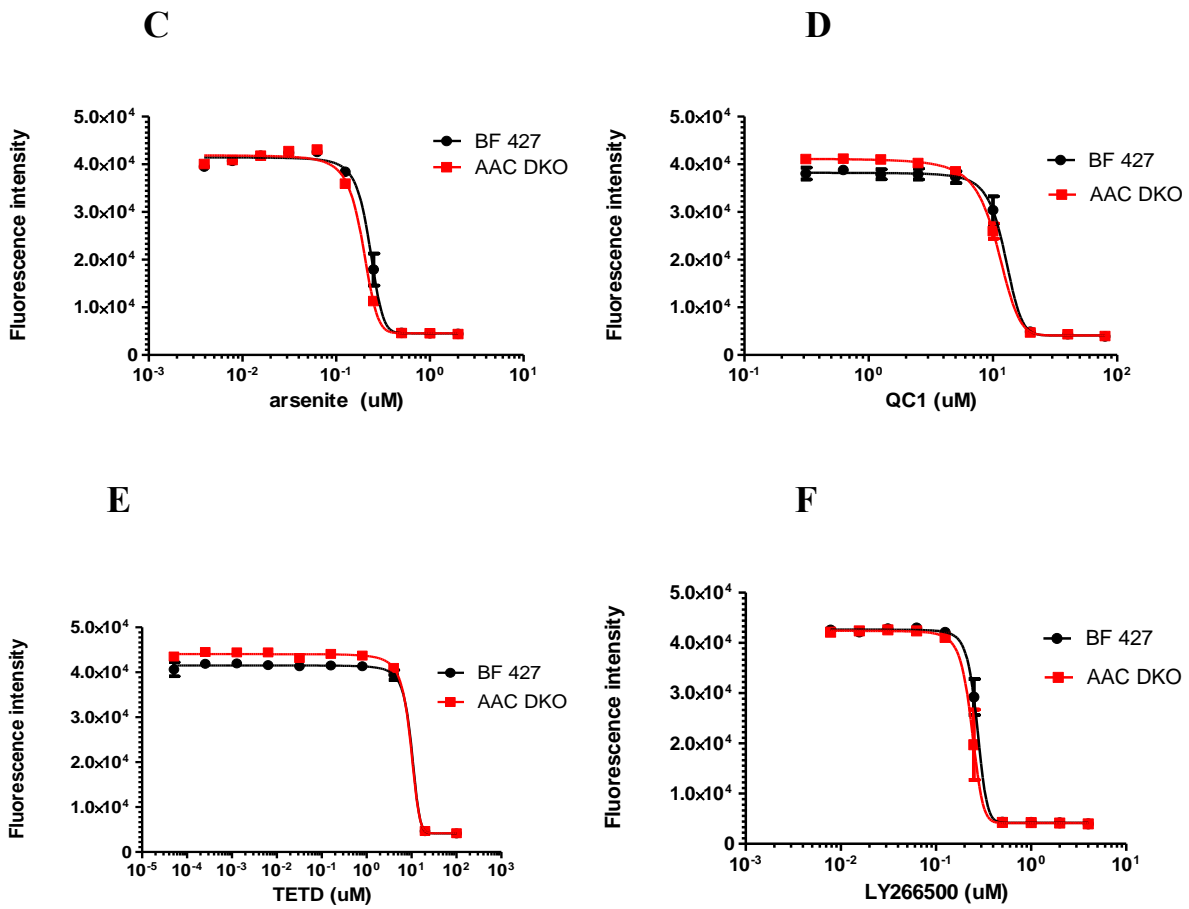


**Fig.8** Alamar blue assay showing sensitivity of BF AAC DKO compared to BF WT towards various SUBPHOS inhibitors (A) TPMP, (B) UK5099, (C) Arsenite, (D) QC1, (E) TETD and (F) LY266500. On the x-axis is show the concentration of the drug in  $\mu\text{M}$ , on the y-axis is the fluorescence intensity. Error bars of 3 technical experiments are shown.

SUBPHOS inhibitor	Main target of the inhibitor	Cell line	EC <sub>50</sub> in $\mu\text{M}$ ( $\pm\text{SD}$ )
<b>TPMP</b>	$\alpha$ -ketoglutarate dehydrogenase (SUBPHOS II)	BF WT	<b>5.12</b> ( $\pm 0.375$ )
		AAC DKO	<b>0.17</b> ( $\pm 0.012$ )
<b>UK5099</b>	mt pyruvate transporter (mt inner membrane, SUBPHOS I)	BF WT	-
		AAC DKO	-
<b>arsenite</b>	pyruvate dehydrogenase complex (SUBPHOS I)	BF WT	0.33 ( $\pm 0.144$ )
		AAC DKO	0.30 ( $\pm 0.160$ )
<b>QC1</b>	l-threonine dehydrogenase (SUBPHOS I)	BF WT	11.37 ( $\pm 1.273$ )
		AAC DKO	9.73 ( $\pm 1.523$ )
<b>TETD</b>	l-threonine dehydrogenase (SUBPHOS I)	BF WT	9.98
		AAC DKO	9.42
<b>LY266500</b>	SCoAS (SUBPHOS I and II)	BF WT	0.27
		AAC DKO	0.24

**Table 1.** EC<sub>50</sub> of at least 2 independent alamar blue experiments (with the exception of TETD and LY266500 where only one experiment was conducted) showing sensitivity of BF AAC DKO compared to BF WT towards various SUBPHOS inhibitors. EC<sub>50</sub> is shown in  $\mu\text{M}$  concentration, SD-standard deviation.

### 3.3. AAC appears to be the only mt ADP/ATP carrier in BF trypanosomes

To exclude the possibility that there is another mt ADP/ATP transporter besides AAC, we assessed whether digitonin-permeabilized AAC DKO cells incubated with ATP can establish the  $\Delta\psi\text{m}$  which is measured by the quenching of the fluorescent dye safranin-O and determined by the Tecan plate reader. In short, WT and AAC DKO cells were pre-incubated in the presence of ATP and safranin-O, and the reaction was initiated by adding 40 $\mu\text{M}$  digitonin to permeabilize only plasma membrane while keeping the mt membrane intact. Therefore, if AAC is the only ADP/ATP carrier in BF trypanosomes, the AAC DKO cells, unlike WT cells, will not be able to establish  $\Delta\psi\text{m}$  because ATP cannot enter the mitochondrion and be hydrolyzed by F<sub>0</sub>F<sub>1</sub>-ATPase. **Fig.9** shows that BF WT cells are able to establish mt  $\Delta\psi\text{m}$  as indicated by the sharp decrease in fluorescence. This is expected since AAC is present, active and imports ATP to the mt matrix. The uncoupler FCCP was added when the  $\Delta\psi\text{m}$  reached plateau and resulted in a rapid membrane depolarization reaching the initial fluorescence levels. In contrast, no significant change in the fluorescence signal was detected in

AAC DKO cells, either upon initiation of the reaction or after addition of FCCP. This indicates that there is no other ATP carrier in AAC DKO cells that can import ATP into the mitochondrion. The veracity of this observation is further supported by experiments performed by my colleague Michaela Husová with the v5-tagged AAC addback cell line in which the AAC gene is expressed from a tubulin gene locus upon the addition of tetracycline. The expression of v5-tagged AAC fully rescued the ability to polarize the inner membrane (Taleva et al., 2023).

In summary, these results suggest that AAC DKO cells are able to produce ATP intramitochondrially, most likely by SUBPHOS pathways.

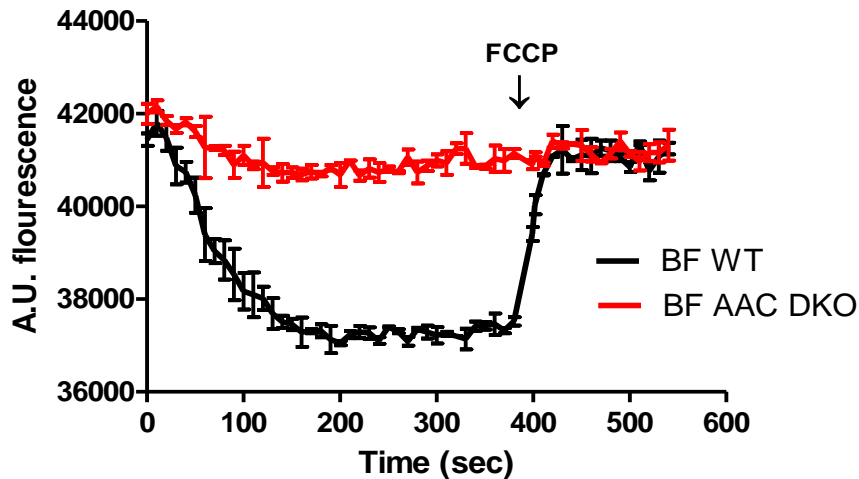


**Fig.9** Membrane potential measurement by quenching mode of Safranin-O. BF WT 427 (in black) and AAC DKO cells (in red) with concentration of  $8.2 \times 10^7$  cells/ml were resuspended in a reaction buffer containing 1mM ATP and 12.5  $\mu$ M safranin O dye to estimate the mt  $\Delta\psi_m$  in situ. The reaction was activated with 40 $\mu$ M digitonin and the fluorescence in arbitrary units was measured by Tecan spectrophotometer every 10 seconds for approximately 9 minutes. After approximately 400 seconds 10 $\mu$ M FCCP was added to dissipate the  $\Delta\psi_m$ . Error bars of 2 experiments are shown.



### 3.4. Succinyl-CoA synthetase (SCoAS) is expressed and active in BF trypanosomes - SCoAS activity assay

Previous data suggest that mt SUBPHOS pathways are potentially active in BF trypanosomes. Succinyl-CoA synthetase (SCoAS) is the only known enzyme in *T. brucei* which is directly involved in the mt ATP production by substrate phosphorylation and it is involved in both SUBPHOS pathways. Therefore, we focus on this enzyme. SCoAS enzyme is responsible for the conversion of succinyl-CoA to succinate which is coupled with ATP synthesis in the mitochondrion. **Fig.10A** shows a schematic of the chemical reaction.

Using a specific SCoAS antibody generated by us we demonstrated by WB (**Fig.7C**) that SCoAS is present and expressed at similar levels in BF WT and AAC DKO. To determine whether the enzyme is active, we developed an SCoAS *in vitro* activity assay. We verified the predicted localization of the enzyme in the mt matrix by WB of fractionated cells (see the Material and Methods). Whole cell lysate (WCL) fraction, the cytosolic (cyto) fraction, the mitochondria-rich organellar (mito) fraction, the mt-insoluble (mito-insol) fraction containing all the organellar membrane debris and the mito-soluble (mito-sol) fraction containing mitochondria matrix-rich proteins were subjected to WB (**Fig.10B**). All the fractions were analyzed for the presence of mtHSP70, a mt marker and APRT, a cytosolic marker. Next, fractions were tested for the presence of SCoAS. In the WT and AAC DKO cell lines mtHSP70 and SCoAS were detected only in the WCL, mito and mito-sol fractions, whereas APRT was found only in the WCL and cyto fractions. These results confirm correct separation of the fractions and localization of SCoAS in the mt matrix.

Next, we measured the SCoAS activity in the mito-sol fraction containing the solubilized mt matrix proteins. In short, we added the substrates for the SCoAS specific reaction (ADP and succinyl-CoA) as well as DTNB (5,5'-Dithiobis 2-nitrobenzoic acid or Ellman's reagent) to the mito-sol fraction. The assay measures the production of Co-A that binds to DTNB, a derived product whose absorbance at 412 nm can be determined using the TECAN plate reader. We also measured the background absorbance (the mito-sol fraction with DTNB only) which was subtracted from the sample absorbance to calculate the specific activity (see Material and Methods). The result presented in **Fig.10C and D** show the absorbance in BF WT (**C**) and AAC DKO cells (**D**) over time. We successfully measured similar SCoAS activity in both BF WT cells ( $23.37 \pm 7.63$  nmoles\*min<sup>-1</sup>\*mg<sup>-1</sup>  $\pm$ SD) and AAC DKO cells ( $18.38 \pm 3.69$  nmoles\*min<sup>-1</sup>\*mg<sup>-1</sup>  $\pm$ SD). With this experiment we demonstrate for the first time that SCoAS is active in BF parasites at least *in vitro*. Furthermore, it is worth mentioning that, as expected, we did not detect any residual SCoAS activity in our SCoAS DKO cell lines (which will be discussed later, **Fig.13**), confirming the reliability of the method.

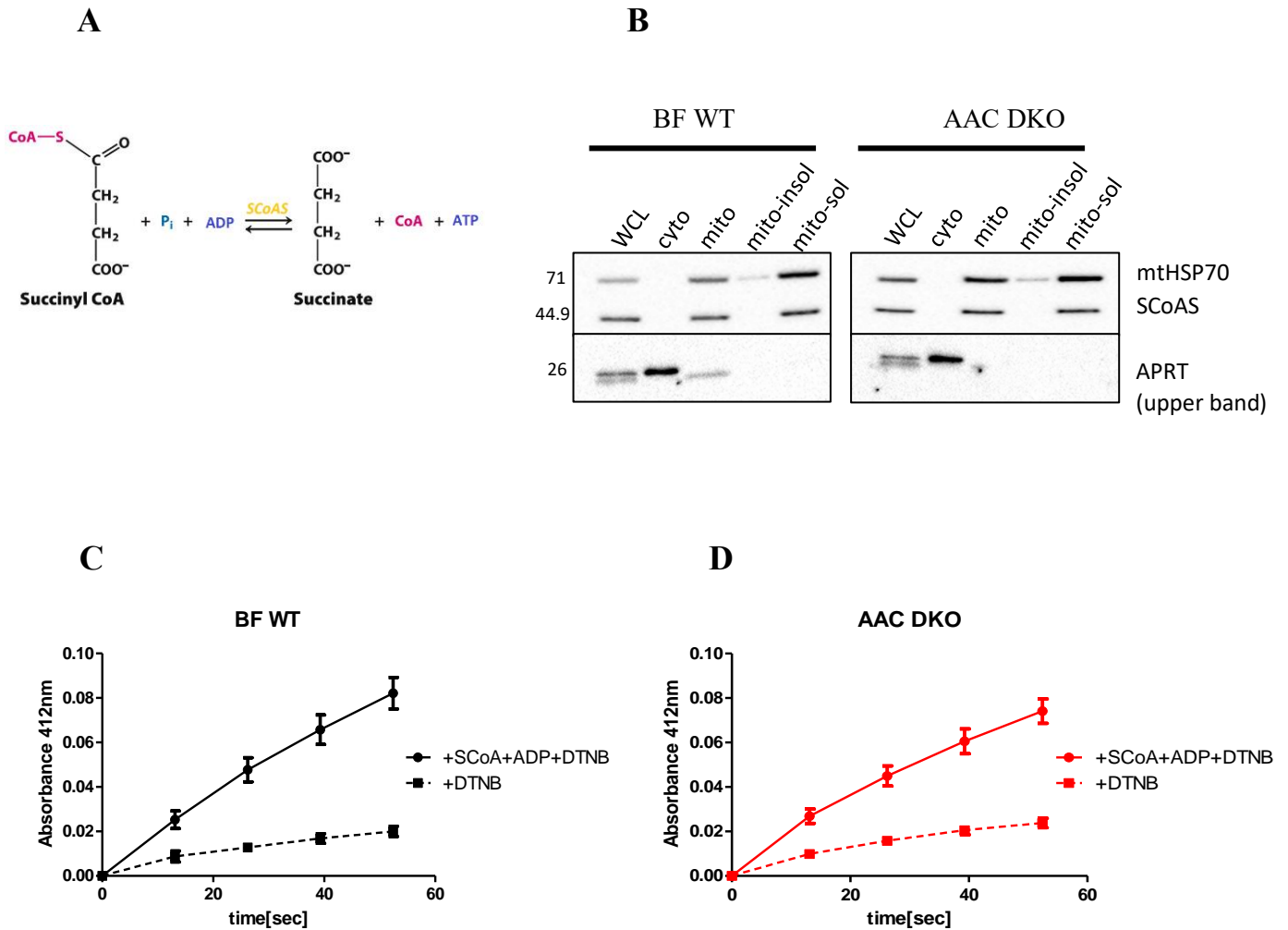


**Fig.10** SCoAS activity assay. **(A)** Schematic representation of the SCoAS chemical reaction producing ATP by SUBPHOS. **(B)** WB analysis of the cellular fractions generated during sample preparation of BF WT and AAC DKO cells. The fractions were tested for the localization of the mtHSP70, SCoAS and APRT proteins. Molecular marker shown on the left side in kDa. **(C)** and **(D)** Activity measured in BF WT **(C)** and AAC DKO cells **(D)**. The increase in absorbance in time represents an active SCoAS enzyme in the sample (+SCoAS+ADP+ DTNB, solid line) compared to the background (+DTNB, dashed line). Error bars of 4 independent experiments are shown.

### **3.5. SCoAS is not essential in BF trypanosomes *in vitro* in standard medium, but becomes potentially important in minimal medium**

Since we have shown that SCoAS is present (**Fig.10B**) and active in the mt matrix of BF cells (**Fig.10C**), next we aimed to determine the consequence of its downregulation. SCoAS is the only known enzyme that directly produces mt ATP by both SUBPHOS pathways. We hypothesize that its ablation will lead to the elimination of intramitochondrially ATP production in BF cells.

#### **3.5.1. SCoAS RNAi cells show growth phenotype in minimal medium**

First, we generated SCoAS RNAi cell line. SCoAS is a dimer, composed of  $\alpha$  and  $\beta$  subunits, each encoded by a single gene (Tb927.3.2230 and Tb927.10.7410, respectively). We chose to downregulate  $\beta$  subunit since in *E.coli* this is the purine nucleotide binding site (Joyce et al., 2000b) and in higher eukaryotes  $\beta$  subunit is believed to determine the substrate specificity of the enzyme (Johnson et al., 1998a). In addition,  $\beta$  subunit of SCoAS has been shown to be highly expressed in BF *T. brucei* and its ablation leads to a significant growth phenotype (Zhang et al., 2010). In short, dsRNAi construct corresponding to 591 bp of the coding region of SCoAS beta was cloned into p2T7-177 plasmid and subsequently electroporated into SM BF *T. brucei* cells, allowing inducible expression of RNAi. The SCoAS RNAi clones were selected by phleomycin resistance. Six clones were obtained, namely B1-B5 and C1. We mainly worked with clone B4.

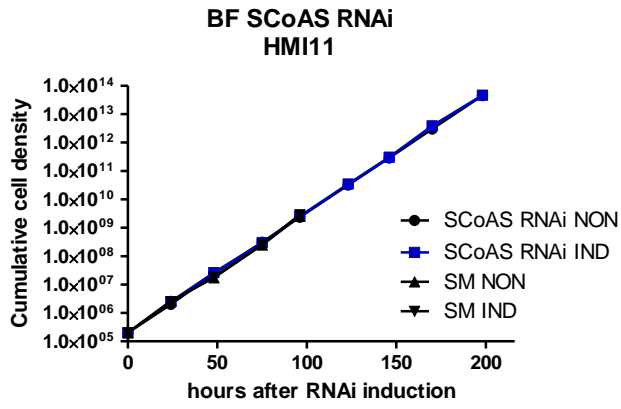
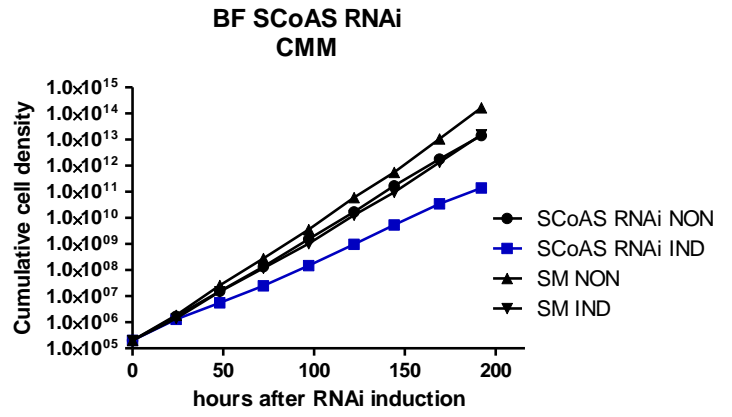
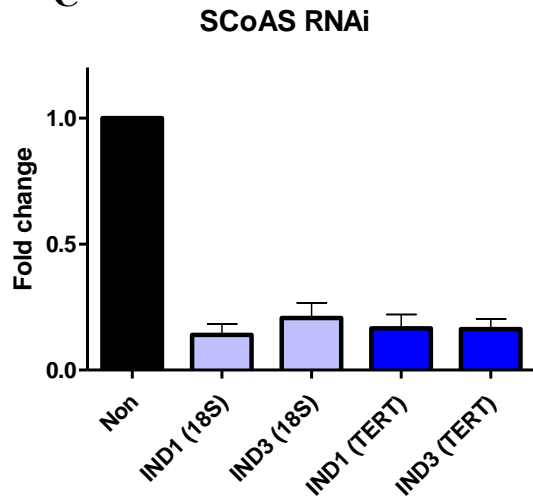
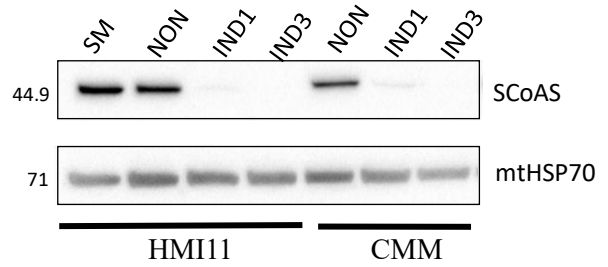
First, we measured the growth rate of all clones obtained in regular HMI-11 medium supplemented with G418 and phleomycin to ensure that the T7 RNA polymerase and tetracycline repressor of the parental SM cell line as well as the integrated RNAi cassette will not be lost during the experiment. We included SM cells as a control (non-induced and induced) grown in the HMI-11 supplemented with G418. **Fig.11A** shows the growth curve for SCoAS RNAi clone B4, but similar results were obtained for the remaining clones (data not shown). Surprisingly, we did not observe any growth defects in HMI-11 medium, and the knockdowns grew at the same rate as the SM cells. In contrast, when SCoAS RNAi was induced in CMM medium supplemented with G418 and phleomycin (**Fig.11B**), we observed small, but significant growth phenotype compared to non-induced cells. It should be noted that parental induced SM cell line grew slightly slower than the non-induced one which could be due to the tetracycline burden. The results show that SCoAS is not essential in BF trypanosomes *in vitro* in standard medium since no growth defect was detected. However, a little growth defect in SCoAS RNAi cells suggests that SCoAS may become potentially important in CMM, an environment closer to the physiological conditions. An explanation could

be that the produced cytosolic ATP is consumed for cellular needs and is not adequately supplied to the mitochondria mt by AAC and the mt ATP pool is decreased due to the downregulation of SCoAS.

Next, the efficiency of RNAi induction in SCoAS RNAi cells was tested on the clones B3 and B4 by qRT-PCR and WB analysis, but only data for clone B4 only are shown as a representative (**Fig 11C and D**). qRT-PCR was performed to determine the levels of the SCoAS mRNA transcripts in the induced cells compared with non-induced cells with the internal reference genes for 18s rRNA and TERT (**Fig.11C**). At day 1 and 3 post-induction, the cells were collected, total RNA was isolated, and cDNA synthesized by RT PCR. The qPCR analysis showed that as early as day 1 postinduction, mRNA levels of SCoAS were significantly reduced compared with non-induced cells (reduced to 14% and 17% using 18S and TERT as a reference, respectively). At day 3, mRNA was reduced to 21% and 16% using 18S or TERT as reference, respectively. The efficiency of SCoAS RNAi was also confirmed by WB analysis (**Fig.11D**, B4 clones shown as a representative result). Cells were grown in either HMI-11 or CMM medium containing the selectable drugs and collected after tetracycline induction on days 1 and 3. It can be observed that in both HMI-11 and CMM medium, protein levels of SCoAS decrease significantly as early as day 1 postinduction compared to non-induced cells, and by day 3 the protein has almost completely disappeared. This, in addition to the qPCR data, indicates that SCoAS was indeed successfully and very efficiently knocked down.

Further, we investigated if the  $\Delta\Psi_m$  is altered upon SCoAS downregulation.  $\Delta\Psi_m$  was measured by TMRE in SCoAS RNAi cell line, clone B4 when tetracycline-induced for 1, 3 and 6 days in HMI-11 (**Fig.11E**) or in CMM (**Fig.11F**). The results show that there is no significant change in the  $\Delta\Psi_m$  in RNAi cell line compared to the non-induced control regardless of the media.

However, even a small trace of residual SCoAS upon downregulation could potentially lead to ATP production by SUBPHOS, explaining the lack of growth phenotype in HMI-11 medium as well as the lack of change in the  $\Delta\Psi_m$  in both media. Therefore, we proceeded to generate SCoAS double knock out cell lines where SCoAS is eliminated.

**A****B****C****D**

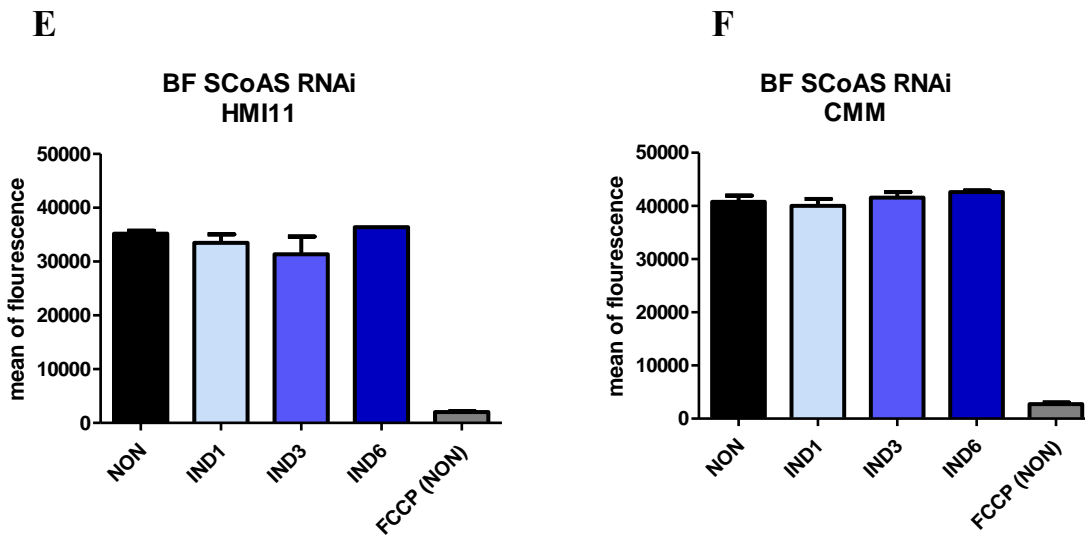


**Fig.11** SCoAS downregulation in BF trypanosomes. **(A and B)** A representative growth curve for SCoAS RNAi cell line clone B4 shown as cumulative cell density in cells/ml measurement for 8 days in HMI-11 **(A)** or CMM **(B)** medium. SCoAS RNAi non-induced (NON) cells are shown in black dots and the tetracycline-induced (IND) cells are in blue squares. SM- single marker parental cell line non-induced (SM NON) shown in black triangles and SM tetracycline-induced (SM IND) are shown in reversed black triangles. **(C)** qRT-PCR analysis on mRNA levels of SCoAS RNAi cell line clone B4 induced for 1 or 3 days shown in fold change compared to non-induced cell line (NON). Data is calculated considering either 18S (light blue) or TERT (dark blue) genes as an internal reference control. Error bars of 3 technical experiments are shown. **(D)** WB analysis of the efficiency of SCoAS downregulation in SCoAS RNAi cell line (clone B4) in HMI-11 (first 4 samples) and CMM (last 3 samples) supplemented with selectable drugs. mtHSP70 antibody was used as a loading control, molecular marker in kDa shown on the left side. **(E and F)** Measurement of the  $\Delta\Psi_m$  by TMRE fluorescence in SCoAS RNAi cell line, clone B4 in HMI-11 medium **(E)** or in CMM **(F)**. SM- single marker, NON – non-induced cells, IND1, 3 and 6 – tetracycline induced cells for 1, 3 and 6 days, respectively. FCCP (carbonyl cyanide 4-(trifluoromethoxy) phenylhydrazone) -  $\Delta\Psi_m$  uncoupler. Error bars represent standard error of at least 3 biological FACS measurements.

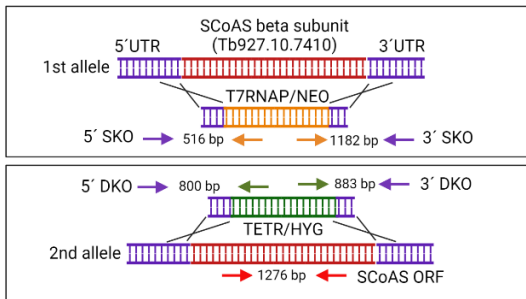
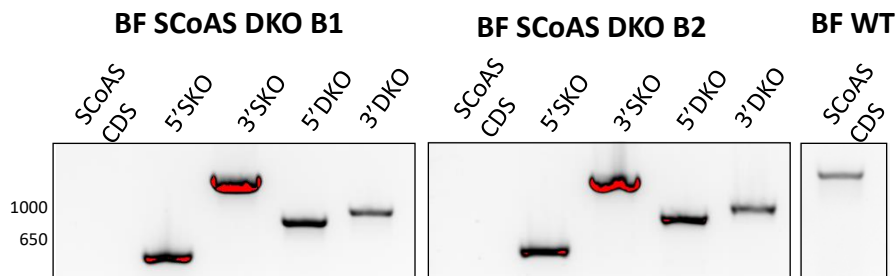
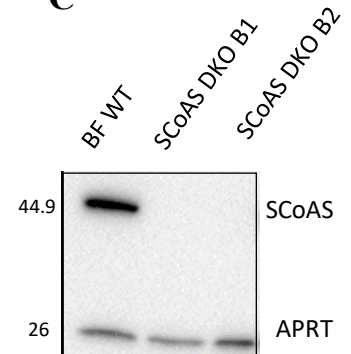
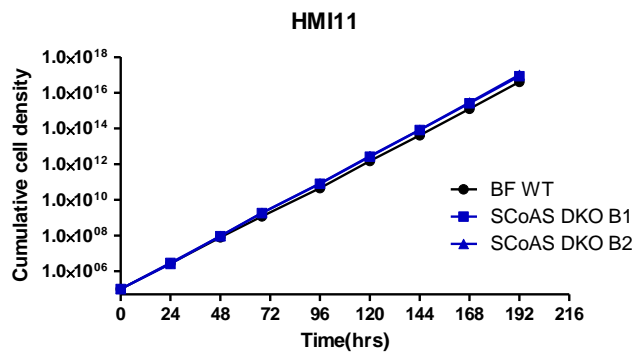
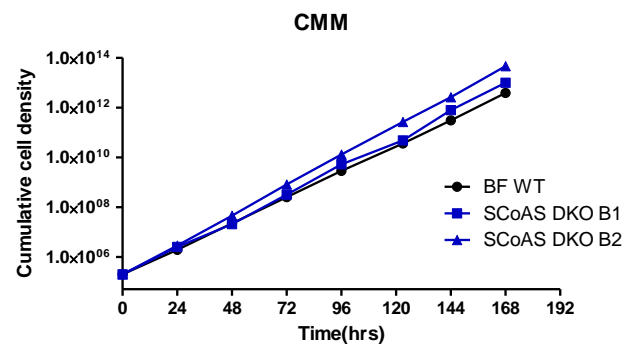
### 3.5.2. SCoAS DKO cell line has no growth defects

BF SCoAS double knock out (DKO) cell line was generated to determine whether SCoAS plays a role in mt ATP production and whether the absence of this enzyme will affect BF mt function. The SCoAS DKO cell line was generated in the same manner as the AAC (**Fig.12A**). The generation of the SKO was successful in the first experiment. We succeeded in generating 6 clones, of which 3 clones were tested by PCR for replacement of the first allele with the gene cassette described below, and all 3 clones were positive. We continued the work with clone B1. The positive SCoAS SKO clone B1 was further transfected to generate DKO cells. The second allelic exchange was also achieved in the first experiment, and we

succeeded in generating five SCoAS DKO clones, two of which (clones B1 and B2) were shown to be SCoAS DKO positive by PCR and WB analysis.

**Fig.12B** shows the PCR verification for SCoAS DKO cell line. Each primer pair, similarly to AAC DKO cell line verification, amplifies genomic region from the genome upstream of the recombination site and from the replacement cassette, thus ensuring the correct position of the integrated cassette. The first allele replacement is verified by 5' (516 bp) and 3' SKO (1182 bp) primer pairs and the second allele replacement by 5' (800 bp) and 3' DKO (883 bp) primer pairs. SCoAS CDS primer pair amplifies 1276 bp region from the SCoAS genes. PCR results show that the integration cassettes have replaced both SCoAS alleles in both clones (B1 and B2) and there is no SCoAS CDS detected in either of the clones. The SCoAS DKO cell line was further verified by WB analysis to ensure the absence of SCoAS protein expression in both B1 and B2 clones (**Fig.12C**). In contrast to BF WT where SCoAS was expressed, no SCoAS protein was detected in SCoAS DKO cells. In conclusion, both PCR and WB results confirm the successful generation of the SCoAS DKO cell line.

Next, we investigated if there is any growth defect in SCoAS DKO cell line. Growth of SCoAS DKOs (clones B1 and B2) was monitored daily for at least seven days in either standard HMI-11 medium (**Fig.12D**) or in CMM medium (**Fig.12E**). In both media no selectable drugs were added during the analysis. The two mutant clones (B1 and B2) did not show any growth phenotype compared to WT in either medium. The lack of growth defects of the SCoAS DKOs in HMI-11 media was not surprising since it correlates with the SCoAS RNAi growth curves. However, in contrast to SCoAS RNAi cell line, the absence of the growth phenotype in CMM medium was rather unexpected. One possible explanation is that DKO cells undergo certain metabolic adaptations due to the lack of SCoAS, whereas the RNAi cell experience a sudden decrease in SCoAS expression after tetracycline induction. Possibly, there is no time to adapt to the decreased levels of SCoAS, which explains the mild growth phenotype of the induced RNAi cells.

**A****B****C****D****E**

**Fig.12** SCoAS DKO BF trypanosomes. (A) A scheme showing the strategy for SCoAS DKO generation. Upper panel – SKO generation (first allele replacement) and the schematic representation of the primer pairs for SKO verification. Lower panel – DKO generation (second allele replacement) and the schematic representation of the primer pairs for DKO verification. (B) PCR verification of SCoAS allele replacement by the integration cassettes of the SKO and DKO as well as the absence of SCoAS CDS in SCoAS DKO cell lines (clones B1, first panel and B2, second panel). BF WT 427 used as a positive control for SCoAS presence,



third panel. (C) WB analysis of lack of SCoAS in SCoAS DKO cells (clones B1 and B2) in contrast to BF WT. APRT antibody was used as a loading control. (D and E) Representative growth curves for SCoAS DKO cell line (clones B1 in blue square and B2 in blue triangle) shown as cumulative cell density (cells/ml) in HMI-11 (D) and CMM (E) medium. BF WT is shown in black dots. In Fig.A and B – molecular marker in kDa is shown on the left side.

### 3.6. $\Delta\Psi_m$ is not changed upon SCoAS loss

Once we generated successful SCoAS DKO mutants we wanted to further characterize them. We checked for any residual SCoAS activity and for change in  $\Delta\Psi_m$  upon SCoAS loss.

#### 3.6.1. SCoAS DKO has no detectable SCoAS activity

To assure there is no residual activity upon SCoAS loss we performed the *in vitro* activity assay in SCoAS DKO cell line. The assay was already explained in the Materials and Methods as well as in **section 3. 4.** The result presented in **Fig.13A** shows the measurements of the absorbance at 412 nm in SCoAS DKO cells clone B1 over time. There was no significant increase in the absorbance suggesting that there is no specific SCoAS activity present in the SCoAS DKO. The lack of any detectable SCoAS activity in BF SCoAS DKO cells shows that when SCoAS is not expressed in BF trypanosomes there is no other mt enzyme that can produce CoA and ATP from succinyl-CoA and thus substitute SCoAS function. The correct localization of the mtHSP70 (mt marker) and APRT (cytosolic marker) demonstrates the validity of the isolated fractions and the lack of SCoAS detection is consistent with the fact that the SCoAS alleles have been successfully deleted and that there is no SCoAS activity in the mt matrix. (**Fig.13A**).

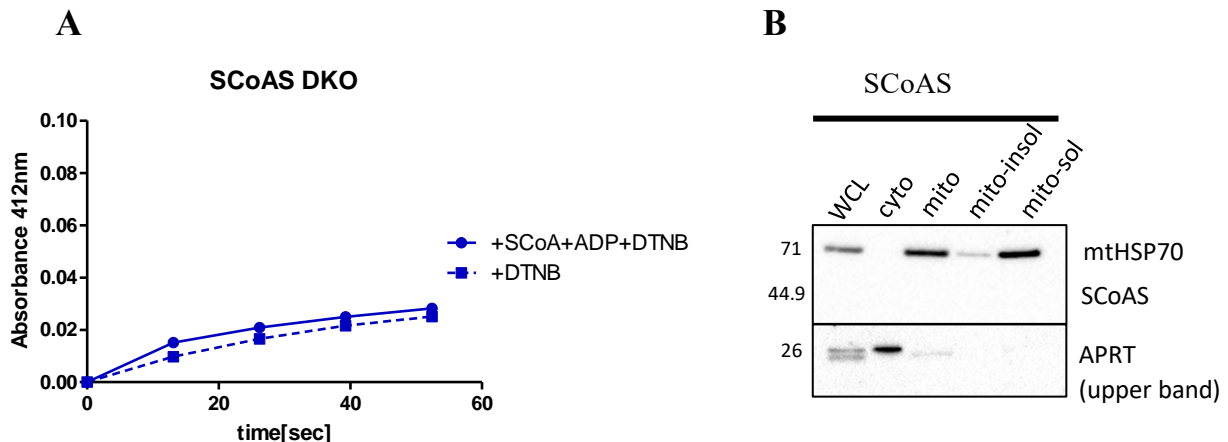


**Fig.13 (A)** SCoAS activity assay in SCoAS DKO cells, clone B1. The increase in absorbance in time represents an active SCoAS enzyme in the sample (+SCoAS+ADP+ DTNB, solid line) compared to the background (+DTNB, dashed line). Error bars of 4 independent experiments are shown. **(B)** WB analysis of the cellular fractions generated during sample preparation of SCoAS DKO cells. The fractions were tested for the localization of the mtHSP70, SCoAS and APRT proteins. Molecular marker shown on the left side in kDa.

### 3.6.2. $\Delta\Psi_m$ was not changed upon SCoAS loss

Further, we investigated if the  $\Delta\Psi_m$  is altered upon SCoAS loss. In **Fig.14**  $\Delta\Psi_m$  was measured by TMRE in SCoAS DKO cell line, clone B1 upon tetracycline induction for 1, 3 and 6 days in HMI-11 **(A)** or in CMM **(B)** medium without the selectable drugs. There was no difference in the  $\Delta\Psi_m$  in the SCoAS DKO cells compared to BF WT 427 parental cell line. It should be mentioned that when  $\Delta\Psi_m$  in SCoAS DKO B1 and B2 clone was compared we found no difference (data not shown).

The fact that we did not observe any decrease in  $\Delta\Psi_m$  was an interesting result, as the AAC DKO data suggested that there should be ATP production in the mitochondria. Thus, it is possible that there is another unknown enzyme in the mitochondrion that is capable of ATP production, and SCoAS DKO takes advantage of this mechanism. A second possible compensatory mechanism is the possible import of ATP from the cytosol by AAC. Considering that the activity and directionality of AAC depends on the mt ADP/ATP ratio, which increases in the absence of SCoAS, this explanation is plausible and will be pursued in a later section.

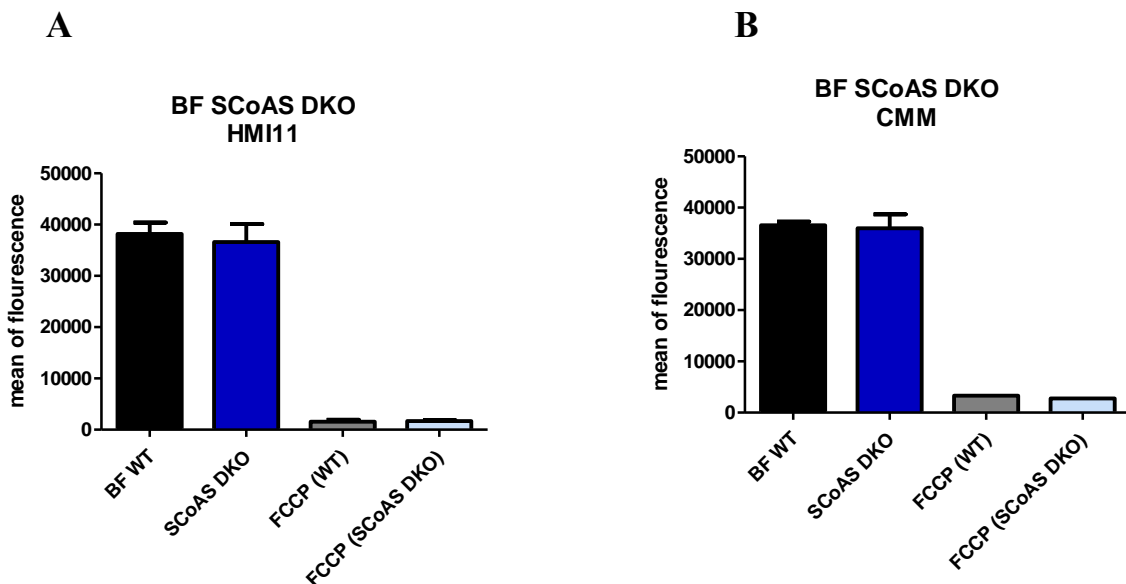


**Fig.14** Measurement of the  $\Delta\Psi_m$  by TMRE fluorescence in SCoAS DKO cell line, clone B1 in HMI-11 medium (A) or in CMM medium (B). Black bars represent BF 427 WT cells, dark blue bars represent SCoAS DKO cells. FCCP (carbonyl cyanide 4-(trifluoromethoxy) phenylhydrazone) -  $\Delta\Psi_m$  uncoupler added to the respective cell line written in brackets. Error bars represent standard error of at least 3 biological FACS measurements.

### **3.7. SCoAS DKO parasites are less virulent in mice than AAC DKO parasites, which are fully virulent**

Both SCoAS and AAC DKO cells grew at normal rates in culture, comparable to WT cells. However, the parasites in culture are not exposed to the same environment as in the mammalian host where the parasites face various different host factors (nutrient fluctuations, immune response, etc.). To test the ability of the parasite to establish infection in the mammalian host, 5-7 female BALB/c mice were infected with an intraperitoneal injection of  $1 \times 10^5$  cells from either BF 427 WT, AAC DKO or SCoAS DKO parasites and a survival curve was plotted (**Fig.15**). The results demonstrate that BF WT parasites developed heavy parasitemia with the need to euthanize all the mice at day 5 or 6 after the infection, which is consistent with the literature (Kodama et al., 2008). AAC DKO cells also developed heavy infection and the infected mice were euthanized at the same times points as WT BF cells (**Fig.15A**). This suggests that AAC activity is not essential for the parasite to establish infection *in vivo*. On the contrary, when mice were infected with SCoAS DKO parasites only 3 mice developed high parasitemia at day 8, one mouse at day 14 and 3 mice were able to clear the infection (**Fig.15B**). The SCoAS DKO addback cell line (Taleva et al., 2023) expressing SCoAS from the tubulin locus was again fully virulent and behaved the same as the BSF 427 parasites. This confirms that the virulence defect was specifically due to the loss of SCoAS.

Since SCoAS DKO parasites are much less virulent compared to WT and AAC DKOs, this indicates that SCoAS is required *in vivo* suggesting that the SUBPHOS pathway may be active in BF *T. brucei* and contribute to the infectivity of the pathogen.

While neither AAC nor SCoAS is essential for BF cells grown in rich culture (HMI-11 medium), it seems possible that the loss of SCoAS, but not AAC, could alter the levels of cellular ATP and impact the ability of the parasite to establish an infection in the more energetically demanding environment of a mammalian host. The data goes in line with the observed slight growth defects when SCoAS RNAi was induced in CMM medium, where the nutrients were scarce and the environment mimics better the bloodstream environment of the parasite.

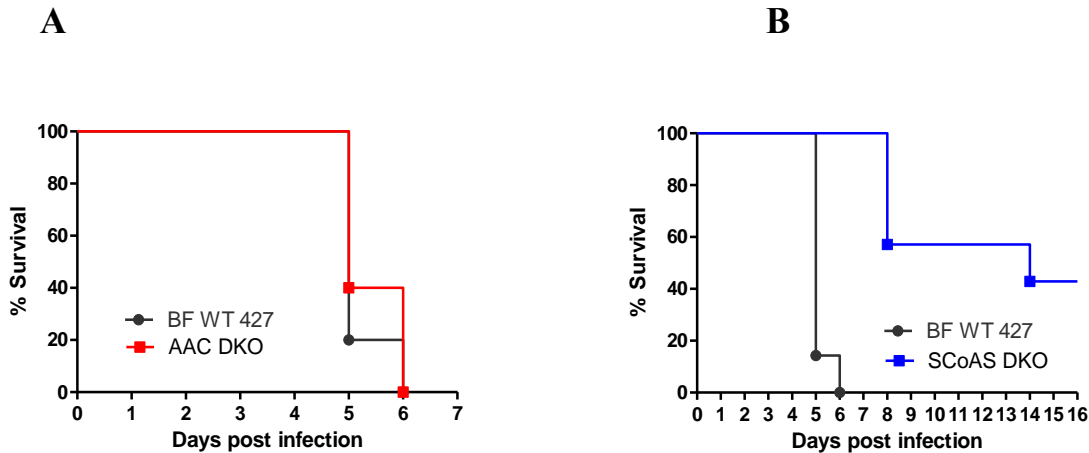


**Fig.15** Mouse survival analysis of 5-7 female BALB/c mice infected with an intraperitoneal injection of  $1 \times 10^5$  parasites (**A**) AAC DKO clone A2 or (**B**) SCoAS DKO clone B1. Mice infected with BF WT 427 were used as a control group (**A and B**). On the x-axis is shown the days after mice infection, on the y-axis is shown the survival of the mice in percentage. The mice were monitored for 20 days.

### 3.8. One clone, but not the other of SCoAS DKO cells become more dependent on the activity of AAC

We have successfully generated SCoAS DKO cell line in BF parasites without any growth defects or alterations in  $\Delta\Psi_m$  in both rich and simplified medium. Since the absence of the mt ATP-producing enzyme has no obvious effect on the fundamental cellular function such division, we aimed to investigate whether there is a compensatory mechanism that allows the cells to supply ATP to the mitochondrion. We also determined that AAC is the only carrier capable of ATP import into the mt matrix. One possible compensatory mechanism could be the increased protein levels or increased activity of AAC. To explore these possibilities, we first examined the AAC protein levels and then the sensitivity of SCoAS DKO cells to carboxyatractylsido (CATR), a well-known AAC inhibitor.

#### 3.8.1. AAC expression levels in SCoAS DKO cells

The protein expression levels of AAC were analyzed in SCoAS DKO cells, clones B1 and B2, by WB. The cells were cultured in either HMI-11 or CMM medium without the selectable drugs. They were collected and analyzed by WB. We found no difference in the expression levels in either clone of SCoAS DKO regardless of the medium (**Fig.16A**).

### 3.8.2. CATR sensitivity in SCoAS DKO cells

Further, we investigated if there is a change in the sensitivity of SCoAS DKO towards CATR, an AAC inhibitor (**Fig.16B**). Alamar blue assay was performed using BF WT 427, AAC DKO and SCoAS DKO cells (clones B1 and B2) in HMI-11 media without the selectable drugs. EC<sub>50</sub> was determined from at least 3 independent experiments.

AAC DKO has no target for CATR, therefore they should be considered CATR insensitive. Its EC<sub>50</sub> was determined to be 0.575 mM. BF WT 427 cells show only twice the higher sensitivity to CATR (0.29 mM ± 0.077 mM) as AAC DKO cells, suggesting that they are also not very sensitive to CATR and therefore not as dependent on AAC activity for mt ATP import. This is in agreement with our AAC DKO data. The significant increase in the sensitivity of SCoAS DKO clone B1 to CATR (0.0189 mM ± 0.003 mM) compared to WT cells indicates that the cells became more dependent on AAC activity after SCoAS loss (approximately 15-fold sensitivity increase). This suggests a possible increase in the activity of AAC to compensate for the lack of mt SUBPHOS ATP production pathways.

In contrast, SCoAS DKO clone B2 had an EC<sub>50</sub> value of 0.222 mM ± 0.06 mM similar to WT. This is a very surprising finding as it suggests that there are more ways how to compensate for the loss of SCoAS. The SCoAS B2 cell line was further investigated by my colleague Michaela Husová in her master's thesis, and it will not be investigated further in this Ph.D. thesis (Husová et al., 2021).

The low sensitivity of BF WT to CATR, followed by the huge increase in sensitivity to CATR in SCoAS DKO clone B1 cells without a detectable change in AAC expression levels, strongly suggests that in BF parasites mt ATP is not primarily provided by the activity of AAC, but is likely produced by mt SUBPHOS. Once SUBPHOS is blocked in SCoAS DKO cells, parasites are more dependent on AAC activity to import the necessary ATP from the cytosol and maintain ΔΨ<sub>m</sub> through F<sub>0</sub>F<sub>1</sub>-ATPase.

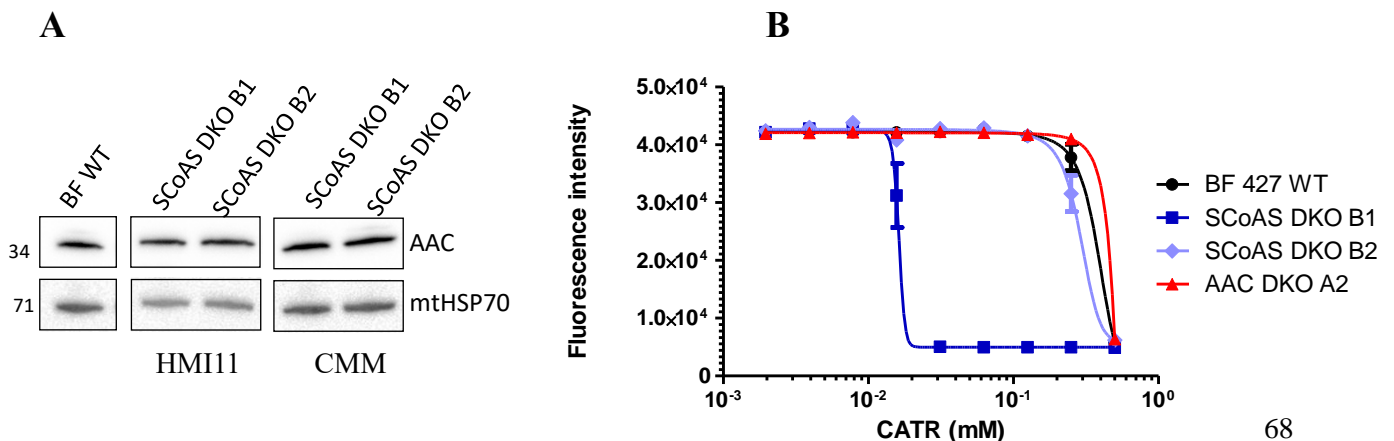


**Fig.16 (A)** WB analysis of BF WT 427, SCoAS DKO B1 and B2 of the AAC expression in HMI-11 or CMM medium. BF WT cells were cultured in HMI-11 medium. Anti-mtHSP70 antibody was used as a loading control. **(B)** Representative graph of alamar blue assay showing sensitivity of SCoAS DKO clones B1 (dark blue) and B2 (light blue) compared to BF WT (black) towards CATR. AAC DKO A2 sensitivity is shown as a negative control in red. On the x-axis is show the concentration of the drug in mM, on the y-axis is the fluorescence intensity. Error bars of 3 technical experiments are shown.

### 3.9. Conditional SCoAS DKO cell line generation

We explain the different sensitivity of SCoAS DKO B1 and B2 clones to CATR by different metabolic adaptations that take place during DKO cell selection. To avoid this period in which the cells adapt to the loss of the protein, we attempted to generate a conditional SCoAS (c)DKO cell line in which we can suddenly switch off the expression of SCoAS and immediately observe the phenotype caused by the decreased expression of SCoAS. SCoAS cDKO cell line was generated from BF 427 WT cells gradually. The first allele was deleted, followed by the introduction of a regulatable copy of SCoAS under the control of tetracycline repressor, and finally, in the presence of tetracycline, the second endogenous allele was deleted.

During SCoAS cDKO generation two clones were generated - AB5 and BB4. Both clones were tested if they are also sensitive to CATR as the SCoAS DKO B1 clone. We tested the sensitivity by alamar blue and the  $EC_{50}$  values are summarized in **Table 2**. The sensitivity of the clone AB5 was similar to WT cells, while the sensitivity of the clone BB4 was 29-folds higher when compared to WT (WT:  $EC_{50} = 0.58 \mu\text{M}$ , SCoAS cDKO BB4 (-TET):  $EC_{50} = 0.02 \mu\text{M}$ ).

These results suggest that only the SCoAS cDKO BB4 clone became dependent on ATP import from the cytosol. The lack of sensitivity of clone AB5 can be explained with either insufficient downregulation of SCoAS in the absence of TET or it may have triggered a similar mechanism to that of the SCoAS B2 clone and maintains  $\Delta\Psi\text{m}$  in the absence of SCoAS and without the involvement of AAC.

Cell line	EC <sub>50</sub> (μM)
BF WT 427	0.58
SCoAS cDKO AB5 (+TET)	0.71
SCoAS cDKO AB5 (-TET)	0.45
SCoAS cDKO BB4 (+TET)	0.31
SCoAS cDKO BB4 (-TET)	<b>0.02</b>

**Table 2.** Sensitivity to CATR: EC<sub>50</sub> values in μM of BF WT, SCoAS cDKO AB5 and BB4 with (+TET) or without tetracycline (-TET) in HMI-11 medium.

The SCoAS cDKO BB4 was tested for the level of expression and regulation of SCoAS in HMI-11 and in CMM medium (**Fig.17A**). Cells were grown in medium without selectable drugs and after 3 days with or without tetracycline exposure, cells were collected and analyzed by WB. The results show that SCoAS cDKO cells express SCoAS in both media when induced (+TET) but to lesser extent than the WT parental cell line. The lower expression can be due to the strong tetracycline repressor which cannot be fully removed by tetracycline or the PARP promoter, a promoter that drives expression of the insect form surface protein, in the plow 79 plasmid is not strong enough to support SCoAS expression at WT level in BF parasites. The lower expression levels of SCoAS cDKO cells when induced (+TET) compared to WT cells may also explain the slight increase in sensitivity to CATR in **Table 2** (EC<sub>50</sub>=0.31μM vs. EC<sub>50</sub>=0.58 μM) and thus higher dependence on AAC.

However, if we compare the SCoAS expression in SCoAS cDKO when it is induced (+TET) and not induced (-TET), we can see that in both media, when tetracycline is absent, no SCoAS is expressed. This shows that the suppression of SCoAS in the non-induced state is very strong and sufficient to completely inhibit SCoAS production. It should be noted that the experiment was also performed in media with selectable drugs, with the same results (data not shown). We performed the experiments without drugs because when grown in CMM with drugs for more than a month the cells very often stop growing and die probably due to extensive cell stress.

Next, we checked how the SCoAS cDKO BB4 clone grows in standard HMI-11 (**Fig.17B**) and in CMM media without selectable drugs (**Fig.17C**). In HMI-11, the non-induced cells showed no growth phenotype compared to the tetracycline-induced and WT cells. However, in CMM medium, non-induced cells (-TET) show significant reduction in growth compared to induced and WT cells. This correlates with the data for the SCoAS RNAi cell line under the same conditions. This suggests that SCoAS appears to be important

for cell growth in a simplified medium where nutrients are limited (representing the blood circulation) and the cell does not have sufficient time to adapt to the loss of SCoAS.

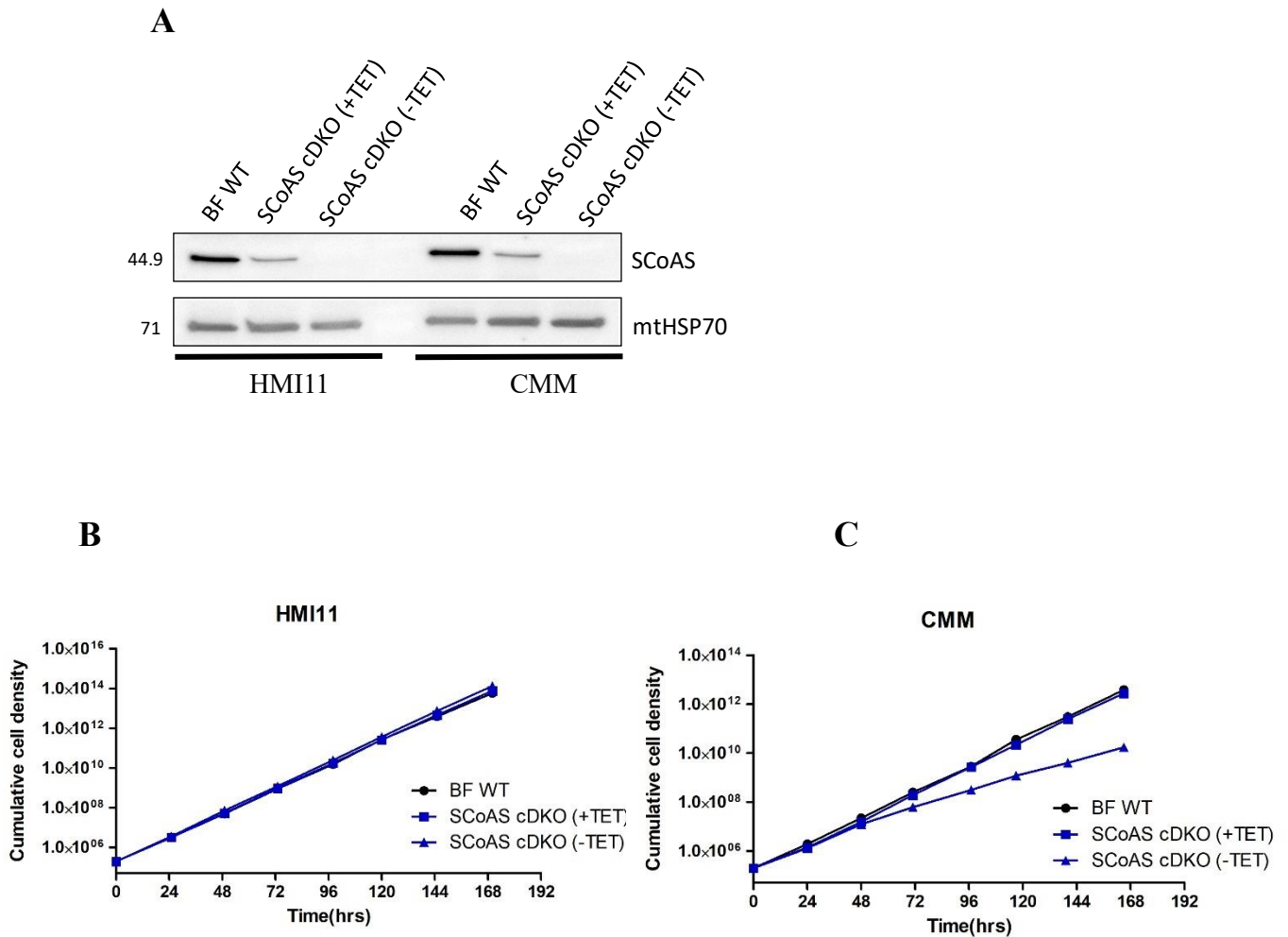


**Fig.17** Conditional SCoAS DKO cell line (clone BB4) in BF trypanosomes. **(A)** WB analysis of the expression and regulation of SCoAS in SCoAS cDKO cells compared to BF WT 427 parental cell line in HMI-11 or in CMM medium without selectable drugs. mtHSP70 antibody was used as a loading control. Molecular marker in kDa is shown on the left side. **(B and C)** Representative growth curves for SCoAS cDKO cell line shown as cumulative cell density (cells/ml) in HMI-11 **(B)** and CMM **(C)** medium. BF WT is in black dots, SCoAS cDKO induced (+TET) is in blue squares and SCoAS cDKO non-induced (-TET) is in blue triangles.



### 3.10. SCoAS DKO/AAC RNAi cell line

Based on our data, we proposed that mt ATP can originate from two different sources, i.e. can be provided by AAC from the cytosol or it can be produced intramitochondrially by SCoAS. Therefore, ablation of both pathways should have a detrimental effect on the cell viability and growth. To test this, we generated a BF cell line in which AAC is downregulated upon tetracycline induction in the background of complete knock-out of SCoAS, SCoAS DKO/AAC RNAi cell line. We obtained four clones, and all were tested for their growth phenotype in HMI-11 media. The clones were induced with tetracycline for 8 days and their growth was compared with the non-induced and the SCoAS DKO B1 parental cell line. Surprisingly, none of the clones tested expressed significant growth phenotype. **Fig.18A** shows a representative growth curve of SCoAS DKO/AAC RNAi clone C2, which exhibited the most pronounced growth phenotype of all clones. The data show that the SCoAS DKO/AAC RNAi induced cells grow slightly slower than the non-induced cells.

Next, we checked the efficiency of AAC downregulation in the SCoAS DKO background. The level of AAC expression was tested on two selected clones by WB analysis. **Fig.18B** shows a representative WB of clone C2. The cells were collected after the tetracycline induction on day 1 and 3. It can be observed that AAC protein levels are decreased compared to non-induced cells with an efficiency of 33% on day 1 and 29% on day 3.

The lack of growth phenotype in the SCoAS DKO/AAC RNAi cell line upon induction can be explained by the insufficient reduction of AAC, which is only down to 29% compared to the downregulation of AAC in the background of BF WT cells, which was down to 8% (**Fig.5B**). This 29% residual AAC expression might be sufficient to supply ATP to the mitochondrion in the absence of SCoAS. Of course, it cannot be excluded that there is another mt metabolic pathway producing ATP that allows the cell to grow normally. It should also be noted that non-induced SCoAS DKO/AAC RNAi were growing slightly slower than the SCoAS DKO B1 parental cell line, pointing at some potential leaky expression of AAC RNAi construct (**Fig.18A**). This is also visible in **Fig.18B** where AAC levels are slightly lower than in the BF WT cells.

In attempt to get potentially tighter regulation and stronger RNAi expression, we repeated the transfection of SCoAS DKO B1 with AAC RNAi, but using AZ0055 stem-loop plasmid. We obtained 6 clones, none of which showed a growth phenotype after RNAi induction (data not shown).

Since 29% residual AAC might be sufficient to supply ATP to the mitochondrion (**Fig.18B**) in SCoAS DKO/AAC RNAi induced cell line, we attempted to generate the reciprocal cell line, RNAi of SCoAS in the background of AAC DKO. We used as a background the AAC DKO A2 which was transfected with

p2T7-177 RNAi plasmid targeting SCoAS mRNA. After 2 transfections we did not obtain viable clones. We can speculate that if the SCoAS RNAi is leaky, i.e. dsRNA is expressed in the absence of tetracycline, this leads to a situation where SCoAS expression is decreased in the background of the AAC DKO and leads to conditions under which it is impossible to survive.

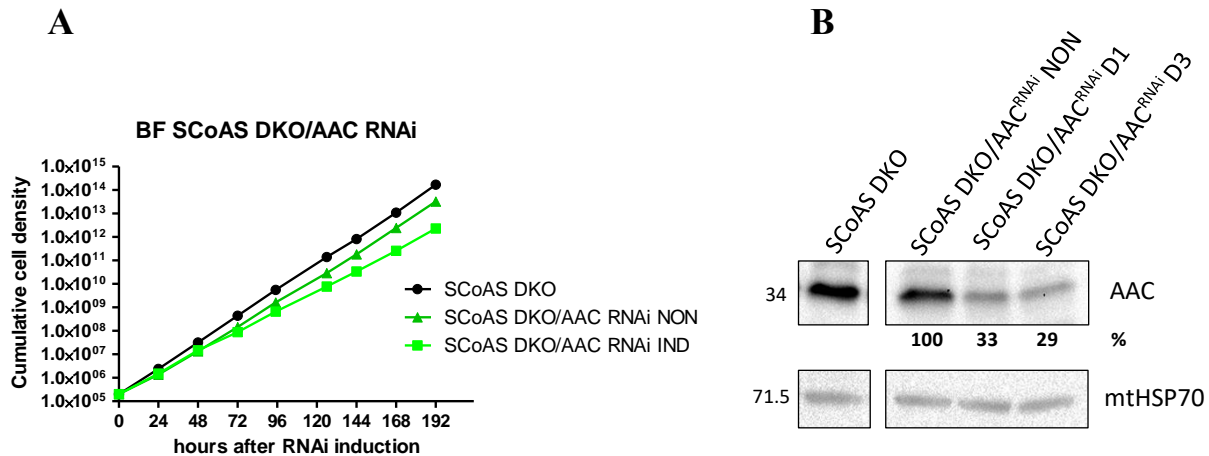


**Fig.18** SCoAS DKO B1/AAC RNAi clone C2 in BF trypanosomes. **(A)** A representative growth curve for SCoAS DKO B1/AAC RNAi clone C2 shown as cumulative cell density (cells/ml) measurement for 8 days in HMI-11 medium. SCoAS DKO B1 parental cell line is shown in black, SCoAS DKO B1/AAC RNAi non-induced (NON) cells are shown in dark green, and the tetracycline-induced (IND) cells are in light green color. **(B)** WB analysis of SCoAS DKO B1/AAC RNAi cell line, clone C2. AAC expression levels were determined after RNAi induction with tetracycline. The levels of AAC are shown in % compared to non-induced cells (100%). SCoAS DKO B1– parental cell line, NON – non-induced RNAi expression, IND D1 and D3 – days after RNAi induction. mtHSP70 used for loading control.  $6.6 \times 10^6$  cells per lane loaded.

### 3.11. Importance of F<sub>0</sub>F<sub>1</sub>-ATPase activity in AAC and SCoAS DKO cell lines

To validate that F<sub>0</sub>F<sub>1</sub>-ATPase is involved in generation of  $\Delta\Psi_m$  in our AAC DKO and SCoAS DKO cell lines, and no other entity complemented for the changes in mt bioenergetics (for example proton pumping activity of complex I), we examined how sensitivity to oligomycin (OLM), specific inhibitor of F<sub>0</sub>F<sub>1</sub>-ATPase, would be affected in the knockouts compared to WT cells and whether inhibition of F<sub>0</sub>F<sub>1</sub>-ATPase would affect  $\Delta\Psi_m$ .

### 3.11.1. Oligomycin sensitivity in AAC DKO and SCoAS DKO cells

First, we performed alamar blue assay to calculate  $EC_{50}$  values towards the  $F_0F_1$ -ATPase inhibitor OLM for AAC DKO, SCoAS DKO (clone B1) and WT BF cells. The cells were grown in HMI-11 media with selectable drugs and at least 24 hours prior to the experiment the drugs were removed. **Fig.19A** shows the graphical representation of the experiment and **Fig.19B** shows the table with the calculated  $EC_{50}$  values. Our results demonstrate that AAC DKO cells are 2.6-folds more sensitive towards OLM compared to WT cells ( $EC_{50}=0.16 \mu\text{g/ml}$  vs.  $EC_{50}=0.41 \mu\text{g/ml}$ ). This can be explained by the activity of AAC, which, if it imports ATP, contributes to the generation of  $\Delta\Psi_m$ , ( $ATP^{4-}/ADP^{3-}$  exchange is electrogenic). Therefore, when AAC is absent, the activity of  $F_0F_1$ -ATPase makes up for this missing part of  $\Delta\Psi_m$ .

One would expect that in SCoAS DKO cell line in which AAC electrogenically contributes to the  $\Delta\Psi_m$  and the cells are therefore, not as dependent on  $F_0F_1$ -ATPase activity compared to WT cells, a decrease in sensitivity would be expected. Surprisingly however, we found almost no difference in the sensitivity of SCoAS DKO cells compared to WT cells to OLM ( $EC_{50}=0.44 \mu\text{g/ml}$  vs.  $EC_{50}=0.41 \mu\text{g/ml}$ ).

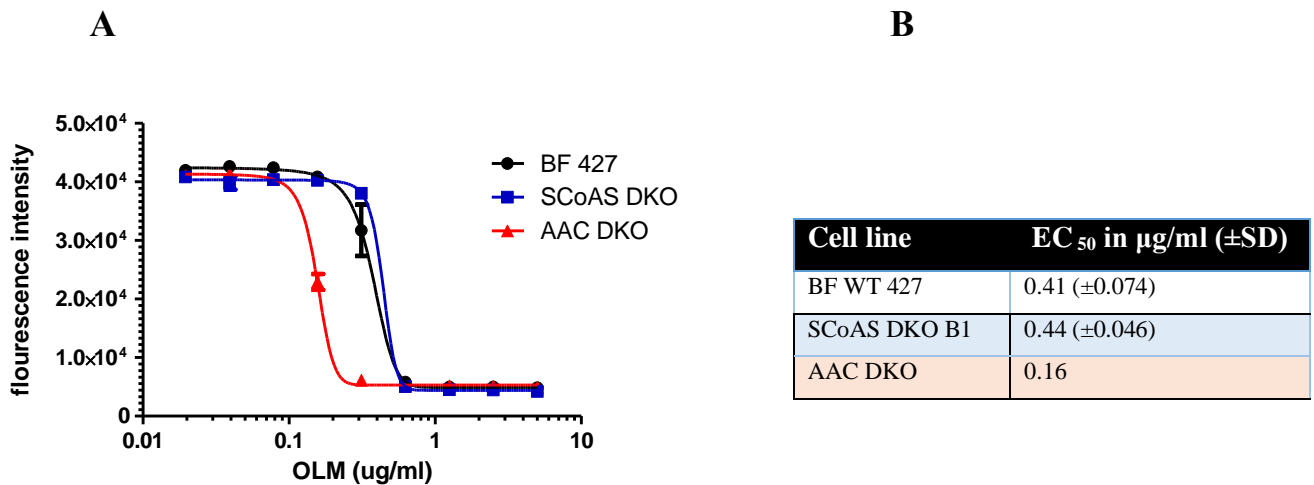


**Fig.19** (A) Alamar blue assay showing sensitivity of SCoAS DKO clone B1 (blue) and AAC DKO (red) compared to BF WT (black) towards OLM. On the x-axis is show the concentration of the drug in  $\mu\text{g/ml}$ , on the y-axis is the fluorescence intensity. Error bars of at least 3 technical experiments are shown. (B) Calculations of the  $EC_{50}$  of at least 2 independent alamar blue experiments (with the exception of AAC DKO cells where only one experiment was conducted) showing sensitivity towards OLM of the respective cell line.  $EC_{50}$  is shown in  $\mu\text{g/ml}$  concentration, SD-standard deviation.

### 3.11.2. $\Delta\Psi_m$ is OLM sensitive in AAC DKO cells

Although the data from the previous experiment indicate that AAC DKO cells are still dependent on  $F_0F_1$ -ATPase activity, we wanted to verify whether  $F_0F_1$ -ATPase is responsible for the generation of  $\Delta\Psi_m$  similarly to BF WT 427 cells. To this end, we measured  $\Delta\Psi_m$  in the cell lines after OLM treatment (**Fig.20A**). In short WT, AAC DKO and SCoAS DKO (B1 clone) were grown in standard HMI-11 medium without the selectable drugs at least 24 hours prior to the experiment. OLM inhibitor was added to the cell cultures at two different concentrations (250 ng/ml and 500 ng/ml) and the cells were incubated for 24 hours under standard conditions. The viability of the cells was observed under a light microscope and the doubling time was calculated based on cell numbers determined after 24 hours. (**Fig.20B**). Concentrations higher than 500ng/ml were not used as the cells already looked less fit at these concentrations and their doubling time increased, especially in the AAC DKO cells. Subsequently, the  $\Delta\Psi_m$  was measured using TMRE as described in Materials and Methods. **Fig.20A** shows the results as a percentage of the non-treated cells (NON), cells without being exposed to the OLM. Since WT, AAC DKO and SCoAS DKO cells have similar measurements for the  $\Delta\Psi_m$  in standard medium (see **Fig.6B** and **Fig.14A**), non-treated cells were considered 100%. When AAC DKO cells are treated with the same concentration of 250 ng/ml OLM as WT cells we can see that the decrease in  $\Delta\Psi_m$  is greater than in the WT cells (42.3% vs.77.3%). At the concentration of 500 ng/ml OLM the  $\Delta\Psi_m$  decreased even more (36.4% vs. 49.2%). The results indicate that in AAC DKO cells the  $\Delta\Psi_m$  is still maintained by the activity of  $F_0F_1$ -ATPase and the cells are even more dependent on  $F_0F_1$ -ATPase for the generation of  $\Delta\Psi_m$  than WT cells. On the other hand, SCoAS DKO cells show considerably less decrease in the  $\Delta\Psi_m$  compared to WT cells when treated either with 250 ng/ml OLM (93.6% vs. 77.3%) or with 500 ng/ml OLM (78.7% vs. 49.2%). It demonstrates that  $\Delta\Psi_m$  of SCoAS DKO cells is less sensitive to inhibition of  $F_0F_1$ -ATPase  $\Delta\Psi_m$  when compared to WT cells. Considering that the SCoAS DKO B1 clone is more sensitive to the AAC inhibitor CATR, it is possible that the higher activity of AAC contributes more to the generation of  $\Delta\Psi_m$  and therefore its levels are less sensitive to OLM treatment. Unfortunately, this experiment was not performed in the presence of CATR which would allow us to better understand the contribution of AAC and  $F_0F_1$ -ATPase to  $\Delta\Psi_m$  in our cell lines.

In conclusion, our results indicate that AAC DKO cells as well as their  $\Delta\Psi_m$  are more sensitive to OLM treatment suggesting that AAC contributes to the  $\Delta\Psi_m$  in WT BF cells through its electrogenic activity. Surprising results were obtained with the SCoAS DKO cells, which have the same  $EC_{50}$  value for OLM as WT cells, although their  $\Delta\Psi_m$  is less sensitive to OLM treatment. This can be explained by increased AAC activity contributing to the  $\Delta\Psi_m$  and it is consistent with the data in **Fig.16B** showing the increased sensitivity of SCoAS DKO (clone B1) to CATR and therefore increased dependence on AAC.

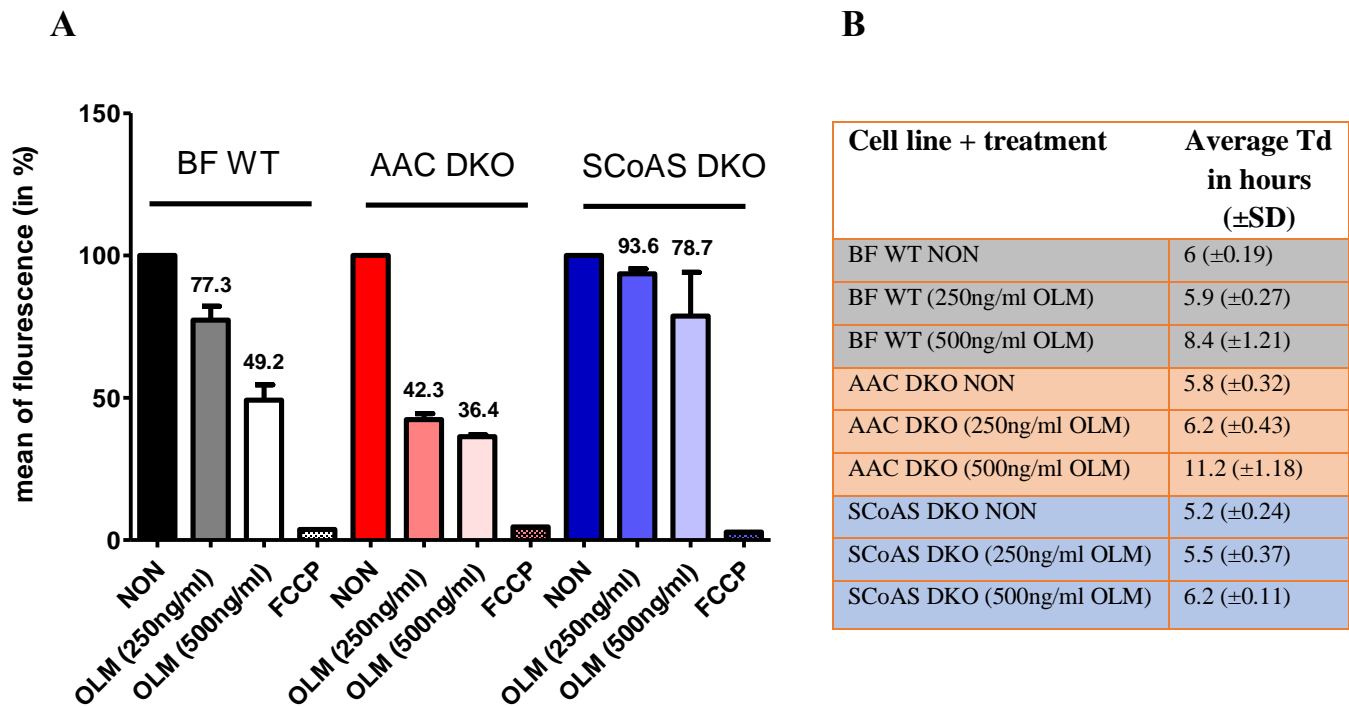


**Fig.20** (A) FACS Measurement of  $\Delta\Psi_m$  by TMRE fluorescence shown as a percentage of the nontreated (NON) cells after treatment with oligomycin (OLM) for 24 hours with 250ng/ml or 500ng/ml. The first 4 columns from black to white represent BF WT cells, the following 4 columns from red to pink represent AAC DKO cells and the last 4 columns from blue to light blue represent SCoAS DKO (B1 clone). FCCP-  $\Delta\Psi_m$  uncoupler used as a negative control in the respective cell line. Error bars represent standard error of 2 biological FACS measurements. The values above the columns show the mean of fluorescence in percentage. (B) Doubling time (Td) shown in hours of BF WT, AAC DKO or SCoAS DKO (B1 clone) either nontreated (NON) or after treatment with oligomycin (OLM) for 24 hours with 250ng/ml or 500ng/ml. SD – standard deviation of 2 independent experiments.

### 3.12. ATP measurements indicate a contribution of SCoAS to the mt ATP pool

To determine whether cellular and mitochondria ATP concentrations levels are affected in the AAC DKO and SCoAS DKO mutants, we implemented two independent approaches. The first approach relied on direct measurements of ATP in the sample using commercial kits, and the second approach relied on measurements of ATP levels in intact living cells using a genetically encoded ATP sensor, the luciferase.

### 3.12.1. *In vitro* ATP measurements

For the purpose of *in vitro* ATP measurements, our AAC DKO and SCoAS DKO mutants as well as BF WT as a control were used. In short, the cells were subjected to subcellular fractionation with digitonin (see Materials and Methods) providing us with two fractions, cytosolic and mt. It should be noted that mt fraction contains genuinely all organelles, nevertheless mitochondrion is considered to have the highest ATP levels among the different organelles and we considered this fraction as mt. In addition, we also prepared a fraction containing the whole cell material to measure total ATP levels. The ATP levels in all three fractions were measured using ATP Bioluminescence Assay Kit HS II (Roche). In **Fig.21A**, the total cellular ATP concentration in AAC DKO cells was measured to be 0.73  $\mu\text{M}$  which was almost the same as for the BF WT cells (0.74  $\mu\text{M}$ ). On the other hand, the total cellular ATP concentration in SCoAS DKO cells was considerably lower, 0.46  $\mu\text{M}$ , which can imply that SCoAS contributes considerably to the total ATP pool. In **Fig.21B** the cytosolic ATP concentration in SCoAS DKO cells was measured to be 0.26  $\mu\text{M}$  which was similar to the concentration of the BF WT cells (0.30  $\mu\text{M}$ ). The cytosolic ATP concentration in AAC DKO cells was significantly higher (0.65  $\mu\text{M}$ ) implying that when AAC is absent ATP accumulates in the cytosol and this suggests that normally AAC participates in supplying BF mitochondrion with ATP. Lower than WT levels in the mt fraction are also seen in SCoAS DKO cells (**Fig.21C**) which would again suggest that SCoAS contributes to the mt ATP pool, however the values are at the limit of the detection therefore we cannot be fully confident with the mt ATP data. Consequently, we further continue with measuring ATP levels *in vivo*.

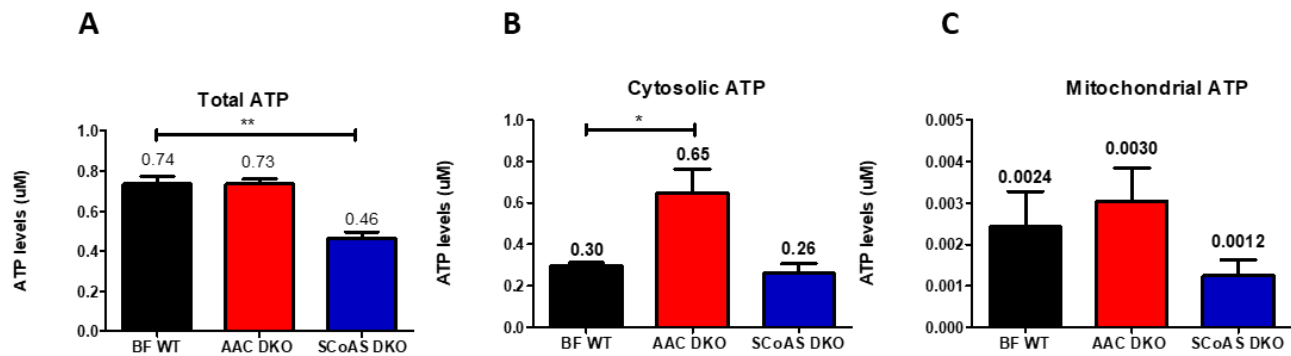


**Fig.21** *In vitro* measurement of ATP concentration using ATP Bioluminescence Assay Kit HS II (Roche) on whole cells (A), digitonin subcellular fractions cytosolic (B) and organellar (C) fractions. Error bars represent standard error of at least 2 independent experiments. statistical analysis performed- Mann Whitney test.\*-P value significant (0.01 to 0.05) \*\*-P value very significant (0.001 to 0.01).

### 3.12.2. *In vivo* ATP measurements

To measure ATP content in living and intact cells *in vivo*, we have developed for the first time a system based on the expression of luciferase targeted to the cytosol or mitochondrion (see Materials and Methods). In short, we have stably expressed firefly luciferase in which we removed the PTS (peroxisomal targeting sequence) and added a C-terminal 3 V5 tag for easier identification. We assume that the luciferase produced from this construct will remain in the cytosol of the transfected cells for a cytosolic ATP evaluation. We have additionally generated another luciferase construct in which we have added an N-terminal MTS (mt targeting sequence) of TbIscU (*T. brucei* iron-sulfur cluster assembly protein) (Mach et al., 2013). We expect the luciferase from this construct to be localized in the mitochondrion of the transfected cells. It should be mentioned that we also tried to use as MLS the predicted mt localization signals from F<sub>o</sub>F<sub>1</sub>-ATPase subunits ( $\alpha$ ,  $\beta$ ,  $\delta$ ,  $\epsilon$  and p18) as well as MLS1 from TAO (Trypanosoma alternative oxidase) (Hamilton et al., 2014). In all these cases, targeting was never efficient enough because different amounts of luciferase remained in the cytosol (data not shown).

The two constructs, luciferase-3V5 (cytosolic luciferase expression) and TbIscU-luciferase-3V5 (mt luciferase expression) were designed for a constitutive expression and they were transfected into our AAC DKO and SCoAS DKO (clone B1) and into in BF WT cells. The transfectants showed no growth or morphological defects. We also checked by WB the localization of the luciferase products (**Fig.22**). BF WT, AAC DKO and SCoAS DKO expressing cytosolic and mt luciferase were subjected to subcellular fractionation with digitonin. The collected fractions WCL (whole cell lysates), Cyto (cytosolic) and Org (organellar) were analyzed by WB for the expression of luciferase with anti-V5 Ab (upper bands in **Fig.22A** and **B**). It is clear that luciferase is almost entirely localized in the correct fraction – cytosolic luciferase in the cytosol (and WCL) and mt luciferase in the organellar fraction (and WCL). To verify the correct fraction isolation, we tested for the presence of specific protein markers for each fraction – APRT as a cytosolic and mtHSP70 as a mt marker.

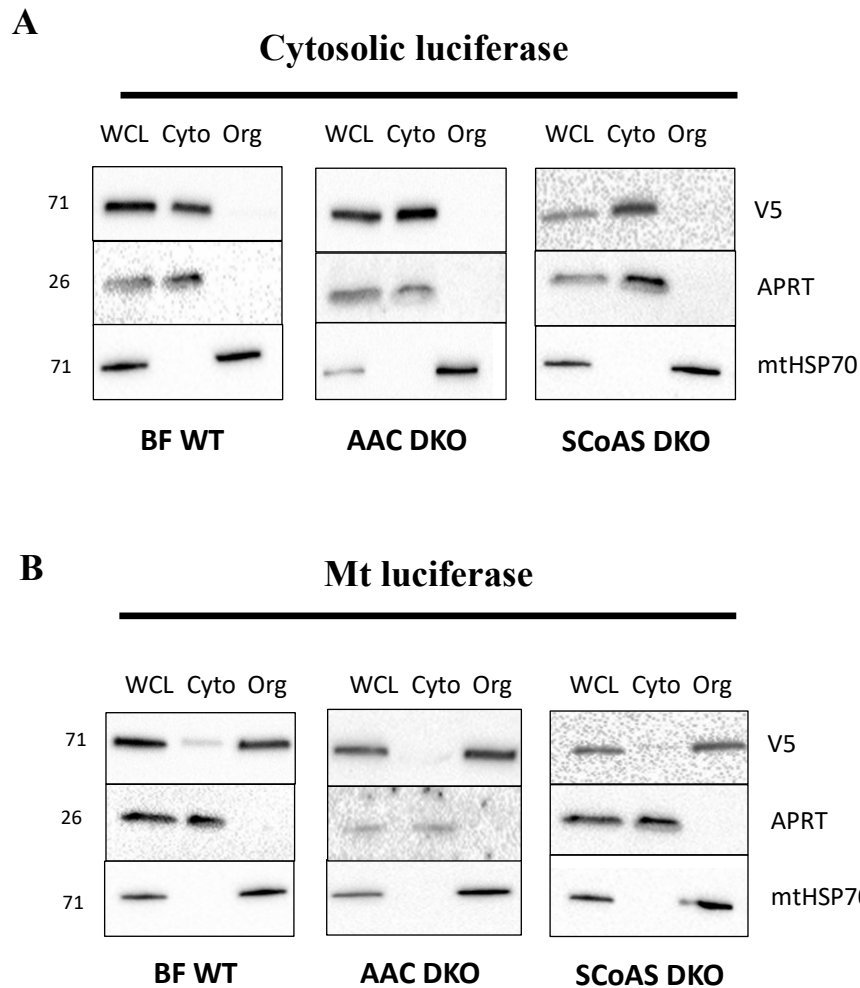


**Fig.22** WB analysis of BF WT, AAC DKO and SCoAS DKO (B1 clone) for cytosolic localization (**A**) or mt localization (**B**) of V5-tagged luciferase after subcellular fractionation (WCL – whole cell lysate, Cyto – cytosolic fraction, Org – organelle fraction). Anti-V5 Ab used to track the luciferase expression with expected size of the tagged product 71 kDa, anti-APRT Ab for a cytosolic control, mtHSP70 Ab used for a mt control. On the left are shown the molecular marker in kDa.

After verifying the correct localization of the cytosolic and mt luciferase in all transfected cell lines (i.e. BF WT, AAC DKO and SCoAS) we further determined the expression levels in order to compare the *in vivo* ATP levels in the transfected cell lines. For this purpose, we performed WB analysis in the cells expressing either mt or cytosolic luciferase using V5 antibody (**Fig.23A**). We used precast gels from Bio-Rad with stain-free technology that allowed us to normalize the luciferase expression to the total protein content. The protein content in the stain-free precast gel is shown in **Fig.23B**. **Fig.23C** shows the normalized expression



levels of luciferase directed to either the cytosol or the mitochondrion compared to the BF WT cells. We assigned a value of 1 for both cytosolic and mt BF WT luciferase expression. The relative levels of mt luciferase in the AAC DKO and SCoAS DKO cells are very similar to the mt expression levels in the BF WT cells (1.15 for AAC DKO and 1.17 for SCoAS DKO). The same is true for the cytosolic luciferase in AAC DKO (1.01) and SCoAS DKO (1.01) compared to BF WT cytosolic expression. Later, the experiment was performed in biological triplicates showing that the expression levels are comparable allowing comparison of ATP-dependent bioluminescence signals between the cell lines.

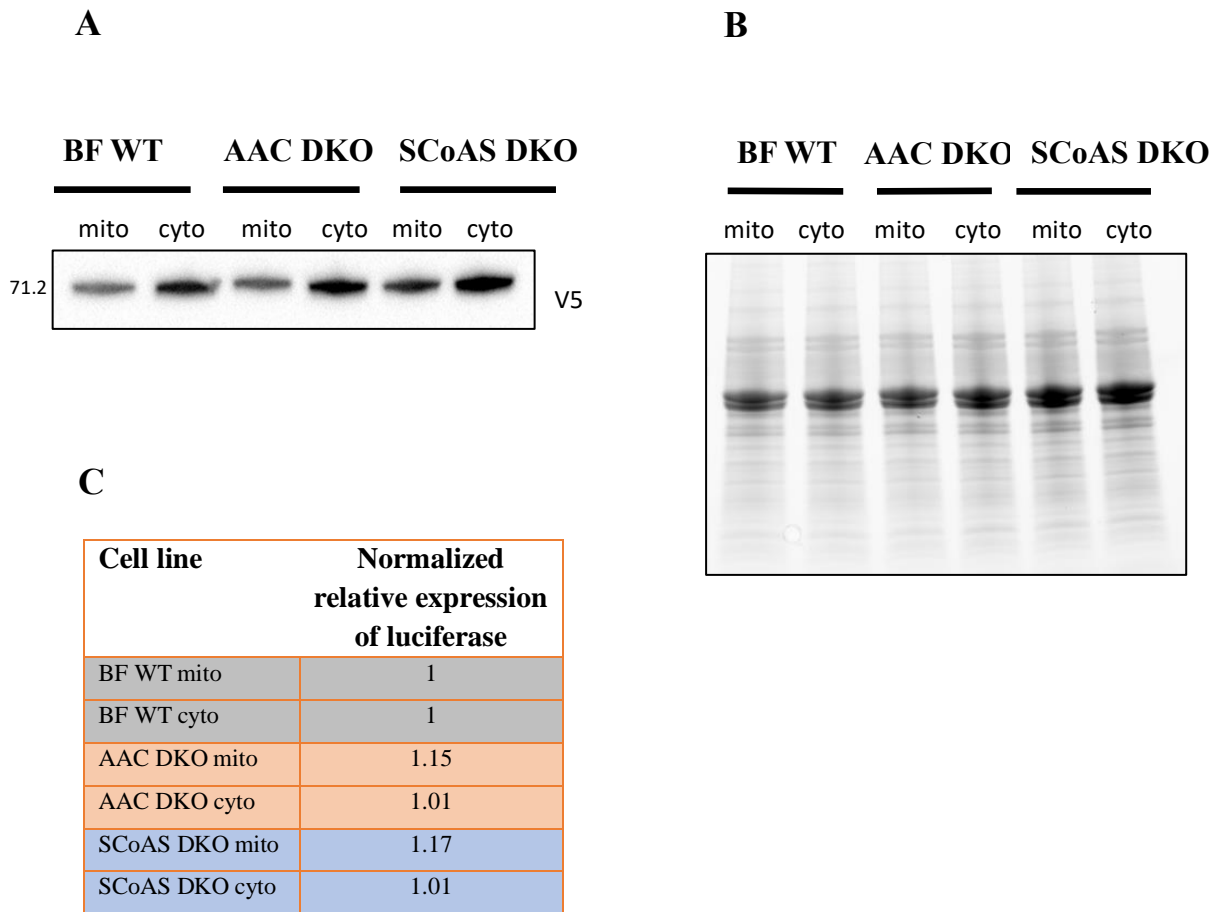


**Fig.23** WB analysis of BF WT, AAC DKO and SCoAS DKO (B1 clone) for luciferase expression targeted to either mitochondrion (mito) or to the cytosol (cyto). (A) Luciferase expression visualized by V5 Ab. (B) Picture of the total protein content of the precast gel of the same gel as on Fig.A. (C) Relative expression levels of the luciferase according to total protein content. On the left are shown the molecular marker in KDa.

After generating the three cell lines, BF WT, AAC DKO and SCoAS DKO, which constitutively express similar amount of firefly luciferase either in the cytosol or in the mitochondrion, we performed *in vivo* ATP measurements in these cell lines. ATP was measured directly in the cells where the luciferase is localized and catalyzes the conversion of ATP to AMP with the help of luciferin. The amount of ATP corresponds to the amount of bioluminescent light emitted during the reaction as shown in **Fig.24A**. The assay was performed in HEPES-Luc buffer, which does not contain any carbon source (see Materials and Methods for more details). This allows us to measure the ATP that has already been produced in the cell compartments at the specific moment. The reaction was initiated by the addition of luciferin and the bioluminescence which is proportional to the ATP content was measured over time.

**Fig.24** shows a representative plot of the time course of bioluminescence levels in either the cytosol (**B**) or the mitochondrion (**C**) in BF WT, AAC DKO and SCoAS DKO expressing luciferase. There was no background bioluminescence signal measured in cells without luciferase or in the buffer. It can be seen that the bioluminescence value increases most at around the 60th second and then gradually decreases again. To compare the values between the cell lines, we decided to measure the bioluminescence at the 60th second (**Fig.24D** and **E**). The bioluminescence signal corresponding to the ATP level was normalized to the BF WT, which was assigned the value 1. In **Fig.24D**, a higher cytosolic ATP level was measured in AAC DKO cells than in WT cells (1.44), which is consistent with the *in vitro* ATP data and suggests that ATP accumulates in the cytosol when AAC is absent, implying that AAC is normally involved in supplying ATP to the mitochondrion. Furthermore, the lower cytosolic ATP concentrations in SCoAS DKO (0.76) compared to WT support the concept of a functional AAC, because when cells lack mt ATP production by SCoAS, AAC supplies ATP from the cytosol, thus reducing cytosolic ATP concentrations. In **Fig.24E**, the mt ATP data also corresponds to the *in vitro* ATP data. Higher mt ATP levels than in WT in AAC DKO cells (1.38) indicate that SCoAS is active and produces a large amount of ATP, probably to compensate for the loss of AAC. An even clearer indication of SCoAS function is the lower mt ATP measurements (0.54) in SCoAS-DKO cells, suggesting that SCoAS contributes to the mt ATP pool and AAC does not fully restore mt ATP levels to WT levels.

Both *in vitro* and *in vivo* measurements indicate that the AAC is able to supply the BF mitochondrion with ATP and that SCoAS also produces mt ATP.

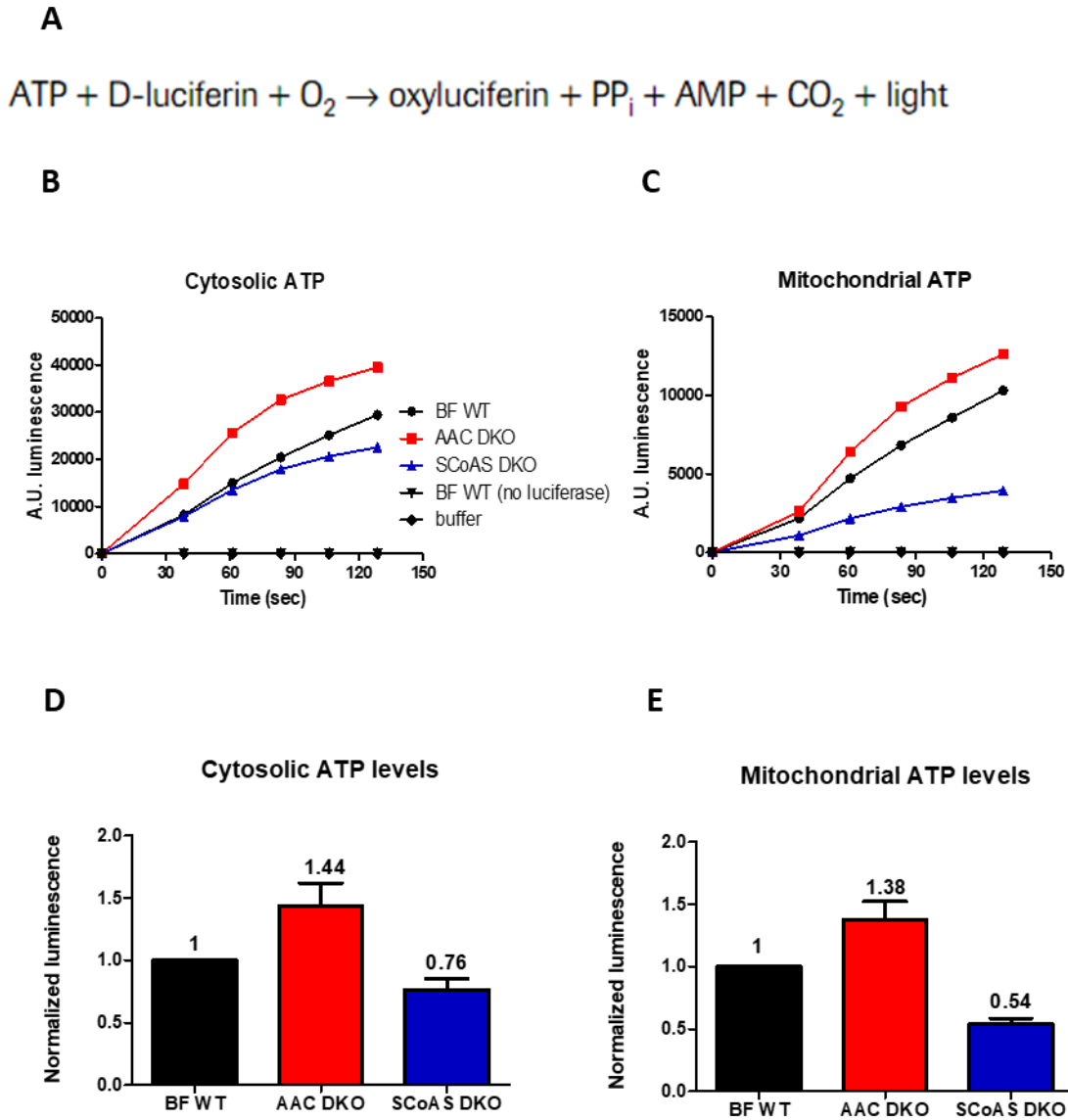


**Fig.24** *In vivo* measurement of ATP – luciferase assay. **(A)** Schematic representation of the luciferase-catalyzed conversion of ATP into light signal, PP<sub>i</sub>-inorganic phosphate. **(B and C)** A representative experiment showing bioluminescent signal representing ATP levels in A.U. (arbitrary units) followed in time in BF WT, AAC DKO and SCoAS DKO (clone B1) cells expressing luciferase either in the cytosol **(B)** or in the mitochondrion **(C)**. **(D and E)** The normalized bioluminescence representing ATP levels measured at 60<sup>th</sup> second after reaction initiation with luciferin in BF WT, AAC DKO and SCoAS DKO (clone B1) cells expressing luciferase either in the cytosol **(D)** or in the mitochondrion **(E)**. Error bars represent standard error of 4 independent experiments.

### 3.13. AAC DKO/ASCT RNAi cell line - Increased sensitivity towards TPMP suggests SUBPHOS I and II activity

Since we failed to generate AAC DKO/SCoAS RNAi cell line, we decided to generate AAC DKO/ASCT RNAi cell line in attempt to show the importance of at least one SUBPHOS pathway. ASCT (acetate:succinate CoA transferase) is the enzyme that catalyzes the conversion of acetyl-CoA to acetate by transferring CoASH to succinate, producing succinyl-CoA, the substrate for SCoAS. To generate this cell line we used our AAC DKO A2 cell line and transfected RNAi vector that produces dsRNA and targets ASCT mRNA. Brief characterization of the cell line showed that ASCT is strongly downregulated on day 2 after tetracycline induction (**Fig.25A**). RNAi induced cells did not exhibited a growth phenotype after 7 days of induction in regular HMI-11 medium supplemented only with phleomycin to avoid loss of the ASCT RNAi construct (**Fig.25B**). We should mention that there was also no growth defect in CMM medium (data not shown). Since the AAC DKO/SCoAS RNAi cell line lacks AAC and ASCT is downregulated, we expected a growth defect after the RNAi induction. The lack of growth phenotype can be explained by the compensatory effect of the potential activity of SUBPHOS II.

In attempt to determine if AAC DKO/SCoAS RNAi relies on the SUBPHOS II pathway, we performed alamar blue assays to check for a change in the sensitivity to the  $\alpha$ -ketoglutarate dehydrogenase inhibitor (and therefore SUBPHOS II inhibitor), TPMP. We already showed that the parental AAC DKO A2 cell line was approximately 30-fold more sensitive towards TPMP compared to WT cells ( $EC_{50}=0.17\mu\text{M}$  vs.  $EC_{50}=5.12\mu\text{M}$ , respectively) (**Fig.8A and table 1**), which already points at BF parasite dependency at least on SUBPHOS II pathway. In AAC DKO/ASCT RNAi cell line, which not only lacks AAC, but simultaneously downregulates the expression of ASCT, for 4 days after induction the sensitivity to TPMP became even higher (AAC DKO/ASCT RNAi NON  $EC_{50} = 0.14\mu\text{M} \pm 0.048$  vs. AAC DKO/ASCT RNAi D4  $EC_{50}=0.03\mu\text{M} \pm 0.002$ ). This shows an increased dependency and therefore activity of SUBPHOS II when all other known alternative mt ATP sources are exhausted. It should be noted that the sensitivity of the parental cell line AAC DKO and AAC DKO/ASCT RNAi NON is similar, indicating tight regulation of dsRNA expression of the ASCT RNAi construct.

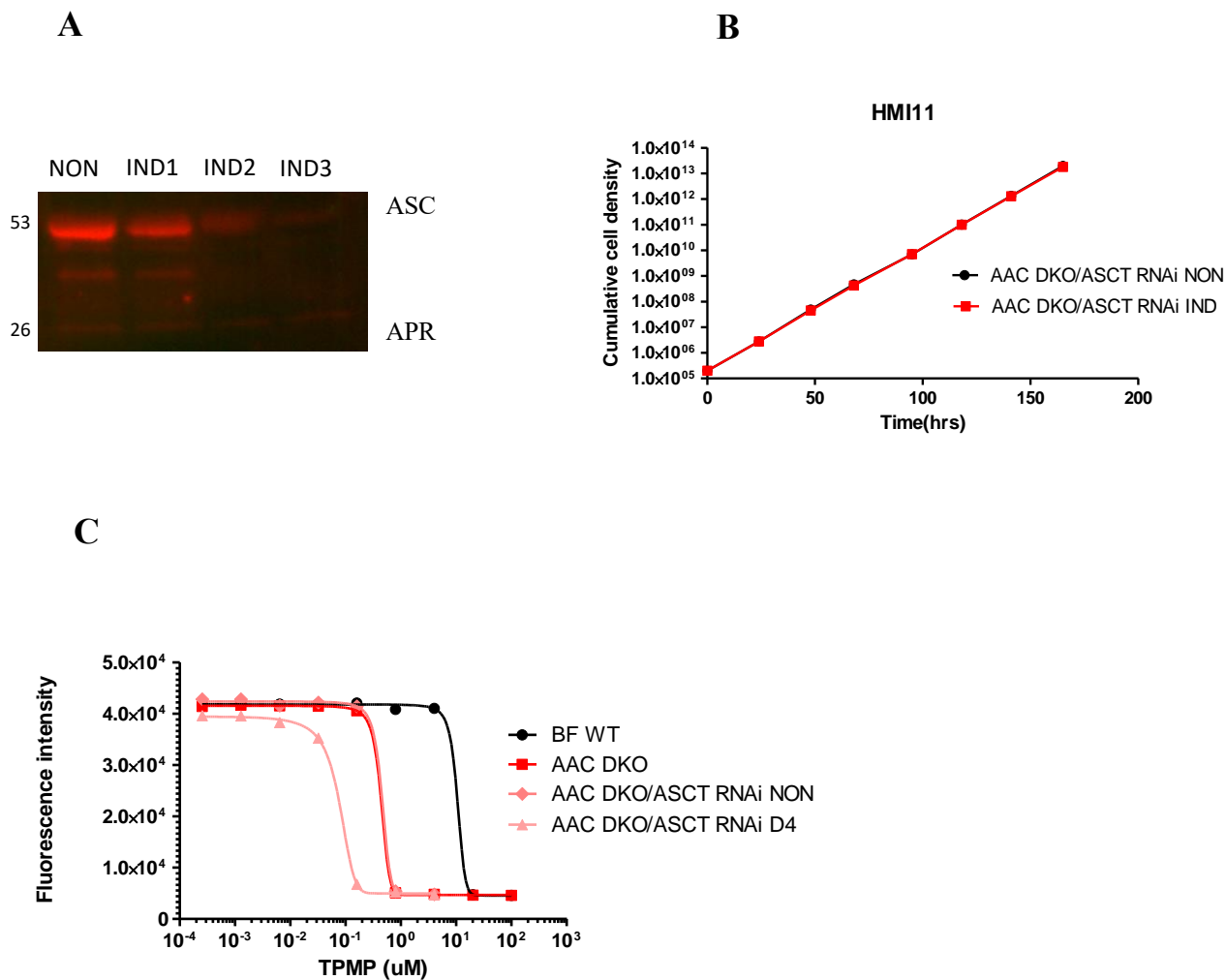


**Fig.25** AAC DKO/ASCT RNAi cell line (A) WB analysis of AAC DKO A2/ASCT RNAi cell line, clone BA4 grown in HMI-11 medium. ASC expression levels were determined after RNAi induction with tetracycline. NON – non-induced RNAi expression, IND 1-3 – days after RNAi induction. APRT used for loading control. (B) A representative growth curve for AAC/ASCT RNAi cell line in HMI-11+phleomycin medium shown as cumulative cell density (cells/ml) measurement for 7 days. AAC/ASCT RNAi non-induced (NON) cells are shown in black and the tetracycline-induced (IND) cells are in red colour. (C) Representative graph of alamar blue assay showing sensitivity of AAC DKO A2/ASCT RNAi towards TPMP, an  $\alpha$ -ketoglutarate inhibitor, when induced for 4 days (pink line), compared to non-induced (dark pink), AAC DKO (red line) and BF WT 427 (black line). On the x-axis is shown the concentration of the drug in  $\mu\text{M}$ , on the y-axis is the fluorescence intensity. Error bars of 3 technical experiments are shown.

### 3.14. Exometabolic analysis supports the SUBPHOS activity

To get a better understanding of what might be happening with the cell metabolism in our mutant cell lines we decided to directly check the excreted metabolic end products. The metabolic end products were

detected based on the ability of  $^1\text{H-NMR}$  spectrometry to distinguish between  $^{13}\text{C}$ -enriched from  $^{12}\text{C}$  molecules. BF WT, AAC DKO and SCoAS DKO trypanosomes were incubated with uniformly labeled 4mM [U- $^{13}\text{C}$ ]-glucose in the presence or absence of the respective unenriched ( $^{12}\text{C}$ -containing) equimolar amino acid – glutamine, glutamate or threonine - as well as  $\alpha$ -ketoglutarate. The same experiment was carried out with ordinary  $^{12}\text{C}$  glucose as the only carbon source mainly for calibration purposes. The quantitative analysis was performed according to (Mazet et al., 2013) and the excreted products deriving either from  $^{13}\text{C}$ -glucose or from  $^{12}\text{C}$ -substrates were quantified in the **Table 3**.

Analyzing the results, we note that there was no significant change in the amount of excreted succinate, pyruvate, alanine, or lactate derived from glucose (either from  $^{13}\text{C}$  or from  $^{12}\text{C}$ -glucose) in either the AAC DKO or in the SCoAS DKO cells compared to the WT cells. Interestingly however, the amount of the excreted acetate derived from  $^{12}\text{C}$ -glucose was significantly lower in SCoAS DKO cells than WT and AAC DKO cells (38 nmoles/h/ $10^8$ cells vs. 346 nmoles/h/ $10^8$ cells in WT and 347 nmoles/h/ $10^8$ cells in AAC DKO cells) and was not even detected from non-labeled glucose. This again demonstrates that SCoAS is directly involved in the ATP producing reaction of SUBPHOS I and it also shows that in the absence of SCoAS acetate production via the ASCT reaction is abolished.

When the cells were incubated with glucose and threonine together the acetate from both sources was abolished in SCoAS DKO cells (undetectable from glucose and 13 nmoles/h/ $10^8$ cells of acetate derived from threonine). This is interesting since it is known that the acetate is crucial substrate for the fatty acid synthesis. A possible explanation is that the parasites produce merely enough acetate through ACH enzyme for its needs, leaving only the 13 nmoles/h/ $10^8$ cells for excretion.

When the BF WT and AAC DKO cells were incubated with glucose and  $\alpha$ -KG together we detected succinate, pyruvate and acetate deriving from  $\alpha$ -KG (direction  $\alpha$ -KG to malate in TCA cycle and from malate in the cytosol to pyruvate and from pyruvate to acetate in the mitochondrion). It has to be emphasized however that this data is very preliminary and needs to be reproduced. This data would suggest that  $\alpha$ -KG can be metabolized to succinate and thus contributing to the SUBPHOS II ATP production via SCoAS. Another interesting observation is that when both glucose and  $\alpha$ -ketoglutarate are used as a carbon source succinate is detected only from  $\alpha$ -ketoglutarate and not from glucose. This suggests that the TCA cycle from  $\alpha$ -ketoglutarate to succinate is the preferred direction in BF parasites compared to the PEP to malate to succinate direction.

However, when we SCoAS DKO cells were incubated with glucose and  $\alpha$ -KG together we also detected succinate, pyruvate and acetate deriving from  $\alpha$ -ketoglutarate. We would expect in SCoAS DKO mutants the succinate production from  $\alpha$ -ketoglutarate to drastically decrease since the enzyme for the reaction is lacking. Succinate excretion decreased only slightly in SCoAS DKO cells (107 nmoles/h/10<sup>8</sup>cells vs. 140 nmoles/h/10<sup>8</sup>cells for WT and 156 nmoles/h/10<sup>8</sup>cells for AAC DKO cells). This discrepancy implies that another unknown enzyme with the same function as SCoAS could exist (see the Discussions).

We should mention that we did not manage to detect any excreted products derived from glutamine or glutamate. Interestingly, glutamine is one of the few amino acids that is taken up by the parasite. While it feeds various metabolic pathways, its primary role lies in the provision of amino groups to the nitrogen pool of the parasite (Johnston et al., 2019).

The overall mt metabolism of AAC DKO cells was not altered compared to WT cells which could imply that the mt SUBPHOS is sufficient to support mitochondrion with ATP and the cell doesn't need to change its metabolism to compensate in any way.

Exometabolomics	Glucose [4mM]			[U- <sup>13</sup> C]-glucose [4mM]			[U- <sup>13</sup> C]-glucose [4mM] Threonine [4mM]			[U- <sup>13</sup> C]-glucose [4mM] $\alpha$ -ketoglutarate [4mM]		
	BF427	TbAAC DKO	SCoAS DKO	BF427	TbAAC DKO	SCoAS DKO	BF427	TbAAC DKO	SCoAS DKO	BF427	TbAAC DKO	SCoAS DKO
Number of samples	18	18	18	15	10	9	12	9	6	6	6	6
Succinate (from glucose)	142±36	168±58	117±22	57±24	67±19	62±14	95±19	96±21	112±12	ND	ND	ND
Succinate ( $\alpha$ -ketoglutarate)										140±11	156±25	107±12
Pyruvate (from glucose)	7115±817	6830±927	8221±830	6478±768	6520±387	7537±1330	7546±810	7527±789	9250±978	7842±413	7992±532	9305±1284
Pyruvate ( $\alpha$ -ketoglutarate)										92±40	66±34	66±41
Acetate (from glucose)	346±62	347±90	38±11	314±66	300±71	ND	310±43	329±72	ND	247±13	255±0	ND
Acetate (threonine/2-oxoglutarate)							294±46	286±36	13±10	51±33	43±14	17±18
Alanine	943±126	906±142	1059±119	820±118	819±83	928±165	944±123	932±112	1147±121	830±45	844±15	926±159
Lactate	366±253	402±352	492±408	522±363	421±210	494±321	482±184	429±116	547±164	223±71	196±8	189±54
Total (from glucose)	8913±1186	8654±1420	9928±1138	8191±1230	8128±693	9021±1677	9376±1147	9313±1062	11055±1259	9170±456	9323±601	10482±1413
Total (threonine/2-oxoglutarate)							294±46	286±36	13±10	283±31	266±63	190±41

**Table 3.** Exometabolomic analysis of the excreted products (succinate, pyruvate, acetate, alanine and lactate) expressed in nmoles/h/10<sup>8</sup>cells, deriving from glucose (black color), threonine (blue color) or  $\alpha$ -ketoglutarate (red color) in BF WT, AAC DKO or SCoAS DKO (B1 clone). ND-non detected.

### **3.15. *In vitro* studies using glycerol as an energy source support the mt SUBPHOS activities**

#### **3.15.1. Glycerol studies: AAC DKO and SCoAS DKO cells**

The BF trypanosomes can utilize glycerol instead of glucose as a carbon source ((Kovářová et al., 2018) , (Pineda et al., 2018)). Since the cellular metabolism changes dramatically when the cells are grown in the presence of glycerol, we decided to look at mt ATP production under these growth conditions. BF WT, AAC DKO and SCoAS DKO (B1 clone) cells were adapted and grown in standard simplified CMM media. CMM normally is supplemented with 10 mM glucose, but for the purpose of simplicity in this section it is referred to as CMM+glc instead of CMM only. At the same time the cells were also adapted to CMM medium supplemented with 10 mM glycerol instead of glucose (CMM+gly). It should be noted that glycerol only medium is not completely glucose free. There is a residual app. 0.5 mM FBS-derived glucose. Despite our attempts to add N-acetylglucosamine in the CMM+gly medium, an inhibitor of *T. brucei* glucose transporters, we were unable to adapt the cells to it.

As we have already discussed in the Introduction (see section **1.3.2.5.2. Glycerol as energy and carbon source**), when medium supplemented with glycerol instead of glucose is used it results in a lower ATP yield in the cytosol of the BF cells. Therefore, we propose that the cells possibly would depend more on ATP produced by SUBPHOS in the mitochondrion. Indeed, when we grow BF WT cells (**Fig.26A black lines**) in CMM supplemented with glycerol the parasites grow slower than when grown in CMM supplemented with glucose only for unlimited time. This could be due to ATP deficiency in the cytosol. The same is also true for AAC DKO cells. When cultured in glycerol, AAC DKO cells can be cultured indefinitely like WT cells but grow slower than WT cells (**Fig.26A red lines**). This indicates that after the loss of AAC, the cells are most likely even more dependent on SUBPHOS to produce ATP. On the other hand, when grown in glycerol conditions SCoAS DKO cells rapidly entered the cytostatic phase followed by cell death (**Fig.26A blue lines**). This result indicates that cytosolic ATP is probably not sufficiently transported from the cytosol to the mitochondria and ATP cannot be produced by mt SUBPHOS due to SCoAS loss. This altogether leads to cell death probably as a result of insufficient ATP, and most likely a collapse of membrane potential. To be able to determine the reason of the cell death we repeated the experiment with the SCoAS RNAi cell lines in which the downregulation of SCoAS occurs after glycerol adaptation, thus eliminating the adaptation period for the cells.



### 3.15.2. Glycerol studies: SCoAS RNAi

When SCoAS RNAi (clone B4) was subjected to tetracycline induction in CMM medium supplemented with either glucose or glycerol, we found that the cells grown in glycerol showed a cytostatic effect at about 7 days after induction, usually leading to cell death or in rare cases, restoration of their growth (**Fig.26B light blue lines**). The phenotype was much more pronounced compared to SCoAS RNAi induction in glucose medium, where the cells only increase their doubling time without leading to cell death or cytostatic effect (**Fig.26B dark blue lines**). The significant downregulation of SCoAS upon induction already at day 1 in both media was confirmed by WB analysis (**Fig.26D**). The severe growth defects following loss of SCoAS under glycerol conditions are further evidence of dependence on SUBPHOS for ATP production. Next, we wanted to see if this cytostatic growth phenotype in glycerol medium in SCoAS RNAi cells leads to a decrease in membrane potential after induction, which would be the case if there is not enough mt ATP to fuel  $F_0F_1$ -ATPase.

When we measured the membrane potential at day 1, 3 and 6 postinduction, we clearly see a significant decrease at day 6  $\Delta\Psi_m$  (53% compared to non-induced cells) when the cells utilize glycerol as sole carbon source. It seems quite plausible that the cytostatic effect we observe at day 7 is due to the severe  $\Delta\Psi_m$  decrease (**Fig.26C**). At the same time, there was no change in  $\Delta\Psi_m$  under the same conditions, but in standard CMM media supplemented with glucose as we already showed in **Fig.11F**. It should be noted that these experiments have been repeated with my colleague Michaela Husová, who has shown that under the glycerol conditions there is indeed a sharp drop in the levels of  $\Delta\Psi_m$ , leading to a significant growth phenotype (Taleva et al., 2023).

In summary, the glycerol studies suggest that under conditions where less cytosolic ATP is generated, SUBPHOS appears to be essential for mt ATP production to maintain  $\Delta\Psi_m$  at physiological levels. Whether parasites encounter such conditions *in vivo* is difficult to assess, but it seems plausible that trypanosomes found in adipose tissues, where glycerol is abundant, could employ mt SUBPHOS and therefore successfully colonize this environmental niche.

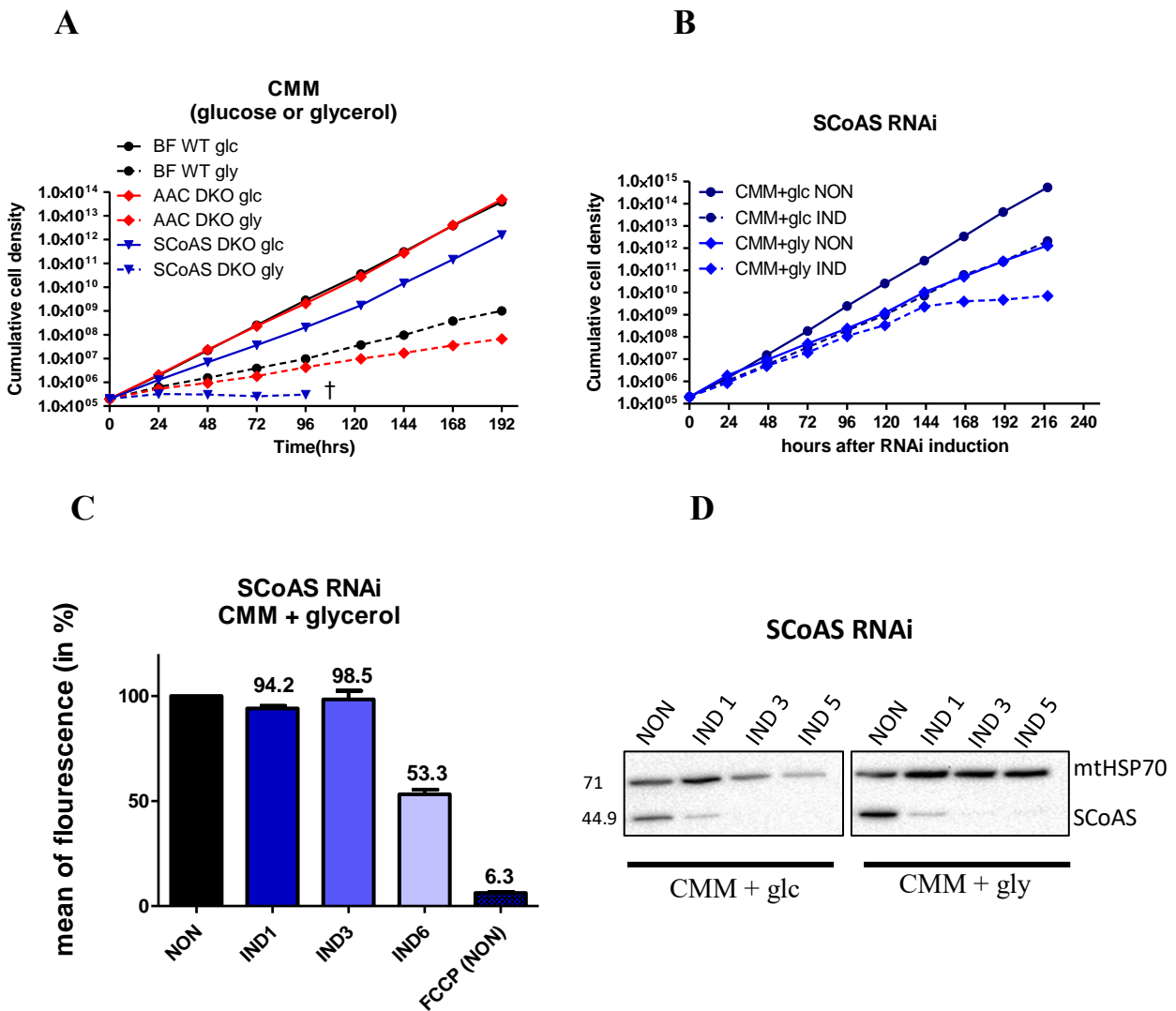


**Fig.26.** Glycerol studies. **(A)** A representative growth curve shown as cumulative cell density (cells/ml) for BF WT (black lines), AAC DKO (red lines) and SCoAS DKO (clone B1) (blue lines) grown in CMM medium supplemented with either 10mM glucose (glc, solid line) or with 10mM glycerol (gly, dashed line), †- cell death. **(B)** A representative growth curve shown as cumulative cell density (cells/ml) for SCoAS RNAi cell line (clone B4) grown in CMM medium supplemented with either 10mM glucose (dark blue line) or with 10mM glycerol (light blue line). SCoAS RNAi non-induced (NON) cells are shown in solid line and the tetracycline-induced (IND) cells are in dashed line. **(C)** FACS Measurement of  $\Delta\Psi_m$  of SCoAS RNAi (clone B4) in CMM medium supplemented with glycerol after tetracycline induction by TMRE fluorescence shown as a percentage of the nontreated (NON) cells at day 1, 3 and 6 of induction (IND 1, 3 and 6). FCCP-  $\Delta\Psi_m$  uncoupler used as a negative control in the non-induced cell line. Error bars represent standard error of 3 biological FACS measurements. The values above the columns show the mean of fluorescence in percentage compared to non-induced cells. **(D)** WB analysis of SCoAS RNAi cell line (clone B4) showing the substantial decrease in the SCoAS enzyme during tetracycline induction in CMM medium supplemented with either glucose or glycerol. mtHSP70 used as a loading control. Molecular marker in kDa shown on the left side.

## 4. DISCUSSION

### 4.1. AAC is active yet not essential in BF *T. brucei*

Bioenergetics of mammalian cells is a well-studied process. Under normal physiological conditions  $F_0F_1$ -ATP synthase works in its forward mode, i.e. combining ADP and inorganic phosphate to generate ATP. Under those conditions AAC works in its forward mode as well, i.e. exporting the generated ATP and importing ADP into the mt matrix. Mathematical models in mammalian cells revealed that under certain conditions ( $\Delta\Psi_m$  decreases under physiologically challenging conditions related to hypoxia or anoxia) the  $F_0F_1$ -ATP synthase reverses, i.e. shifts from ATP-forming to ATP-consuming mode. The value of the  $\Delta\Psi_m$  at which  $F_0F_1$ -ATP synthase reverses is termed 'reversal potential' (Erev\_ATPase) (Chinopoulos, 2011). Chinopoulos and colleagues show that first  $F_0F_1$ -ATP synthase reverses and if the conditions keep deteriorating (further decrease in  $\Delta\Psi_m$ , changes in mt matrix ATP/ADP ratio, disturbance of cytosolic ATP levels) then it is followed by AAC reversal, i.e. it imports ATP and exports ADP from the mt matrix (Chinopoulos et al., 2010). The value of the  $\Delta\Psi_m$  at which AAC reverses is termed Erev\_AAC. Therefore, it seems that the  $F_0F_1$ -ATP synthase and AAC can have the same or different directionality depending on the cellular needs, and thus they can work independently from each other. When Erev\_ANT and Erev\_ATPase are plotted as a function of mt ATP/ADP ratio, then they define four spaces – A, B, C and D space. When both  $F_0F_1$ -ATP synthase and AAC work in forward mode, which is the case in mammalian cells under normal physiological conditions, they define the mt A space. When both are reversal, then the space is defined as C space. When  $F_0F_1$ -ATP synthase reverses and AAC is in a forward mode, then the mt B space is defined. D space is considered biologically irrelevant.

In BF *T. brucei* the  $F_0F_1$ -ATP synthase in contrast to mammalian cells works under normal physiological condition in reverse mode and AAC is believed, however without any direct proof, to work also in reverse mode, supplying mt matrix with the necessary ATP (Nolan & Voorheis, 1992), (Schnauffer et al., 2005), (Brown et al., 2006). It is generally accepted that BF mitochondrion is only an ATP consuming organelle, supplied by the reverse mode of AAC alone. Hence, in BF *T. brucei* the mitochondrion, the plot of Erev\_ANT and Erev\_ATPase as a function of mt ATP/ADP ratio must correspond to C space.

We show that AAC indeed is functional in its reverse mode in BF cells as suggested by the luciferase-based ATP measurements. The cytosolic ATP concentration measured in AAC DKO cells was significantly higher compared to WT cells both *in vitro* and *in vivo* implying that when AAC is absent ATP accumulates in the cytosol and this suggests that normally AAC participates in supplying BF mitochondrion with ATP. In addition, the lower *in vivo* measured cytosolic ATP levels in SCoAS DKO compared to WT cells

additionally support the concept of functional AAC since when the cells lack mt ATP production by SCoAS (discussed next) then AAC supplies it from the cytosol and thus decreases ATP cytosolic levels.

Surprisingly however, the successful achievement of both knock-out and knock-down of AAC in BF *T. brucei* without either growth defects *in vitro* or loss of virulency of AAC DKO parasites in mice shows undoubtedly that AAC is dispensable in this life stage. Furthermore, AAC DKO cells did not show any change in the  $\Delta\Psi_m$  or the overall mt metabolism based on the excreted end products compared to WT cells. This indicates that mt ATP can be supplied by other means. We can exclude the activity of other ADP/ATP carrier as we demonstrate that AAC is the only functional mt ATP transporter in our cells, which correlates with previous functional studies determining the AAC as the only functional ADP/ATP carrier in *T. brucei* (Peña-Diaz et al., 2012). Therefore, it all suggests that ATP can be produced intramitochondrially, a notion neglected in the past. This is also in line with the recent metabolomics and proteomics data showing that certain metabolic mt pathways can be in fact activated in BF parasites under certain conditions (Zíková et al., 2017).

#### **4.2. SUBPHOS pathways are present and active in BF mitochondrion**

The intramitochondrial production of ATP in *T. brucei* can be achieved by SUBPHOS and the responsible enzyme is SCoAS, generating ATP with a direct transfer of a phosphoryl group to ADP from a phosphorylated compound. To my knowledge, no other enzyme has been found as a possible mt ATP-producing candidate in trypanosomes. While in higher eukaryotes SCoAS can produce either ATP or GTP, in trypanosomes it was found to produce only ATP (Bochud-Allemann & Schneider, 2002), (Hunger-Glaser, Linder, et al., 1999). In PF cells it is expressed and active and has an important role in both ASCT/SCoAS cycle and TCA cycle (Zhang et al., 2010), (Bochud-Allemann & Schneider, 2002), but data for BF cells are sparse. We demonstrated by WB that SCoAS is expressed in BF stage although at lower levels compared to PF stage. Importantly, we show that SCoAS is active in both WT and AAC DKO cells at similar levels which also corresponds to previously published data (Durieux I et al., 1991). No activity was detected in SCoAS DKO cells, as expected, determining that the activity is specific. Since measurements were done *in vitro* on mt-enriched cell fraction, the data does not necessarily represent *in vivo* activity, which depends on many factors, including enzyme quantity, which is the same in AAC DKO and WT cells according to WB data, substrate availability and product accumulation.

As we show SCoAS is expressed and active in BF trypanosomes, we further investigated the role of the enzyme and mapped the pathways it participates, namely SUBPHOS I and II. It is known that SCoAS is active at least in SUBPHOS I after the discovery that BF cells produce acetate via the ASCT. ASCT is

integrated into the ASCT/SCoAS cycle, which must therefore be active, which is why SCoAS must also be active as part of it. Recently, the participation of SCoAS also in SUBPHOS II as part of the TCA cycle can be deduced from the detection of glutamine-derived succinate (Johnston et al., 2019). However, in BF cells, the role of SCoAS as a mt ATP-producing enzyme has never been investigated. We showed that SCoAS contributes to the mt ATP pool as exemplified by the lower total ATP concentration measured *in vitro* as well as the lower mt ATP levels measured *in vivo* in SCoAS DKO cells compared to WT cells. Higher mt ATP in AAC DKO cells also indicates that SCoAS contributes to the mt ATP pool probably to compensate for the loss of AAC.

### **4.3. Interplay between the two pathways: AAC and SUBPHOS I/II work together and can compensate for each other**

Given that both SCoAS and AAC seem to be active in BF cells, one of the most interesting questions is the interplay between them. It seems that the ATP production by SCoAS becomes indispensable *in vivo* or when grown in glycerol conditions, where the cytosolic ATP levels are assumed to be lowered. The question is now what compensates for the loss of SCoAS when grown in regular HMI-11 medium since neither SCoAS RNAi cells nor SCoAS DKO cells show any growth defects or  $\Delta\Psi_m$  change. Interestingly, we observed that SCoAS DKO cells have 15-fold and SCoAS cDKO cells have 29-fold increased sensitivity to CATR, an AAC inhibitor. This greatly increased dependency on AAC upon SCoAS loss points at the necessity of the ATP production by SCoAS in BF cells and the need for compensation when lost by the reversal activity of AAC. Indeed, this is in line with the mammalian mathematical model, which shows that when ATP/ADP intramitochondrial ratio drops, which would be the case when SCoAS is lacking, then the AAC would reverse more easily and would start supplying mitochondrion with ATP, placing the mitochondrion to C space. At the same time, it seems that SCoAS in turn is able to compensate for the AAC loss as evident from the 30-fold increased sensitivity of AAC DKO cells to TPMP, an  $\alpha$ -KgdH inhibitor.  $\alpha$ -KgdH is located immediately upstream of SCoAS in the TCA cycle and it produces succinyl-CoA which is the substrate for SCoAS in SUBPHOS II pathway, therefore its inhibition must lead to inhibition of ATP production by SUBPHOS II.

These results show that BF cells can compensate for the loss of AAC by becoming more dependent on SUBPHOS for ATP production and *vice versa*, when they lose ATP produced by SUBPHOS upon SCoAS loss, they become more dependent on AAC and it all seems to be dictated from the intramitochondrially ATP levels.

It is interesting that only one of the two tested clones for both SCoAS DKO and SCoAS cDKO cells display such an adaptation. The other clones did not show such striking differences in the sensitivity towards CATR, suggesting a different mechanism of adaptation to SCoAS loss. In the Master's thesis of my colleague (Husová et al., 2021) she investigates the possible adaptations. According to her data, SCoAS DKO B2 clone is very sensitive to TPMP, an  $\alpha$ -KgdH inhibitor and at the same time has a decreased MCP14 levels, a mt transporter connected to the proline uptake. Therefore, she speculates that a possible adaptation of this clone is the increased proline consumption to feed glutamate to  $\alpha$ -KG and then to succinyl-CoA via  $\alpha$ -KgdH with the goal to generate NADH, which then passes electrons through respiratory complex I, which in turn contributes to the  $\Delta\Psi_m$ . Interestingly, this hypothesis would mean that complex I can be activated to pump protons and that proline can be consumed as an energy source by BF cells, which is not supposed to be the case. However, when the BF parasites are challenged with mt SUBPHOS inactivity then the parasites could exploit such a mechanism.

In line with the increased dependency of SCoAS mutants on AAC, is the decreased dependency on  $F_0F_1$ -ATP synthase for mt  $\Delta\Psi_m$  generation, demonstrated by the considerably lower decrease in the mt  $\Delta\Psi_m$  compared to WT cells when treated with OLM,  $F_0F_1$ -ATP synthase inhibitor. It demonstrates that SCoAS DKO cells are less dependent on  $F_0F_1$ -ATP synthase for the generation of the mt  $\Delta\Psi_m$  compared to WT cells. It seems there is some level of electrogenic contribution to the  $\Delta\Psi_m$  by ATP import to the mitochondrion via AAC at the expense of ADP. At the same time when this electrogenic contribution of AAC to the mt  $\Delta\Psi_m$  is lost in AAC DKO cells, they become more dependent on  $F_0F_1$ -ATP synthase for the mt  $\Delta\Psi_m$  generation, exemplified by the increased by 2.6-folds sensitivity towards OLM compared to WT cells together with the slight decrease in the mt  $\Delta\Psi_m$  compared to WT cells when treated with OLM. It seems like AAC can at least to some extent contribute electrogenically to mt  $\Delta\Psi_m$  in BF cells. This is a well-known phenomenon in the dyskinetoplasmic (Dk) *T. brucei* parasites. Those cells lack mt DNA and thus the lack proton pore of  $F_0F_1$ -ATP synthase. Dk cells have their mt  $\Delta\Psi_m$  uncoupled from proton pumping of  $F_0F_1$ -ATP synthase, but it is rather generated through increased ATP hydrolysis by  $\gamma$ -mutated  $F_1$ -moiety, which generates ADP. The  $\Delta\Psi_m$  is produced by the electrogenic exchange of cytosolic  $ADP^{3-}$  for mt  $ATP^{4-}$  by AAC. ATP has one extra negative charge compared to ADP and thus makes the matrix side of the inner mt membrane more negative (Dean et al., 2013). Probably such compensation mechanism is exploit by BF cells when they lose SCoAS.

#### 4.4. Both SUBPHOS I and II are active and compensate for the AAC loss

It is plausible that both the SUBPHOS I and SUBPHOS II pathways are active, as shown by comparing the sensitivity of cells to TPMP, an  $\alpha$ -KGDH and thus SUBPHOS II inhibitor. We have previously discussed the increased sensitivity of AAC DKO cells to TPMP, indicating an increased dependence of the BF parasite on the SUBPHOS II pathway upon loss of AAC. When ASCT is also downregulated in addition to loss of AAC (AAC DKO/ASCT RNAi cells), sensitivity to TPMP increases even further. ASCT is the enzyme involved in the ASCT/SCoAS cycle and is thus responsible for the generation of succinyl-CoA, which is subsequently utilized by SCoAS to produce ATP through SUBPHOS I. This shows that BF cells exhibit an increased dependence and thus activity on SUBPHOS II when the other known alternative mt ATP sources are depleted. You can also look at it the other way around – once ASCT returns to its normal levels, only in the AAC DKO cell line, the sensitivity to TPMP decreases, which means that the cells become less dependent on SUBPHOS II, which can be explained by the activity of SUBPHOS I.

Since SCoAS is involved in both SUBPHOS pathways, we would expect that AAC DKO cells would express high sensitivity shift compared to WT cells towards LY266500, an inhibitor of histidine phosphorylation in SCoAS (Hunger-Glaser, Brun, et al., 1999). However, no shift was detected ( $EC_{50}=0.24\mu\text{M}$  for AAC DKO cells vs.  $EC_{50}=0.27\mu\text{M}$  in WT cells). In addition, SCoAS DKO cells showed similar sensitivity ( $EC_{50}=0.23\mu\text{M}$ , data not shown). This would mean that SCoAS is not active in our BF parasites, but it seems rather unlikely considering the rest of the results. A more plausible explanation is that LY266500 is not that specific towards SCoAS considering the same high sensitivity even in the absence of the enzyme in SCoAS DKO cells. Regarding the low  $EC_{50}$  in our BF cells compared to the literature (BF  $IC_{50}=28.5\mu\text{M}$  (Hunger-Glaser, Brun, et al., 1999)) seems probable the inhibitor acts in our cell lines on some other enzymes or cells structures may be nonspecifically. It is also possible that the inhibitor acts specifically on other kinases which possess histidine phosphorylation, although it was shown that it does not inhibit such kinase as nucleoside diphosphate kinase in *T. brucei* (Hunger-Glaser et al., 2000).

When we used exometabolomics to shed light on energy metabolism of BF trypanosomes, we confirmed what is already known that BF cells can utilize glucose and threonine for acetate production, which is in line with the activity of SUBPHOS I. Interestingly, we also found that BF cells could possibly utilize  $\alpha$ -KG. Although the data is very preliminary and needs to be reproduced, we could detect  $\alpha$ -KG-derived succinate, pyruvate and acetate ( $\alpha$ -KG to succinate to malate in TCA cycle, to pyruvate to acetate, see **Fig.4**), which suggests possible activity of SUBPHOS II and partial (or maybe even complete) activity of TCA cycle in this life stage. When both glucose and  $\alpha$ -KG were used as a carbon source succinate was

detected only from  $\alpha$ -KG and not from glucose in both WT and AAC mutants. This could mean that  $\alpha$ -KG is converted to succinate, and this is the preferred TCA cycle direction rather than from malate to succinate (from glucose to pyruvate and then to malate and succinate). TCA cycle intermediates (succinate, malate, citrate/isocitrate) deriving from glutamine were found recently in BF trypanosomes, again pointing at possible TCA activity (Johnston et al., 2019). These observations, however, needs to be further investigated to be further supported. To my knowledge, we are the first to test the  $\alpha$ -KG metabolism in long slender BF 427 strain, monomorphic cells which cannot differentiate into stumpy form.  $\alpha$ -KG was also shown to be utilized as a substrate for mt ATP production by TCA cycle reactions in transitional and stumpy form of *T. brucei*, however not in long slender BF form (BIENEN et al., 1993). In addition,  $\alpha$ -KG can be consumed and metabolized in PF parasites in the presence of 2mM proline and absence of glucose (Villafranz et al., 2021). Therefore, the cells are perfectly equipped to utilize the metabolite, however if this is the case for BF cells is difficult to assess yet.  $\alpha$ -KG could be in theory either taken up from the environment or be generated intracellularly. Although for exometabolomics we used 4mM  $\alpha$ -KG when incubating the cells, it is possible that its concentration in blood (5-10  $\mu$ M in humans (Aragonès et al., 2016), (Wagner et al., 2010)) could be sufficient for the parasites to take it up.  $\alpha$ -KG could be produced intracellularly from the transamination reactions employing by ALT and AST. For the purpose cells need to utilize glutamine-derived glutamate, however we could not detect any utilization of either glutamine or glutamate.

Exometabolomics revealed in addition that SCoAS indeed is involved in both SUBPHOS I and II. In SCoAS DKO cells the decreased threonine-derived acetate and the lack of detected glucose-derived acetate points at the direct involvement of SCoAS in the ATP produced by SUBPHOS I. Threonine-derived acetate however was not completely abolished, suggesting that this baseline level of acetate production is due to the ACH activity and seems to be sufficient to support fatty acid biosynthesis without affecting parasite growth rate (Millerioux et al., 2018), (Millerioux et al., 2012).  $\alpha$ -KG-derived acetate ( $\alpha$ -KG to malate to pyruvate to acetate) is decreased upon SCoAS loss, however only 3 times compared to WT cells, which suggests some SUBPHOS II activity as well.

Interestingly, when SCoAS DKO cells were incubated with glucose and  $\alpha$ -ketoglutarate together we also detected succinate, pyruvate and acetate deriving from  $\alpha$ -ketoglutarate. We would expect in SCoAS DKO mutants the succinate production from  $\alpha$ -ketoglutarate to drastically decrease since the enzyme for the reaction is lacking. Succinate excretion decreased only slightly in SCoAS DKO cells. This discrepancy implies that another unknown enzyme with the same function as SCoAS to produce succinate from succinyl-CoA could exist. This unknown enzyme probably does not produce ATP since we show that SCoAS mutants become more dependent on AAC for mt ATP supply (significantly increased sensitivity to CATR). Therefore, we are looking for an enzyme that possibly just removes the CoASH-group from



succinyl-CoA and thus produces succinate for further reactions. Such enzymes are acyl-CoA thioesterases which are found in most eukaryotes and catalyze the hydrolysis of the CoA esters of various lipids to free acids with the release of CoASH. Specifically, the peroxisomal acyl-CoA thioesterases 4 was found in liver and kidney of mice to be succinyl-CoA thioesterase, producing succinate from succinyl-CoA with CoASH removal (Westin et al., 2005). We don't know however if trypanosomes have a homologue of acyl-CoA thioesterases 4 since it has not been investigated. Interestingly, the acetyl-CoA thioesterase, ACH, was shown to be active in *T. brucei* in both PF and BF stages and important for acetate production (Millerioux et al., 2012), (Mochizuki et al., 2020), (Mazet et al., 2013). Although specific for acetyl-CoA, it shows similar level of specificity towards acetoacetyl-CoA and even higher specificity towards butyryl-CoA (Millerioux et al., 2012). Acetyl-CoA is C2 compound (has 2 carbon atoms without considering the CoA group), whereas acetoacetyl-CoA and butyryl-CoA are C4 compounds as is succinyl-CoA. In addition, structurally succinyl-CoA is similar to butyryl-CoA with the difference that the carboxylic group in the succinyl-CoA is replaced by a methyl group in butyryl-CoA. Consequently, in theory would be possible that ACH acts on succinyl-CoA as well promiscuously under physiologically challenging conditions such as loss of SCoAS and the consequent accumulation of the substrate succinyl-CoA.

As we demonstrated, AAC and SUBPHOS pathways seem to work together and compensate each other to supply mt with ATP. Therefore, ablation of AAC and SUBPHOS simultaneously should be detrimental for the cell and would indicate that these are indeed the only possible pathways for the BF cells to supply mitochondrion with ATP to generate membrane potential. However, we achieved SCoAS DKO/AAC RNAi mutants with almost no growth phenotype. Since the residual AAC was as high as 29% at day 3, we speculate that this amount is still quite sufficient for the cells to supply the mitochondrion with ATP when SCoAS is absent. Our attempt to achieve the reciprocal cell mutant (AAC DKO/SCoAS RNAi) was unsuccessful since no viable clones were generated. This suggests that it is possible to have a leaky expression of SCoAS RNAi already without tetracycline induction. If this is the case, it implies that upon induction the growth phenotype would be severe, as expected.

#### **4.5. SCoAS is essential in glycerol medium as well as in the mouse model**

The successful achievement of both SCoAS RNAi (protein reduction level down to 86% already at day 1) and SCoAS DKO cells without growth defects in standard HMI-11 medium with no mt  $\Delta\Psi_m$  change shows that SCoAS is not essential in BF cells for mt  $\Delta\Psi_m$  generation when glucose is well-abundant (25mM). However, when grown in CMM+glu medium, where the glucose concentration is lower (10mM), SCoAS knockdowns as well as SCoAS cDKO showed slight growth defects. Moreover, the decreased virulency of

SCoAS DKO in mice, a more challenging environment with even lower glucose concentration (~5mM (Zuo et al., 2014)) shows that SCoAS becomes indispensable. It seems that in mice models, representing the natural environment of the parasites in the mammalian host, the glycolysis is not sufficient to provide ATP to the mitochondrion via AAC and SCoAS determining SUBPHOS becomes essential. If SCoAS is essential in the mammalian host, it emphasizes the importance of mt ATP production by SUBPHOS *in vivo*. SCoAS seems to become essential when glycerol is the energy source as well. In CMM+gly medium both SCoAS RNAi and SCoAS DKO cells display strong growth defects. Since cytosolic ATP levels were shown to be reduced when BF cells utilize glycerol instead of glucose (Pineda et al., 2018), this growth phenotype additionally supports the essentiality of SUBPHOS when ATP is not sufficiently delivered by AAC to the mitochondrion.

The question now is what are the reasons for this severe growth phenotype under glycerol conditions? The most obvious reason would be that the insufficient mt ATP in the SCoAS deficient cells restricts F<sub>0</sub>F<sub>1</sub>-ATP synthase from generating mt  $\Delta\Psi_m$ . When measuring the mt membrane potential in SCoAS knockdowns in CMM+gly medium, we observed that it collapsed to 53.3 % on day 6 postinduction and not before, which was exactly one day before the cytostatic growth effect occurred. This suggests that the growth defects are due to a decrease of mt  $\Delta\Psi_m$ . This collapse is consistent with other data showing that a drop in mt  $\Delta\Psi_m$  below about 50% is ultimately detrimental to BF cells (Šubrtová et al., 2015), (Procházková et al., 2018). The lack of change in mt  $\Delta\Psi_m$  in SCoAS knockdowns in lower glucose-containing media (CMM+glu) explains their minor growth defect. The presence and activity of AAC in these cells seems to be sufficient to supply mitochondria with ATP, which is necessary for cell viability, although not optimal. The glycerol studies suggest that under the conditions where cytosolic ATP is lower, SUBPHOS seems to become essential for mitochondrial ATP production to keep the mt  $\Delta\Psi_m$  at physiological levels. Such conditions are observed in adipose tissues, which are rich in glycerol compared to blood (~50 $\mu$ M in blood (Samra et al., 1996), (Sjöstrand et al., 2002) vs. adipose interstitial space ranging between 0.2 – 2.8 mM) (Sjöstrand et al., 2002), (Maggs et al., n.d.)). Glycerol is released by the adipocytes during lipolysis together with fatty acids. BF parasites are found to reside in adipose tissue (Trindade et al., 2016) and they are known as ATF parasites. In addition, it is possible that these ATF can utilize also fatty acids via  $\beta$ -oxidation, shown to be possible in BF cells (Trindade et al., 2016) and consequently to produce acetyl-CoA which may be used by SUBPHOS I to generate mt ATP. The ability of BF cells to use glycerol or even fatty acids for energy production may be crucial for adaptation to invade other environments, such as adipose tissue, revealing the high adaptation potential of the parasites. These parasites could potentially serve as reservoirs and could be the cause for patient relapses especially in asymptomatic carriers with low or even undetected blood parasites. It seems that SUBPHOS ATP production by SCoAS is essential for parasite virulency and when

occupying other diverse niches with various carbon sources within the mammalian host, such as adipose tissue.

In conclusion, we have shown that BF *T. brucei* is capable of mt ATP production by SUBPHOS I and II and that there is a clear interplay between SUBPHOS pathways and AAC activity. These interchangeable activities allow parasites to generate mt ATP through different metabolic pathways depending on the available carbon source. A fascinating metabolic flexibility allows the parasite to adapt to different environmental niches in its mammalian host.

## 5. MATERIALS AND METHODS

### 5.1. Cultivation media

All *T. brucei* BF cell lines were routinely grown at 37°C in the presence of 5% CO<sub>2</sub>. For most of the experiments the cultivation medium was the nutrient-rich HMI-11 (Invitrogen) supplemented with 3g/L sodium bicarbonate (Merck) serving as a pH buffer together with CO<sub>2</sub> (pH 7.3), 100U-100µg/ml Penicillin-Streptomycin (Gibco™, Thermo Fisher Scientific) as antibacterial agent and 10% FBS (Biosera). To keep a healthy population of cells the cultures were grown to not more than 2x10<sup>6</sup> cells/ml in 25cm<sup>2</sup> flasks in 5ml or 10 ml medium. For most of the experiments the cells were grown for few days in mid-log phase, which is 0.6 – 0.8x10<sup>6</sup> cells/ml, ensuring well growing and healthy cell population. The cell density was measured with Z2 Coulter Counter (Beckman Coulter Inc.). BF trypanosomes can be spilt harshly but should not be let overgrow. When higher cell number needed for experiments, the cell culture can be expanded in 75cm<sup>2</sup> or 150cm<sup>2</sup> flasks which can contain around 100 ml of culture. It is important to have in mind that HMI-11 is not only amino acid-rich but also glucose-rich medium, containing 25 mM glucose.

For specific experiment the cells were grown in Creeks minimal media (CMM) (Creek et al., 2013) containing either 10mM glucose (CMM+glu) (Sigma) or 10mM glycerol (CMM+gly) (Lach-ner), both supplemented with 10% FBS. If CMM only is indicated, it is considered CMM+glu as it is the original medium. Since the recipe is slightly modified, I present a table with the CMM content (**table 4**). The cells grown in HMI-11 medium were first adapted to CMM+glu medium by gradually decreasing the HMI-11 volume in favor of CMM+glu for approximately 2 weeks. Once the cells are well-adapted to CMM+glu conditions, the cells can be further adapted to CMM+gly medium following the same procedure with the important remark to be grown in flask with maximum 5 ml of culture in a lying position of the flask probably due to the need for a better aeration knowing that the BF cells consume more oxygen when glycerol is utilized instead of glucose (Pineda et al., 2018).

All media unless otherwise stated contained the respective for each cell line selectable drug(s) for the cell population to keep the transfected construct. The selectable drugs (also referred as antibiotics) were used in the following concentrations: G418 (analogue of neomycin)- 2.5µg/ml, hygromycin - 5µg/ml, puromycin - 0.1µg/ml, phleomycin - 2.5µg/ml. When tetracycline was used the applicable concentration was 1µg/ml.

Component	Manufacturer	Final concentration
MilliQ		
D-glucose/ Glycerol anhydrous	Sigma / Lach-ner	10mM/10mM
L-glutamine	AppliChem	1mM
L-cysteine	AppliChem	1mM
L-tyrosine	AppliChem	100uM
L-phenylalanine	AppliChem	100uM
L-tryptophan	AppliChem	100uM
L-leucine	AppliChem	100uM
L-methionine	AppliChem	100uM
L-arginine	AppliChem	100uM
Hypoxanthine	Molekula	100uM
NaCl	Lach-ner	77.59mM
CaCl <sub>2</sub> ·2H <sub>2</sub> O	AppliChem	1.49mM
KCl	Sigma	4.4mM
MgSO <sub>4</sub> ·7H <sub>2</sub> O	AppliChem	814uM
NaHCO <sub>3</sub>	Merck	35.95mM
HEPES	Sigma/Merck	25.032mM
Phenol Red	Sigma/Merck	42uM
Bathocuproinedisulfonic acid	Molekula	52uM
B-mercaptoethanol	Sigma	192uM
Pen/Strep	Gibco™, Thermo Fisher Scientific	100U/100µg/ml
NaOH to bring pH to 7.4		
FBS	Biosera	10%

**Table 4.** The recipe for CMM+glu or CMM+gly medium used for the specific experiments.

## 5.2. Cell lines

### 5.2.1. Bloodstream form (BF) WT cell line

A very well studied and commonly used cell line in the labs is BF *Trypanosoma brucei brucei* WT monomorphic strain Lister 427 (G. A. M. Cross & Manning, 1973). This cell line is used in multiple experiments as a control, and it serves as a background cell line for generation of all double knock-out (DKO) cell lines.

### 5.2.2. BF Single-marker (SM) cell line

In many experiments we used as a parental cell line for RNAi-expressing cells the genetically modified BF single-marker (SM) cell line which encodes in the tubulin locus the genes for the T7 RNA polymerase and tetracycline repressor under the control of 10% T7 promoter. All genes are in tandem with a neomycin-resistance marker gene which ensures the presence of the genes in the genome (Wirtz et al., 1999). This constitutive expression of T7 polymerase and tetracycline repressor makes it a wonderful system for RNAi studies.

### 5.2.3. AAC RNAi (GT)

AAC ORF-specific 402 bp dsRNAi fragment was amplified (purple Taq polymerase, 50°C annealing temperature) from BF WT 427 genomic DNA with the following PCR primers: forward primer 5-GATGGATCCAAGTCTGTGAAGGGTGGTGG-3 with 20 bp AAC gene homology and BamHI restriction site, reverse primer 5-GCACTCGAGCGATACCGCGTAGGATGTTT-3 with 20 bp AAC gene homology and XhoI restriction site. Next, the construct was cloned by removing GFP from the p2T7-177 parental plasmid containing genes for 2 head-to-head T7 promoters and 2 T7 terminators for AAC dsRNAi expression, 2 tetracycline operators, repeats for integration into *T. brucei* 177 mini-chromosome and phleomycin resistance cassette. The final plasmid was verified by Sanger sequencing. It was linearized by NotI and transfected into SM BF trypanosomes by homologous recombination into transcriptionally silent 177-bp repeats in *T. brucei* minichromosomes, where the constitutive expression of T7 RNA polymerase and tetracycline repressor keep tight regulation of the uninduced cells. The AAC dsRNAi fragment was being transcribed upon 1µg/ml tetracycline induction. Tetracycline binds and removes the tetracycline repressor from the operator sites allowing the expression of the dsRNAi construct leading to downregulation of the AAC at mRNA and subsequently at protein level. The AAC RNAi cell line was grown in the presence of G418 and phleomycin.

### 5.2.4. SCoAS RNAi

For the generation of SCoAS RNAi cells we utilized the same strategy as for the AAC RNAi cells with the only difference in generation of the dsRNAi fragment which is 591bp SCoAS ORF-specific. The PCR primers used to amplify the fragment were: forward primer 5-AAAGGATCCCTTCCCACGAAGGCTGCG-3 with 18bp SCoAS gene homology and BamHI restriction

site, reverse primer 5- CCCAAGCTTAGCATTTTCAGCGGCGCG-3 with 18 bp SCoAS gene homology and HindIII restriction site. The SCoAS RNAi cell line was grown in the presence of G418 and Phleomycin.

### 5.2.5. AAC DKO

Two constructs, 5' intergenic region (with 401bp T. brucei 427 genome homology) and 3' intergenic region (with 308bp T. brucei 427 genome homology), flanking the all tree consecutive AAC gene copies from T. brucei 427 : AACa (Tb927.10.14840), AACb (Tb927.10.14830) and AACc (Tb927.10.14820), were amplified by KOD proofreading polymerase with PCR primers as follows: 5' intergenic region forward primer 5-AAAGCGGCCCGCCATGTGTGCTCCATCTTG-3 (18 bp 5' intergenic homology region and NotI restriction site) and 5' intergenic region reverse primer 5-GGAACGCGTCTCGAGCGTAGACGCATGCCCTTAAATG-3 (22 bp 5' intergenic homology region and MluI and XhoI restriction sites); 3' intergenic region forward primer 5-GGGTCTAGAATTAAATGCAGTTTGAAGTGATGCATGGAC-3 (24 bp 3' intergenic homology region and XbaI and SmaI restriction sites) and 3' intergenic region reverse primer 5-AAAAGGCCTGCGGCCGCTAAAGAGGTTAAAGATGTGG-3 (20 bp 3' intergenic homology region and StuI and NotI restriction sites). The constructs were amplified from genomic BF WT 427 DNA and both constructs were cloned into pLew13 parental plasmid, already containing the gene for T7 polymerase and the Neomycin resistance to generate pLew13-5'IR-3'IR plasmid. Following Sanger sequencing verification and NotI linearization of the pLew13-5'IR-3'IR, BF WT 427 cells were transfected with the plasmid and the first allele of the AAC gene was substituted by the gene cassette of T7 polymerase and the Neomycin resistance gene. Having replaced the first AAC allele (verified by PCR) and the BF AAC single knock-out cells generated we continued with the replacement of the second AAC allele. We used the already generated pLew13-5'IR-3'IR plasmid where we replaced the gene cassette for T7 polymerase and the Neomycin resistance with the gene cassette for 10% T7 promoter, tetracycline repressor and Hygromycin resistance. This was achieved by cloning the later cassette from the pLew90 plasmid which already contained it into the pLew13-5'IR-3'IR plasmid with concomitant removal of the gene cassette for T7 polymerase and the Neomycin resistance with the restriction enzymes XhoI and the blunt end inducing enzymes – StuI and SmaI and thus we generated the plasmid pLew90-5'IR-3'IR. Following NotI linearization, pLew90-5'IR-3'IR plasmid was transfected into the BF AAC single knock out cells and after numerous attempts the second AAC allele from those cells was replaced by the gene cassette of 10% T7 promoter, tetracycline repressor and Hygromycin resistance, thus generating AAC DKO cells. The final achievement of AAC DKO cells was verified by PCR and WB analysis. The cells were grown in the presence of G418 and hygromycin to keep the integrated constructs.

### 5.2.6. SCoAS DKO

For the generation of SCoAS DKO cells we used the same strategy as for the AAC DKO cells with the only difference in the initial two constructs. The two constructs were generated with homology to *T. brucei* 427 genome of the 5' and 3' flanking regions of the SCoAS CDS. The 5' construct had 210bp homology with the 5' intergenic region and 5' UTR of the SCoAS CDS and was amplified with forward primer 5-ATAGCGGCCCGCCGTTTCGTTTTGCTTCCGTAG-3 and reverse primer 5-GATACGCGTCTCGAGCGATACCCTCAGCGAAATAAA-3. The 3' construct had 285bp homology with the 3' UTR of the SCoAS CDS and was amplified with forward primer 5-GCGTCTAGAATTTAAATACTTGAAAGGAGGCGGTTCT-3 and reverse primer 5-TATAGGCTGCGGCCCGCCGTGGATTAACATGCACGA-3. The final SCoAS DKO cell line contained the replacement of the two SCoAS alleles with either gene cassette for T7 polymerase and the Neomycin resistance or the gene cassette for 10% T7 promoter, tetracycline repressor and Hygromycin resistance. The final achievement of SCoAS DKO cells was verified by PCR and WB analysis.

### 5.2.7. AAC DKO/ASCT RNAi

The cell line was kindly given to me by a colleague. It was generated from AAC DKO A2 cells with transfection of plasmid p2T7-177 containing the ASCT RNAi construct.

### 5.2.8. Conditional SCoAS DKO

We generated conditional SCoAS (c)DKO cell line, where SCoAS protein can be switched off and on by request. The first allele of SCoAS gene in BF WT 427 cells was substituted with the same strategy as for the generation of SCoAS DKO cell line - by the gene cassette of T7 polymerase and the Neomycin resistance gene. Next, SCoAS ectopic regulatable copy was introduced in the following way. SCoAS CDS was cloned into pLew79 plasmid, which already contained T7 promoter and phleomycin resistance cassette, as well as PARP promoter and tetracycline operators for regulation of SCoAS ectopic expression. From that moment on the cells were grown in the presence of tetracycline (1µg/ml) to ensure SCoAS constant expression until needed. Finally, the second SCoAS allele was removed with the same strategy as for the generation of SCoAS DKO cell line – by replacement with T7 promoter, tetracycline repressor and Hygromycin resistance. To ensure the SCoAS copy was introduced in the correct place we performed a PCR verification (data not shown) with forward primer complementary to the PARP 5'UTR and the reverse



primer complementary to SCoAS CDS. The final verification was achieved by checking the regulation of expression the protein in the SCoAS cDKO cell line upon request showing that system can work in both HMI-11 and CMM medium. The cell line was grown in the presence of G418, hygromycin and phleomycin drugs, and tetracycline. Tetracycline binds the tetracycline repressor and due to a conformational change, the repressor cannot any longer bind the operator site and thus the introduced copy of SCoAS is constantly expressed under PARP promoter. 2-3 days before an experiment the cells would be spun down and washed in medium without tetracycline twice and grown in tetracycline-free medium during the experiments. Thus, the cells are suddenly compelled to the absence of SCoAS with no preadaptation time to its loss.

### **5.2.9. SCoAS DKO/AAC RNAi**

SCoAS DKO/AAC RNAi is a cell line which is lacking SCoAS and at the same time AAC levels can be downregulated upon tetracycline induction. The parental cell line, SCoAS DKO (B1 clone sensitive to CATR) already generated and containing T7 RNA polymerase, 10% T7 promoter and tetracycline repressor was subsequently transfected with p2T7-177 plasmid, containing dsRNAi construct targeting AAC mRNA (already generated, see AAC RNAi cell line) under two T7 promoters and two tetracycline operators. This system allows for tetracycline-inducible expression of AAC RNAi in the background of SCoAS DKO. The cells were grown in the presence of G418, hygromycin and phleomycin.

### **5.3. Mitochondrial or cytosolic luciferase expression in AAC DKO, SCoAS DKO and BF WT cells**

For the in vivo ATP measurements in the cytosol or in the mitochondrion we generated BF cell lines expressing firefly luciferase into those compartments. We generated two constructs either containing or not the MTS from TbIscU (*T. brucei* iron-sulfur cluster assembly protein, Tb927.9.11720) (Mach et al., 2013), followed by ORF from *P.pyralis* (accession version M15077.1), commonly known as firefly luciferase with restriction sites for N-terminal HindIII and C-terminal BamHI and C-terminal 3 V5-tags. The constructs were amplified using as a template a previously generated in the lab pHD1344 plasmid, containing puromycin resistance cassette, tubulin CDS and luciferase CDS. The reverse PCR primer common for both constructs used was with 16 bp homology regions with the luciferase and BamHI restriction site: 5-GCTGGATCCCTTCTTGGCCTTTAATG-3. The forward PCR primer for the mitochondrial expression contained 21 bp luciferase homology region together with MTS predicted from TbIscU and HindIII restriction site was: 5-

GCCAAGCTTATGCGGCGACTGATATCATCACACATTGTACTGCCGACGCTGGCAGCCTCACTT  
CGGTCACTGTACAGCCCACTAGAAGACGCCAAAAACATAAAG-3. The forward PCR primer for  
cytosolic luciferase expression contained 18 bp luciferase homology and HindIII restriction site was: 5-  
CCGAAGCTTATGGAAGACGCCAAAAAC-3. The parental plasmid used was modified pHD-1344-tub-  
B5-3v5, containing beta tubulin CDS, TbKREPB5 CDS with C-terminally fused 3 v5 tags followed by  
NcoI restriction site N-terminally to GFP CDS. Via site-directed mutagenesis we introduced another NcoI  
site C-terminally to GFP CDS which allowed us to remove GFP via NcoI restriction enzyme. TbKREPB5  
was flanked by HindIII and BamHI. The constructs with firefly luciferase ORF with or without MTS were  
cloned into the modified pHD-1344-tub-B5-3v5 vector using HindIII and BamHI restriction enzymes by  
removing TbKREPB5 to generate LUC MTS pHD 3v5 or LUC NoMTS pHD 3v5 plasmids. The final  
plasmids were linearized with NotI prior to transfection in BF WT, AAC DKO and SCoAS DKO and  
contained the MTS firefly luciferase CDS (for mito expression) or firefly luciferase CDS only (for cyto  
expression) fused C-terminally with 3V5 tags under the control of the tubulin promoter and thus allow the  
expression to be constitutive. The plasmids were verified by Sanger sequencing and transfected for either  
mitochondrial (TbIscU-luciferase-3V5) or cytosolic (luciferase-3V5) expression into our mutant cell lines  
- AAC DKO and SCoAS DKO (clone B1) as well as in BF WT 427 cells.

#### **5.4. Transfections of *T. brucei***

All the genetically modified BF *T. brucei* cell lines we used were generated by transfection with the  
respective linearized plasmid and the following integration into the parasite genome due to homologous  
recombination. The plasmids were designed to have only one NotI restriction site which is linearized by  
NotI restriction enzyme and the generated ends of the linearized plasmid are engineered to be homologous  
to specific sequences of the *T. brucei* genome. The linearization of the plasmid was achieved by digestion  
of 15 µg of the circular plasmid with 2 µl NotI restriction enzyme at 37°C overnight followed by ethanol  
precipitation (1/10 of the volume 3M Sodium Acetate, pH 5.2, 2.5x vol 97% EtOH, 30 min incubation at -  
80 °C). After full-speed centrifugation and wash with 70% EtOH the plasmid was resuspended in 30 µl  
sterile water. Few days prior to transfection the cells were grown in mid-log phase and  $3 \times 10^7$  cells were  
centrifuged (1300xg, 10min), washed in PBS buffer containing 6mM glucose (PBS-G) and resuspended in  
100 µl Amaxa Cell Line Nucleofactor (Lonza). The resuspended cells were transferred into electroporation  
cuvette, mixed with 10 µg of the linearized plasmid and electroporated (program X-001) by Nucleofactor  
II electroporator (Lonza). The transfected cells were transferred in 30ml HMI-11 medium. 3ml of the HMI-  
11- diluted transfectant were further diluted in 27 ml HMI-11 to achieve  $1 \times 10^5$  cells/ml concentration and  
another dilution (3ml of the  $1 \times 10^5$  cells/ml into 27 ml HMI-11) to achieve  $1 \times 10^4$  cells/ml concentration.

Aliquots of 1ml from each of the 3 dilutions were distributed into 24-well plates and incubated at 37°C. After 16 hours incubation 1 ml of the HMI-11 medium containing twice concentrated respective selectable drugs were added to each well. 5-6 days later the positive transformants are starting to appear.

## **5.5. Western blots**

Western blots are used to determine the relative amount of a specific protein in the sample.  $1 \times 10^7$  cells were harvested at 1300xg at 4°C for 10 minutes, washed with 1x PBS and the whole cells lysates (WCL) were resuspended in 20µl 1xPBS and 10µl SDS solution (6% SDS, 300mM DTT, 150mM Tris HCl, 30% glycerol, and 0.02% Bromophenol Blue). Samples were boiled for 7 minutes at 97°C and stored at -20°C. The SDS functions to give proteins negative charge so they could migrate to the positively charged electrode during electrophoresis. Proteins were resolved on SDS-PAGE gels (BioRad, Invitrogen) using  $3.3 \times 10^6$  cells/line loaded. Proteins were blotted onto PVDF membrane (Thermo Scientific) which was preactivated with methanol. The membrane was probed with corresponding primary mouse monoclonal (mAb) or rabbit polyclonal (pAb) antibodies diluted in 5% skimmed milk. Primary antibodies used are with the following dilutions: pAb anti-AAC (1:1000, 34kDa), pAb anti-SCoAS (1:1000, 44.9kDa), pAb anti-APRT (1:500, 26kDa), and mAb anti-HSP70 (1:5000, 71.5kDa, pAb anti-TDH (1:2000, 36.5kDa), pAb anti-ASCT (1:1000, 53kDa), pAb anti-p18 (1:1000, 18kDa), pAb anti-ATPaseTb2 (1:2000, 43.3kDa), pAb anti-OSCP (1:1000, 27kDa), mAb anti-V5 tag (1:2000).

This was followed by probing with secondary HRP conjugated anti-mouse or anti-rabbit antibody (1:2000 dilution) respectively. Proteins were visualized using the Clarity Western ECL substrate (Bio-Rad 1705060EM) on a ChemiDoc instrument (Bio-Rad). The PageRuler prestained protein standard (Fermentas) was used to determine the molecular size of the detected bands.

## **5.6. Quantitative reverse transcriptase-PCR (qRT-PCR)**

In order to verify the successful downregulation of the target SCoAS transcript in the induced SCoAS RNAi cell lines, q RT-PCR was performed.

### **5.6.1. Total RNA isolation (Phenol-Chloroform extraction)**

To determine the decrease in the SCoAS mRNA levels, first we have to isolate total RNA. SCoAS (clones B3 and B4) were grown in HMI-11 media with the appropriate selectable drugs in order to keep the RNAi

construct.  $2.5 \times 10^8$  cells 1- and 3-days post-induction with tetracycline as well as non-induced cells were collected by centrifugation at 1500xg for 5 min at 4°C. Next, the cell pellet was washed once in PBS and centrifuged again. The pellet was collected, flash-frozen in liquid nitrogen and stored at -80°C. Frozen cell pellet was dissolved in 0.8 ml solution, containing 4M guanidine isothiocyanate (for protein denaturation, cell lysis and RNase inhibition), 25mM sodium citrate, pH 7.0, 0.5% sarcosyl-sodium salt and 0.1M  $\beta$ -mercaptoethanol. Next, the following compound were added and mixed gradually: 0.1ml of 2M sodium acetate, 0.9 ml of phenol and 0.3 ml of chloroform, rotated for 10 min at 4°C and incubate on ice for 10-15 min. Immediately the aqueous supernatant (containing RNA molecules) was transferred to 2 ml Phase-lock tube (Thermo Fisher). The organic phase contains DNA molecules and proteins. Next, to the RNA-containing solution, 0.8 ml chloroform was added and vortexed at max speed for at least 1 min, next was centrifuged at RT for 5 min max speed and the aqueous supernatant was transferred to a new tube. Next, the RNA was precipitated by addition of 2ml isopropanol, incubated for 1h at -20°C, centrifuged at 4°C for 30 min max speed. The pellet was washed in 80% ice-cold ethanol and centrifuged again at 4°C for 10 min max speed. The supernatant was removed and the pellet, containing the RNA fraction was air-dried and resuspended in 0.2ml water. This sample was further subjected to the precipitation by 20 $\mu$ l sodium acetate (pH 5) and 0.6ml 96% ethanol for 1h at -20°C. Next, the samples were centrifuged at 4°C for 30 min max speed and washed with 80% ethanol. The pellet was dissolved in water and the concentration of the RNA in the RNA-rich entity was measured by nanodrop.

### **5.6.2. DNase treatment**

The samples containing RNA were further treated with DNase to remove any residual DNA from the samples. For the purpose Turbo DNase, Ambion (Invitrogen) kit was used. Briefly, the samples were incubated in the buffer and Turbo DNase for 30 min at 37°C. Then it was preceded directly to RNA re-purification by RNeasy MiniElute Cleanup Kit (Qiagen), where the protocol was followed. The final product was the purified total RNA diluted in grade water from the kit.

### **5.6.3. Copy DNA (cDNA) synthesis**

The purified total RNA from the samples was further converted to its ssDNA copy (cDNA) using TagMan Reverse Transcription Kit (Applied Biosciences). Briefly, the RNA samples were incubated with RT buffer and random hexamers from the kit at 80°C for 2 min (to unwind any double stranded nucleic acids to allow the hexamers bind) at the thermal cycler and then kept on ice. Next, according to the protocol, to the samples were added to their final concentration 1.75mM MgCl<sub>2</sub>, 0.5mM each dNTP, 1U/ $\mu$ l RNase inhibitor, 2.5U/ $\mu$ l

reverse transcriptase (RT) and the samples were placed back to the thermal cycler and the actual cDNA synthesis was achieved by the following steps: 25 °C for 10 min, 48 °C for 30min, 95 °C for 5 min, 10 °C hold. The cDNA samples were stored at -80 °C. In addition, the procedure was repeated with the same samples and conditions with the only difference that RT was not added. It was used for contamination control.

#### 5.6.4. Quantitative PCR (qPCR) and data analysis

Next, we proceeded to quantification of the downregulation of SCoAS transcripts relative to reference gene transcripts in the induced vs. non-induced SCoAS RNAi cells. We used quantitative PCR (qPCR) and LC480 SYBR Green I Master kit (Roche). For the reference gene transcripts we used trypanosome transcripts for the house-keeping genes 18S rRNA and trypanosome telomere reverse transcriptase (TERT) which should be equally expressed in both NON and induced cells. The qPCR primers for the target cDNA of SCoAS CDS were designed to target cDNA region outside of the RNAi targeted region. Each sample was measured in triplicates. Into each well of the 96-well plate 10µl of 2xSYBR Green I Master mix, 8µl of the respective primer pair mix (1.5 µM each) and 2 µl of the samples. It should be mentioned that the samples used for reference genes targets were diluted 1:500 since these reference gene transcripts are highly abundant. Samples without RT treatment were also included as a contamination control. The primers sequence used are shown on **table 5**. Next, the plate was introduced to the Light Cycler 480 (Roche) and the program was initiated according to **table 6**. SYBR Green is a fluorescent dye which accumulates into dsDNA and the dsDNA-SYBR Green complex emits green light, recorded by the Light Cycler. During the PCR reaction the respective amplicons amplify exponentially, and the fluorescence corresponds to the amount of DNA after each cycle. The cycle at which the fluorescence is above the set threshold is called Ct (threshold cycle). The Ct values for all the samples were exported to excel for analysis.

The method used for determining the SCoAS transcript relative levels in the samples was the  $2^{-\Delta\Delta Ct}$  method (Livak & Schmittgen, 2001). Briefly, the amount of the target SCoAS gene transcript in the induced cells which was normalized to the reference gene transcripts (either to 18s rRNA or to TERT) and it is relative to the SCoAS gene transcript in the non-induced cells, equals  $2^{-\Delta\Delta Ct}$ .  $-\Delta\Delta Ct$  equals  $-(\Delta Ct_{Ind} - \Delta Ct_{NON})$ .  $\Delta Ct_{Ind}$  equals  $(Ct_{ScoAS ind} - Ct_{ref.gene ind})$ .  $\Delta Ct_{non}$  equals  $(Ct_{ScoAS NON} - Ct_{ref.gene NON})$ . We assume that the efficiency of the target amplicons is one.

Reaction Step	Temperature	Time	Cycle numbers
Initial denaturing step	95°C	30 sec	
Denaturation	95°C	15 sec	45 cycles
Annealing	60°C	15 sec	
Extension	72°C	15 sec	
Hold	4°C	forever	

**Table 5** - The program used to perform qPCR in the light cycler for the experiment.

Target gene transcript for qPCR	Primer pair sequence
18S rRNA	For: GCGAAACGCCAAGCTAATAC Rev: AGCCGCGACATAGAAAAAGA
TERT (Trypanosome telomere reverse transcriptase)	FOR: AGGAACTGTCACGGAGTTTGC REV: GGTATCGTTGCGGCGTCT
SCoAS	FOR: GGTATCGTTGCGGCGTCT REV: CGCTTGCTTCTTCTTCCTTG

**Table 6** - qPCR primer sequence used in the experiment.

### 5.7. Membrane potential measurements by TMRE

The mitochondrial membrane potential (mt  $\Delta\Psi_m$ ) of trypanosome cell population is an important component of the fitness of the cell population. mt  $\Delta\Psi_m$  represents the difference in ion concentration and thus the charge between the intermembrane space and the mitochondrial matrix. Changes in the mt  $\Delta\Psi_m$  was measured by flow cytometry using the fluorescent dye tetramethylrhodamine ethyl ester (TMRE). TMRE accumulates in active mitochondria according to  $\Delta\Psi_m$  and its fluorescence can be measured by FACS.

### 5.7.1. Cell staining

Each experiment was conducted in technical triplicates for statistical purposes.  $3 \times 10^6$  BF cells grown in mid-log phase for few days prior to the experiment in the appropriate medium were collected by centrifugation at 1300xg for 10 minutes at RT. The cells were resuspended in 10 ml of the appropriate media without the selectable drugs to avoid interfering with the experiment in the presence of 60nM TMRE and incubated for 30 min under standard for BF cell cultivation conditions. The positively charged membrane permeable TMRE accumulates into the functional mitochondrion with the net negative charge of the mitochondrial matrix in oppose to parasites with impaired mitochondria. The cells were harvested by centrifugation at 1300xg for 10 minutes at RT and resuspended in 1ml PBS buffer, pH 7.4 supplemented with 6mM glucose. Additionally, as a negative control for mitochondrial membrane depolarization, the experiment was conducted under the same conditions in the presence of 20 $\mu$ M Carbonyl cyanide 4-(trifluoromethoxy) phenylhydrazone (FCCP),  $\Delta\Psi_m$  uncoupler. FCCP is a protophore which translocates protons across the membrane causing membrane depolarization and therefore mt  $\Delta\Psi_m$  collapse. Next, we proceeded to FACS measurements.

### 5.7.2. FACS measurements

The accumulation of TMRE in the mitochondrial matrix, representing the mt  $\Delta\Psi_m$ , was measured by Becton Dickinson FACS Canto II flow cytometer. During the flow of the cells through a laser beam TMRE was activated by excitation energy at 488 nm and the emitted light at 585nm was recorded by the detector. The data from FACS flow cytometer were exported into Excel sheet and further analyzed.

### 5.8. Membrane potential measurement by quenching mode of Safranin-O

The changes in mitochondrial membrane potential (mt  $\Delta\psi_m$ ) were measured *in situ* in time on digitonin-permeabilized cells using safranin O dye (Sigma, S2255-25G). Safranin O is a lipophilic cationic dye, and it is used as a fluorescent indicator of mt  $\Delta\psi$  in isolated mitochondria or digitonin-permeabilized cells. It accumulates into the mitochondrion and its stacking to the inner mitochondrial membrane anionic sites leads to the aggregation of the safranin O into dimers and polymers. As a result, the higher the mt  $\Delta\psi_m$  the more safranin O accumulates and aggregates and therefore less safranin O is available for detection, also known as fluorescence self-quenching. Safranin O has an excitation wavelength of 496 nm and emission wavelength of 586 nm, which can be measured by Tecan Infinite M200. The experiment was performed in

the following way. Each experiment was conducted in technical triplicates for statistical purposes. Prior to the experiment the cells were grown for few days in mid-log phase. WT and AAC DKO cells were collected by centrifugation at 1300xg for 10 minutes at RT, washed with PBS-G and resuspended in a buffer containing 125 mM sucrose, 65mM KCL, 10mM Hepes-KOH (pH 7.2), 1mM MgCl<sub>2</sub>, 2.5mM KH<sub>2</sub>PO<sub>4</sub>, 20μM EGTA, 0.5mM Na<sub>3</sub>O<sub>4</sub>V. In a total volume of 100μl/well, 8.2x10<sup>6</sup> cells were distributed into each well in a 96-well plate and safranin O was added (12.5μM final concentration) followed by ATP (1mM final concentration). The assay was initiated by adding digitonin (40μM final concentration) to permeabilize only plasma membrane but keep the mt membrane intact. The fluorescence was measure by Tecan every 10 seconds. Where indicated 5 μl of the membrane-depolarizing protophore FCCP (10μM final concentration) was injected by the machine and the measurements continued. Data were analyzed using GraphPad Prism.

## **5.9. Oligomycin treatment**

BF WT and AAC DKO cells were grown in mid-log phase in standard cultivation conditions in HMI-11 medium without the selectable drugs at least 24 hours prior to the experiment. 500 ng/ml final concentration of Oligomycin (OLM), complex V inhibitor, purchased from Sigma (cat.num.O4876-25MG) was either added or not to 10 ml cell culture with 1x10<sup>5</sup> cells/ml cell density and incubated under standard conditions for 24 hours. The viability of the cells was observed under light microscope and the doubling time was estimated. Next, the mt ΔΨ<sub>m</sub> was measured with TMRE by FACS as already described with the only difference that 500 ng/ml OLM was added and always kept in the media and buffers during the measurements since the inhibition is reversible and OLM would be washed away. It should be mentioned that OLM was dissolved and kept in 96% ethanol and the final concentration in the cell culture was estimated to contain 0.04% ethanol. Therefore, we also checked if the mt ΔΨ<sub>m</sub> would be affected when cells were incubated with 0.04% ethanol, and we saw no difference compared to non-treated cells (data not shown).

## **5.10. *In vitro* ATP measurements**

### **5.10.1. Sample preparation – subcellular fractionation**

*In vitro* ATP levels were measured on the total, mitochondrial and cytosolic cell fraction of BF WT cells and our AAC DKO and SCoAS DKO mutants. The cells were grown in HMI-11 medium with the respective



drugs in mid-log phase for few days prior to the experiment. For the cytosolic and organellar fraction  $5 \times 10^7$  cells from each cell line were harvested by centrifugation at 1300xg for 10 minutes at 4°C, washed with PBS and resuspended in 500µl So-TE buffer (20 mM Tris-HCL, pH 7.5, 0.6 M sorbitol, 2 mM EDTA). After adding preboiled and let to room-temperature 500 µl So-TE supplemented with 0.03% digitonin, the test tube was inverted once. Samples were incubated for 5 min on ice and spun down (3 minutes, 4°C, 4500xg). The supernatant is the cytosolic fraction (containing the cytosol), and the pellet is the mitochondrial-rich organellar fraction (containing the membrane-bound organelles). The pellet is resuspended in the same volume as the supernatant in So-Te buffer and both fractions are diluted in the same volume of So-TE. For the total cell fraction, where the levels of ATP in the whole cell are measured,  $5 \times 10^7$  cells from each cell line were collected similarly by centrifugation at 1300xg for 10 minutes at 4°C, washed with PBS and resuspended in 400µl So-TE buffer.

### **5.10.2. ATP measurements**

Next, we measured the ATP levels in all 3 fractions (total, cytosolic and mitochondrial) using ATP Bioluminescence Assay Kit HS II (Roche, Cat. No. 11 699 709 001) according to the protocol. Briefly, 100µl sample from each fraction were mixed with 100µl cell lysis reagent 3 from the kit and kept for 5 min at room temperature. 50µl was distributed in triplicates in each well of 96-well white bioluminescence plate. The plate was inserted in the luminometer Orion II. 50µl luciferase reagent 1 (containing luciferase reagent) from the kit was added to initiate the reaction by injection protocol. The bioluminescence was measured by luminometer, and the data was saved on a separate excel sheet for analysis. The ATP concentration was calculated according to the ATP standard in the kit. Briefly, an ATP standard (from the kit) with known concentration was diluted serially by 10 folds and measured together with the samples. Then bioluminescent vs. concentration values are plotted and from the obtained linear curve (trendline) the equation was generated and from the sample bioluminescent values the corresponding ATP values in mM were calculated.

### **5.11. *In vivo* ATP measurements – luciferase assay**

*In vivo* ATP measurements were performed directly in cytosol and in the mitochondrion of the intact cells by targeted expression of luciferase into those compartments. For the purpose, BF WT, AAC DKO and SCoAS DKO (clone B1) cells were transfected to stably express luciferase, either in the cytosol or in the mitochondrion of the cells (see M&M section 1.2.10). ATP was measured directly in the cytosol or the mitochondrion, where the luciferase is localized. Luciferase catalyzes the conversion of ATP to AMP with the help of luciferin and the amount of ATP corresponds to the amount of emitted bioluminescent light

during the reaction. The cells were grown in HMI-11 medium with the respective drugs in mid-log phase for few days prior to the experiment.  $1 \times 10^7$  cells from each cells line were harvested by centrifugation at 1300xg for 10 minutes at room temperature, washed with PBS (pH 7.4) and the cell pellet was resuspended in 160  $\mu$ l HEPES-Luc buffer, pH 7.4 containing 20mM HEPES, 116mM NaCl, 5.6mM KCl, 8mM MgSO<sub>4</sub> and 1.8mM CaCl<sub>2</sub>. The samples were transferred into 96-well white bioluminescence plate. In addition, BF WT cells without luciferase expression as well as HEPES-Luc buffer without cells used as controls were also distributed in the plate. The reaction was initiated by injection of 40 $\mu$ l of 250 $\mu$ M D-luciferin (Sigma, L6882), which is cell membrane permeable. The produced bioluminescence was measured in time by Tecan Infinite Spectrophotometer and the bioluminescent values corresponding to the ATP levels was normalized to the BF WT which were given the value of 1.

### 5.12. Animal experiments

Animal experimental work was performed by Brian Panicucci and Michaela Husová. Mice were treated according to Czech and EU legislation and were euthanized when they displayed an impaired health or the parasitemia levels were higher than  $1 \times 10^8$  cells/ml of blood. Groups of 5-7 BALB/c mice were used for each of the cell lines and were infected with  $1 \times 10^5$  cells (harvested at 1300xg for 10min and resuspended in PBS containin 6mM glucose) via 100ul intraperitoneal injection of either BF WT 427, AAC DKO or SCoAS DKO parasites. Blood samples from a tail vein were mixed with 1x SSC and 3.7% formaldehyde, and the parasitemia levels were counted using a hemocytometer (Counting Chamber CE Neubauer IMP DL). Parasitemia counts were observed for 20 days.

### 5.13. Alamar blue assay

Alamar blue assay is a widely used method to determine the sensitivity of cells towards different drugs. The BF trypanosome cells were treated with increasing concentration of the respective compound and resazurin dye is used to determine the cell viability. The viable cells are able to reduce the non-fluorescent dye resazurin to the strongly fluorescent resorufin by the metabolically active mitochondrion and the fluorescent output is proportional to the viable cell count. Then the effective concentration of the drug which kills half of the cell population is estimated (EC<sub>50</sub>). The method was performed in the following way. The respective cells line was grown in mid-log phase for few days before the experiment.  $5 \times 10^3$  cells/ml in the appropriate medium were plated in transparent 96-well plates in a total volume of 200 $\mu$ l/well in triplicates. Then the respective test compound was added in gradually increasing concentration. The summary of the drugs used in the method in this thesis is shown on **table 7**. The range of the concentration of the drug must

be chosen carefully ensuring that the lowest concentration keeps all the cells viable, and the highest concentration kills all the cells. The cells were incubated under standard conditions and after 72 hours 20ul of 125ug/ml of resazurin (Sigma, R7017-1G) was added to each well. After 24 hours the fluorescence was measured by Tecan Spark set up using excitation wavelength of 544nm and emission wavelength of 590nm. Data were analyzed using GraphPad Prism and the EC<sub>50</sub> values were estimated.

Compound	Manufacturer	Solvent
TPMP	Sigma/Merck	methanol
UK5099	Sigma/Merck	DMSO
arsenite	Sigma/Merck	H <sub>2</sub> O
QC1	Merck	DMSO
TETD	Sigma/Merck	H <sub>2</sub> O
LY266500	MolPort	DMSO
CATR	Sigma	DMSO
OLM	Sigma	ethanol

**Table 7-** Test compounds used in alamar blue assay.

#### 5.14. Succinyl-CoA synthetase (SCoAS) activity assay

The of the Succinyl-CoA synthetase (SCoAS) activity in the BF trypanosomes to my knowledge is measured for the first time in that thesis. The method is based on Alarcon et al., 2002 with modifications from Lambeth et al., 2004 and suggestions from Christos Chinopoulos MD, PhD.

##### 5.14.1. Sample preparation – digitonin subcellular fractionation:

The activity of SCoAS enzyme was measured on the mitochondrial matrix-rich fraction from BF WT, AAC DKO and SCoAS DKO trypanosomes. 5x10<sup>8</sup> cells grown in mid-log phase were harvested and spun down (10 minutes, 4°C, 1300xg). Next, the cells were washed once with PBS (a few µl taken for WB for WCL fraction) and resuspended in 500 µl So-TE (20 mM Tris-HCL, pH 7.5, 0.6 M sorbitol, 2 mM EDTA). After adding preboiled and let to room-temperature 500 µl So-TE supplemented with 0.03% digitonin, the test

tube was inverted once. Samples were incubated for 5 min on ice and spun down (3 minutes, 4°C, 4500xg). The supernatant is the cytosolic fraction (a few µl taken for WB for cyto fraction), and the pellet is the mitochondrial-rich organellar fraction (a few µl taken for WB for mito fraction).

#### **5.14.2. Sample preparation of the mitochondrial matrix-rich fraction**

The pellet (the mitochondrial-rich organellar fraction) was further resuspended in 500 µl ANT buffer, pH 7.25, containing 8 mM KCl (Lach-ner), 110 mM K-gluconate (Sigma), 10 mM NaCl (Sigma), 10 mM Hepes -free acid (Sigma), 10 mM K<sub>2</sub>HPO<sub>4</sub> (Sigma), 0.015 mM EGTA (K<sup>+</sup> salt) (Sigma), 0.5 mg/ml BSA (FA-free) (Sigma), 10 mM mannitol (Sigma) and 10 mM MgCl<sub>2</sub> (Sigma) added immediately before use. The samples were sonicated in order to break the organellar membranes and to release mitochondrial matrix content so that the SCoAS enzyme can be accessible for the assay. The sonication was done 3 times for 10 sec at 20% power and kept on ice for 1 min between pulses. The samples were spun down at max speed (1600xg) at 4°C for 5 min. Supernatant containing the mitochondrial matrix-rich entity (mito-soluble fraction) was collected (a few µl taken for WB) and further being a subject of SCoAS activity assay. The pellet containing organellar membrane debris (mito-insoluble fraction) was resuspended in the same volume of PBS and a few µl were taken for WB. WB analysis was utilized for assessing the quality of the generated fractions, efficiency of the sonication as well as the presence of SCoAS in the respective fractions.

#### **5.14.3. Activity assay - measurements**

SCoAS enzyme triggers the conversion of succinyl-CoA to succinate together with the conversion of ADP to ATP in trypanosomes with the release of CoA-SH. It also requires Pi, Mg<sup>2+</sup> as cofactor and 30°C to be carried. SCoAS activity was measured on the supernatant after sonication of all 3 cell lines, BF WT, AAC DKO and SCoAS DKO cells (negative control). It was diluted 8 folds in ANT buffer and a few µl were used to determine mitochondrial protein concentration by BCA assay (Pierce). During the reaction the release of CoA-SH was monitored spectrophotometrically at 412 nm on its reaction with DTNB (5,5'-Dithiobis 2-nitrobenzoic acid or Ellman's reagent) forming thio-nitrobenzoate anion (TNB) at 30°C over time every 10 sec using a plate reader Tecan Infinite M200. Final concentration of 2mM ADP was added to the sonicated in ANT buffer sample and the reaction was initiated by adding in a quick succession of succinyl-CoA (0.2mM final concentration) and DTNB (0.2mM final concentration) in the total reaction volume of 100 µl. In parallel as a background control, we used the respective cell lines without addition of the substrates (succinyl-CoA and ADP) but only DTNB. 4 independent experiments were carried out.

The specific SCoAS enzymatic activity was calculated in mg of mitochondrial protein where one unit of activity converts one nanomole of succinyl-CoA to CoA for 1 minute. First, we calculated the change in the absorbance for TNB at 412nm for 1 min for the sample and for the background control and subtracted the later. Next, we calculated the change in the concentration in nanomoles\*100  $\mu\text{l}^{-1}*\text{min}^{-1}$  of TNB as a results of SCoAS enzymatic activity by Lambert-Beer's Law:  $A=c.l.e$ , where A is the change in absorbance for 1 min, c is the change in the concentration for 1 min, l is the length in solution the light is passing through, considered to be to be 0.58cm for 100ul in standard microplate well, e is the molar extinction coefficient value which at 412 nm for the TNB was considered as 13 600  $\text{L.M}^{-1}.\text{cm}^{-1}$ . And finally, the change in the concentration of TNB of each sample in nanomoles\*100  $\mu\text{l}^{-1}*\text{min}^{-1}$  was divided by the total mitochondrial protein for the respective sample measured by BCA assay in mg/100 $\mu\text{l}$  to get the specific SCoAS activity expressed in nmoles\*min<sup>-1</sup>\*mg<sup>-1</sup>.

### 5.15. Exometabolomics

The exometabolomics experiments were performed in collaboration with the laboratory of F. Bringaud, University of Bordeaux, Bordeaux, France. BF WT, AAC DKO and SCoAS DKO trypanosomes were grown in mid-log phase in HMI-11 media supplemented with the respective drugs.  $1 \times 10^7$  cells were collected by centrifugation at 1400xg for 10 min at RT and washed with incubation buffer (PBS buffer supplemented with 5 g/L  $\text{NaHCO}_3$ , pH 7.4) with the addition of 1mM of the respective carbon source. Next, the cells were incubated in preheated plates until the cells manage to keep cell integrity (validated by microscopic observation, appr.2,5 hours) at 37°C with incubation buffer containing uniformly labeled [U-<sup>13</sup>C]-glucose (4 mM) in the presence or absence of the respective 4 mM compound – glutamine, glutamate,  $\alpha$ -ketoglutarate or threonine in a total volume of 1ml. The same experiment was carried out with ordinary <sup>12</sup>C glucose as the only carbon source mainly for calibration purposes. Following centrifugation at 8000xg for 1 min at RT, the supernatant was collected and a proton NMR (<sup>1</sup>H-NMR) spectra were performed as described in (Mazet et al., 2013).

## 6. REFERENCE LIST (ALPHABETICAL ORDER):

- Acestor, N., Zíková, A., Dalley, R. A., Anupama, A., Panigrahi, A. K., & Stuart, K. D. (2011). Trypanosoma brucei mitochondrial respiratome: Composition and organization in procyclic form. *Molecular and Cellular Proteomics*, 10(9), 1–14. <https://doi.org/10.1074/mcp.M110.006908>
- Alarcon, C., Wicksteed, B., Prentki, M., Corkey, B. E., & Rhodes, C. J. (2002). Succinate is a preferential metabolic stimulus-coupling signal for glucose-induced proinsulin biosynthesis translation. *Diabetes*, 51(8), 2496–2504. <https://doi.org/10.2337/diabetes.51.8.2496>
- Alexander, P. B., Wang, J., & McKnight, S. L. (2011). Targeted killing of a mammalian cell based upon its specialized metabolic state. *Proceedings of the National Academy of Sciences of the United States of America*, 108(38), 15828–15833. <https://doi.org/10.1073/pnas.1111312108>
- Alkhaldi, A. A. M., Martinek, J., Panicucci, B., Dardonville, C., Zíková, A., & de Koning, H. P. (2016). Trypanocidal action of bisphosphonium salts through a mitochondrial target in bloodstream form Trypanosoma brucei. *International Journal for Parasitology: Drugs and Drug Resistance*, 6(1), 23–34. <https://doi.org/10.1016/j.ijpddr.2015.12.002>
- Allmann, S., Mazet, M., Ziebart, N., Bouyssou, G., Fouillen, L., Dupuy, J. W., Bonneu, M., Moreau, P., Bringaud, F., & Boshart, M. (2014). Triacylglycerol storage in lipid droplets in procyclic trypanosoma brucei. *PLoS ONE*, 9(12). <https://doi.org/10.1371/journal.pone.0114628>
- Allmann, S., Morand, P., Ebikeme, C., Gales, L., Biran, M., Hubert, J., Brennand, A., Mazet, M., Franconi, J. M., Michels, P. A. M., Portais, J. C., Boshart, M., & Bringaud, F. (2013). Cytosolic NADPH homeostasis in glucose-starved procyclic trypanosoma brucei relies on malic enzyme and the pentose phosphate pathway fed by gluconeogenic flux. *Journal of Biological Chemistry*, 288(25), 18494–18505. <https://doi.org/10.1074/jbc.M113.462978>
- Allmann, S., Wargnies, M., Plazolles, N., Cahoreau, E., Biran, M., Morand, P., Pineda, E., Kulyk, H., Asencio, C., Villafraz, O., Rivière, L., Tetaud, E., Rotureau, B., Mourier, A., Portais, J. C., & Bringaud, F. (2021). Glycerol suppresses glucose consumption in trypanosomes through metabolic contest. *PLoS Biology*, 19(8). <https://doi.org/10.1371/journal.pbio.3001359>
- Alsford, S., Currier, R. B., Guerra-Assunção, J. A., Clark, T. G., & Horn, D. (2014). Cathepsin-L Can Resist Lysis by Human Serum in Trypanosoma brucei brucei. *PLoS Pathogens*, 10(5). <https://doi.org/10.1371/journal.ppat.1004130>

- Aragonès, G., Auguet, T., Berlanga, A., Guiu-Jurado, E., Martinez, S., Armengol, S., Sabench, F., Ras, R., Hernandez, M., Aguilar, C., Colom, J., Sirvent, J. J., Del Castillo, D., & Richart, C. (2016). Increased circulating levels of alpha-ketoglutarate in morbidly obese women with non-alcoholic fatty liver disease. *PLoS ONE*, *11*(4). <https://doi.org/10.1371/journal.pone.0154601>
- Aranda, A., Maugeri, D., Uttaro, A. D., Opperdoes, F., Cazzulo, J. J., & Nowicki, C. (2006). The malate dehydrogenase isoforms from *Trypanosoma brucei*: Subcellular localization and differential expression in bloodstream and procyclic forms. *International Journal for Parasitology*, *36*(3), 295–307. <https://doi.org/10.1016/j.ijpara.2005.09.013>
- Babokhov, P., Sanyaolu, A. O., Oyibo, W. A., Fagbenro-Beyioku, A. F., & Iriemenam, N. C. (2013). A current analysis of chemotherapy strategies for the treatment of human African trypanosomiasis. In *Pathogens and Global Health* (Vol. 107, Issue 5, pp. 242–252). <https://doi.org/10.1179/2047773213Y.0000000105>
- Bagga, P., Behar, K. L., Mason, G. F., De Feyter, H. M., Rothman, D. L., & Patel, A. B. (2014). Characterization of cerebral glutamine uptake from blood in the mouse brain: Implications for metabolic modeling of <sup>13</sup>C NMR data. *Journal of Cerebral Blood Flow and Metabolism*, *34*(10), 1666–1672. <https://doi.org/10.1038/jcbfm.2014.129>
- Bailey, D. L., Fraser, M. E., Bridger, W. A., James, M. N. G., & Wolodko, W. T. (1999). *A Dimeric Form of Escherichia coli Succinyl-CoA Synthetase Produced by Site-Directed Mutagenesis*. <http://www.idealibrary.com>
- Balogun, R. A. (1974). STUDIES ON THE AMINO ACIDS OF THE TSETSE FLY, GLOSSINA MORBITANS, MAINTAINED ON IN VITRO AND IN VIVO FEEDING SYSTEMS. In *Comp. B&hem. Physiol* (Vol. 49). Pergamon Press.
- Bamber, L., Harding, M., Monné, M., Slotboom, D. J., & Kunji, E. R. S. (2007). The yeast mitochondrial ADP/ATP carrier functions as a monomer in mitochondrial membranes. *Proceedings of the National Academy of Sciences of the United States of America*, *104*(26), 10830–10834. <https://doi.org/10.1073/pnas.0703969104>
- Bergquist, E. R., Fischer, R. J., Sugden, K. D., & Martin, B. D. (2009). Inhibition by methylated organoarsenicals of the respiratory 2-oxo-acid dehydrogenases. *Journal of Organometallic Chemistry*, *694*(6), 973–980. <https://doi.org/10.1016/j.jorganchem.2008.12.028>
- Besteiro, S., Biran, M., Biteau, N., Coustou, V., Baltz, T., Canioni, P., & Bringaud, F. (2002). Succinate secreted by *Trypanosoma brucei* is produced by a novel and unique glycosomal enzyme, NADH-

- dependent fumarate reductase. *Journal of Biological Chemistry*, 277(41), 38001–38012. <https://doi.org/10.1074/jbc.M201759200>
- BIENEN, E. J., MATURI, R. K., POLLAKIS, G., & CLARKSON, A. B. (1993). Non-cytochrome mediated mitochondrial ATP production in bloodstream form *Trypanosoma brucei brucei*. *European Journal of Biochemistry*, 216(1), 75–80. <https://doi.org/10.1111/j.1432-1033.1993.tb18118.x>
- Birney, M., Um, H.-D., & Klein, C. (1996). Novel Mechanisms of *Escherichia coli* Succinyl-Coenzyme A Synthetase Regulation. In *JOURNAL OF BACTERIOLOGY* (Vol. 178, Issue 10). <https://journals.asm.org/journal/jb>
- Bochud-Allemann, N., & Schneider, A. (2002). Mitochondrial substrate level phosphorylation is essential for growth of procyclic *Trypanosoma brucei*. *Journal of Biological Chemistry*, 277(36), 32849–32854. <https://doi.org/10.1074/jbc.M205776200>
- Boschmann, M., Murphy, F. P., & Krueger, J. G. (2001). *Clinical and Laboratory Investigations Microdialysis Can Detect Age-Related Differences in Glucose Distribution within the Dermis and Subcutaneous Adipose Tissue*. [www.karger.com/journals/drm](http://www.karger.com/journals/drm)
- Boundenga, L., Mombo, I. M., Augustin, M. O., Barthélémy, N., Nzassi, P. M., Moukodoum, N. D., Rougeron, V., & Prugnolle, F. (2022). Molecular Identification of Trypanosome Diversity in Domestic Animals Reveals the Presence of *Trypanosoma brucei gambiense* in Historical Foci of Human African Trypanosomiasis in Gabon. *Pathogens*, 11(9). <https://doi.org/10.3390/pathogens11090992>
- Bringaud, F., Barrett, M., & Zilberstein, D. (2012). Multiple roles of proline transport and metabolism in trypanosomatids. *Frontiers in Bioscience*, 17, 349–374. <https://www.ncbi.nlm.nih.gov/pubmed/22201748>
- Bringaud, F., Rivière, L., & Coustou, V. (2006). Energy metabolism of trypanosomatids: Adaptation to available carbon sources. In *Molecular and Biochemical Parasitology* (Vol. 149, Issue 1, pp. 1–9). Elsevier. <https://doi.org/10.1016/j.molbiopara.2006.03.017>
- Brown, S. V., Hosking, P., Li, J., & Williams, N. (2006). ATP synthase is responsible for maintaining mitochondrial membrane potential in bloodstream form *Trypanosoma brucei*. *Eukaryotic Cell*, 5(1), 45–53. <https://doi.org/10.1128/EC.5.1.45-53.2006>



- Bursell, E. (1963). *Aspects of the Metabolism of Amino Acids in the Tsetse Fly, Glossina* (Vol. 9). Pergamon Press Ltd.
- Büscher, P., Cecchi, G., Jamonneau, V., & Priotto, G. (2017). Human African trypanosomiasis. In *The Lancet* (Vol. 390, Issue 10110, pp. 2397–2409). Lancet Publishing Group. [https://doi.org/10.1016/S0140-6736\(17\)31510-6](https://doi.org/10.1016/S0140-6736(17)31510-6)
- Capewell, P., Cren-Travaillé, C., Marchesi, F., Johnston, P., Clucas, C., Benson, R. A., Gorman, T.-A., Calvo-Alvarez, E., Crouzols, A., Gory Jouvion, G., Jamonneau, V., Weir, W., Stevenson, L., O’neill, K., Cooper, A., Swar, N.-R. K., Bucheton, B., Ngoyi, M., Garside, P., ... Macleod, A. (2016). *The skin is a significant but overlooked anatomical reservoir for vector-borne African trypanosomes*. <https://doi.org/10.7554/eLife.17716.001>
- Carruthers, L. V., Munday, J. C., Ebiloma, G. U., Steketee, P., Jayaraman, S., Campagnaro, G. D., Ungogo, M. A., Lemgruber, L., Donachie, A. M., Rowan, T. G., Peter, R., Morrison, L. J., Barrett, M. P., & De Koning, H. P. (2021). Diminazene resistance in *Trypanosoma congolense* is not caused by reduced transport capacity but associated with reduced mitochondrial membrane potential. *Molecular Microbiology*, *116*(2), 564–588. <https://doi.org/10.1111/mmi.14733>
- Cayla, M., Rojas, F., Silvester, E., Venter, F., & Matthews, K. R. (2019). African trypanosomes. *Parasites and Vectors*, *12*(1). <https://doi.org/10.1186/s13071-019-3355-5>
- Cestari, I., & Stuart, K. (2017). Transcriptional Regulation of Telomeric Expression Sites and Antigenic Variation in Trypanosomes. *Current Genomics*, *19*(2). <https://doi.org/10.2174/1389202918666170911161831>
- Chaudhuri, M., Ajayi, W., & Hill, G. C. (1998). Biochemical and molecular properties of the *Trypanosoma brucei* alternative oxidase. In *Molecular and Biochemical Parasitology* (Vol. 95).
- Chaudhuri, M., Ott, R. D., & Hill, G. C. (2006). Trypanosome alternative oxidase: from molecule to function. *Trends in Parasitology*, *22*(10), 484–491. <https://doi.org/10.1016/j.pt.2006.08.007>
- Chinopoulos, C. (2011). The “B space” of mitochondrial phosphorylation. In *Journal of Neuroscience Research* (Vol. 89, Issue 12, pp. 1897–1904). <https://doi.org/10.1002/jnr.22659>
- Chinopoulos, C., Gerencser, A. A., Mandi, M., Mathe, K., Töröcsik, B., Doczi, J., Turiak, L., Kiss, G., Konrád, C., Vajda, S., Vereczki, V., Oh, R. J., & Adam-Vizi, V. (2010). Forward operation of adenine nucleotide translocase during F<sub>0</sub>F<sub>1</sub>-ATPase reversal: Critical role of matrix substrate-level phosphorylation. *FASEB Journal*, *24*(7), 2405–2416. <https://doi.org/10.1096/fj.09-149898>

- Clark, M. S., & Worland, M. R. (2008). How insects survive the cold: Molecular mechanisms - A review. In *Journal of Comparative Physiology B: Biochemical, Systemic, and Environmental Physiology* (Vol. 178, Issue 8, pp. 917–933). <https://doi.org/10.1007/s00360-008-0286-4>
- Colasante, C., Peña Diaz, P., Clayton, C., & Voncken, F. (2009). Mitochondrial carrier family inventory of *Trypanosoma brucei brucei*: Identification, expression and subcellular localisation. *Molecular and Biochemical Parasitology*, *167*(2), 104–117. <https://doi.org/10.1016/j.molbiopara.2009.05.004>
- Cooper, A., Capewell, P., Clucas, C., Veitch, N., Weir, W., Thomson, R., Raper, J., & MacLeod, A. (2016). A Primate APOL1 Variant That Kills *Trypanosoma brucei gambiense*. *PLoS Neglected Tropical Diseases*, *10*(8). <https://doi.org/10.1371/journal.pntd.0004903>
- Coustou, V., Biran, M., Besteiro, S., Rivière, L., Baltz, T., Franconi, J. M., & Bringaud, F. (2006). Fumarate is an essential intermediary metabolite produced by the procyclic *Trypanosoma brucei*. *Journal of Biological Chemistry*, *281*(37), 26832–26846. <https://doi.org/10.1074/jbc.M601377200>
- Coustou, V., Biran, M., Breton, M., Guegan, F., Rivière, L., Plazolles, N., Nolan, D., Barrett, M. P., Franconi, J. M., & Bringaud, F. (2008). Glucose-induced remodeling of intermediary and energy metabolism in procyclic *Trypanosoma brucei*. *Journal of Biological Chemistry*, *283*(24), 16343–16354. <https://doi.org/10.1074/jbc.M709592200>
- Creek, D. J., Nijagal, B., Kim, D. H., Rojas, F., Matthews, K. R., & Barrett, M. P. (2013). Metabolomics guides rational development of a simplified cell culture medium for drug screening against *trypanosoma brucei*. *Antimicrobial Agents and Chemotherapy*, *57*(6), 2768–2779. <https://doi.org/10.1128/AAC.00044-13>
- Cross, G. A., Klein, R. A., & Linstead, D. J. (1975). Utilization of amino acids by *Trypanosoma brucei* in culture: L-threonine as a precursor for acetate. *Parasitology*, *71*(2), 311–326. <https://doi.org/10.1017/S0031182000046758>
- Cross, G. A. M., & Manning, J. C. (1973). Cultivation of *Trypanosoma brucei* spp. in semi-defined and defined media. In *Parasitology* (Vol. 67).
- Dahout-Gonzalez, C., Nury, H., Trézéguet, V., Lauquin, G. J. M., Pebay-Peyroula, E., & Brandolin, G. (2006). Molecular, functional, and pathological aspects of the mitochondrial ADP/ATP carrier. *Physiology*, *21*(4), 242–249. <https://doi.org/10.1152/physiol.00005.2006>

- Davies, K. M., Anselmi, C., Wittig, I., Faraldo-Gómez, J. D., & Kühlbrandt, W. (n.d.). *Structure of the yeast F<sub>1</sub>F<sub>o</sub>-ATP synthase dimer and its role in shaping the mitochondrial cristae*. <https://doi.org/10.1073/pnas.1204593109/-/DCSupplemental>
- de Aquino, G. P., Gomes, M. A. M., Salinas, R. K., & Laranjeira-Silva, M. F. (2021). Lipid and fatty acid metabolism in trypanosomatids. In *Microbial Cell* (Vol. 8, Issue 11, pp. 262–275). Shared Science Publishers OG. <https://doi.org/10.15698/mic2021.11.764>
- De Simone, G., Di Masi, A., & Ascenzi, P. (2021). Serum albumin: A multifaced enzyme. In *International Journal of Molecular Sciences* (Vol. 22, Issue 18). MDPI. <https://doi.org/10.3390/ijms221810086>
- Dean, S., Gould, M. K., Dewar, C. E., & Schnauffer, A. C. (2013). Single point mutations in ATP synthase compensate for mitochondrial genome loss in. *Source*, *110*(36), 14741–14746. <https://doi.org/10.1073/pnas.13054041>
- Dewar, C. E., Casas-Sanchez, A., Dieme, C., Crouzols, A., Haines, L. R., Acosta-Serrano, Á., Rotureau, B., & Schnauffer, A. (2022). *Oxidative Phosphorylation Is Required for Powering Motility and Development of the Sleeping Sickness Parasite Trypanosoma brucei in the Tsetse Fly Vector*. <https://journals.asm.org/journal/mbio>
- Dickie, E. A., Giordani, F., Gould, M. K., Mäser, P., Burri, C., Mottram, J. C., Rao, S. P. S., & Barrett, M. P. (2020). New drugs for human African trypanosomiasis: A twenty first century success story. In *Tropical Medicine and Infectious Disease* (Vol. 5, Issue 1). MDPI AG. <https://doi.org/10.3390/tropicalmed5010029>
- Divakaruni, A. S., Wiley, S. E., Rogers, G. W., Andreyev, A. Y., Petrosyan, S., Loviscach, M., Wall, E. A., Yadava, N., Heuck, A. P., Ferrick, D. A., Henry, R. R., McDonald, W. G., Colca, J. R., Simon, M. I., Ciaraldi, T. P., & Murphy, A. N. (2013). Thiazolidinediones are acute, specific inhibitors of the mitochondrial pyruvate carrier. *Proceedings of the National Academy of Sciences of the United States of America*, *110*(14), 5422–5427. <https://doi.org/10.1073/pnas.1303360110>
- Doleželová, E., Kunzová, M., Dejung, M., Levin, M., Panicucci, B., Regnault, C., Janzen, C. J., Barrett, M. P., Butter, F., & Ziková, A. (2020). Cell-based and multi-omics profiling reveals dynamic metabolic repurposing of mitochondria to drive developmental progression of *Trypanosoma brucei*. *PLoS Biology*, *18*(6). <https://doi.org/10.1371/journal.pbio.3000741>

- Drgoň, T., Šabová, L., Gavurniková, G., & Kolarov, J. (1992). Yeast ADP/ATP carrier (AAC) proteins exhibit similar enzymatic properties but their deletion produces different phenotypes. *FEBS Letters*, *304*(2–3), 277–280. [https://doi.org/10.1016/0014-5793\(92\)80637-V](https://doi.org/10.1016/0014-5793(92)80637-V)
- Durieux I, P. O., Schtitz, P., & Brun, R. (1991). *Alterations in Krebs cycle enzyme activities and carbohydrate catabolism in two strains of T13'panosoma brucei during in vitro differentiation of their bloodstream to procyclic stages* (Vol. 45).
- DUYCKAERTS, C., SLUSE-GOFFART, C. M., FUX, J. -P, SLUSE, F. E., & LIEBECQ, C. (1980). Kinetic Mechanism of the Exchanges Catalysed by the Adenine-Nucleotide Carrier. *European Journal of Biochemistry*, *106*(1), 1–6. <https://doi.org/10.1111/j.1432-1033.1980.tb05990.x>
- Ebikeme, C. E., Peacock, L., Coustou, V., Riviere, L., Bringaud, F., Gibson, W. C., & Barrett, M. P. (2008). N-acetyl D-glucosamine stimulates growth in procyclic forms of *Trypanosoma brucei* by inducing a metabolic shift. *Parasitology*, *135*(5), 585–594. <https://doi.org/10.1017/S0031182008004241>
- Ebikeme, C., Hubert, J., Biran, M., Gouspillou, G., Morand, P., Plazolles, N., Guegan, F., Diolez, P., Franconi, J. M., Portais, J. C., & Bringaud, F. R. (2010). Ablation of succinate production from glucose metabolism in the procyclic trypanosomes induces metabolic switches to the glycerol 3-phosphate/ dihydroxyacetone phosphate shuttle and to proline metabolism. *Journal of Biological Chemistry*, *285*(42), 32312–32324. <https://doi.org/10.1074/jbc.M110.124917>
- Elkalaf, M., Tuma, P., Weiszenstein, M., Polák, J., & Trnka, J. (2016). Mitochondrial Probe Methyltriphenylphosphonium (TPMP) Inhibits the Krebs Cycle Enzyme 2- Oxoglutarate Dehydrogenase. *PLoS ONE*, *11*(8), 1–16. <https://doi.org/10.1371/journal.pone.0161413>
- Else, A. J., Clarke, J. F., Willis, A., Jackman, S. A., Hough, D. W., & Danson, M. J. (1994). Dihydrolipoamide dehydrogenase in the *Trypanosoma* subgenus, *Trypanozoon*. In *Molecular and Biochemical Parasitology* (Vol. 64).
- Evanst, D. A., & Brown, R. C. (1972). The Utilization of Glucose and Proline by Culture Forms of *Trypanosoma brucei*\*. In *J. PROTOZOOL* (Vol. 19, Issue 4).
- Eyram Adjogatse. (2014). *Structure-based drug design for the discovery of new treatments for trypanosomiasis, Ph.D. Thesis.*
- Eze, A. A., Gould, M. K., Munday, J. C., Tagoe, D. N. A., Stelmanis, V., Schnauffer, A., & De Koning, H. P. (2016a). Reduced Mitochondrial Membrane Potential Is a Late Adaptation of *Trypanosoma*

- brucei brucei to Isometamidium Preceded by Mutations in the  $\gamma$  Subunit of the F1Fo-ATPase. *PLoS Neglected Tropical Diseases*, 10(8). <https://doi.org/10.1371/journal.pntd.0004791>
- Eze, A. A., Gould, M. K., Munday, J. C., Tagoe, D. N. A., Stelmanis, V., Schnauffer, A., & De Koning, H. P. (2016b). Reduced Mitochondrial Membrane Potential Is a Late Adaptation of *Trypanosoma brucei brucei* to Isometamidium Preceded by Mutations in the  $\gamma$  Subunit of the F1Fo-ATPase. *PLoS Neglected Tropical Diseases*, 10(8). <https://doi.org/10.1371/journal.pntd.0004791>
- Fang, J., & Beattie, D. S. (2002). Novel FMN-containing rotenone-insensitive NADH dehydrogenase from *Trypanosoma brucei* mitochondria: Isolation and characterization. *Biochemistry*, 41(9), 3065–3072. <https://doi.org/10.1021/bi015989w>
- Fang, J., & Beattie, D. S. (2003). Identification of a gene encoding a 54 kDa alternative NADH dehydrogenase in *Trypanosoma brucei*. *Molecular and Biochemical Parasitology*, 127(1), 73–77. [https://doi.org/10.1016/S0166-6851\(02\)00305-5](https://doi.org/10.1016/S0166-6851(02)00305-5)
- Franco, J. R., Cecchi, G., Paone, M., Diarra, A., Grout, L., Ebeja, A. K., Simarro, P. P., Zhao, W., & Argaw, D. (2022). The elimination of human African trypanosomiasis: Achievements in relation to WHO road map targets for 2020. *PLoS Neglected Tropical Diseases*, 16(1). <https://doi.org/10.1371/JOURNAL.PNTD.0010047>
- Frauwirth, K. A., Riley, J. L., Harris, M. H., Parry, R. V., Rathmell, J. C., Plas, D. R., Elstrom, R. L., June, C. H., & Thompson, C. B. (2002). The CD28 Signaling Pathway Regulates Glucose Metabolism ability of resting cells to take up and utilize nutrients at levels sufficient to maintain viability (Rathmell et al in fat and muscle cells insulin induces glucose uptake in excess of that required to maintain. In *Immunity* (Vol. 16).
- Frenkel, D., Zhang, F., Guirnalda, P., Haynes, C., Bockstal, V., Radwanska, M., Magez, S., & Black, S. J. (2016). *Trypanosoma brucei* Co-opts NK Cells to Kill Splenic B2 B Cells. *PLoS Pathogens*, 12(7). <https://doi.org/10.1371/journal.ppat.1005733>
- Furuya, T., Kessler, P., Jardim, A., Schnauffer, A., Crudder, C., & Parsons, M. (n.d.). *Glucose is toxic to glycosome-deficient trypanosomes*. [www.who.int/inf-fsenfact259.html](http://www.who.int/inf-fsenfact259.html)
- Gatto, C., Grandi, M., Solaini, G., Baracca, A., & Giorgio, V. (2022). The F1Fo-ATPase inhibitor protein IF1 in pathophysiology. In *Frontiers in Physiology* (Vol. 13). Frontiers Media S.A. <https://doi.org/10.3389/fphys.2022.917203>
- Gibson. (1986). *Will the real Trypanosoma b. gambiense please stand up*.

- Ginger, M. L., Ngazoa, E. S., Pereira, C. A., Pullen, T. J., Kabiri, M., Becker, K., Gull, K., & Steverding, D. (2005). Intracellular positioning of isoforms explains an unusually large adenylate kinase gene family in the parasite *Trypanosoma brucei*. *Journal of Biological Chemistry*, *280*(12), 11781–11789. <https://doi.org/10.1074/jbc.M413821200>
- Gnipová, A., Panicucci, B., Paris, Z., Verner, Z., Horváth, A., Lukeš, J., & Zíková, A. (2012). Disparate phenotypic effects from the knockdown of various *Trypanosoma brucei* cytochrome c oxidase subunits. *Molecular and Biochemical Parasitology*, *184*(2), 90–98. <https://doi.org/10.1016/j.molbiopara.2012.04.013>
- Gnipová, A., Šubrtová, K., Panicucci, B., Horváth, A., Lukeš, J., & Zíková, A. (2015). The ADP/ATP carrier and its relationship to oxidative phosphorylation in ancestral protist *trypanosoma brucei*. *Eukaryotic Cell*, *14*(3), 297–310. <https://doi.org/10.1128/EC.00238-14>
- Greig, N., Wyllie, S., Patterson, S., & Fairlamb, A. H. (2009). A comparative study of methylglyoxal metabolism in trypanosomatids. *FEBS Journal*, *276*(2), 376–386. <https://doi.org/10.1111/j.1742-4658.2008.06788.x>
- Guerra, D. G., Decottignies, A., Bakker, B. M., & Michels, P. A. M. (2006). The mitochondrial FAD-dependent glycerol-3-phosphate dehydrogenase of Trypanosomatidae and the glycosomal redox balance of insect stages of *Trypanosoma brucei* and *Leishmania* spp. *Molecular and Biochemical Parasitology*, *149*(2), 155–169. <https://doi.org/10.1016/j.molbiopara.2006.05.006>
- Gunasekera, K., Wüthrich, D., Braga-Lagache, S., Heller, M., & Ochsenreiter, T. (2012). Proteome remodelling during development from blood to insect-form *Trypanosoma brucei* quantified by SILAC and mass spectrometry. *BMC Genomics*, *13*(1). <https://doi.org/10.1186/1471-2164-13-556>
- Haindrich, A. C., Ernst, V., Naguleswaran, A., Oliveres, Q. F., Roditi, I., & Rentsch, D. (2021). Nutrient availability regulates proline/alanine transporters in *Trypanosoma brucei*. *Journal of Biological Chemistry*, *296*. <https://doi.org/10.1016/j.jbc.2021.100566>
- Halestrap, A. P. (1976). The Mechanism of the Inhibition of the Mitochondrial Pyruvate Transporter by  $\alpha$ -Cyanocinnamate Derivatives. In *Biochem. J* (Vol. 156).
- Hall, R. J., Flanagan, L. A., Bottery, M. J., Springthorpe, V., Thorpe, S., Darby, A. C., Wood, A. J., & Thomas, G. H. (2019). *A Tale of Three Species: Adaptation of Sodalis glossinidius to Tsetse Biology, Wigglesworthia Metabolism, and Host Diet*. <https://doi.org/10>

- Hamilton, V., Singha, U. K., Smith, J. T., Weems, E., & Chaudhuri, M. (2014). Trypanosome alternative oxidase possesses both an N-terminal and internal mitochondrial targeting signal. *Eukaryotic Cell*, 13(4), 539–547. <https://doi.org/10.1128/EC.00312-13>
- Hammond, D. J., Aman, R. A., & Wang, C. C. (1985). The role of compartmentation of glycerol kinase in the synthesis of ATP within the glycosome of *Trypanosoma brucei*. *Journal of Biological Chemistry*, 260(29), 15646–15654. [https://doi.org/10.1016/s0021-9258\(17\)36307-x](https://doi.org/10.1016/s0021-9258(17)36307-x)
- Helfert, S., Este! Vez, A. M., Bakker, B., Michels, P., & Clayton, C. (2001). Roles of triosephosphate isomerase and aerobic metabolism in *Trypanosoma brucei*. In *Biochem. J* (Vol. 357). [www.who.int](http://www.who.int)
- Hierro-Yap, C., Subrtová, K., Gahura, O., Panicucci, B., Dewar, C., Chinopoulos, C., Schnauffer, A., & Zíková, A. (2021). Bioenergetic consequences of FoF1–ATP synthase/ATPase deficiency in two life cycle stages of *Trypanosoma brucei*. *Journal of Biological Chemistry*, 296. <https://doi.org/10.1016/j.jbc.2021.100357>
- Hirumi, H., Hirumi, ' K, Moloo, S. K., & Shaw, M. K. (1992). *Trypanosoma brucei brucei*: In Vitro Production of Metacyclic Forms. In *J. Protozool* (Vol. 39, Issue 5).
- Horáková, E., Lecordier, L., Cunha, P., Sobotka, R., Changmai, P., Langedijk, C. J. M., Abbeele, J., Van Den, Vanhollebeke, B., & Lukeš, J. (2022). Heme-deficient metabolism and impaired cellular differentiation as an evolutionary trade-off for human infectivity in *Trypanosoma brucei gambiense*. *Nature Communications*, 13(1). <https://doi.org/10.1038/s41467-022-34501-4>
- Horváth, A., Horáková, E., Dunajčíková, P., Verner, Z., Pravdová, E., Šlapetová, I., Cuninková, L., & Lukeš, J. (2005). Downregulation of the nuclear-encoded subunits of the complexes III and IV disrupts their respective complexes but not complex I in procyclic *Trypanosoma brucei*. *Molecular Microbiology*, 58(1), 116–130. <https://doi.org/10.1111/j.1365-2958.2005.04813.x>
- Hunger-Glaser, I., Brun, R., Linder, M., & Seebeck, T. (1999). Inhibition of succinyl CoA synthetase histidine-phosphorylation in *Trypanosoma brucei* by an inhibitor of bacterial two-component systems. *Molecular and Biochemical Parasitology*, 100(1), 53–59. [https://doi.org/10.1016/S0166-6851\(99\)00032-8](https://doi.org/10.1016/S0166-6851(99)00032-8)
- Hunger-Glaser, I., Hemphill, A., Shalaby, T., Hänni, M., & Seebeck, T. (2000). Nucleoside diphosphate kinase of *Trypanosoma brucei*. In *Gene* (Vol. 257). [www.elsevier.com/locate/gene](http://www.elsevier.com/locate/gene)

- Hunger-Glaser, I., Linder, M., & Seebeck, T. (1999). Histidine-phosphorylation of succinyl CoA synthetase from *Trypanosoma brucei*. In *Molecular and Biochemical Parasitology* (Vol. 100).
- Husová, B. M., Alena, R., Zíková, P., & Panicucci, B. (2021). *Elucidating the source of bloodstream Trypanosoma brucei mitochondrial ATP (Master thesis)*.
- Intlekofer, A. M., Wang, B., Liu, H., Shah, H., Carmona-Fontaine, C., Rustenburg, A. S., Salah, S., Gunner, M. R., Chodera, J. D., Cross, J. R., & Thompson, C. B. (2017). L-2-Hydroxyglutarate production arises from noncanonical enzyme function at acidic pH. *Nature Chemical Biology*, 13(5), 494–500. <https://doi.org/10.1038/nchembio.2307>
- J. F. Ryley. (1955). *Comparative Carbohydrate Metabolism of Eleven Species Of Trypanosome*.
- J H Smith, B. M., & Taylor, K. W. (1908). Blood, 3, 1259. Ellinger, F. (1945). Radiology, 44, 125. In *British Medical Journal* (Vol. 20). London. In press.
- James C. Morris, Z. W. M. E. D. and P. T. E. (2002). Glycolysis modulates trypanosome glycoprotein expression as revealed by an RNAi library. *Embo J* 21, 4429–4438.
- Jeacock, L., Baker, N., Wiedemar, N., Mäser, P., & Horn, D. (2017). Aquaglyceroporin-null trypanosomes display glycerol transport defects and respiratory-inhibitor sensitivity. *PLoS Pathogens*, 13(3), 1–16. <https://doi.org/10.1371/journal.ppat.1006307>
- Johnson, J. D., Mehus, J. G., Tews, K., Milavetz, B. I., & Lambeth, D. O. (1998a). Genetic evidence for the expression of ATP- and GTP-specific succinyl- CoA synthetases in multicellular eucaryotes. *Journal of Biological Chemistry*, 273(42), 27580–27586. <https://doi.org/10.1074/jbc.273.42.27580>
- Johnson, J. D., Mehus, J. G., Tews, K., Milavetz, B. I., & Lambeth, D. O. (1998b). *Genetic Evidence for the Expression of ATP-and GTP-specific Succinyl-CoA Synthetases in Multicellular Eucaryotes\**. <http://www.jbc.org/>
- Johnston, K., Kim, D. H., Kerkhoven, E. J., Burchmore, R., Barrett, M. P., & Achcar, F. (2019). Mapping the metabolism of five amino acids in bloodstream form *Trypanosoma brucei* using U-13C-labelled substrates and LC–MS. *Bioscience Reports*, 39(5). <https://doi.org/10.1042/BSR20181601>
- Joyce, M. A., Fraser, M. E., James, M. N. G., Bridger, W. A., & Wolodko, W. T. (2000a). ADP-binding site of *Escherichia coli* succinyl-CoA synthetase revealed by X-ray crystallography. *Biochemistry*, 39(1), 17–25. <https://doi.org/10.1021/bi991696f>



- Joyce, M. A., Fraser, M. E., James, M. N. G., Bridger, W. A., & Wolodko, W. T. (2000b). ADP-binding site of *Escherichia coli* succinyl-CoA synthetase revealed by X-ray crystallography. *Biochemistry*, *39*(1), 17–25. <https://doi.org/10.1021/bi991696f>
- Kasozi, K. I., MacLeod, E. T., Waiswa, C., Mahero, M., Ntulume, I., & Welburn, S. C. (2022). Systematic Review and Meta-Analysis on Knowledge Attitude and Practices on African Animal Trypanocide Resistance. In *Tropical Medicine and Infectious Disease* (Vol. 7, Issue 9). MDPI. <https://doi.org/10.3390/tropicalmed7090205>
- Kieft, R., Capewell, P., Turner, C. M. R., Veitch, N. J., MacLeod, A., & Hajduk, S. (2010). Mechanism of *Trypanosoma brucei gambiense* (group 1) resistance to human trypanosome lytic factor. *Proceedings of the National Academy of Sciences of the United States of America*, *107*(37), 16137–16141. <https://doi.org/10.1073/pnas.1007074107>
- King, M. S., Kerr, M., Crichton, P. G., Springett, R., & Kunji, E. R. S. (2016). Formation of a cytoplasmic salt bridge network in the matrix state is a fundamental step in the transport mechanism of the mitochondrial ADP/ATP carrier. *Biochimica et Biophysica Acta - Bioenergetics*, *1857*(1), 14–22. <https://doi.org/10.1016/j.bbabi.2015.09.013>
- Klingenberg, M. (2008). The ADP and ATP transport in mitochondria and its carrier. *Biochimica et Biophysica Acta - Biomembranes*, *1778*(10), 1978–2021. <https://doi.org/10.1016/j.bbamem.2008.04.011>
- Kodama, H., Okazaki, F., & Ishida, S. (2008). Protective Effect of Humus Extract Against *Trypanosoma brucei* Infection in Mice. In *J. Vet. Med. Sci* (Vol. 70, Issue 11).
- Kolev, N. G., Ramey-Butler, K., Cross, G. A. M., Ullu, E., & Tschudi, C. (2012). Developmental progression to infectivity in *Trypanosoma brucei* triggered by an RNA-binding protein. *Science*, *338*(6112), 1352–1353. <https://doi.org/10.1126/science.1229641>
- Kovářová, J., Nagar, R., Faria, J., Ferguson, M. A. J., Barrett, M. P., & Horn, D. (2018). Gluconeogenesis using glycerol as a substrate in bloodstream-form *Trypanosoma brucei*. *PLoS Pathogens*, *14*(12). <https://doi.org/10.1371/journal.ppat.1007475>
- Kristensson, K., Masocha, W., & Bentivoglio, M. (2013). Mechanisms of CNS invasion and damage by parasites. In *Handbook of Clinical Neurology* (Vol. 114, pp. 11–22). Elsevier B.V. <https://doi.org/10.1016/B978-0-444-53490-3.00002-9>

- Kuemmerle, A., Schmid, C., Bernhard, S., Kande, V., Mutombo, W., Ilunga, M., Lumpungu, I., Mutanda, S., Nganzobo, P., Tete, D. N., Kisala, M., Burri, C., Blesson, S., & Mordt, O. V. (2021). Effectiveness of nifurtimox eflornithine combination therapy (NECT) in *T. b. gambiense* second stage sleeping sickness patients in the Democratic Republic of Congo: Report from a field study. *PLoS Neglected Tropical Diseases*, *15*(11). <https://doi.org/10.1371/journal.pntd.0009903>
- Kühlbrandt, W. (2019). *Annual Review of Biochemistry Structure and Mechanisms of F-Type ATP Synthases*. <https://doi.org/10.1146/annurev-biochem-013118>
- Lambeth, D. O., Tews, K. N., Adkins, S., Frohlich, D., & Milavetz, B. I. (2004a). Expression of two succinyl-CoA synthetases with different nucleotide specificities in mammalian tissues. *Journal of Biological Chemistry*, *279*(35), 36621–36624. <https://doi.org/10.1074/jbc.M406884200>
- Lambeth, D. O., Tews, K. N., Adkins, S., Frohlich, D., & Milavetz, B. I. (2004b). Expression of two succinyl-CoA synthetases with different nucleotide specificities in mammalian tissues. *Journal of Biological Chemistry*, *279*(35), 36621–36624. <https://doi.org/10.1074/jbc.M406884200>
- Lamour, N., Rivière, L., Coustou, V., Coombs, G. H., Barrett, M. P., & Bringaud, F. (2005). Proline metabolism in procyclic *Trypanosoma brucei* is down-regulated in the presence of glucose. *Journal of Biological Chemistry*, *280*(12), 11902–11910. <https://doi.org/10.1074/jbc.M414274200>
- Lewis, A. M., Waterhouse, C., & Jacobs, L. S. (1980). Whole-Blood and Plasma Amino Acid Analysis: Gas-Liquid and Cation-Exchange Chromatography Compared. In *CLINICAL CHEMISTRY* (Vol. 26, Issue 2).
- Li, X., Wu, F., & Beard, D. A. (2013). Identification of the kinetic mechanism of succinyl-CoA synthetase. *Bioscience Reports*, *33*(1), 145–163. <https://doi.org/10.1042/BSR20120069>
- Linstead, D. J., & Cross, G. A. M. (1977). Threonine Catabolism in *Trypanosoma brucei*. In *Journal of General Microbiology (1977): Vol. IOI*. [www.microbiologyresearch.org](http://www.microbiologyresearch.org)
- Livak, K. J., & Schmittgen, T. D. (2001). Analysis of relative gene expression data using real-time quantitative PCR and the  $2^{-\Delta\Delta CT}$  method. *Methods*, *25*(4), 402–408. <https://doi.org/10.1006/meth.2001.1262>
- Loi'c, L., Re, R., Moreau, P., Allmann, S., Hahn, M., Biran, M., Plazolles, N., Franconi, J.-M., Boshart, M., & Dé Ric Bringaud, F. (n.d.). *Acetate produced in the mitochondrion is the essential precursor for lipid biosynthesis in procyclic trypanosomes*. <http://www.genedb.org/genedb/trypl/>

- Luévano-Martínez, L. A., Girard, R. M. B. M., Alencar, M. B., & Silber, A. M. (2020). ATP regulates the activity of an alternative oxidase in *Trypanosoma brucei*. *FEBS Letters*, *594*(13), 2150–2158. <https://doi.org/10.1002/1873-3468.13790>
- Mach, J., Poliak, P., Matušková, A., Žárský, V., Janata, J., Lukes, J., & Tachezy, J. (2013). An advanced system of the mitochondrial processing peptidase and core protein family in *Trypanosoma brucei* and multiple origins of the Core I subunit in eukaryotes. *Genome Biology and Evolution*, *5*(5), 860–875. <https://doi.org/10.1093/gbe/evt056>
- Maggs, D. G., Jacob, R., Rife, F., Lange, R., Leone, P., During, M. J., Tamborlane, W. V., & Sherwin, R. S. (n.d.). *Interstitial fluid Concentrations of Glycerol, Glucose, and Amino Acids in Human Quadriceps Muscle and Adipose Tissue Evidence for Significant Lipolysis in Skeletal Muscle*.
- Mantilla, B. S., Marchese, L., Casas-Sánchez, A., Dyer, N. A., Ejeh, N., Biran, M., Bringaud, F., Lehane, M. J., Acosta-Serrano, A., & Silber, A. M. (2017). Proline Metabolism is Essential for *Trypanosoma brucei brucei* Survival in the Tsetse Vector. *PLoS Pathogens*, *13*(1). <https://doi.org/10.1371/journal.ppat.1006158>
- Marciano, D., Llorente, C., Mageri, D. A., de la Fuente, C., Opperdoes, F., Cazzulo, J. J., & Nowicki, C. (2008). Biochemical characterization of stage-specific isoforms of aspartate aminotransferases from *Trypanosoma cruzi* and *Trypanosoma brucei*. *Molecular and Biochemical Parasitology*, *161*(1), 12–20. <https://doi.org/10.1016/j.molbiopara.2008.05.005>
- Markos, A. B. A. K. M. B. E. B. K. N. E. (1989). *Metabolic differentiation of bloodstream forms of Trypanosoma brucei brucei into procyclic forms. Effect of hydroxyurea, arabinosyl adenine, and serum omission*. *36*(3), 225–238.
- Matthews, K. R. (2005). The developmental cell biology of *Trypanosoma brucei*. *Journal of Cell Science*, *118*(2), 283–290. <https://doi.org/10.1242/jcs.01649>
- Mazet, M., Morand, P., Biran, M., Bouyssou, G., Courtois, P., Daulouède, S., Millerieux, Y., Franconi, J. M., Vincendeau, P., Moreau, P., & Bringaud, F. (2013). Revisiting the Central Metabolism of the Bloodstream Forms of *Trypanosoma brucei*: Production of Acetate in the Mitochondrion Is Essential for Parasite Viability. *PLoS Neglected Tropical Diseases*, *7*(12), 1–14. <https://doi.org/10.1371/journal.pntd.0002587>
- Michels, P. A. M., Villafraz, O., Pineda, E., Alencar, M. B., Cáceres, A. J., Silber, A. M., & Bringaud, F. (2021). Carbohydrate metabolism in trypanosomatids: New insights revealing novel

- complexity, diversity and species-unique features. In *Experimental Parasitology* (Vol. 224). Academic Press Inc. <https://doi.org/10.1016/j.exppara.2021.108102>
- Millerioux, Y., Ebikeme, C., Biran, M., Morand, P., Bouyssou, G., Vincent, I. M., Mazet, M., Riviere, L., Franconi, J. M., Burchmore, R. J. S., Moreau, P., Barrett, M. P., & Bringaud, F. (2013). The threonine degradation pathway of the *Trypanosoma brucei* procyclic form: The main carbon source for lipid biosynthesis is under metabolic control. *Molecular Microbiology*, *90*(1), 114–129. <https://doi.org/10.1111/mmi.12351>
- Millerioux, Y., Mazet, M., Bouyssou, G., Allmann, S., Kiema, T. R., Bertiaux, E., Fouillen, L., Thapa, C., Biran, M., Plazolles, N., Dittrich-Domergue, F., Cruzols, A., Wierenga, R. K., Rotureau, B., Moreau, P., & Bringaud, F. (2018). De novo biosynthesis of sterols and fatty acids in the *Trypanosoma brucei* procyclic form: Carbon source preferences and metabolic flux redistributions. *PLoS Pathogens*, *14*(5). <https://doi.org/10.1371/journal.ppat.1007116>
- Millerioux, Y., Morand, P., Biran, M., Mazet, M., Moreau, P., Wagnies, M., Ebikeme, C., Deramchia, K., Gales, L., Portais, J. C., Boshart, M., Franconi, J. M., & Bringaud, F. (2012). ATP synthesis-coupled and -uncoupled acetate production from acetyl-CoA by mitochondrial acetate:Succinate CoA-transferase and acetyl-CoA thioesterase in *Trypanosoma*. *Journal of Biological Chemistry*, *287*(21), 17186–17197. <https://doi.org/10.1074/jbc.M112.355404>
- Mochizuki, K., Inaoka, D. K., Mazet, M., Shiba, T., Fukuda, K., Kurasawa, H., Millerioux, Y., Boshart, M., Balogun, E. O., Harada, S., Hirayama, K., Bringaud, F., & Kita, K. (2020). The ASCT/SCS cycle fuels mitochondrial ATP and acetate production in *Trypanosoma brucei*. *Biochimica et Biophysica Acta - Bioenergetics*, *1861*(11). <https://doi.org/10.1016/j.bbabi.2020.148283>
- Morrison, L. J., Steketee, P. C., Tettey, M. D., & Matthews, K. R. (2023). Pathogenicity and virulence of African trypanosomes: From laboratory models to clinically relevant hosts. *Virulence*, *14*(1). <https://doi.org/10.1080/21505594.2022.2150445>
- Moxley, M. A., Tanner, J. J., & Becker, D. F. (2011). Steady-state kinetic mechanism of the proline:ubiquinone oxidoreductase activity of proline utilization A (PutA) from *Escherichia coli*. *Archives of Biochemistry and Biophysics*, *516*(2), 113–120. <https://doi.org/10.1016/j.abb.2011.10.011>

- Njiokou, F., Nimpaye, H., Simo, G., Njitchouang, G. R., Asonganyi, T., Cuny, G., & Herder, S. (2010). Domestic animals as potential reservoir hosts of *trypanosoma brucei gambiense* in sleeping sickness foci in Cameroon. *Parasite*, *17*(1), 61–66. <https://doi.org/10.1051/parasite/2010171061>
- Nolan, D. P., & Voorheis, H. P. (1992). The mitochondrion in bloodstream forms of *Trypanosoma brucei* is energized by the electrogenic pumping of protons catalysed by the F1F0-ATPase. *European Journal of Biochemistry*, *209*(1), 207–216. <https://doi.org/10.1111/j.1432-1033.1992.tb17278.x>
- O’Gorman, G. M., Park, S. D. E., Hill, E. W., Meade, K. G., Coussens, P. M., Agaba, M., Naessens, J., Kemp, S. J., & MacHugh, D. E. (2009). Transcriptional profiling of cattle infected with *Trypanosoma congolense* highlights gene expression signatures underlying trypanotolerance and trypanosusceptibility. *BMC Genomics*, *10*. <https://doi.org/10.1186/1471-2164-10-207>
- Ong, H. B., Lee, W. S., Patterson, S., Wyllie, S., & Fairlamb, A. H. (2015). Homoserine and quorum-sensing acyl homoserine lactones as alternative sources of threonine: A potential role for homoserine kinase in insect-stage *Trypanosoma brucei*. *Molecular Microbiology*, *95*(1), 143–156. <https://doi.org/10.1111/mmi.12853>
- Opperdoes, F. R., & Borst, P. (1977). Localization of nine glycolytic enzymes in a microbody-like organelle in *Trypanosoma brucei*: The glycosome. *FEBS Letters*, *80*(2), 360–364. [https://doi.org/10.1016/0014-5793\(77\)80476-6](https://doi.org/10.1016/0014-5793(77)80476-6)
- Opperdoes FR. (1981). *Localization of malate dehydrogenase, adenylate kinase and glycolytic enzymes in glycosomes and the threonine pathway in the mitochondrion of cultured procyclic trypanomastigotes of Trypanosoma brucei.*
- Panicucci, B., Gahura, O., & Ziková, A. (2017). *Trypanosoma brucei* TbIF1 inhibits the essential F1-ATPase in the infectious form of the parasite. *PLoS Neglected Tropical Diseases*, *11*(4), 1–21. <https://doi.org/10.1371/journal.pntd.0005552>
- Pebay-Peyroula, E., Dahout-Gonzalez, C., Kahn, R., Trézéguet, V., Lauquin, G. J. M., & Brandolin, G. (2003). Structure of mitochondrial ADP/ATP carrier in complex with carboxyatractyloside. *Nature*, *426*(6962), 39–44. <https://doi.org/10.1038/nature02056>
- Peña-Díaz, P., Pelosi, L., Ebikeme, C., Colasante, C., Gao, F., Bringaud, F., & Voncken, F. (2012). Functional characterization of TbMCP5, a conserved and essential ADP/ATP carrier present in the mitochondrion of the human pathogen *Trypanosoma brucei*. *Journal of Biological Chemistry*, *287*(50), 41861–41874. <https://doi.org/10.1074/jbc.M112.404699>

- Pereira, S. S., Trindade, S., De Niz, M., & Figueiredo, L. M. (2019). Tissue tropism in parasitic diseases. In *Open Biology* (Vol. 9, Issue 5). Royal Society Publishing. <https://doi.org/10.1098/rsob.190036>
- Perham, R. N. (2000). *S WINGING A RMS AND S WINGING D OMAINS IN M ULTIFUNCTIONAL E NZYMES : Catalytic Machines for Multistep Reactions*. 961–1004.
- Pineda, E., Thonnus, M., Mazet, M., Mourier, A., Cahoreau, E., Kulyk, H., Dupuy, J. W., Biran, M., Masante, C., Allmann, S., Rivière, L., Rotureau, B., Portais, J. C., & Bringaud, F. (2018). Glycerol supports growth of the *Trypanosoma brucei* bloodstream forms in the absence of glucose: Analysis of metabolic adaptations on glycerol-rich conditions. *PLoS Pathogens*, *14*(11), 1–25. <https://doi.org/10.1371/journal.ppat.1007412>
- Poudyal, N. R., & Paul, K. S. (2022). Fatty acid uptake in *Trypanosoma brucei*: Host resources and possible mechanisms. In *Frontiers in Cellular and Infection Microbiology* (Vol. 12). Frontiers Media S.A. <https://doi.org/10.3389/fcimb.2022.949409>
- Procházková, M., Panicucci, B., & Zíková, A. (2018). Cultured bloodstream *Trypanosoma brucei* adapt to life without mitochondrial translation release factor 1. *Scientific Reports*, *8*(1). <https://doi.org/10.1038/s41598-018-23472-6>
- Pullman, M. E., & Monroy, G. C. (1963). A Naturally Occurring Inhibitor of Mitochondrial Adenosine Triphosphatase. *Journal of Biological Chemistry*, *238*(11), 3762–3769. [https://doi.org/10.1016/S0021-9258\(19\)75338-1](https://doi.org/10.1016/S0021-9258(19)75338-1)
- Pyrih, J., Hammond, M., Alves, A., Dean, S., Sunter, J. D., Wheeler, R. J., Gull, K., & Lukeš, J. (2023). Comprehensive sub-mitochondrial protein map of the parasitic protist *Trypanosoma brucei* defines critical features of organellar biology. *Cell Reports*, *42*(9). <https://doi.org/10.1016/j.celrep.2023.113083>
- Rex Sheu, K.-F., & Blass, J. P. (1999). The alpha-Ketoglutarate Dehydrogenase Complex. *Annals of the New York Academy of Sciences*, *893*(1 OXIDATIVE/ENE), 61–78. <https://doi.org/10.1111/j.1749-6632.1999.tb07818.x>
- Rivière, L., Van Weelden, S. W. H., Glass, P., Vegh, P., Coustou, V., Biran, M., Van Hellemond, J. J., Bringaud, F., Tielens, A. G. M., & Boshart, M. (2004). Acetyl:succinate CoA-transferase in procyclic *Trypanosoma brucei*. Gene identification and role in carbohydrate metabolism. *Journal of Biological Chemistry*, *279*(44), 45337–45346. <https://doi.org/10.1074/jbc.M407513200>

- Roldán, A., Comini, M. A., Crispo, M., & Krauth-Siegel, R. L. (2011). Lipoamide dehydrogenase is essential for both bloodstream and procyclic *Trypanosoma brucei*. *Molecular Microbiology*, *81*(3), 623–639. <https://doi.org/10.1111/j.1365-2958.2011.07721.x>
- Rose, C., Casas-Sánchez, A., Dyer, N. A., Solórzano, C., Beckett, A. J., Middlehurst, B., Marcello, M., Haines, L. R., Lisack, J., Engstler, M., Lehane, M. J., Prior, I. A., & Acosta-Serrano, Á. (2020). *Trypanosoma brucei* colonizes the tsetse gut via an immature peritrophic matrix in the proventriculus. *Nature Microbiology*, *5*(7), 909–916. <https://doi.org/10.1038/s41564-020-0707-z>
- Samra, S., Ravell, C. L., Giles, S. L., Arnert, P., & Frayn, K. N. (1996). Rapid Communication Interstitial glycerol concentration in human skeletal muscle and adipose tissue is close to the concentration in blood. In *Clinical Science* (Vol. 90).
- Sanchez, M. A. (2013). Molecular identification and characterization of an essential pyruvate transporter from *trypanosoma brucei*. *Journal of Biological Chemistry*, *288*(20), 14428–14437. <https://doi.org/10.1074/jbc.M113.473157>
- Schnauffer, A., Clark-Walker, G. D., Steinberg, A. G., & Stuart, K. (2005). The F1-ATP synthase complex in bloodstream stage trypanosomes has an unusual and essential function. *EMBO Journal*, *24*(23), 4029–4040. <https://doi.org/10.1038/sj.emboj.7600862>
- Sharma, R., Gluenz, E., Peacock, L., Gibson, W., Gull, K., & Carrington, M. (2009). The heart of darkness: growth and form of *Trypanosoma brucei* in the tsetse fly. In *Trends in Parasitology* (Vol. 25, Issue 11, pp. 517–524). <https://doi.org/10.1016/j.pt.2009.08.001>
- Sjöstrand, M., Sjöstrand, S., Gudbjörnsdóttir, S., Gudbjörnsdóttir, G., Holmáing, A., Holmáing, H., Strindberg, L., Ekberg, K., Lönnroth, P., & Lönnroth, L. (2002). *Measurements of Interstitial Muscle Glycerol in Normal and Insulin-Resistant Subjects*. <https://academic.oup.com/jcem/article/87/5/2206/2847168>
- Škodová, I., Verner, Z., Bringaud, F., Fabian, P., Lukeš, J., & Horvátha, A. (2013). Characterization of two mitochondrial flavin adenine dinucleotide-dependent glycerol-3-phosphate dehydrogenases in *Trypanosoma brucei*. *Eukaryotic Cell*, *12*(12), 1664–1673. <https://doi.org/10.1128/EC.00152-13>
- Smith, T. K., Bringaud, F., Nolan, D. P., & Figueiredo, L. M. (2017). Metabolic reprogramming during the *Trypanosoma brucei* life cycle [ version 2; referees : 4 approved ] Referee Status : *F1000Research*, *6*(May), 1–12. <https://doi.org/10.12688/f1000research.10342.1>

- Smith, T. K., & Bütikofer, P. (2010). Lipid metabolism in *Trypanosoma brucei*. In *Molecular and Biochemical Parasitology* (Vol. 172, Issue 2, pp. 66–79). <https://doi.org/10.1016/j.molbiopara.2010.04.001>
- Spitznagel, D., Ebikeme, C., Biran, M., Nicabháird, N., Bringaud, F., Henehan, G. T. M., & Nolan, D. P. (2009). Alanine aminotransferase of *Trypanosoma brucei*- a key role in proline metabolism in procyclic life forms. *FEBS Journal*, 276(23), 7187–7199. <https://doi.org/10.1111/j.1742-4658.2009.07432.x>
- Štáfková, J., Mach, J., Biran, M., Verner, Z., Bringaud, F., & Tachezy, J. (2016). Mitochondrial pyruvate carrier in *Trypanosoma brucei*. *Molecular Microbiology*, 100(3), 442–456. <https://doi.org/10.1111/mmi.13325>
- Šubrtová, K., Panicucci, B., & Zíková, A. (2015). ATPaseTb2, a Unique Membrane-bound FoF1-ATPase Component, Is Essential in Bloodstream and Dyskinetoplastic *Trypanosomes*. *PLoS Pathogens*, 11(2). <https://doi.org/10.1371/journal.ppat.1004660>
- Surve, S., Heestand, M., Panicucci, B., Schnauffer, A., & Parsons, M. (2012). Enigmatic presence of mitochondrial complex I in *Trypanosoma brucei* bloodstream forms. *Eukaryotic Cell*, 12(2), 183–193. <https://doi.org/10.1128/EC.05282-11>
- Surve, S. V., Jensen, B. C., Heestand, M., Mazet, M., Smith, T. K., Bringaud, F., Parsons, M., & Schnauffer, A. (2017). NADH dehydrogenase of *Trypanosoma brucei* is important for efficient acetate production in bloodstream forms. *Molecular and Biochemical Parasitology*, 211, 57–61. <https://doi.org/10.1016/j.molbiopara.2016.10.001>
- Sykes, S. E., & Hajduk, S. L. (2013). Dual functions of  $\alpha$ -ketoglutarate dehydrogenase E2 in the Krebs cycle and mitochondrial DNA inheritance in *Trypanosoma brucei*. *Eukaryotic Cell*, 12(1), 78–90. <https://doi.org/10.1128/EC.00269-12>
- Sykes, S., Szempruch, A., & Hajduk, S. (2015). The Krebs cycle enzyme  $\alpha$ -ketoglutarate decarboxylase is an essential glycosomal protein in bloodstream African trypanosomes. *Eukaryotic Cell*, 14(3), 206–215. <https://doi.org/10.1128/EC.00214-14>
- Taleva, G., Husová, M., Panicucci, B., Hierro-Yap, C., Pineda, E., Biran, M., Moos, M., Šimek, P., Butter, F., Bringaud, F., & Zíková, A. (2023). Mitochondrion of the *Trypanosoma brucei* long slender bloodstream form is capable of ATP production by substrate-level phosphorylation. *PLoS Pathogens*, 19(10), e1011699. <https://doi.org/10.1371/journal.ppat.1011699>



- Tielens, A. G. M., van Grinsven, K. W. A., Henze, K., van Hellemond, J. J., & Martin, W. (2010). Acetate formation in the energy metabolism of parasitic helminths and protists. In *International Journal for Parasitology* (Vol. 40, Issue 4, pp. 387–397). <https://doi.org/10.1016/j.ijpara.2009.12.006>
- Trindade, S., Rijo-Ferreira, F., Carvalho, T., Pinto-Neves, D., Guegan, F., Aresta-Branco, F., Bento, F., Young, S. A., Pinto, A., Van Den Abbeele, J., Ribeiro, R. M., Dias, S., Smith, T. K., & Figueiredo, L. M. (2016). Trypanosoma brucei Parasites Occupy and Functionally Adapt to the Adipose Tissue in Mice. *Cell Host and Microbe*, 19(6), 837–848. <https://doi.org/10.1016/j.chom.2016.05.002>
- Uzcátegui, N. L., Figarella, K., Bassarak, B., Meza, N. W., Mukhopadhyay, R., Ramirez, J. L., & Duszenko, M. (2013). Trypanosoma Brucei Aquaglyceroporins Facilitate the Uptake of Arsenite and Antimonite in a pH Dependent Way. *Cell Physiol Biochem*, 32, 880–888. <https://doi.org/10.1159/000354490>
- Uzcátegui, N. L., Figarella, K., Segnini, A., Marsiccobetre, S., Lang, F., Beitz, E., Rodríguez-Acosta, A., & Bertl, A. (2018). Trypanosoma brucei aquaglyceroporins mediate the transport of metabolic end-products: Methylglyoxal, D-lactate, L-lactate and acetate. *Biochimica et Biophysica Acta - Biomembranes*, 1860(11), 2252–2261. <https://doi.org/10.1016/j.bbamem.2018.09.008>
- Uzcategui, N. L., Szallies, A., Pavlovic-Djuranovic, S., Palmada, M., Figarella, K., Boehmer, C., Lang, F., Beitz, E., & Duszenko, M. (2004). Cloning, heterologous expression, and characterization of three aquaglyceroporins from Trypanosoma brucei. *Journal of Biological Chemistry*, 279(41), 42669–42676. <https://doi.org/10.1074/jbc.M404518200>
- Uzureau, P., Uzureau, S., Lecordier, L., Fontaine, F., Tebabi, P., Homblé, F., Grélard, A., Zhendre, V., Nolan, D. P., Lins, L., Crowet, J. M., Pays, A., Felu, C., Poelvoorde, P., Vanhollebeke, B., Moestrup, S. K., Lyngsø, J., Pedersen, J. S., Mottram, J. C., ... Pays, E. (2013). Mechanism of Trypanosoma brucei gambiense resistance to human serum. *Nature*, 501(7467), 430–434. <https://doi.org/10.1038/nature12516>
- Van Hellemond, J. J., Bakker, B. M., & Tielens, A. G. M. (2005). Energy metabolism and its compartmentation in Trypanosoma brucei. In *Advances in Microbial Physiology* (Vol. 50). Elsevier Masson SAS. [https://doi.org/10.1016/S0065-2911\(05\)50005-5](https://doi.org/10.1016/S0065-2911(05)50005-5)

- Van Hellemond, J. J., Opperdoes, F. R., & Tielens, A. G. M. (1998). Trypanosomatidae produce acetate via a mitochondrial acetate:succinate CoA transferase. *Proceedings of the National Academy of Sciences of the United States of America*, 95(6), 3036–3041. <https://doi.org/10.1073/pnas.95.6.3036>
- Van Hellemond, J. J., Opperdoes, F. R., & Tielens, A. G. M. (2005). The extraordinary mitochondrion and unusual citric acid cycle in *Trypanosoma brucei*. *Biochemical Society Transactions*, 33(5), 967–971. <https://doi.org/10.1042/BST20050967>
- Van Weelden, S. W. H., Fast, B., Vogt, A., Van der Meer, P., Saas, J., Van Hellemond, J. J., Tielens, A. G. M., & Boshart, M. (2003). Procyclic *Trypanosoma brucei* do not use Krebs cycle activity for energy generation. *Journal of Biological Chemistry*, 278(15), 12854–12863. <https://doi.org/10.1074/jbc.M213190200>
- Van Weelden, S. W. H., Van Hellemond, J. J., Opperdoes, F. R., & Tielens, A. G. M. (2005). New functions for parts of the krebs cycle in procyclic *Trypanosoma brucei*, a cycle not operating as a cycle. *Journal of Biological Chemistry*, 280(13), 12451–12460. <https://doi.org/10.1074/jbc.M412447200>
- Vaupel, P., & Multhoff, G. (2021). Revisiting the Warburg effect: historical dogma versus current understanding. In *Journal of Physiology* (Vol. 599, Issue 6, pp. 1745–1757). John Wiley and Sons Inc. <https://doi.org/10.1113/JP278810>
- Verner, Z., Basu, S., Benz, C., Dixit, S., Dobáková, E., Faktorová, D., Hashimi, H., Horáková, E., Huang, Z., Paris, Z., Peña-Díaz, P., Ridlon, L., Týč, J., Wildridge, D., Zíková, A., & Lukeš, J. (2015). Malleable Mitochondrion of *Trypanosoma brucei*. *International Review of Cell and Molecular Biology*, 315, 73–151. <https://doi.org/10.1016/bs.ircmb.2014.11.001>
- Verner, Z., Čermáková, P., Škodová, I., Kriegová, E., Horváth, A., & Lukeš, J. (2011). Complex i (NADH:ubiquinone oxidoreductase) is active in but non-essential for procyclic *Trypanosoma brucei*. *Molecular and Biochemical Parasitology*, 175(2), 196–200. <https://doi.org/10.1016/j.molbiopara.2010.11.003>
- Verner, Z., Škodová, I., Poláková, S., Ďurišová-Benkovičová, V., Horváth, A., & Lukeš, J. (2013). Alternative NADH dehydrogenase (NDH2): Intermembrane-space-facing counterpart of mitochondrial complex i in the procyclic *Trypanosoma brucei*. *Parasitology*, 140(3), 328–337. <https://doi.org/10.1017/S003118201200162X>

- Villafranz, O., Biran, M., Pineda, E., Plazolles, N., Cahoreau, E., Souza, R. O. O., Thonnus, M., Allmann, S., Tetaud, E., Rivière, L., Silber, A. M., Barrett, M. P., Zíková, A., Boshart, M., Portais, J. C., & Bringaud, F. R. (2021). Procylic trypanosomes recycle glucose catabolites and TCA cycle intermediates to stimulate growth in the presence of physiological amounts of proline. *PLoS Pathogens*, *17*(3). <https://doi.org/10.1371/journal.ppat.1009204>
- Vourchakbé, J., Tiofack, Z. A. A., Kante, T. S., Mpoame, M., & Simo, G. (2020). Molecular identification of *Trypanosoma brucei gambiense* in naturally infected pigs, dogs and small ruminants confirms domestic animals as potential reservoirs for sleeping sickness in Chad. *Parasite*, *27*. <https://doi.org/10.1051/parasite/2020061>
- Wagner, B. M., Donnarumma, F., Wintersteiger, R., Windischhofer, W., & Leis, H. J. (2010). Simultaneous quantitative determination of  $\alpha$ -ketoglutaric acid and 5-hydroxymethylfurfural in human plasma by gas chromatography-mass spectrometry. *Analytical and Bioanalytical Chemistry*, *396*(7), 2629–2637. <https://doi.org/10.1007/s00216-010-3479-0>
- Wargnies, M., Bertiaux, E., Cahoreau, E., Ziebart, N., Crouzols, A., Morand, P., Biran, M., Allmann, S., Hubert, J., Villafranz, O., Millerioux, Y., Plazolles, N., Asencio, C., Rivière, L., Rotureau, B., Boshart, M., Portais, J. C., & Bringaud, F. (2018). Gluconeogenesis is essential for trypanosome development in the tsetse fly vector. *PLoS Pathogens*, *14*(12). <https://doi.org/10.1371/journal.ppat.1007502>
- Westin, M. A. K., Hunt, M. C., & Alexson, S. E. H. (2005). The identification of a succinyl-CoA thioesterase suggests a novel pathway for succinate production in peroxisomes. *Journal of Biological Chemistry*, *280*(46), 38125–38132. <https://doi.org/10.1074/jbc.M508479200>
- Wheeler, R. J. (2010). The trypanolytic factor-mechanism, impacts and applications. In *Trends in Parasitology* (Vol. 26, Issue 9, pp. 457–464). <https://doi.org/10.1016/j.pt.2010.05.005>
- Wilkes, J. M., Mulugeta, W., Wells, C., & Peregrine, A. S. (1997). Modulation of mitochondrial electrical potential: a candidate mechanism for drug resistance in African trypanosomes. In *Biochem. J* (Vol. 326). <http://portlandpress.com/biochemj/article-pdf/326/3/755/625369/bj3260755.pdf>
- Williams, N. (1994). The Mitochondrial ATP Synthase of *Trypanosoma brucei*: Structure and Regulation. In *Journal of Bioenergetics and Biomembranes* (Vol. 26, Issue 2).
- Wirtz, E., Leal, S., Ochatt, C., & Cross, G. A. M. (1999). A tightly regulated inducible expression system for conditional gene knock-outs and dominant-negative genetics in *Trypanosoma brucei*.

In *Molecular and Biochemical Parasitology* (Vol. 99).  
www.rockefeller.edu/labheads/cross/cross-

Wyatt, G. R., & Meyer, A. W. L. (n.d.). *T H E CHEMISTRY OF INSECT HEMOLYMPH III. GLYCEROL* \* *The Journal of General Physiology*.

Zhang, X., Cui, J., Nilsson, D., Gunasekera, K., Chanfon, A., Song, X., Wang, H., Xu, Y., & Ochsenreiter, T. (2010). The *Trypanosoma brucei* MitoCarta and its regulation and splicing pattern during development. *Nucleic Acids Research*, 38(21), 7378–7387. <https://doi.org/10.1093/nar/gkq618>

Zíková, A. (2022). Mitochondrial adaptations throughout the *Trypanosoma brucei* life cycle. *Journal of Eukaryotic Microbiology*. <https://doi.org/10.1111/jeu.12911>

Zíková, A., Schnauffer, A., Dalley, R. A., Panigrahi, A. K., & Stuart, K. D. (2009). The F0F1-ATP synthase complex contains novel subunits and is essential for procyclic *Trypanosoma brucei*. *PLoS Pathogens*, 5(5). <https://doi.org/10.1371/journal.ppat.1000436>

Zíková, A., Verner, Z., Nenarokova, A., Michels, P. A. M., & Lukeš, J. (2017). A paradigm shift: The mitoproteomes of procyclic and bloodstream *Trypanosoma brucei* are comparably complex. *PLoS Pathogens*, 13(12), 1–9. <https://doi.org/10.1371/journal.ppat.1006679>

Zuo, Z., Wu, T., Lin, M., Zhang, S., Yan, F., Yang, Z., Wang, Y., & Wang, C. (2014). Chronic exposure to tributyltin chloride induces pancreatic islet cell apoptosis and disrupts glucose homeostasis in male mice. *Environmental Science and Technology*, 48(9), 5179–5186. <https://doi.org/10.1021/es404729p>

## 7. CURRICULUM VITAE

**Surname, name:** Taleva, Gergana (born in Sofia, Bulgaria, 1986)

### **Education**

**Ph.D. studies:** 2015 – currently (University of South Bohemia, České Budějovice, Czech Republic)

**Master of Science (Biology–Biotechnology):** 2010 – 2012 (The University of Copenhagen, Faculty of Science, Copenhagen, Denmark)

**Bachelor of Science (Molecular Biology):** 2005 – 2009 (Sofia University “St. Kliment Ohridski”, Faculty of Biology, Sofia, Bulgaria)

### **Stays**

**Laboratory of Frédéric Bringaud:** June 2018, 4 weeks (University of Bordeaux, Bordeaux, France)

### **Awards**

**European award for extra university activities** - April 2010, Sofia, Bulgaria

**Award for an excellent presentation in the fourth workshop – ‘Biological activity of metal and metal compounds’**, November 2009, Sofia, Bulgaria

### **Conferences**

**18<sup>th</sup> FEBS Young Scientists' Forum (YSF)**, 4-7 July 2018 and 43<sup>rd</sup> FEBS congress, 7-12 July 2018, Prague, Czech Republic, with poster presentation ‘Identifying the source of bloodstream Trypanosoma brucei mitochondrial ATP.’

**British Society for Parasitology Trypanosomiasis and Leishmaniasis Seminar**, 4-7

September 2016, České Budějovice, Czech Republic, with poster presentation: ‘Exploring the bioenergetics of the bloodstream *T. brucei* mitochondrion.’

**11th MiP conference on Mitochondrial Physiology Luční Bouda**, 7-11 September 2015, Pec pod Snezkou, Czech Republic, with poster presentation: ‘A new look at the bioenergetics of the bloodstream *Trypanosoma brucei* mitochondrion.’

**‘Protodny’**, 2015, Dubovice, Czech Republic, with poster presentation: ‘Bioenergetics of the bloodstream *T. brucei* mitochondrion: a new look.’

## **Publications**

**Taleva G**, Husová M, Panicucci B, Hierro-Yap C, Pineda E, Biran M, Moos M, Šimek P, Butter F, Bringaud F, Zíková A. Mitochondrion of the *Trypanosoma brucei* long slender bloodstream form is capable of ATP production by substrate-level phosphorylation. *PLoS Pathog.* 2023 Oct 11;19(10):e1011699. doi: 10.1371/journal.ppat.1011699. PMID: 37819951; PMCID: PMC10593219.

Zoltner M, Campagnaro GD, **Taleva G**, Burrell A, Cerone M, Leung KF, Achcar F, Horn D, Vaughan S, Gadelha C, Zíková A, Barrett MP, de Koning HP, Field MC. Suramin exposure alters cellular metabolism and mitochondrial energy production in African trypanosomes. *J Biol Chem.* 2020 Jun 12;295(24):8331-8347. doi: 10.1074/jbc.RA120.012355. Epub 2020 Apr 30. PMID: 32354742; PMCID: PMC7294092.

Signature: Gergana Taleva